Evaluation of κ^4-Diimine Nickel and Cobalt Hydrofunctionalization Catalysts

By

Christopher L. Rock

A Dissertation Presented in Partial Fulfillment
of the Requirements for the Degree of
Doctor of Philosophy

Approved November 2018 by the
Graduate Supervisory Committee

Ryan Trovitch, Chair
John Kouvetakis
George Pettit

ARIZONA STATE UNIVERSITY

December 2018

ABSTRACT

The search for highly active, inexpensive, and earth abundant replacements for existing transition metal catalysts is ongoing. Our group has utilized several redox non-innocent ligands that feature flexible arms with donor substituents. These ligands allow for coordinative flexibility about the metal centre, while the redox non-innocent core helps to overcome the one electron chemistry that is prevalent in first row transition metals. This dissertation focuses on the use of ^{Ph2PPr}DI, which can adopt a κ^4-configuration when bound to a metal. One reaction that is industrially useful is hydrosilylation, which allows for the preparation of silicones that are useful in the lubrication, adhesive, and cosmetics industries. Typically, this reaction relies on highly active, platinum-based catalysts. However, the high cost of this metal has inspired the search for base metal replacements. In Chapter One, an overview of existing alkene and carbonyl hydrosilylation catalysts is presented. Chapter Two focuses on exploring the reactivity of (^{Ph2PPr}DI)Ni towards carbonyl hydrosilylation, as well as the development of the 2nd generation catalysts, (^{iPr2PPr}DI)Ni and (^{tBu2PPr}DI)Ni. Chapter Three presents a new C-O bond hydrosilylation reaction for the formation of silyl esters. It was found the (^{Ph2PPr}DI)Ni is the most active catalyst in the literature for this transformation, with turnover frequencies of up to 900 h^{-1}. Chapter Four explores the activity and selectivity of (^{Ph2PPr}DI)Ni for alkene hydrosilylation, including the first large scope of *gem*-olefins for a nickel-based catalyst. Chapter Five explores the chemistry of (^{Ph2PPr}DI)CoH, first through electronic structure determinations and crystallography, followed by an investigation of its reactivity towards alkyne hydroboration and nitrile dihydroboration. (^{Ph2PPr}DI)CoH is the first reported cobalt nitrile dihydroboration catalyst.

ACKNOWLEDGEMENTS

Throughout my graduate school career, there are so many people that have had an impact on my experiments, my studies, and my life. I must begin with my advisor for the last 5 years, Prof. Ryan Trovitch. I cannot think of a single time when he was unavailable to go over data, experiments, or have time to read drafts of papers that I had written. I am grateful I had the opportunity to join his lab when I arrived at ASU and have my own small part in building what the group has become.

I must also thank all those who guided and assisted me throughout this whole process. My committee members, Prof. George Pettit and Prof. John Kouvetakis, for their input during my exam and dissertation writing process. Prof. Anne Jones for teaching the scientific writing course during my first year, that I found incredibly valuable. Thank you to Tom Groy for his work with the X-ray diffractometer, Marco Flores for his work with EPR, and Brian Cherry for his assistance with the NMR. Thank you to Amanda Bowman at Colorado College for her work with DFT calculations. Thank you to all the Trovitch group members for all the fun times in lab, the assistance with experiments, and the discussions on science. I feel fortunate to have joined a group with so many talented individuals. Thank you to my professors at UBC for fostering my love of chemistry and setting me on the path. Thank you to Prof. Alaa Abd-El-Aziz for getting me started in a research lab as an undergrad and helping me work all the way through my Masters.

Beyond my studies, I must thank my extraordinary group of friends, who helped to make this experience so much more enjoyable. Thank you so much for all the great conversations, coffees, nights out, taco Tuesdays, football games, training days at jiujitsu, and Thanksgivings, it was all a blast.

Finally, I will finish by thanking my family. Mom, Dad, Bets, Lauren, and Andrew: thank you for your unwavering support over the last 12 years. I don't think we anticipated when I left for UBC at 18 that my studies would take me to all the places it did. To my wonderful wife Amanda: when I was going through my exam in my second year, you stepped up to make it easier on me and have been doing it ever since. I don't think I can express what your daily support means to me.

Your TALENT determines what you can do.

Your MOTIVATION determines how much you are willing to do.

Your ATTITUDE determines how well you do it.

~Lou Holtz~

TABLE OF CONTENTS

Page

CHAPTER Page

APPENDIX Page

LIST OF TABLES

TABLE Page

LIST OF FIGURES

FIGURE Page

FIGURE Page

FIGURE Page

FIGURE Page

FIGURE Page

LIST OF SCHEMES

SCHEME Page

CHAPTER ONE

INTRODUCTION

1.1 Transition Metal Catalysis

Synthetically important organic transformations such as hydrogenation, C-C bond coupling, olefin polymerization, and metathesis often rely on a transition metal catalyst to facilitate reactivity. Indeed, several Nobel Prizes in Chemistry have been awarded on these successes. They include the 1963 prize shared by Ziegler and Natta for their work in olefin polymerization (an example catalyst is shown in **Fig. 1.1**, **a**),[1] the 2001 prize shared by Knowles, Noyori, and Sharpless for their work in asymmetric synthesis catalyzed by ruthenium, rhodium, and osmium reagents (**Fig. 1.1**, **b**),[2] the 2005 prize shared by Shrock, Grubbs, and Chauvin for their work in metathesis catalyzed by molybdenum (**Fig. 1.1**, **c**) and ruthenium (**Fig. 1.1**, **d**),[3] and the 2010 prize shared by Heck, Negishi, and Suzuki for their work in C-C cross coupling reactions catalyzed by palladium (**Fig. 1.1**, **e**).[4]

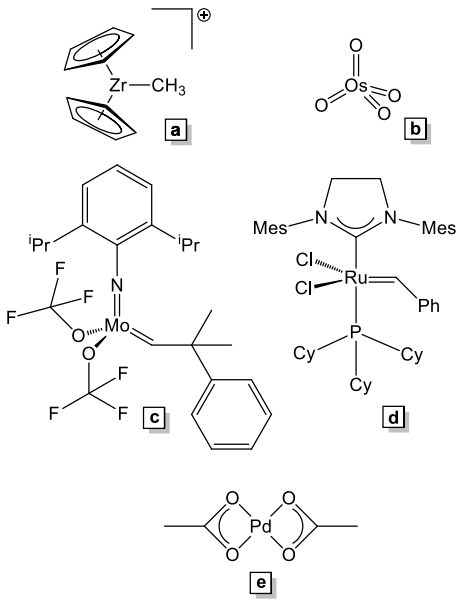

Fig. 1.1 Nobel Prize winning transition metal catalysts.

These complexes and others have had profound effects on many industries, including plastics and pharmaceuticals, allowing for more efficient synthesis of valuable materials.[5]

Scheme 1.1 Example transition metal catalyzed reactions: hydrogenation (top),[6] olefin metathesis (2nd), asymmetric dihydroxylation (3rd), and C-C cross coupling (bottom).

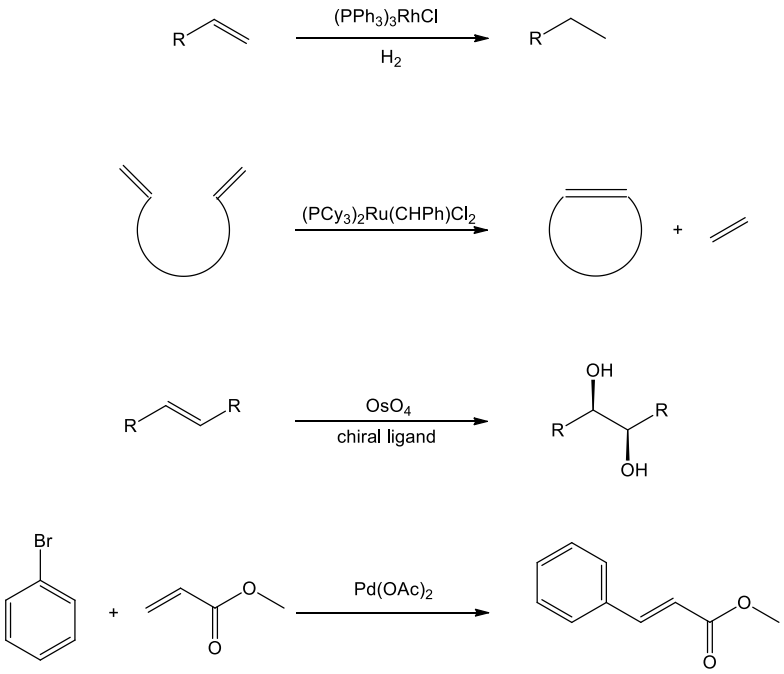

1.2 Base Metal Catalysis

One draw back of several catalysts described in **Scheme 1.1** is their reliance on precious metals. While their efficiency and versatility will likely ensure their continued use, the cost[7] and toxicity[8] of these elements leads to the search for base metal alternatives, which do not share the same concerns. Indeed, the abundance of base metals in the earth's crust is significantly higher than the precious metals that many catalysts rely on (**Table 1.1**).

Table 1.1 Abundance of transition metals in ppm within the Earth's crust.[9]

Sc 16	**Ti** 5 600	**V** 160	**Cr** 100	**Mn** 950	**Fe** 41 000	**Co** 20	**Ni** 80	**Cu** 50	**Zn** 75
Y 30	**Zr** 190	**Nb** 20	**Mo** 1.5	**Tc** -	**Ru** 0.001	**Rh** 0.0002	**Pd** 0.0006	**Ag** 0.07	**Cd** 0.11
La 32	**Hf** 5.3	**Ta** 2	**W** 160	**Re** 0.0004	**Os** 0.0001	**Ir** 0.0003	**Pt** 0.003	**Au** 0.0011	**Hg** 0.05

With these thoughts in mind, there has been significant work done to develop highly efficient, cost effective replacements for precious metal catalysts. Some examples of recent work on base metal alternatives include development of an alkene hydrogenation catalyst, ($^{2,6\text{-iPrPh}}$CNC)Fe(N_2)$_2$ (**Fig. 1.2**, **a**, replacing rhodium),[10] nickel catalyzed Kumada cross coupling with Ni(OAc)$_2$ (**Fig. 1.2**, **b**, replacing palladium),[11] and the electrocatalytic reduction of CO_2 with (bipy)(CO_3)MnBr (**Fig. 1.2**, **c**, replacing rhenium).[12]

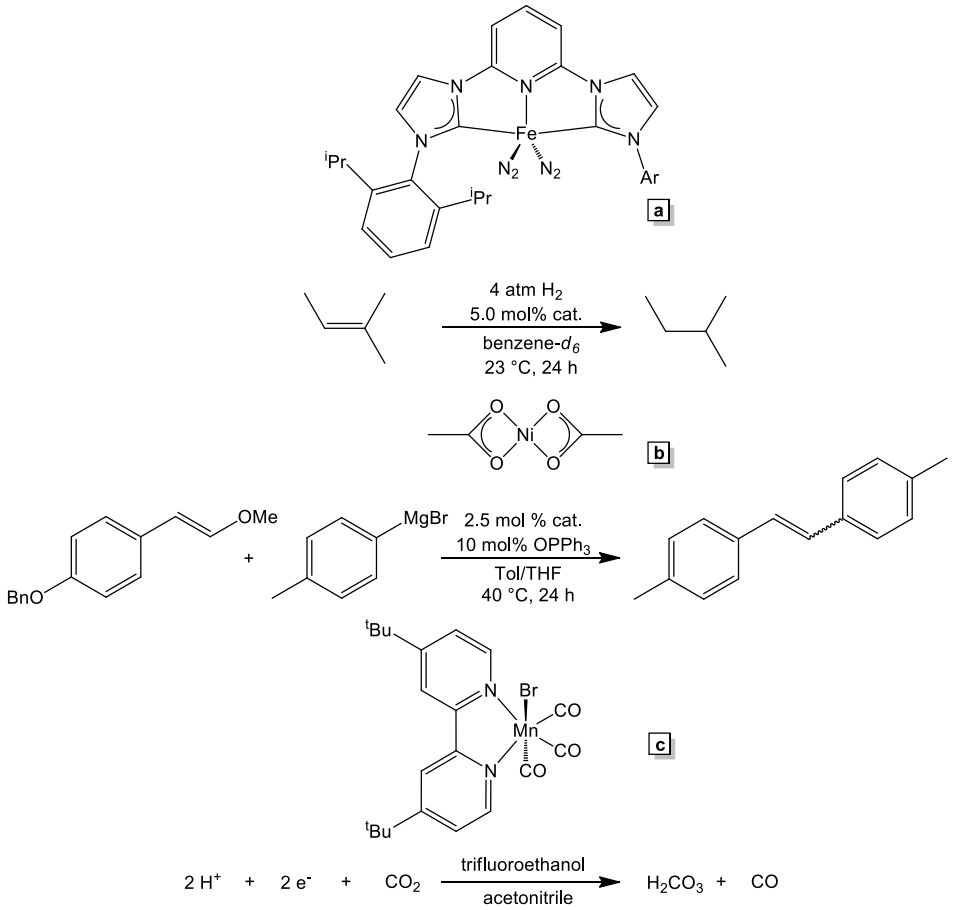

Fig. 1.2 Examples of base metal catalysis and their corresponding organic transformation.

Base metals are not without their drawbacks, however. Base metals tend to undergo single electron chemistry, with numerous oxidation states commonly seen. Single electron chemistry can lead to radical transformations, which can be useful, but for traditional organic transformations requiring 2 electrons or the 2 electron oxidative addition/reductive elimination pathways common to 2nd and 3rd row transition metals, this can be problematic. Base metal compounds also tend to adopt high-spin, paramagnetic configurations, which can be challenging to characterize, as the commonly used methods of ^{1}H, ^{13}C, and heteronuclear NMR spectroscopy may not be as informative as those run on diamagnetic samples.

1.3 Redox Non-Innocent Ligands

One of the methods used the help overcome the high-spin, one electron issues observed for base metals is to employ a redox non-innocent ligand.[13] First described by Jørgensen in 1966, innocent ligands allow oxidation states of the central atom to be defined, while non-innocent ligands can accept electrons from the metal, changing it from its classical oxidation state.[14] With an extended π-network, redox non-innocent ligands can stabilize metals in their preferred oxidation state. This is accomplished by accepting electrons from reduced metal centres, allowing for organic transformations to be catalyzed. A number of base metal catalysts utilizing this ligand type have been reported, with reactions such as water reduction,[15] proton reduction,[16] and alcohol oxidation[17] being observed. Two notable members of this ligand family are bis(imino)pyridine (pyridine diimine, PDI) and 1,4-diaza-1,3-butadiene (α-diimine, DI). Systems featuring PDI ligands were popularized by Brookhart and Gibson, where iron and cobalt containing complexes were shown to mediate olefin polymeraztion.[1] Later, Chirik and coworkers developed PDI-supported complexes of iron and cobalt, which can catalyze a number of reactions such as hydrogenation, hydrosilylation, 2+2 cyclization and polymerization.[19] Like PDI, several DI containing compounds capable of olefin polymerization have been reported.[20]

One advantage of the PDI and DI ligands is that the electronic structure and oxidation state of the metal can be determined from spectroscopic, crystallographic, and computational methods.[21] As seen in **Fig. 1.3**, the bond distances as the ligand becomes reduced are consistent across metals, allowing for electronic structure determinations to be made.

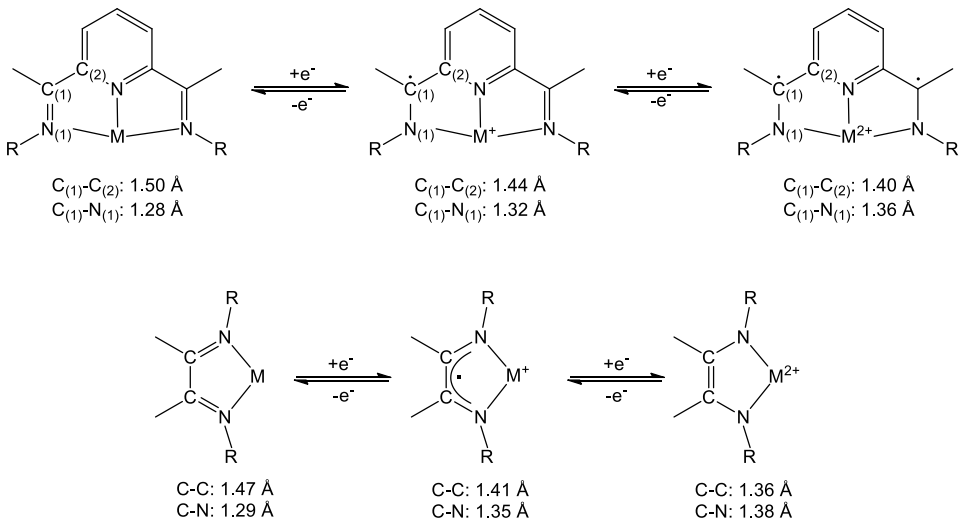

Fig. 1.3 Single crystal X-ray diffraction bond distances within PDI and DI ligand fragments as the ligand becomes more reduced.

Typically, PDI and DI ligands are made by condensing an aryl amine with a diketone. Early work with these ligands increased the steric bulk about the metal centre by placing various substituents on the parent amine.[18-20] One of the most popular is 2,6-di-*i*-propylanaline. However, recently our group has utilized alkyl amines featuring donor groups to develop ligands with coordinative flexibility. Notable examples are 3-(diphenylphosphino)propylamine and 2-pyridinylethylamine, generating ligands that can coordinate with up to 5 and 4 donor atoms, respectively.

Scheme 1.2 Synthesis of donor substituted PDI[22] and DI[23] ligands.

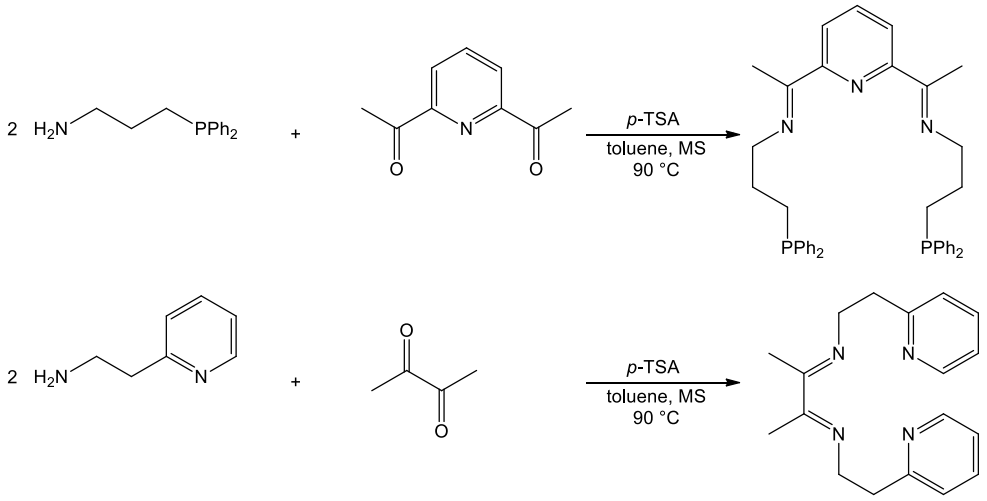

Ligands of this nature have an advantage over their unfunctionalized counterparts by allowing reversible ligand loss during catalysis. When the catalyst is at rest, the donor arms can coordinate to the metal and prevent catalyst decomposition. In the presence of substrate, the donors can dissociate to allow for binding and transformation, re-coordinating after elimination of product.

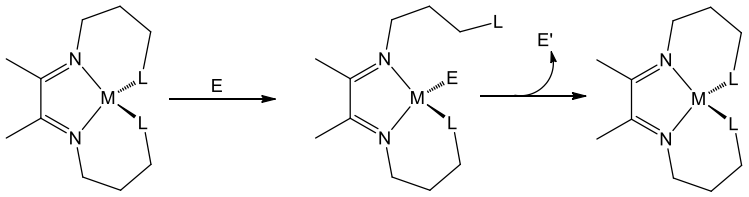

Fig. 1.4 Reversible donor group coordination allowing for substrate modification.

1.4 Olefin Hydrosilylation

One transformation that is synthetically important in the lubricants, adhesives, and cosmetics industries is hydrosilylation, which traditionally involves the addition of an Si-H bond across an olefin.

Scheme 1.3 Platinum catalyzed olefin hydrosilylation.

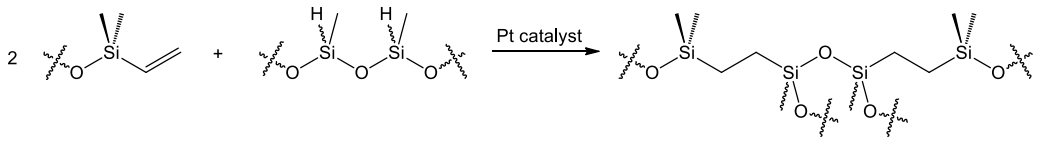

Industrially, the cross linking of siloxanes is catalyzed on large scales by either Karstedt's[24] or Speier's[25] catalysts, which are based on platinum. Speier initially reported the hydrosilylation of 1-pentene with $MeHSiCl_2$ at 100 °C with 0.00005 mol% catalyst loading, with 93% product silane being isolated (turnover frequencies (TOFs) up to 3 720 000 h^{-1} (1033 s^{-1})).[26]

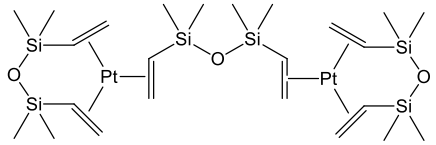

$H_2PtCl_6 \cdot 6H_2O$

Fig. 1.5 Karstedt's (top) and Speier's (bottom) catalysts.

While the remarkable efficiency and versatility of the platinum hydrosilylation catalysts ensures their continued use, the search for more cost-effective replacements is ongoing. A number of olefin hydrosilylation studies featuring base metal catalysts have recently emerged.[27] Some notable examples of manganese based systems are ($^{2,6\text{-Et2Ph}}$PDI)$MnBr_2$, published by Thomas,[28] which catalyzed olefin hydrosilylation after the addition of NaO^tBu with $PhSiH_3$ at TOFs up to 12.4 h^{-1} at ambient temperature, and [($^{2,6\text{-}i\text{Pr2Ph}}$BDI)Mn(μ-H)]$_2$ by our group,[29] which catalyzed olefin hydrosilylation with $PhSiH_3$ with TOFs up to 4.1 h^{-1} at 130 °C.

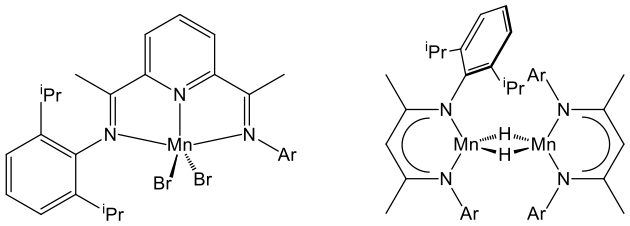

Fig. 1.6 Manganese based-olefin hydrosilylation pre-catalysts by Thomas (left) and Trovitch (right).

As the most abundant transition metal in the earth's crust, iron replacements for precious metal catalysts are continuously sought after. The first example of iron catalyzed olefin hydrosilylation, $Fe(CO)_5$, was reported by Nesmeyanov in 1960.[30] Further mechanistic studies showed that photoirradiation or thermolysis (at up to 140 °C) was required to generate the active species, thought to be either $[Fe(CO)_4]$ or $[Fe(CO)_3]$.[31] This precatalyst produced anti-Markovnikov added products from α-olefins with a variety of silanes. In 2013, Nagashima and coworkers reported mild conditions for the hydrosilylation of ethylene using (κ^2-*Si*,*Si*-1,2-bis(dimethylsilyl)benzene)(κ^2-η^2-SiH,η^2-SiH-1,2-bis(dimethylsilyl)benzene)$Fe(CO)_2$ (**Fig. 1.7**, **a**). This compound utilized either internal or α-olefins and tertiary silanes with 0.01-1.0 mol% catalyst loading at either 23 or 80 °C.[32] Rather than utilize ligands such as CO, Chirik proposed the use of redox non-innocent ligands to generate the same effect, beginning with ($^{2,6\text{-iPrPh}}$PDI)$Fe(N_2)_2$ (**Fig. 1.7**, **b**) in 2004. This compound catalyzed the conversion of terminal olefins to the anti-Markovnikov alkene hydrosilylation products with either Ph_2SiH_2 or $PhSiH_3$ using 0.3 mol% catalyst at ambient temperature with TOFs up to 2970 h^{-1}.[33] Building off of this work, a less sterically demanding PDI ligand was used that resulted in the formation of the dimer, [(($^{2,6\text{-MePh}}$PDI)$Fe(N_2)$)$_2$(μ^2-N_2)] (**Fig. 1.7**, **c**), which exhibited higher activity, catalyzing olefin hydrosilylation with tertiary silanes at catalyst loadings as low as 0.004 mol% (TOFs up to

100 000 h^{-1}).[34] These reports inspired extensive studies on iron utilizing ligands of a similar nature. One noted problem with such compounds is their high sensitivity towards oxygen and moisture. To overcome this problem, bench stable iron dihalides were used, with the active catalyst being generated *in situ* after the addition of an external activator (ie: $NaEt_3BH$). It was shown by Thomas, through addition to ($^{2,6\text{-EtPh}}$PDI)$FeCl_2$, that many different activators can be utilized.[35] This technique was utilized to perform the hydrosilylation of olefins using $PhSiH_3$ without the need for air or moisture free precautions by adding an excess of ($^{i}Pr)_2NEt$ to ($^{2,6\text{-EtPh}}$PDI)$Fe(OTf)_2$, (**Fig. 1.7**, **d**). These bench stable catalysts needed a higher catalyst loading than Chirik's nitrogen complexes, with operating between 2.0-4.0 mol%, though the ambient temperature catalysis was complete in as little as 1 h.[36] Catalysts do not necessarily need to utilize a PDI ligand to exhibit high activity; Nakazawa and Chirik independently published terpyridine type complexes like ^{mes}(terpy)$FeBr_2$ (**Fig. 1.7**, **e**), that catalyze olefin hydrosilylation at catalyst loadings between 0.05-0.1 mol% with Ph_2SiH_2 or $PhSiH_3$ after the addition of $NaEt_3BH$.[37] Chirik published iron alkyl variations of (PDI)Fe and (terpy)Fe (**Fig. 1.7**, **f**) that catalyzed olefin hydrosilylation with 1.0 mol% catalyst loading utilizing tertiary silanes at 60 °C.[37b] Nakazawa later used a iminobipyride ligand to generate a series of complexes similar to ($^{2,6\text{-iPrPh}}$BPI)$FeBr_2$ ((**Fig. 1.7**, **g**), which catalyze the hydrosilylation of 1-octene with TOFs up to 5353 h^{-1} at ambient temperature with Ph_2SiH_2 after activation with $NaEt_3BH$.[38] Moving away from strictly nitrogen based ligands, Huang and coworkers reported the hydrosilylation of olefins with ($P^{O}NN$)$FeBr_2$ (**Fig. 1.7**, **h**) after activation with of $NaEt_3BH$.[39] Changing the alkyl substitution on the phosphine ligand allowed for tailoring of the silane that could be utilized; less sterically bulky substituents allowed for the use of

secondary and tertiary silanes, while more bulky substituents favoured use of primary silanes. Complexes of the ($P^{O}NN$)$FeBr_2$ type are much less active than the (PDI)Fe nitrogen complexes, as they are susceptible to P-O bond cleavage and catalyst deactivation. Recently, ($P^{C}NN$)$FeBr_2$ variants were prepared, which allowed for the lowering of the catalyst loading from between 1.0-5.0 mol% to 0.02 mol%. The ambient temperature reduction of 1-octene proceeded with $PhSiH_3$ at TOFs up to 65.8 h^{-1} (vs. a maximum of 33 h^{-1} for ($P^{O}NN$)$FeBr_2$ type complexes).[40, 41]

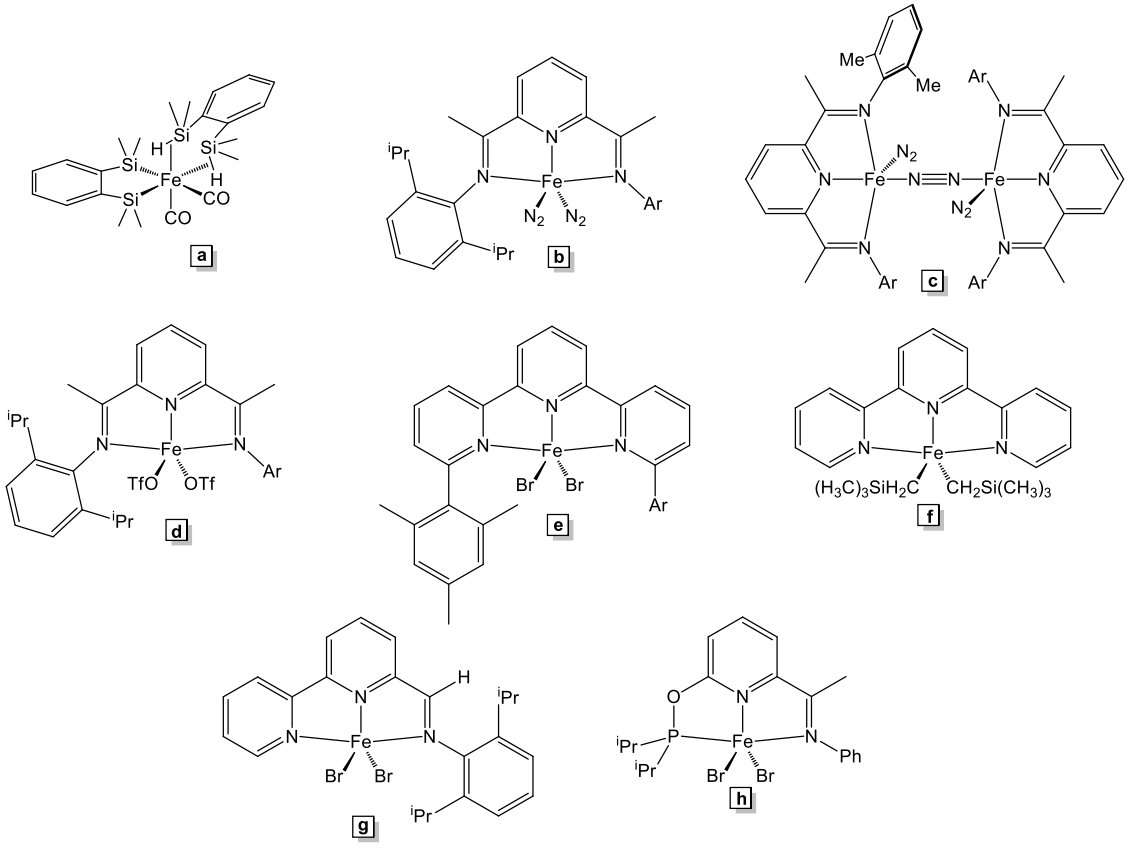

Fig. 1.7 Examples of iron-based olefin hydrosilylation catalysts.

The first reported cobalt based hydrosilylation catalyst, $Co_2(CO)_8$, was reported by Chalk and Harrod in 1965.[42] This catalyst operated under milder conditions than its iron analogue, catalyzing the *anti*-Markovnikov hydrosilylation of terminal alkenes with tertiary silanes.

Moving from simple metal carbonyl complexes, Grant and Brookhart reported that $[Cp^{*}(P(OMe)_3CoCH_2CH_2\text{-}\mu\text{-}H)]^{+}[BAr^{F}{}_4]^{-}$ (**Fig. 1.8**, **a**) catalyzed the *anti*-Markovikov hydrosilylation of 1-hexene with Et_3SiH within 6 h at ambient temperature with 1.0 mol% catalyst loading (TOF of 16.5 h^{-1}).[43] In 2013, Deng and coworkers reported a (κ^2-*N*,*Si*-silylNHC)(κ^2-*N*,*C*-alkylNHC)Co complex (**Fig. 1.8**, **b**) that demonstrated very high activity, showing 70% conversion of 1-octene with $PhSiH_3$ at ambient temperature within 24 h at 0.005 mol% catalyst loading (TOF of 583.3 h^{-1}).[44] Two β-diketiminate (BDI) η^6-arene Co complexes reported by Holland catalyzed olefin hydrosilylation with $(EtO)_3SiH$ at loadings from 0.05-2.0 mol% at either 23 or 60 °C, with the less sterically bulky example (**Fig. 1.8**, **c**) being more efficient.[45] Despite their high activity and selectivity, the sensitivity of the (PDI)Fe(N_2) complexes reported by Chirik (**Fig. 1.7**, **c**), limits their industrial application. Seeking bench stable alternatives led to the synthesis of complexes of the (^{TF}APDI)Co(κ^2-OAc)(κ^1-OAc) type (**Fig. 1.8**, **d**), where the carboxylates are activated by tertiary silanes to form an active catalyst that operated at ambient temperature between 0.25-1.0 mol% catalyst loading.[46] In 2016, Fout and coworkers reported (^{DIPP}CCC)Co(N_2), a bis-carbene complex (**Fig. 1.8**, **e**), which hydrosilylated a number of terminal alkenes featuring reactive functional groups (ie: formyl, carbonyl, hydroxyl, nitrile) at 5.0 mol% catalyst loading with secondary and tertiary silanes (TOFs up to 13.2 h^{-1}).[47] The cobalt analogue (**Fig. 1.8**, **f**) of the (P^{C}NN)Fe(II) complex reported by Huang (**Fig. 1.7**, **g**), provides the opposite regioselectivity, with Markovnikov products being isolated from the hydrosilylation of aliphatic olefins with $PhSiH_3$. These reactions had TOFs up to 82.5 h^{-1} after reacting at 60 °C for 24 h.[48, 49]

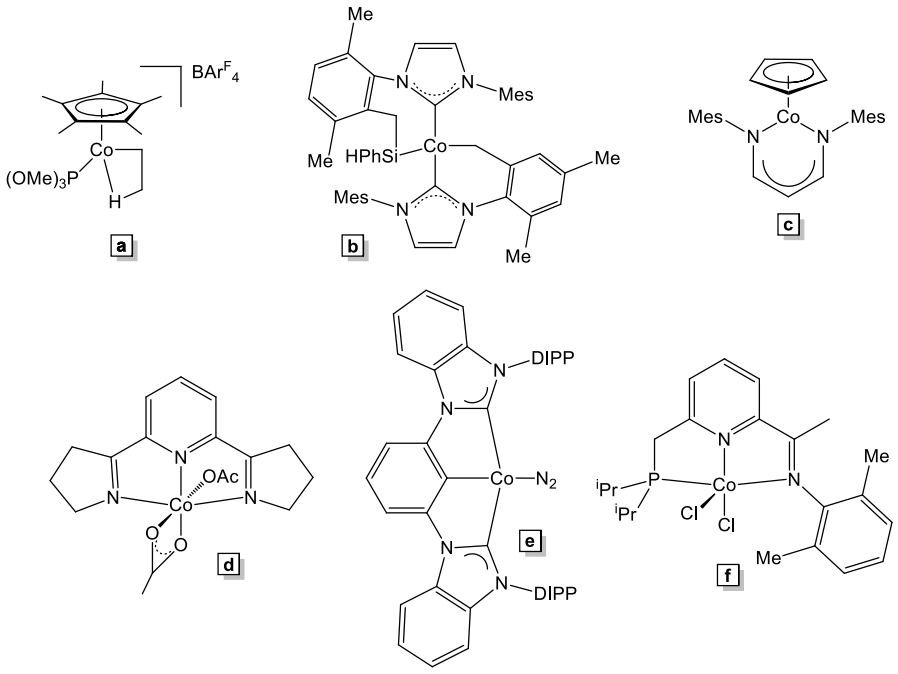

Fig. 1.8 Examples of cobalt-based olefin hydrosilylation catalysts.

Due to its presence in the same group as platinum, nickel has proved to be a viable alternative and has received extensive study.[50] Notable Ni catalysts for Markovnikov-selective alkene hydrosilylation include indenyl pre-catalysts having the general formula (R-Ind)NiCl(PPh_3),[51] as well as [(allyl)Ni(NHC)][BAr^F_4], which have been found to catalyze alkene hydrosilylation with TOFs up to 25 h^{-1} at 60 °C.[52] Catalysts that result in *anti*-Markovnikov product selectivity are more common, with Kuznetsov and Gevorgyan reporting that $(PPh_3)_2NiBr_2$ catalyzes the hydrosilylation of styrenes using Ph_2SiH_2 with TOF up to 8 h^{-1} at 80 °C.[53] Lipschutz and Tilley employed Ni[N($SiMe_3$)(DIPP)]$_2$ (**Fig. 1.9**, **a**) to hydrosilylate 1-octene with Ph_2SiH_2 (TOFs of up to 24.7 h^{-1}),[54] while Shimada and co-workers utilized (salicylaldiminato)$NiCH_3$ complexes (**Fig. 1.9**, **b**) and secondary silanes to convert internal and α-olefins to linear alkyl silanes at ambient temperature.[55] The Shimada group has also demonstrated efficient alkene hydrosilylation at room

temperature using *in situ* activated $(acac)_2Ni$ compounds[56] and cationic Ni allyl catalysts (**Fig. 1.9**, **c**).[57] To date, the most efficient nickel catalyst for alkene hydrosilylation is $(MeN_2N)Ni(OMe)$ (**Fig. 1.9**, **d**), which has been found to convert 1-octene to $Ph_2SiH(octyl)$ within 3 min at ambient temperature, allowing for TOFs of up to 83 000 h^{-1}.[58] Chirik and co-workers found that the *in situ* generated compound, $[(^{2,6\text{-iPr2Ph}}DI)NiH]_2$ (**Fig. 1.1**, **e**), hydrosilylates 1-octene with TOFs up to 166 h^{-1} at 40 °C (up to 33 h^{-1} at ambient temperature).[59]

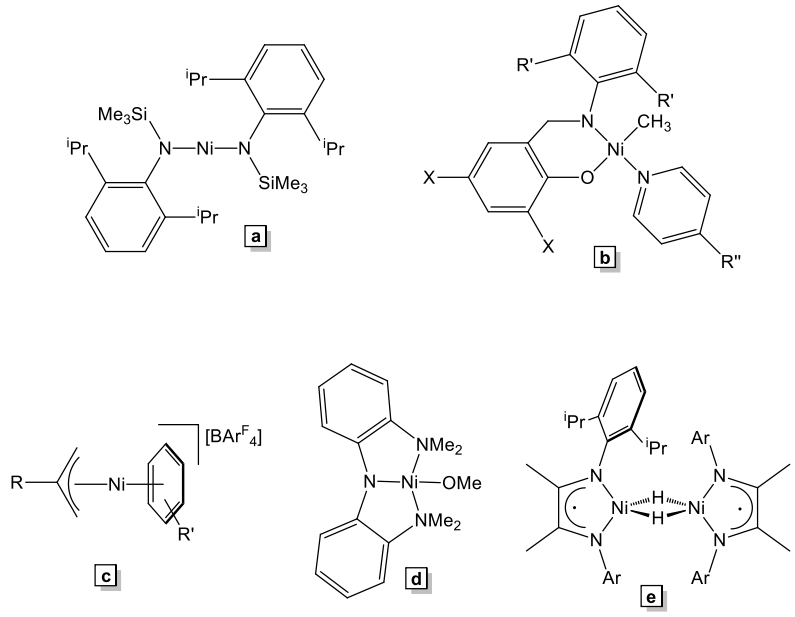

Fig. 1.9 Examples of nickel-based olefin hydrosilylation catalysts.

1.5 Carbonyl Hydrosilylation

Approximately 15 years after alkene hydrosilylation was first demonstrated, Ojima and coworkers[60] reported a related reaction, carbonyl hydrosilylation, using Wilkinson's catalyst.[6] Though typically used as a mild route for the synthesis of alcohols,[61] carbonyl

hydrosilylation has recently been utilized as an alternate route for the preparation of silicones.[62]

Scheme 1.4 Silicone preparation *via* carbonyl hydrosilylation.

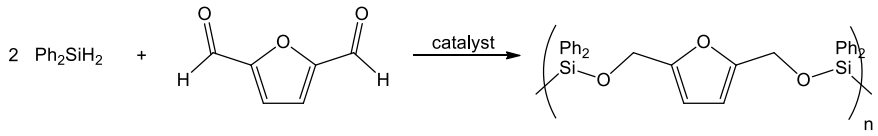

Over the last few years, several highly active catalysts for carbonyl hydrosilylation have appeared. Some early examples include $(PPh_3)(CO)_4MnC(O)CH_3$ reported by Cutler, which catalyzed acetone hydrosilylation with $PhMe_2SiH$ at 2.4 mol% catalyst loading in benzene within 5 min. (TOF of 8.1 min^{-1}),[63] (η^5-1*H*-naphthyl)$Mn(CO)_3$ (**Fig. 1.10**, **a**)by Lee, which reduced cyclohexanone with Ph_2SiH_2 at 5 mol% loading in 3 h (TOF of 6.6 h^{-1}),[64] and $[(\eta^6$-naphthalene)$Mn(CO)_3][BF_4]$ (**Fig. 1.10**, **b**)by Chung, which catalyzed acetophenone with $PhMe_2SiH$ at 5.0 mol% catalyst loading in 2 h (TOF of 9.9 h^{-1}).[65] To date, the most efficient base metal catalyst reported is the manganese complex (^{Ph2PPr}PDI)Mn reported by our group (**Fig. 1.10**, **c**), which converted aldehydes[66] to silyl ethers with TOFs up to 4 900 min^{-1} and ketones[67] to silyl ethers with TOFs up to 76 800 h^{-1} under neat conditions at ambient temperature. Related compounds published by our group also showed remarkable carbonyl hydrosilylation activity.[68] Other notable examples include a Mn(salen) compound by Du (**Fig. 1.10**, **d**), which catalyzed the formation of silicones (**Scheme 1.4**) with 1.0 mol% catalyst within 24 h at ambient temperature.[62b] In 2017, Stadiotto and Turculet reported $[(\kappa^2$-*P*,*N*)$Mn(N(SiMe_3)_2)]$ (**Fig. 1.10**, **e**), which catalyzed a broad scope of carbonyl containing substrates (TOFs up to 24.7 h^{-1} for ketone and aldehyde hydrosilylation).[69]

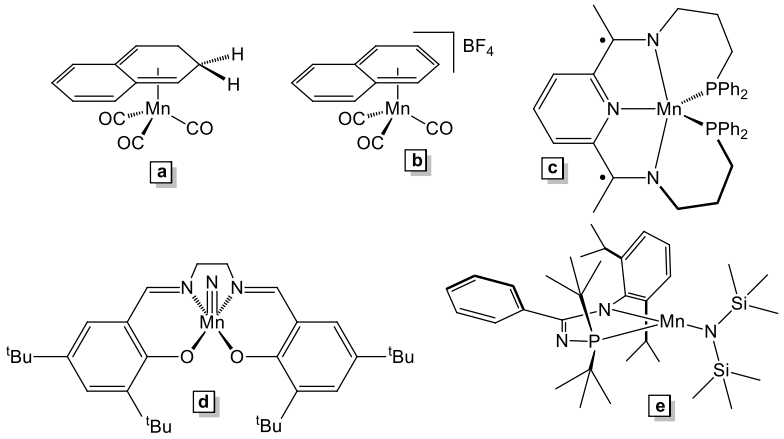

Fig. 1.10 Examples of manganese-based carbonyl hydrosilylation catalysts.

The iron catalysts reported by Chirik for alkene hydrosilylation are also active for carbonyl hydrosilylation. ($^{2,6\text{-iPrPh}}$PDI)Fe(N_2)$_2$ (**Fig. 1.7**, **b**) was capable of acetophenone hydrosilylation with Ph_2SiH_2 at 1.0 mol% catalyst loading within 3 h at ambient temperature, while the dialkyl analogue, ($^{2,6\text{-iPrPh}}$PDI)Fe($CH_2(SiMe_3)$)$_2$ (**Fig. 1.11**, **a**) was more efficient, operating at 0.1 mol%, both at ambient temperature.[70] Enantiopure PyBox iron compounds (**Fig. 1.11**, **b**) showed some enantioselectivity in the hydrosilylation of acetophenone with Ph_2SiH_2, while showing similar activity to the PDI iron alkyl complexes previously reported.[71] The half-sandwich compound (Cp*-NHC)FeCl published by Royo (**Fig. 1.11**, **c**) catalyzed aldehyde hydrosilylation at 70 °C with 1.0 mol% catalyst loading in under 2 h for certain substrates (TOF up to 49.5 h^{-1}).[72] Tilley used a simple amide complex, Fe($N(SiMe_3)_2$)$_2$ (**Fig. 1.11**, **d**), to catalyze ambient temperature ketone hydrosilylation with TOFs up to 163 h^{-1}.[73] A PCP-pincer iron hydride compound developed by Guan (**Fig. 1.11**, **e**) was found to catalyze aldehyde hydrosilylation with $(EtO)_3SiH$ at 50 °C at 1.0 mol% catalyst loading within 1.5 h (TOFs up to 66 h^{-1}).[74] The iron analogue of Stradiotto and Turculet's manganese hydrosilylation catalyst (**Fig. 1.10**, **e**) was also

active for carbonyl hydrosilylation. Operating at the much lower catalyst loading of 0.015 mol%, ketone hydrosilylation reached >99% conversion within 4 h (TOF up to 1650 h^{-1}).[75]

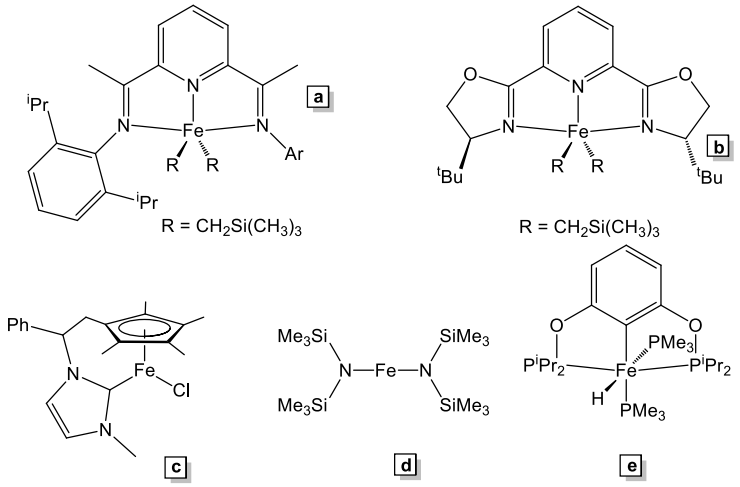

Fig. 1.11 Examples of iron-based carbonyl hydrosilylation catalysts.

In 1991, Brunner and Amberger demonstrated that addition of an excess of PyBox ligand to [Co(pyridine)$_6$][(BF_4)] resulted in an *in situ* generated catalyst that was capable of ketone hydrosilylation. These reactions were completed within 18 h at 20 °C with 0.5 mol% catalyst loading and generated very modest enantioselectivity in the products (TOFs up to 10.4 h^{-1}).[76] Chan and coworkers added a series of chiral, bidentate phosphine ligands to cobalt salts and used that in situ catalyst to form chiral alcohols (after hydrolysis) with 90-95% enantiomeric excess from ketones, using 6.0 mol% catalyst.[77] Using a series of (BPI)Co(CH_2SiMe_3) compounds (**Fig. 1.12**, **a**), Gade and coworkers were able to isolate chiral alcohols (following hydrolysis) after hydrosilylating ketones with $(EtO)_2MeSiH$ after 8 h at ambient temperature with 2.5 mol% catalyst loading (TOFs up to 5.0 h^{-1}).[78] in 2013, Florke and coworkers utilized a mercapto trimethylphosphine cobalt hydride ((**Fig. 1.12**, **b**) to hydrosilylate aldehydes with $(EtO)_3SiH$ at 40 °C (TOFs up to 49.5 h^{-1}).[79] A

CNC timethylphosphino cobalt hydride (**Fig. 1.12**, **c**) was developed by Li and used to hydrosilylate aldehydes with TOFs up to 33 h^{-1} at 60 °C.[80] In 2015, Peters used (DPB)Co(N_2) (**Fig. 1.12**, **d**) to hydrosilylate aldehydes with $PhSiH_3$ in minutes (TOFs up to 49.5 min^{-1}), while ketones took significantly longer (up to 99 h, TOFs up to 7.5 min^{-1}).[81]

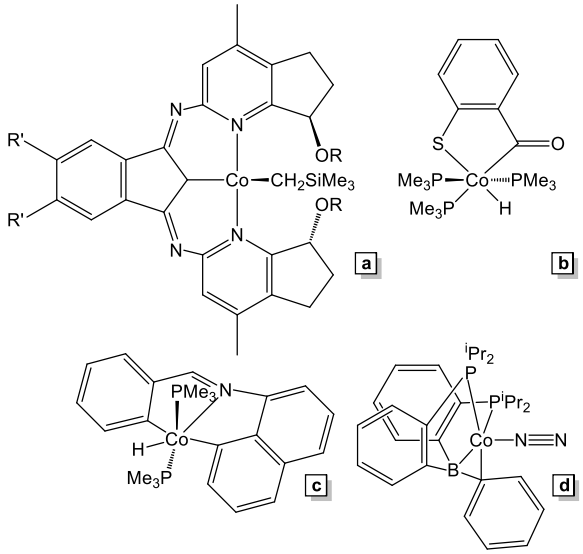

Fig. 1.12 Examples of cobalt-based carbonyl hydrosilylation catalysts.

In 2009, Guan reported that [2,6-($^{i}Pr_2PO)_2C_6H_3$]NiH (**Fig. 1.13**, **a**) catalyzes aldehyde hydrosilylation with turnover frequencies (TOFs) of 250 h^{-1}.[82] Later that year, Mindiola and coworkers achieved aldehyde and ketone hydrosilylation TOFs of 287 h^{-1} and 14 h^{-1}, respectively, upon heating solutions of substrate, Et_3SiH [(PN^{i}Pr$_3$)Ni(μ^2-Br)]$_2$ (**Fig. 1.13**, **b**), and KO^{t}Bu to 100 °C.[83] The leading example of Ni-catalyzed aldehyde hydrosilylation was published by Postigo and Royo in 2012, whereby TOFs of up to 2304 h^{-1} were achieved using $PhSiH_3$ and (Cp*-NHC^{Me})Ni(O^{t}Bu) (**Fig. 1.13**, **c**).[84] At 60 °C, a half-sandwich Ni complex (**Fig. 1.13**, **d**) developed by Albrecht and coworkers was found to hydrosilylate aldehydes with initial TOFs of up to 23,000 h^{-1}.[85] Compounds of this type have also been

employed to reduce aldehydes and ketones in the presence of Ph_2SiH_2.[86] A (PBP)Ni borane complex developed by the Peters group has been used to reduce benzaldehydes in the presence of $PhSiH_3$ and extensive mechanistic studies suggest that the ligand is chemically non-innocent.[87] Most recently, Schmidt and coworkers reported a cationic (κ^2-PN)Ni(allyl) pre-catalyst for carbonyl hydrosilylation.[88]

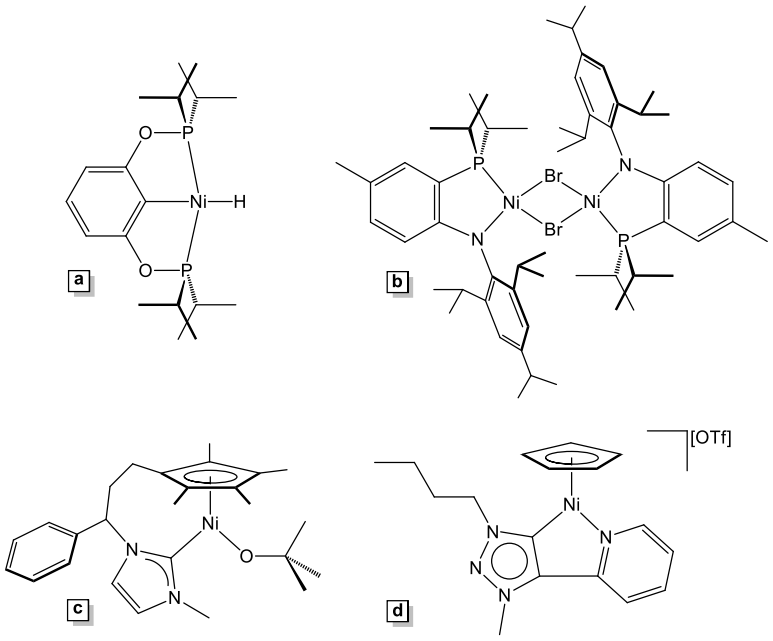

Fig. 1.13 Examples of nickel-based carbonyl hydrosilylation catalysts.

1.6 Scope of Work

Encouraged by the success of recently reported base metal hydrosilylation catalysts, but also aware that reported activity still does not yet offer a replacement for the use of platinum catalysts, the reactivity of new nickel catalysts was explored. A redox non-innocent DI ligand featuring phosphine substituted donor arms bound to nickel was used ((^{Ph2PPr}DI)Ni), which allowed for the stabilization of the metal centre. Using this catalyst, the hydrosilylation of carbonyls (Chapter 2), esters (Chapter 3), and alkenes (Chapter 4)

was explored, and comparable activity for carbonyl (TOF up to 41 h^{-1}) and alkene (TOF up to 990 h^{-1}) hydrosilylation was noted compared to the existing nickel catalysts described in **1.4** and **1.5**. Additionally, a new C-O bond hydrosilylation pathway was noted when allyl esters were combined with $PhSiH_3$, yielding silaneyl triesters with the highest reported TOF to date (990 h^{-1}). Also explored in Chapter 4 is the reduction of *gem*-olefins, yielding enantiomeric mixtures of products. In Chapter 5, the hydroboration of alkynes (TOF up to 900 h^{-1}) and dihydroboration of nitriles (TOF up to 4.1 h^{-1}) with a phosphine substituted donor DI cobalt hydride catalyst, (^{Ph2PPr}DI)CoH, was explored. This cobalt catalyst is the first reported for nitrile dihydroboration and provides the foundation for the development of more active 2nd generation reagents.

CHAPTER TWO

κ^4-DIIMINE NICKEL CATALYST DEVELOPMENT AND CARBONYL HYDROSILYLATION

2.1 Abstract

Seeking to expand on initial studies performed with the previously reported (^{Ph2PPr}DI)Ni (**1**), the alkyl phosphine variants, (^{iPr2PPr}DI)Ni (**2**) and (^{tBu2PPr}DI)Ni (**3**) were prepared. Comparing their hydrosilylation activity towards benzaldehyde with $PhSiH_3$ at 1.0 mol% catalyst loading revealed that **1** reached >99% conversion within 3 h at ambient temperature to a mixture of silyl ethers, while **2** and **3** achieved 8 and 67% conversion, respectively. Utilizing **1** and benzaldehyde, it was determined that $PhSiH_3$ was the most efficient silane for this reaction, with only Ph_2SiH_2 exhibiting any conversion (14%) amongst 7 other silanes that were screened. Lowering of the catalyst loading to 0.1 mol% under neat conditions resulted in >99% conversion within 24 h at ambient temperature. With optimized conditions in hand, a further 11 aldehydes were screened, with **1** showing functional group tolerance for fluoro, chloro, nitrile, ether, and alkene functionalities, although 4-bromobenzaldehyde did likely result in C-Br oxidative addition. Moving to the more demanding ketones, it was found that ketones can be reduced with 1.0 mol% **1** and $PhSiH_3$ at 60 °C within 24 h. All silyl ether products were hydrolyzed with 10% $NaOH_{(aq)}$ to their parent alcohol to allow for simplified isolation. Throughout these experiments, several insights into the mechanism were acquired. Noting that the stronger σ-donating phosphine ligands of **2** and **3** make for poorer catalytic activity, exogenous PMe_3 was added to a benzaldehyde hydrosilylation trial with $PhSiH_3$ and 1.0 mol% **1**, resulting in a decrease in conversion to 3% within 3 h. Independent addition of 2 equivalents of PMe_3 to **1** resulted in partial conversion to several products, including $Ni(PMe_3)_4$. It is proposed that **1** operates

through a modified Ojima carbonyl hydrosilylation mechanism, where the pendant phosphine arms are displaced during silane oxidative addition, prior to alkene insertion into the Ni-H bond. The reductive elimination of the silyl product rapidly occurs after this step.

2.2 (^{Ph2PPr}DI)Ni

In 2013, we reported the synthesis of a κ^4-diimine nickel catalyst featuring pendant phosphine donor arms. Using an acid catalyzed Schiff base condensation between diacetyl and 2 equivalents of $H_2N(CH_2)_3PPh_2$, ^{Ph2PPr}DI was synthesized and crystallized in good yield. Adding this ligand to $Ni(COD)_2$ rapidly displaced the COD ligands to form (^{Ph2PPr}DI)Ni (**1**), which was characterized *via* NMR and single crystal XRD.[23]

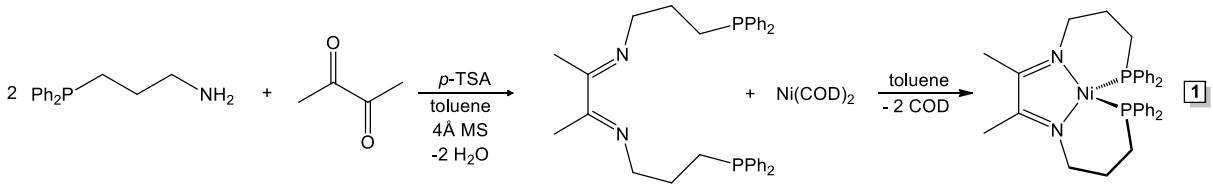

Scheme 2.1 Preparation of catalyst **1**.

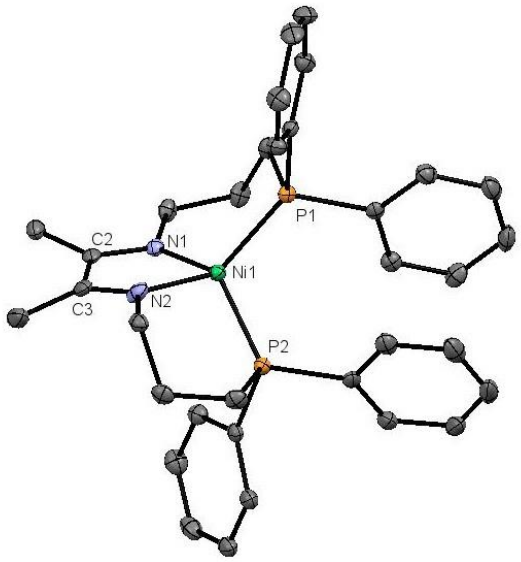

Fig. 2.1 Solid state structure of **1**, drawn with 30% probability ellipsoids. Hydrogen atoms are removed for clarity.

To gain insight into the electronic structure of the compound, the bond lengths of the redox non-innocent chelate were compared to literature values for neutral and reduced DI ligands. Compound **1** features a DI C-C bond distance of 1.414 (3) Å and C-N distances of 1.340 (3) and 1.341 (3) Å. Comparing these distances to accepted literature values[21e] indicates that **1** likely posses a singly reduced DI fragment, with the radical being antiferromagnetically coupled to a metal based electron.

Table 2.1 Selected bond distances for **1**.

Bonds	Distance (Å)
C2-C3	1.414 (3)
C2-N1	1.340 (3)
C3-N2	1.341 (3)
N1-Ni	1.9369 (17)
N2-Ni	1.9250 (18)
P1-Ni	2.1343 (6)
P2-Ni	2.1345 (6)

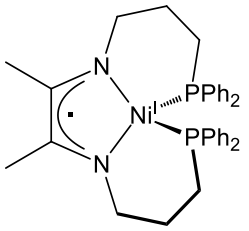

Fig. 2.2 A more accurate electronic structure description of **1**.

Investigating the catalytic abilities of **1** revealed that it is active for alkyne and carbonyl hydrosilylation at 5.0 mol% loading, yielding an alkenyl silane or silyl ethers, respectively.[23]

2.3 Next Generation Catalysts

Having previously shown that the donor functionality of the pendant arms plays a key role in catalyst formation,[23] changing the donor substituents on the phosphines was explored. Utilizing 2 equivalents of either $^{i}Pr_2P(CH_2)_3NH_2$ or $^{t}Bu_2P(CH_2)_3NH_2$ in an acid catalyzed Schiff base condensation allowed for the preparation of ^{iPr2PPr}DI and ^{tBu2PPr}DI, respectively.

While ^{tBu2PPr}DI was successfully crystallized from a solution of diethyl ether and pentane at -35 °C, ^{iPr2PPr}DI proved more difficult to isolate from unreacted phosphine amine and partially condensed materials. Fortunately, adding this mixed material directly to $Ni(COD)_2$ resulted in the formation of (^{iPr2PPr}DI)Ni (**2**), which was cleanly recrystallized from diethyl ether. (^{tBu2PPr}DI)Ni (**3**) was prepared by adding the isolated ^{tBu2PPr}DI to an equimolar amount of $Ni(COD)_2$ in toluene, isolated, and recrystallized from diethyl ether. Both **2** and **3** are diamagnetic complexes with ^{31}P NMR resonances at 52.33 and 73.59 ppm, respectively (**Fig. 2.5**). As these signals are significantly shifted from the parent ligands (^{iPr2PPr}DI at -1.83 ppm, ^{tBu2PPr}DI at 26.58 ppm), coordination of the phosphine arms to the metal centre is confirmed.

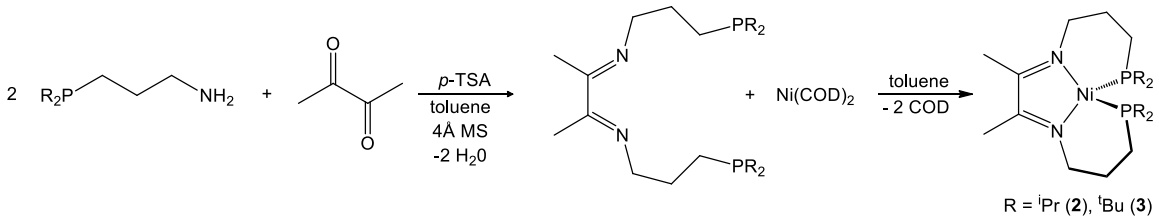

Scheme 2.2 Synthesis of catalysts **2** and **3**.

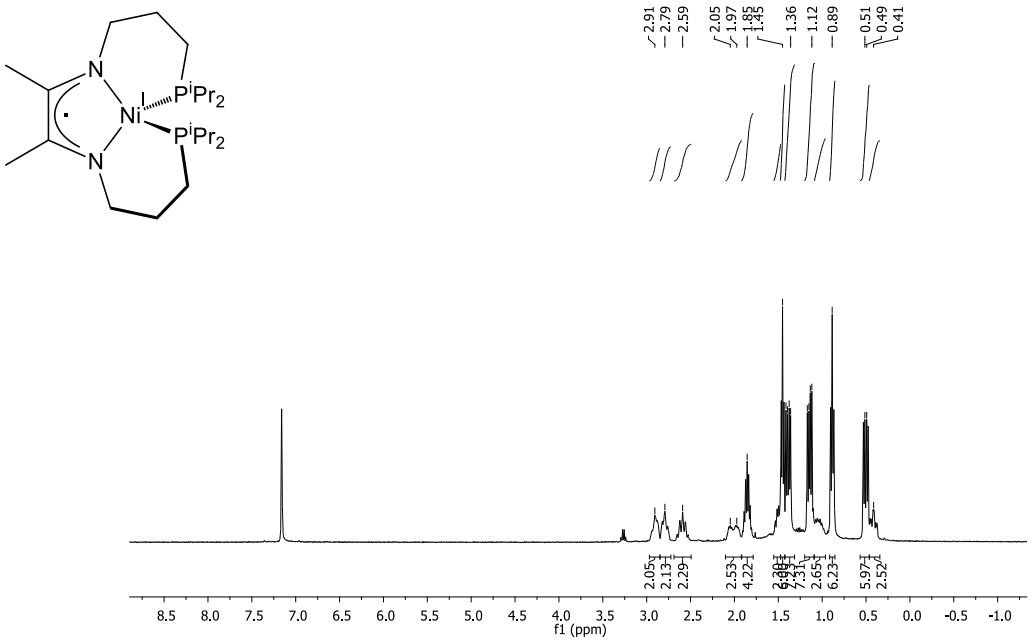

Fig. 2.3 ^{1}H NMR spectrum of **2** in benzene-d_6.

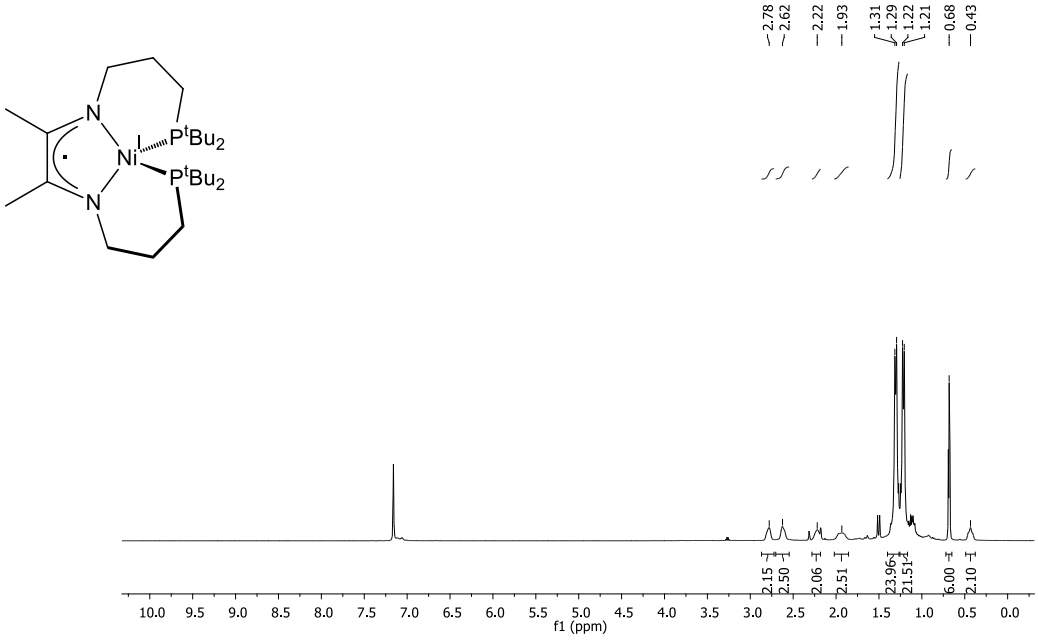

Fig. 2.4 ^{1}H NMR spectrum of **3** in benzene-d_6.

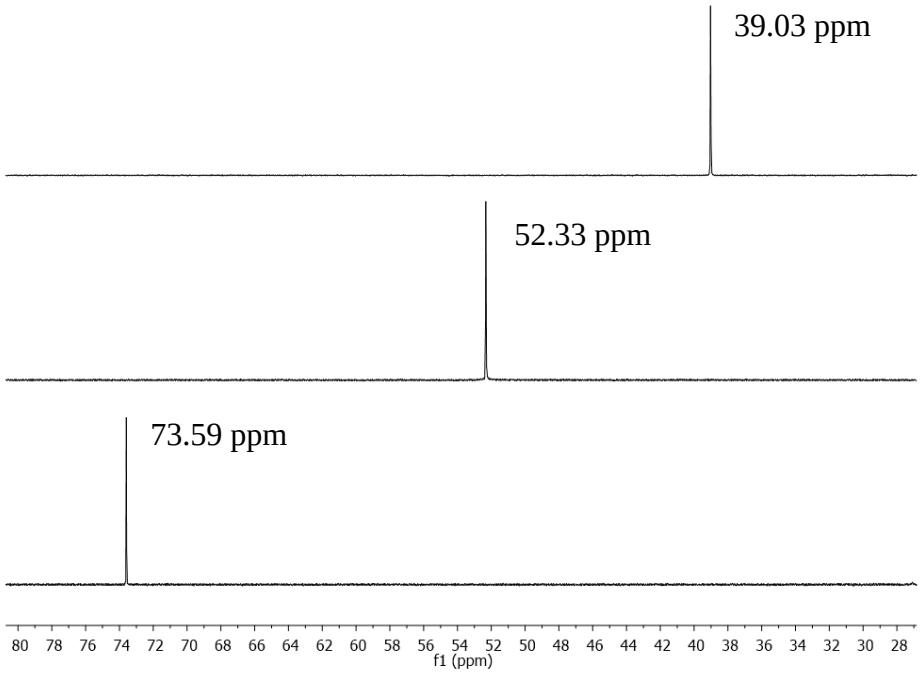

Fig. 2.5 ^{31}P NMR spectra of **1** (top), **2** (middle), and **3** (bottom).

Crystals suitable for single crystal XRD of both **2** and **3** were grown from saturated solutions of diethyl ether at -35 °C. Both structures have distorted tetrahedral geometries and analysis of the bond lengths of the compounds revealed C-C bond distances of 1.420(4) Å (**2**) and 1.423(4) Å (**3**) and C-N distances of 1.350(3) Å (**2**) and 1.339(3) Å (**3**). These values, like those for **1**, indicate that **2** and **3** posses singly reduced DI chelates, with the mono-anion being antiferromagnetically coupled to a Ni electron.

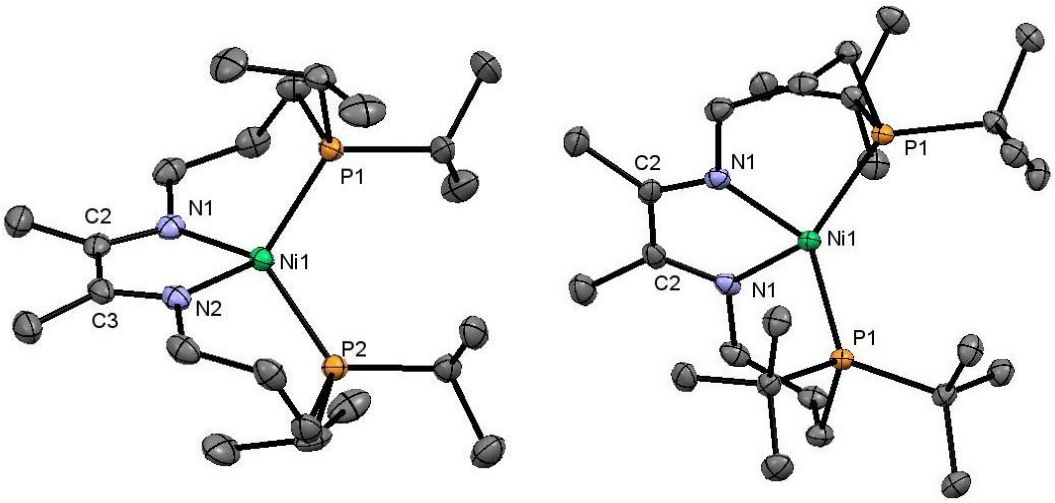

Fig. 2.6 Solid state structures of **2** (left) and **3** (right), drawn with 30% probability ellipsoids. Hydrogen atoms removed for clarity.

Table 2.2 Selected bond distances for **2** and **3**.

2	**Bonds**	**3**
1.420(3)	C2-C3	1.423(4)
1.350(3)	C2-N1	1.339(3)
1.350(3)	C3-N2	-
1.933(2)	N1-Ni	1.9582(17)
1.931(2)	N2-Ni	-
2.1455(7)	P1-Ni	2.2262(5)
2.1554(7)	P2-Ni	-

2.4 Comparing Hydrosilylation Activity

With catalysts **1-3** in hand, comparison of their catalytic activity was investigated. Combining benzaldehyde with an equimolar amount of $PhSiH_3$ in benzene-d_6 with 1.0 mol% catalyst, conversion to a mixture of silyl ethers was observed *via* ^{1}H NMR

spectroscopy. Interestingly, while **1** was able to consume benzaldehyde in >99% conversion within 3 h, **2** and **3** were only able to convert 8 and 67%, respectively.

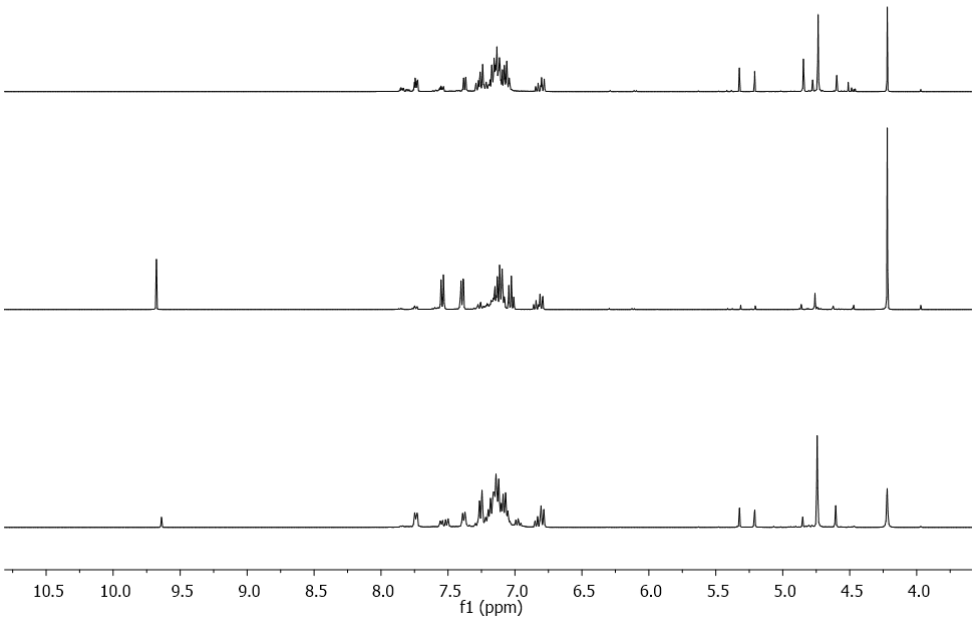

Fig. 2.7 ^{1}H NMR spectra showing conversion of benzaldehyde with $PhSiH_3$ by catalyst **1** (top), **2** (middle), and **3** (bottom) in benzene-d_6.

Knowing that **1** is superior to the alkyl phosphine variants, the optimum silane reductant was then investigated. Combining benzaldehyde with either $PhSiH_3$, Ph_2SiH_2, or Ph_3SiH in benzene-d_6 with 1.0 mol% **1** resulted in >99%, 14%, and 0% conversion, respectively, within 3 hours. Additionally, no conversion was noted with Et_2SiH_2, $^{i}Pr_2SiH_2$, $^{t}Bu_2SiH_2$, Et_3SiH, or Me_2PhSiH.

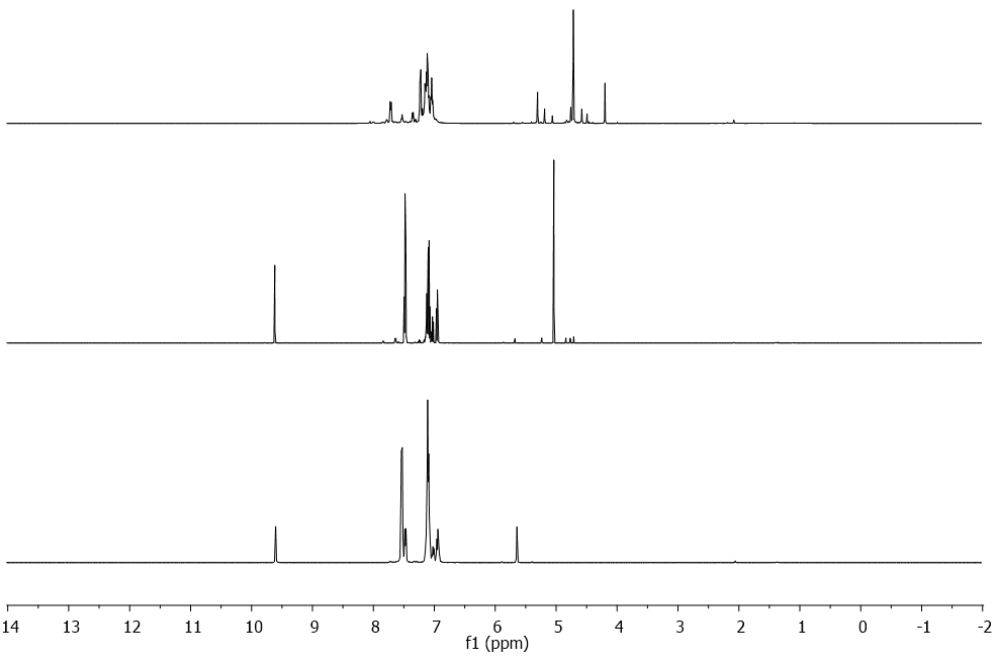

Fig. 2.8 ^{1}H NMR spectra showing conversion of benzaldehyde with $PhSiH_3$ (top), Ph_2SiH_2 (middle), and Ph_3SiH (bottom) with 1.0 mol% **1** in benzene-d_6.

2.5 Carbonyl Hydrosilylation Scope

With initial aldehyde hydrosilylation operating with a turnover frequency (TOF) of 33 h^{-1}, optimal conditions for this reaction were sought. Decreasing the catalyst loading from 1.0 to 0.1 mol% and running the reaction in the absence of solvent resulted in >99% conversion of benzaldehyde to a mixture of silyl ethers within 24 h at ambient temperature. Owing to the complex nature of isolating mixed silyl ethers, the neat solution was treated with 10% aqueous NaOH to hydrolyze all the ethers to their parent alcohol. This allowed for more efficient product isolation and characterization. Benzyl alcohol was isolated after hydrolysis in 81% yield (**Fig. 2.9**).

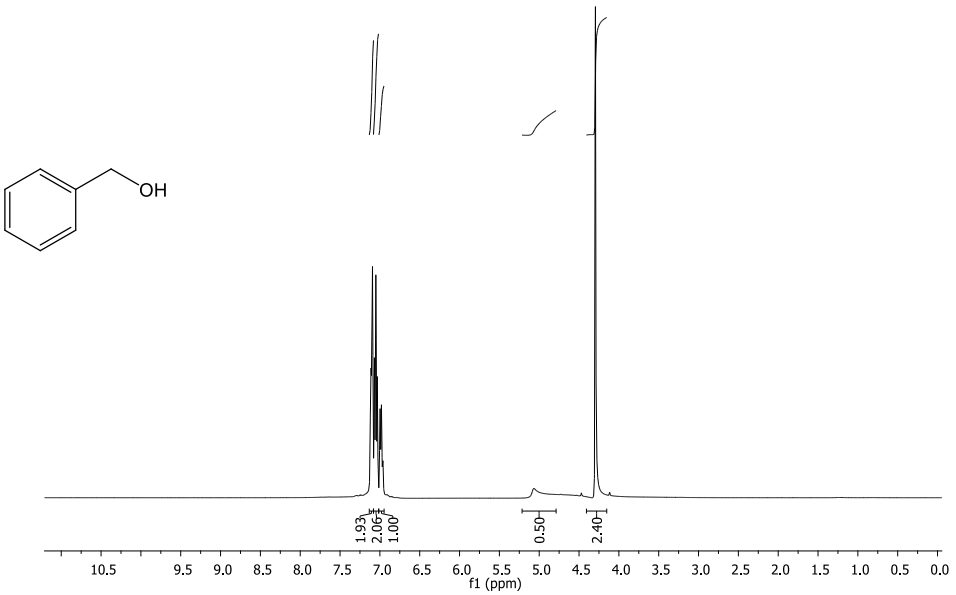

Fig. 2.9 ^{1}H NMR spectrum of benzyl alcohol, isolated after hydrosilylation and hydrolysis.

A further 11 aldehydes were screened, achieving TOFs of 41 h^{-1}, with **1** showing good tolerance for fluoro, chloro, and ether substituents (**Table 2.3**). **1** also showed good chemoselectivity for carbonyls, as nitriles and alkenes were unreactive, despite **1** being known to mediate alkyne hydrosilylation. Interestingly, the addition of 4-bromobenzaldehyde to **1** resulted in an immediate colour change from the characteristic red of **1** to blue, with no substrate conversion being observed in the presence of $PhSiH_3$. These observations are likely a result of oxidative addition of the C-Br bond to the nickel catalyst, leading to catalyst deactivation. Unfortunately, this species is paramagnetic and attempts to characterize it *via* NMR and single crystal XRD were unsuccessful.

Table 2.3 Hydrosilylation of aldehydes using 0.1 mol% **1** and $PhSiH_3$ at 25 °C.[a,b]

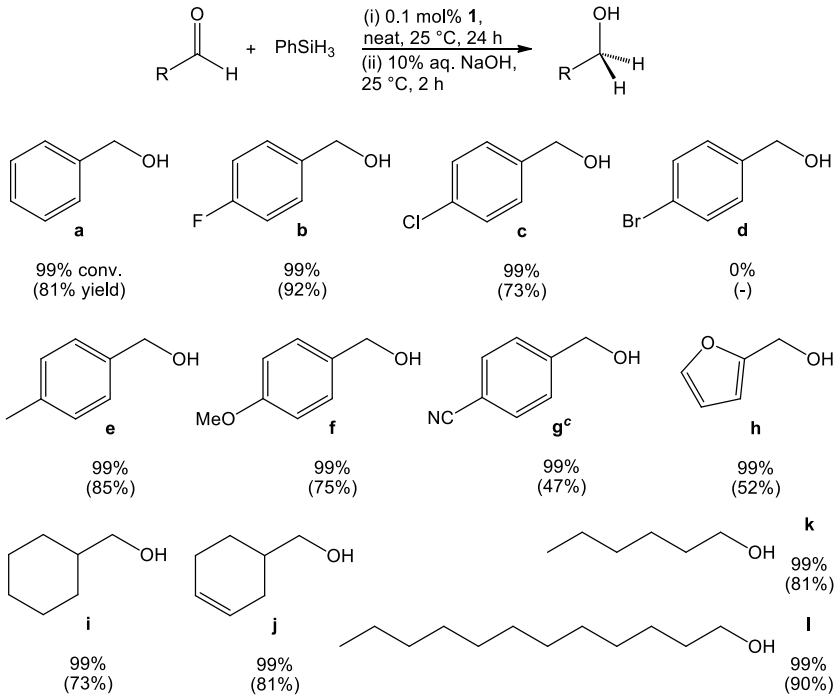

[a]Percent conversion determined by ^1H NMR spectroscopy (TOF = 41 h^{-1} for all substrates except **d**). [b]Isolated yields of the corresponding alcohol in parentheses. [c]Approximately 0.5 mL of benzene was added to aid solubility.

Moving from aldehydes to ketones (**Table 2.4**), it was found that they were more challenging to hydrosilylate. Heating to 60 °C for 24 h at a 1.0 mol% catalyst loading was required for complete conversion, equating to a TOF of 4.1 h^{-1}. Hydrolysis of the mixed silyl ethers with 10% aqueous NaOH again allowed for the isolation of a single product. Sterically demanding ketones such as dicyclohexylketone and 2,4-dimethylpentanone were successfully hydrosilylated, and the incorporation of various functional groups on acetophenone did not affect the catalytic rate.

Table 2.4 Hydrosilylation of ketones using 1.0 mol% **1** and $PhSiH_3$ at 60 °C.[a,b]

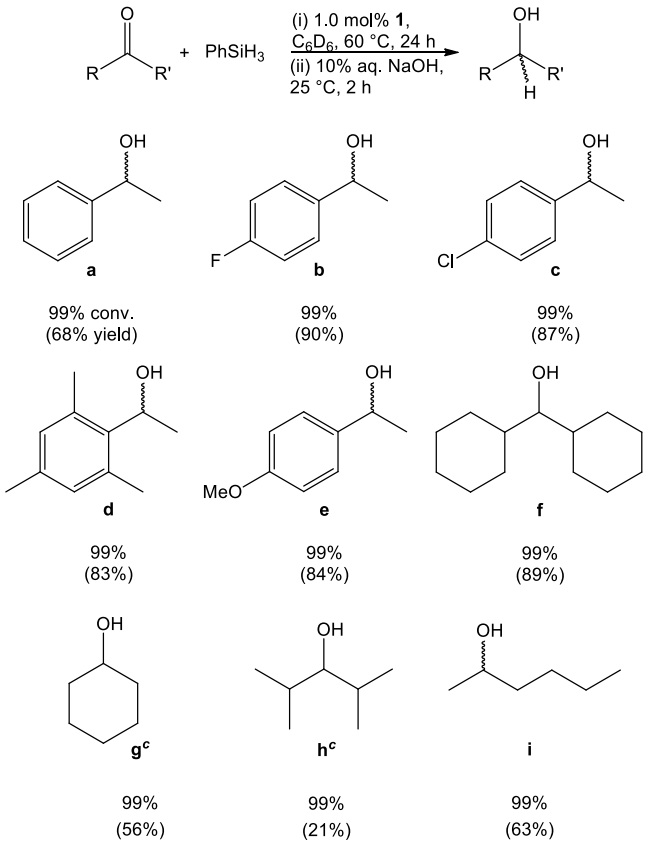

[a] Percent conversion determined by ^1H NMR spectroscopy (TOF = 4 h^{-1} for all substrates). [b]Isolated yields of the corresponding alcohol in parentheses. [c]This substrate was previously converted to a mixture of silyl ethers using 5.0 mol% **1** and $PhSiH_3$.[23]

2.6 Mechanism

It is proposed that catalysts **1**-**3** operate *via* a modified Ojima mechanism,[89] where the phosphine arms are displaced to allow for silane coordination and oxidative addition. The substrate is then inserted into the Ni-H bond, followed by rapid reductive elimination to form a silyl ether.

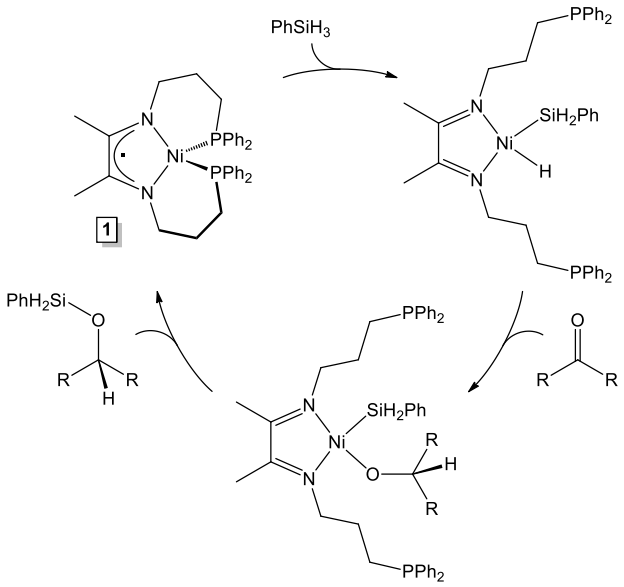

Fig. 2.10 Proposed modified Ojima mechanism for **1**-mediated carbonyl hydrosilylation.

During the course of catalysis, several clues to the mechanism have been noted. First, addition of an aldehyde or ketone directly to the catalyst elicits no changes. However, addition of 100 equivalents of $PhSiH_3$ to **1** results in conversion to coupled silanes. ^{29}Si NMR revealed the presence of two coupled silanes in appreciable quantity, (PhH_2SiSiH_2Ph (-61.50 ppm)[90] and $(PhSiH_2)_2SiHPh$ (-58.85 ppm),[91] as well as a small amount of $(PhSiH_2)_3SiPh$ (-56.12 ppm).[91] This process is slow, with 35% conversion being observed after 24 hours at ambient temperature.

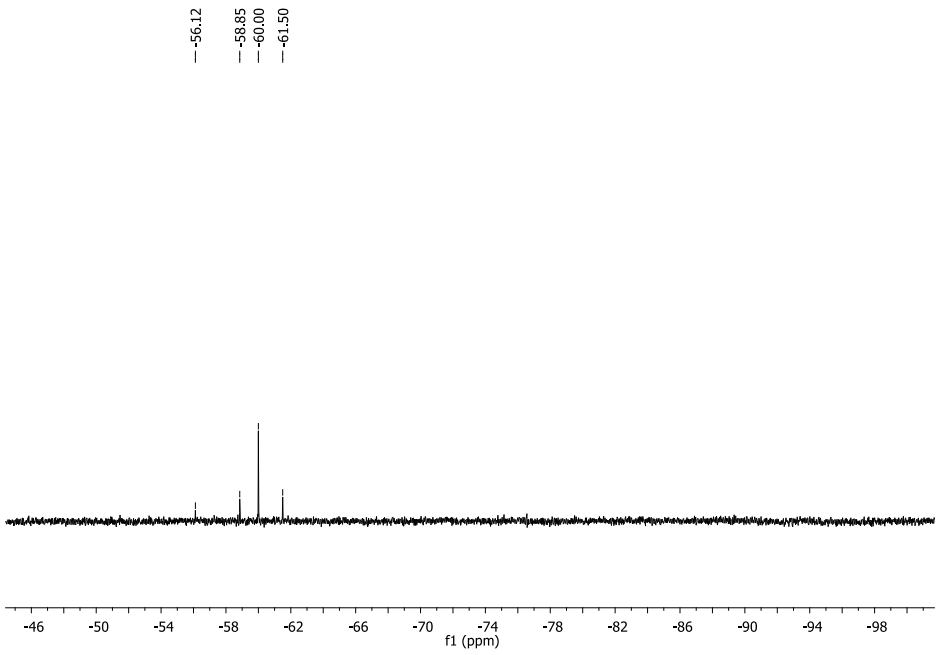

Fig. 2.11 DEPT135 ^{29}Si NMR spectrum of $PhSiH_3$ coupling using 1.0 mol% **1** in benzene-d_6.

Coupled silanes are also observable during catalysis, although no changes to the ^{31}P NMR spectrum were noted, indicating that while the Si-H oxidative addition is accessible, the resulting Ni(II) products are not persistent. In the presence of an aldehyde or ketone substrate, coordination to the metal and insertion into the Ni-H bond, followed by reductive elimination, yielding a silyl ether, is rapid.

To explain the relatively poor catalytic activity of **2** and **3** compared to **1**, the hydrosilylation of benzaldehyde with $PhSiH_3$ in the presence of 1.0 mol% **1** was carried out after the addition of 20 equivalents (relative to catalyst) of PMe_3. This exogenous phosphine significantly impacted the rate of catalysis, as it was determined there was only 3% conversion of benzaldehyde after 3 h (*via* ^{1}H NMR spectroscopy) and new signals were observed in the ^{31}P NMR spectrum.

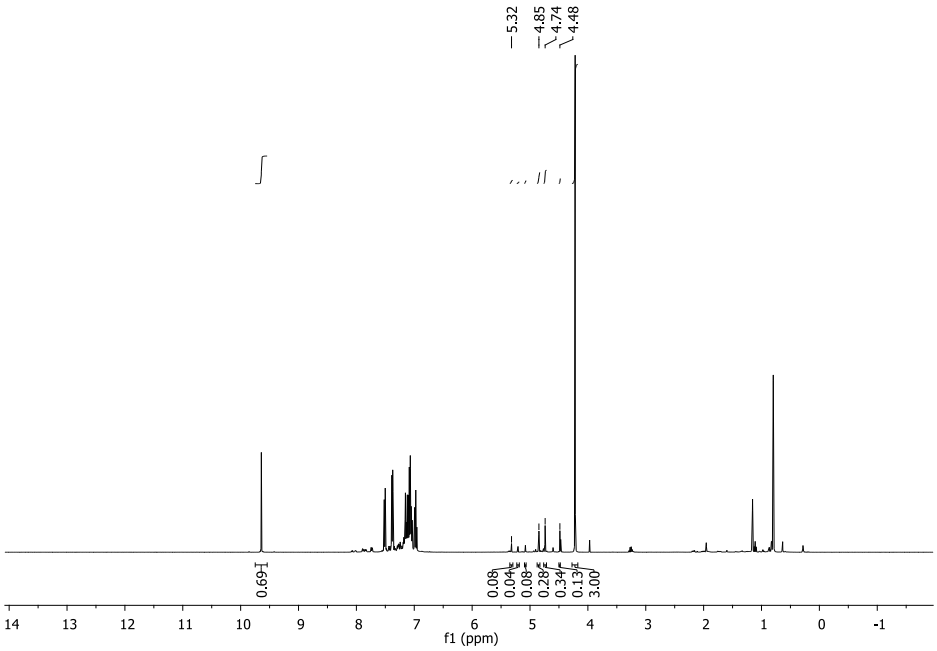

Fig. 2.12 ^{1}H NMR spectrum of attempted benzaldehyde hydrosilylation using $PhSiH_3$ and 1.0 mol% **1** in the presence of 20 mol% PMe_3 in benzene-d_6.

Addition of 2 equivalents of PMe_3 to **1** resulted in the formation of two new products after 1 h, as determined by ^{31}P NMR spectroscopy. While **1** is still present, $Ni(PMe_3)_4$ was formed as ^{Ph2PPr}DI was completely displaced. Additionally, a complex proposed to be (κ^1-*P*-^{Ph2PPr}DI)$Ni(PMe_3)_3$ was also identified.

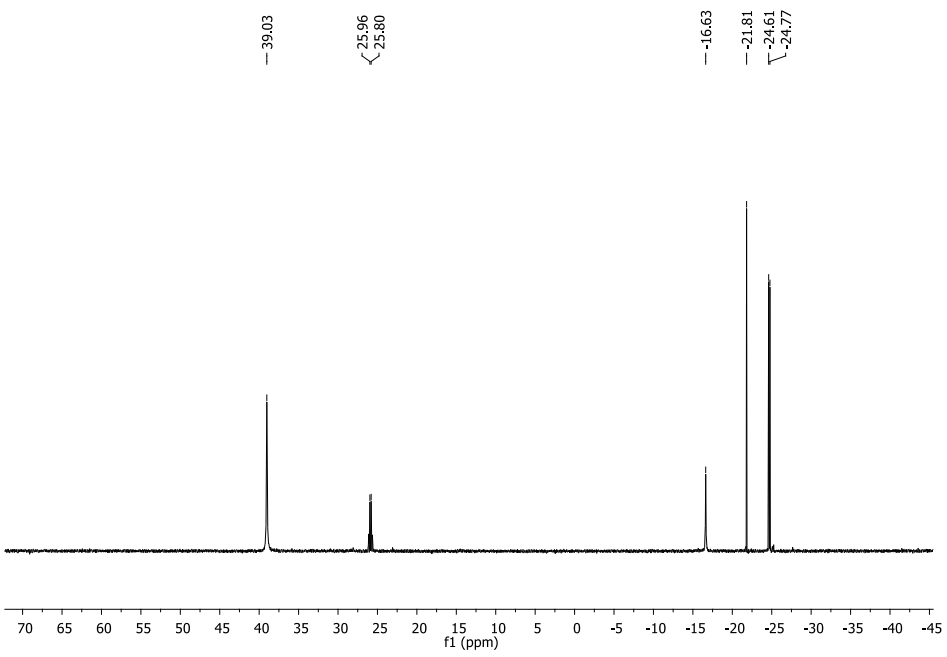

Fig. 2.13 ^{31}P NMR spectrum collected upon adding two equivalents of PMe_3 to **1** in benzene-d_6.

Given that the phosphine donor arms of ^{Ph2PPr}DI are readily displaced by a stronger σ-donating phosphine (PMe_3), it is likely that alkyl phosphines are less likely to dissociate than aryl phosphines. The Tolman Electronic Parameters (TEP),[92] which indicate σ-donating ability, dictate that P^tBu_3>P^iPr_3>PPh_3, with PMe_3 fitting in between P^iPr_3 and PPh_3. This leads credence to the proposed modified Ojima mechanism (**Fig. 2.10**), as the less strongly bound phenyl phosphine arms are more readily displaced by incoming silane to form a Ni(II) intermediate. However, to account for the superiority of catalyst **3** over **2**, which should not be the case according to the TEP, the cone angles of the phosphines must also be considered. The cone angles of the similar analogues $PEtPh_2$, PEt^iPr_2, and PEt^tBu_2 are 140°, 151°, and 165°, respectively, so catalyst **3** should experience significantly more steric repulsion between the phosphine ligands than **2**, which allows them to be more

readily displaced by substrate. This is borne out in the crystal structure data, as **3** has a much wider P-Ni-P angle of 131.35° compared to either **1** (113.58(2)°) or **2** (113.80(3)°).

2.7 Conclusion

In summary, building on the previously reported activity of (^{Ph2PPr}DI)Ni (**1**), two alkyl phosphine variants, (^{iPr2PPr}DI)Ni (**2**) and (^{tBu2PPr}DI)Ni (**3**) were synthesized. The catalytic activity of each was compared by combining benzaldehyde and $PhSiH_3$ with 1.0 mol% catalyst. After 3 h at ambient temperature, it was determined via ^{1}H NMR spectroscopy that **1** resulted in >99% conversion, **2** in 8% conversion, and **3** in 67% conversion. Using **1**, a scope of silanes was screened for benzaldehyde reduction, where it was determined that $PhSiH_3$ was the optimum silane. A scope of aldehydes was then converted to a mixture of silyl ethers using 0.1 mol% **1** within 24 h at ambient temperature, while a scope of ketones was converted to a mixture of silyl ethers using 1.0 mol% **1** within 24 h at 60 °C. Mechanistically, it was proposed that **1**-mediated carbonyl hydrosilylation follows a modified Ojima pathway. **1** is a superior catalyst than either **2** or **3** due to the weaker σ-donating ability of the phenyl phosphine ligands, allowing them to be more readily displaced by substrate during catalysis. This was confirmed through the addition of exogenous PMe_3 during a trial of benzaldehyde hydrosilylation with $PhSiH_3$ and 1.0 mol% **1**, where only 3% conversion was observed after 3 h at ambient temperature.[93]

2.8 Experimental Data

General Considerations: All reactions were performed inside an MBraun glovebox under an atmosphere of purified nitrogen. Toluene, tetrahydrofuran, diethyl ether, and pentane were purchased from Sigma-Aldrich, purified using a Pure Process Technology solvent system, and stored in the glovebox over activated 4Å molecular sieves and sodium before use. Benzene-d_6 was purchased from Cambridge Isotope Laboratories or Oakwood Chemicals and dried over 4Å molecular sieves and potassium. Celite was obtained from Acros Organics. Bis(1,5-cyclooctadiene) nickel was purchased from Strem. Benzaldehyde, *p*-tolualdehyde, *p*-methoxybenzaldehyde, furfural, cyclohexanecarboxaldehyde, *p*-chloroacetophenone, diisopropyl ketone, cyclohexanone, and 2-hexanone were sourced from Sigma Aldrich. *p*-Chlorobenzaldehyde, hexanal, decanal, cyclohex-3-enylcarbaldehyde, acetophenone, 2,4,6-trimethylacetophenone, *p*-methoxyacetophenone, dicyclohexylketone, and 2,3-butanedione were purchased from TCI America. *p*-Bromobenzaldehyde, *p*-cyanobenzaldehyde, *p*-fluoroacetophenone, and phenyl silane were purchased from Oakwood Chemicals. *p*-Fluorobenzaldehyde was obtained from Acros. All liquid substrates were dried over 4Å molecular sieves prior to use. All solid substrates were recrystallized from diethyl ether prior to use. 3-(Di-*i*-propylphosphino)-propylamine,[94] 3-(di-*t*-butylphosphino) propylamine,[94] 3-(diphenylphosphino) propylamine,[95] **^{Ph2PPr}DI**,[23] and **(^{Ph2PPr}DI)Ni**[23] were synthesized according to literature procedure.

Solution nuclear magnetic resonance (NMR) spectra were recorded at room temperature on either a Varian 400 MHz, Bruker 400 MHz, or Varian 500 MHz NMR spectrometer. All ^{1}H NMR and ^{13}C NMR chemical shifts (ppm) are reported relative to Si(Me)$_4$ using ^{1}H

(residual) and ^{13}C chemical shifts of the solvent as secondary standards. ^{31}P NMR chemical shifts (ppm) are reported relative to phosphoric acid.

X-ray Crystallography. Single crystals suitable for X-ray diffraction were coated with polyisobutylene oil in the glovebox and transferred to glass fiber with Apiezon N grease, which was then mounted on the goniometer head of a Bruker APEX Diffractometer equipped with Mo Kα radiation (Arizona State University). A hemisphere routine was used for data collection and determination of the lattice constants. The space group was identified and the data was processed using the Bruker SAINT+ program and corrected for absorption using SADABS. The structures were solved using direct methods (SHELXS) completed by subsequent Fourier synthesis and refined by full-matrix, least-squares procedures on [F^2] (SHELXL). The crystallographic data collected for compounds **2** and **3** has been deposited with The Cambridge Crystallographic Data Centre (CCDC) and assigned the numbers 1586336 and 1586337, respectively.

Preparation of ^{tBu2PPr}DI. In a glove box, a 100 mL thick-walled glass bomb was charged with 2,3-butanedione (98.9 mg, 1.15 mmol), *p*-toluenesulfonic acid (4 mg, 0.029 mmol), and 5 mL of toluene. After stirring for 5 min, 3-(di-*t*-butylphosphino)propylamine (465.0 mg, 2.31 mmol) in 5 mL toluene and 4 Å molecular sieves were added. The vessel was sealed and stirred at 90 °C for 4 days. The reaction was subsequently cooled to room temperature, filtered through a bed of Celite, and the solvent removed *in vacuo*. The resulting yellow oil was dissolved in a minimal mixture of diethyl ether and pentane and cooled to -35 °C. White crystals identified as **^{tBu2PPr}DI** were isolated in 26.2% yield (136.6 mg, 0.302 mmol). Analysis for $C_{26}H_{54}N_2P_2$: Calc. C, 68.38% H, 11.92%, N, 6.13% Found C, 68.36% H, 11.99% N, 6.01%.^1H NMR (benzene-d_6): 3.39 (t, J = 6.4 Hz, 4H),

2.09 (s, 6H), 2.02 (dd, *J* = 14.8, 7.0 Hz, 4H), 1.55 (m, 4H), 1.13 (d, *J* = 10.9 Hz, 36H). ^{13}C NMR (benzene-d_6): 168.23, 53.68 (d, *J* = 14.2 Hz), 32.40 (d, *J* = 25.8 Hz), 31.74 (d, *J* = 22.7 Hz), 30.25 (d, *J* = 13.8 Hz), 19.75 (d, *J* = 21.8 Hz). ^{31}P NMR (benzene-d_6): 26.58 (s).

Preparation of (^{iPr2PPr}DI)Ni (2). In a glove box, a 100 mL thick-walled glass bomb was charged with 2,3-butanedione (90.0 mg, 1.05 mmol), *p*-toluenesulfonic acid (4 mg, 0.029 mmol), and 5 mL of toluene. After stirring for 5 min, 3-(di-*i*-propylphosphino)propyl amine (388.0 mg, 2.21 mmol) in 5 mL toluene and 4 Å molecular sieves were added. The vessel was sealed and stirred at 70 °C for 5 d. The reaction was subsequently cooled to room temperature, filtered through a bed of Celite, and solvent removed *in vacuo*. The resulting yellow oil was dissolved in a minimal amount of toluene and added to Ni(COD)$_2$ (178.0 mg, 0.65 mmol) dissolved in 10 mL toluene in a 20 mL scintillation vial. The resulting red solution was stirred overnight, filtered through a bed of Celite, and solvent removed *in vacuo*. The red solid was dissolved in a minimal amount of diethyl ether and cooled to -35 °C. A red crystalline solid identified as **2** was isolated in 84% yield relative to Ni(COD)$_2$ (249.0 mg, 0.54 mmol). Analysis for $C_{22}H_{46}N_2P_2Ni$: Calc. C, 57.54% H, 10.10%, N, 6.10% Found C, 57.66% H, 10.45% N, 5.99%.^{1}H NMR (benzene-d_6): 2.90 (m, 1H), 2.79 (m, 1H), 2.59 (m, 1H), 2.01 (m, 1H), 1.85 (m, 2H), 1.45 (t, *J* = 6.2 Hz, 3H), 1.39 (dd, *J* = 14.6, 6.7 Hz, 3H), 1.14 (dd, *J* = 13.5, 7.2 Hz, 3H), 0.89 (t, *J* = 7.4 Hz, 3H), 0.50 (dd, *J* = 15.1, 6.7 Hz, 3H), 0.41 (m, 1H). ^{13}C NMR (benzene-d_6): 140.97, 57.01, 30.10 (d, *J* = 5.2 Hz), 30.03 (d, *J* = 5.7 Hz), 29.66 (d, *J* = 3.2 Hz), 29.56 (d, *J* = 3.8 Hz). 22.97 (d, *J* = 5.7 Hz), 22.88 (d, *J* = 5.4 Hz), 19.87 (t, *J* = 3.7 Hz), 19.63 (t, *J* = 4.9 Hz), 18.52 (t, *J* = 5.3 Hz), 17.02 (t, *J* = 2.7 Hz), 15.98 (t, *J* = 3.7 Hz), 15.35 (d, *J* = 5.6 Hz), 15.26 (d, *J* = 5.1 Hz). ^{31}P NMR (benzene-d_6): 52.33 (s).

Preparation of (^{tBu2PPr}DI)Ni (3). In a glove box, a 20 mL scintiallation vial was charged with 18.9 mg of $Ni(COD)_2$ (0.0689 mmol) and 10 mL of toluene. Recrystallized ^{tBu2PPr}DI (31.2 mg, 0.0689 mmol) in 5 mL toluene was slowly added. The solution immediately turned red and was stirred for 24 h, followed by filtration through Celite and removal of solvent *in vacuo*. The material was dissolved in a minimal quantity of diethyl ether and cooled to -35 °C. A red crystalline solid identified as **3** was isolated in 74% yield (26.3 mg, 0.0512 mmol). Analysis for $C_{26}H_{54}N_2P_2Ni$: Calc. C, 60.60% H, 10.56%, N, 5.43% Found C, 59.64% H, 10.32% N, 5.25%. ^{1}H NMR (benzene-d_6): 2.78 (m, 2H), 2.62 (m, 2H), 2.22 (m, 2H), 1.96 (m, 2H), 1.30 (d, J = 9.9 Hz, 18H), 1.21 (d, J = 9.9 Hz, 18H), 0.68 (t, J = 4.8 Hz, 6H), 0.43 (t, J = 12.0 Hz, 2H). ^{13}C NMR (benzene-d_6): 140.64 (t, J = 4.1 Hz), 55.20 (s), 30.82 (bs), 30.72 (bs), 26.12 (t, J = 7.3 Hz), 17.70 (t, J = 1.8 Hz), 16.28 (t, J = 5.8 Hz). ^{31}P NMR (benzene-d_6): 73.59 (s).

General Procedure for Hydrosilylation of Aldehydes with 0.1 mol% 1: Under inert atmosphere, a 20 mL scintillation vial was charged with approximately 0.0030 g of **1** (0.00504 mmol). Aldehyde (approx. 5.04 mmol) and $PhSiH_3$ (approx. 5.04 mmol) were combined and added to the catalyst. The resulting solution was stirred at room temperature for 24 h. Using ^{1}H NMR spectroscopy, >99% conversion was observed after 2 h (except for **Table 2.3**, entry **d**). The solution was then hydrolyzed with 2 mL of 10% aqueous NaOH and the organic product was extracted with diethyl ether (3x2 mL). The combined organic layers were dried with Na_2SO_4 and the solvent was removed *in vacuo* to isolate the alcohol.

General Procedure for Hydrosilylation of Ketones with 1.0 mol% 1: In a glove box, ketone (approx. 0.7 mmol) and $PhSiH_3$ (approx. 0.7 mmol) were added sequentially to a

20 mL scintillation vial containing **1** (approx. 4.0 mg, 0.007 mmol). The resulting red solution was dissolved in benzene-d_6, transferred into a J. Young NMR tube, and heated at 60 °C for 24 h. Conversion of >99% was observed by ^{1}H NMR spectroscopy. The solution was hydrolyzed with 1 mL of 10% $NaOH_{(aq)}$ and the organic product was extracted using Et_2O and dried over Na_2SO_4. The solvent was removed *in vacuo* and the alcohol product was isolated.

Aldehyde Hydrosilylation:

Hydrosilylation of Benzaldehyde Using 0.1 mol% 1: In a glove box, benzaldehyde (478 μL, 3.88 mmol) and $PhSiH_3$ (395 μL, 3.88 mmol) were added sequentially to a 20 mL scintillation vial containing **1** (2.3 mg, 0.00388 mmol). The resulting red solution was stirred at room temperature for 24 h. Greater than 99% conversion was observed *via* ^{1}H NMR spectroscopy. The solution was hydrolyzed with 2 mL of 10% $NaOH_{(aq)}$ and the organic product was extracted using Et_2O and dried over Na_2SO_4. The solvent was removed *in vacuo* and the product was identified as benzyl alcohol (337.8 mg, 3.12 mmol, 80.5%). ^{1}H NMR (benzene-d_6): 7.10 (m, 2H), 7.06 (m, 2H), 7.03 (m, 1H), 5.12 (s, 1H), 4.34 (s, 2H). ^{13}C NMR (benzene-d_6): 141.83, 128.95, 127.85, 127.81, 64.88.

Hydrosilylation of 4-Fluorobenzaldehyde Using 0.1 mol% 1: In a glove box, 4-fluorobenzaldehyde (378 μL, 3.53 mmol) and $PhSiH_3$ (435 μL, 3.53 mmol) were added sequentially to a 20 mL scintillation vial containing **1** (2.1 mg, 0.00353 mmol). The resulting red solution was stirred at room temperature for 24 h. Greater than 99% conversion was observed *via* ^{1}H NMR spectroscopy. The solution was hydrolyzed with 2 mL of 10% $NaOH_{(aq)}$ and the organic product was extracted using Et_2O (2x3 mL) and dried over Na_2SO_4. The solvent was removed *in vacuo* and the product was identified as 4-

fluorobenzyl alcohol (408.8 mg, 3.24 mmol, 91.9%). ^{1}H NMR (benzene-d_6): 6.93 (m, 2H), 6.79 (m, 2H), 4.18 (s, 2H), 2.37 (bs, 1H). ^{13}C NMR (benzene-d_6): 162.88 (d, J = 244.7 Hz), 137.47 (d, J = 3.1 Hz), 129.23 (d, J = 8.0 Hz), 115.67 (d, J = 21.3 Hz), 64.24.

Hydrosilylation of 4-Chlorobenzaldehyde Using 0.1 mol% 1: In a glove box, 4-chlorobenzaldehyde (371 μL, 2.64 mmol) and $PhSiH_3$ (326 μL, 2.64 mmol) were added sequentially to a 20 mL scintillation vial containing **1** (1.5 mg, 0.00264 mmol). The resulting red solution was stirred at room temperature for 24 h. Greater than 99% conversion was observed *via* ^{1}H NMR spectroscopy. The solution was hydrolyzed with 2 mL of 10% $NaOH_{(aq)}$ and the organic product was extracted using Et_2O and dried over Na_2SO_4. The solvent was removed *in vacuo* and the product was identified as 4-chlorobenzyl alcohol (273.0 mg, 1.91 mmol, 72.5%). ^{1}H NMR (benzene-d_6): 7.09 (d, J = 8.4 Hz, 2H), 6.85 (d, J = 8.4 Hz, 2H), 4.11 (s, 2H), 1.83 (s, 1H). ^{13}C NMR (benzene-d_6): 140.41, 133.58, 129.03, 128.62, 64.38.

Hydrosilylation of 4-Methylbenzaldehyde Using 0.1 mol% 1: In a glove box, 4-methylbenzaldehyde (911 μL, 7.73 mmol) and $PhSiH_3$ (952 μL, 7.73 mmol) were added sequentially to a 20 mL scintillation vial containing **1** (4.6 mg, 0.00773 mmol). The resulting red solution was stirred at room temperature for 24 h. Greater than 99% conversion was observed *via* ^{1}H NMR spectroscopy. The solution was hydrolyzed with 2 mL of 10% $NaOH_{(aq)}$ and the organic product was extracted using Et_2O and dried over Na_2SO_4. The solvent was removed *in vacuo* and the product was identified as 4-methylbenzyl alcohol (762.5 mg, 6.24 mmol, 85.3%). ^{1}H NMR (benzene-d_6): 7.14 (d, J = 7.8 Hz, 2H), 6.98 (d, J = 7.8 Hz, 2H), 4.38 (s, 2H), 2.58 (bs, 1H), 2.09 (s, 3H). ^{13}C NMR (benzene-d_6): 139.29, 137.17, 129.62, 127.61, 65.17, 21.45.

Hydrosilylation of 4-Methoxybenzaldehyde Using 0.1 mol% 1: In a glove box, 4-methoxybenzaldehyde (515 μL, 4.23 mmol) and $PhSiH_3$ (521 μL, 4.23 mmol) were added sequentially to a 20 mL scintillation vial containing **1** (2.4 mg, 0.00423 mmol). The resulting red solution was stirred at room temperature for 24 h. Greater than 99% conversion was observed *via* ^{1}H NMR spectroscopy. The solution was hydrolyzed with 2 mL of 10% $NaOH_{(aq)}$ and the organic product was extracted using Et_2O and dried over Na_2SO_4. The solvent was removed *in vacuo* and the product was identified as 4-methoxybenzyl alcohol (437.5 mg, 3.17 mmol, 74.9%). ^{1}H NMR (benzene-d_6): 7.17 (d, J = 8.4 Hz, 2H), 6.76 (d, J = 8.4 Hz, 2H), 4.44 (s, 2H), 4.39 (s, 1H), 3.35 (s, 3H). ^{13}C NMR (benzene-d_6): 159.71, 134.23, 129.18, 114.41, 64.74, 55.21.

Hydrosilylation of 4-Cyanobenzaldehyde Using 0.1 mol% 1: In a glove box, 4-cyanobenzaldehyde (859 mg, 6.55 mmol) and $PhSiH_3$ (807 μL, 6.55 mmol) were added sequentially to a 20 mL scintillation vial containing **1** (3.9 mg, 0.00655 mmol). The resulting red solution was stirred at room temperature for 24 h. Greater than 99% conversion was observed *via* ^{1}H NMR spectroscopy. The solution was hydrolyzed with 2 mL of 10% $NaOH_{(aq)}$ and the organic product was extracted using Et_2O and dried over Na_2SO_4. The solvent was removed *in vacuo* and the product was identified as 4-cyanobenzyl alcohol (413.4 mg, 3.10 mmol, 47.4%). ^{1}H NMR (benzene-d_6): 7.12 (d, J = 8.2 Hz, 2H), 7.03 (d, J = 8.2 Hz, 2H), 4.38 (s, 2H), 4.20 (s, 1H). ^{13}C NMR (benzene-d_6): 147.62, 132.57, 127.40, 119.63, 110.80, 63.91.

Hydrosilylation of Furfural Using 0.1 mol% 1: In a glove box, furfural (292 μL, 3.52 mmol) and $PhSiH_3$ (435 μL, 3.52 mmol) were added sequentially to a 20 mL scintillation vial containing **1** (2.1 mg, 0.00352 mmol). The resulting red solution was stirred at room

temperature for 24 h. Greater than 99% conversion was observed *via* ^{1}H NMR spectroscopy. The solution was hydrolyzed with 2 mL of 10% $NaOH_{(aq)}$ and the organic product was extracted using Et_2O and dried over Na_2SO_4. The solvent was removed *in vacuo* and the product was identified as furfuryl alcohol (178.2 mg, 1.81 mmol, 51.6%). ^{1}H NMR (benzene-d_6): 7.10 (m, 1H), 6.06 (m, 2H), 4.36 (s, 2H), 3.92 (s, 1H). ^{13}C NMR (benzene-d_6): 155.35, 142.72, 110.89, 108.02, 57.38.

Hydrosilylation of Cyclohexanecarboxaldehyde Using 0.1 mol% 1: In a glove box, cyclohexanecarboxaldehyde (726 μL, 5.99 mmol) and $PhSiH_3$ (739 μL, 5.99 mmol) were added sequentially to a 20 mL scintillation vial containing **1** (3.6 mg, 0.00599 mmol). The resulting red solution was stirred at room temperature for 24 h. Greater than 99% conversion was observed *via* ^{1}H NMR spectroscopy. The solution was hydrolyzed with 2 mL of 10% $NaOH_{(aq)}$ and the organic product was extracted using Et_2O and dried over Na_2SO_4. The solvent was removed *in vacuo* and the product was identified as cyclohexanemethanol (499.3 mg, 4.37 mmol, 73.0%). ^{1}H NMR (benzene-d_6): 3.18 (s, 2H), 1.64 (s, 5H), 1.25 (m, 1H), 1.11 (m, 3H), 0.80 (s, 2H), 0.69 (m, 1H). ^{13}C NMR (benzene-d_6): 68.70, 41.26, 30.54, 27.50, 26.77.

Hydrosilylation of 3-Cyclohexenecarboxaldehyde Using 0.1 mol% 1: In a glove box, 3-cyclohexenecarboxaldehyde (541 μL, 4.76 mmol) and $PhSiH_3$ (586 μL, 4.76 mmol) were added sequentially to a 20 mL scintillation vial containing **1** (2.8 mg, 0.00476 mmol). The resulting red solution was stirred at room temperature for 24 h. Greater than 99% conversion was observed *via* ^{1}H NMR spectroscopy. The solution was hydrolyzed with 2 mL of 10% $NaOH_{(aq)}$ and the organic product was extracted using Et_2O and dried over

Na_2SO_4. The solvent was removed *in vacuo* and the product was identified as 3-cyclohexene-1-methanol (431.4 mg, 3.84 mmol, 80.1%). ^{1}H NMR (benzene-d_6): 5.65 (s, 2H), 3.21 (s, 2H), 1.94 (m, 3H), 1.62 (m, 3H), 1.14 (m, 1H), 0.75 (s, 1H). ^{13}C NMR (benzene-d_6): 127.64, 126.76, 67.84, 37.05, 28.98, 26.07, 25.44.

Hydrosilylation of Hexanal Using 0.1 mol% 1: In a glove box, hexanal (682 μL, 5.54 mmol) and $PhSiH_3$ (683 μL, 5.54 mmol) were added sequentially to a 20 mL scintillation vial containing **1** (3.3 mg, 0.00554 mmol). The resulting red solution was stirred at room temperature for 24 h. Greater than 99% conversion was observed *via* ^{1}H NMR spectroscopy. The solution was hydrolyzed with 2 mL of 10% $NaOH_{(aq)}$ and the organic product was extracted using Et_2O and dried over Na_2SO_4. The solvent was removed *in vacuo* and the product was identified as hexanol (459.6 mg, 4.50 mmol, 81.2%). ^{1}H NMR (benzene-d_6): 4.04 (s, 1H), 3.55 (t, J = 6.7 Hz, 2H), 1.52 (pseudo p, J = 7.0 Hz, 2H), 1.25 (m, 6H), 0.87 (t, J = 7.0 Hz, 3H). ^{13}C NMR (benzene-d_6): 63.04, 33.49, 32.43, 26.26, 23.41, 14.64.

Hydrosilylation of Decanal Using 0.1 mol% 1: In a glove box, decanal (948 μL, 5.04 mmol) and $PhSiH_3$ (621 μL, 5.04 mmol) were added sequentially to a 20 mL scintillation vial containing **1** (3.0 mg, 0.00504 mmol). The resulting red solution was stirred at room temperature for 24 h. Greater than 99% conversion was observed *via* ^{1}H NMR spectroscopy. The solution was hydrolyzed with 2 mL of 10% $NaOH_{(aq)}$ and the organic product was extracted using Et_2O and dried over Na_2SO_4. The solvent was removed *in vacuo* and the product was identified as decanol (716 mg, 4.52 mmol, 89.8%). ^{1}H NMR (benzene-d_6): 4.29 (s, 1H), 3.46 (s, 2H), 1.49 (d, 2H), 1.24 (s, 16H), 0.87 (s, 3H). ^{13}C NMR (benzene-d_6): 62.93, 33.66, 32.86, 30.70, 30.65, 30.54, 30.34, 26.86, 23.58, 14.80.

Ketone Hydrosilylation:

Hydrosilylation of Acetophenone with 1.0 mol% 1: In a glove box, acetophenone (80.3 μL, 0.689 mmol) and $PhSiH_3$ (84.8 μL, 0.689 mmol) were added sequentially to a 20 mL scintillation vial containing **1** (4.1 mg, 0.00689 mmol). The resulting red solution was dissolved in benzene-d_6 and transferred into a J. Young NMR tube and heated at 60 °C for 24 h. Greater than 99% conversion was observed *via* ^{1}H NMR spectroscopy. The solution was hydrolyzed with 1 mL of 10% $NaOH_{(aq)}$ and the organic product was extracted using Et_2O and dried over Na_2SO_4. The solvent was removed *in vacuo* and the product was identified as 1-phenylethanol (56.8 mg, 0.465 mmol, 67.5%). ^{1}H NMR (benzene-d_6): 7.23 (d, J = 7.5 Hz, 2H), 7.14 (t, J = 7.5 Hz, 2H), 7.06 (t, J = 7.3 Hz, 1H), 4.57 (q, J = 6.5 Hz, 1H), 2.52 (s, 1H), 1.29 (d, J = 6.5 Hz, 3H). ^{13}C NMR (benzene-d_6): 147.17, 128.88, 127.66, 126.08, 70.50, 25.97.

Hydrosilylation of 4-Fluoroacetophenone with 1.0 mol% 1: In a glove box, 4-fluoroacetophenone (116 μL, 0.957 mmol) and $PhSiH_3$ (117 μL, 0.957 mmol) were added sequentially to a 20 mL scintillation vial containing **1** (5.7 mg, 0.00957 mmol). The resulting red solution was dissolved in benzene-d_6 and transferred into a J. Young NMR tube and heated at 60 °C for 24 h. Greater than 99% conversion was observed *via* ^{1}H NMR spectroscopy. The solution was hydrolyzed with 1 mL of 10% $NaOH_{(aq)}$ and the organic product was extracted using Et_2O and dried over Na_2SO_4. The solvent was removed *in vacuo* and the product was identified as 1-(4-fluorophenyl)ethanol (120.9 mg, 0.863 mmol, 90.1%). ^{1}H NMR (benzene-d_6): 7.00 (m, 2H), 6.81 (m, 2H), 4.44 (q, J = 6.5 Hz, 1H), 2.15 (s, 1H), 1.20 (d, J = 6.5 Hz, 3H). ^{13}C NMR (benzene-d_6): 162.02 (d, J = 244.2 Hz), 142.02 (d, J = 3.3 Hz), 126.92 (d, J = 7.9 Hz), 114.83 (d, J = 21.4 Hz), 69.06, 25.15.

Hydrosilylation of 4-Chloroacetophenone with 1.0 mol% 1: In a glove box, 4-chloroacetophenone (94.0 μL, 0.723 mmol) and $PhSiH_3$ (89.0 μL, 0.723 mmol) were added sequentially to a 20 mL scintillation vial containing **1** (4.3 mg, 0.00723 mmol). The resulting red solution was dissolved in benzene-d_6 and transferred into a J. Young NMR tube and heated at 60 °C for 24 h. Greater than 99% conversion was observed *via* ^{1}H NMR spectroscopy. The solution was hydrolyzed with 1 mL of 10% $NaOH_{(aq)}$ and the organic product was extracted using Et_2O and dried over Na_2SO_4. The solvent was removed *in vacuo* and the product was identified as 1-(4-chlorophenyl)ethanol (97.8 mg, 0.624 mmol, 86.5%). ^{1}H NMR (benzene-d_6): 7.11 (d, J = 8.5 Hz, 2H), 6.92 (d, J = 8.5 Hz, 2H), 4.39 (q, J = 6.5 Hz, 1H), 2.48 (s, 1H), 1.16 (d, J = 6.5 Hz, 3H). ^{13}C NMR (benzene-d_6): 145.34, 133.39, 129.01, 127.44, 69.77, 25.74.

Hydrosilylation of 2,4,6-Trimethylacetophenone with 1.0 mol% 1: In a glove box, 2,4,6-trimethylacetophenone (109.0 μL, 0.655 mmol) and $PhSiH_3$ (80.7 μL, 0.655 mmol) were added sequentially to a 20 mL scintillation vial containing **1** (3.9 mg, 0.00655 mmol). The resulting red solution was dissolved in benzene-d_6 and transferred into a J. Young NMR tube and heated at 60 °C for 24 h. Greater than 99% conversion was observed *via* ^{1}H NMR spectroscopy. The solution was hydrolyzed with 1 mL of 10% $NaOH_{(aq)}$ and the organic product was extracted using Et_2O and dried over Na_2SO_4. The solvent was removed *in vacuo* and the product was identified as 1-mesitylethanol (89.7 mg, 0.546 mmol, 83.3%). ^{1}H NMR (benzene-d_6): 6.70 (s, 2H), 5.10 (q, J = 6.7 Hz, 1H), 2.45 (s, 1H), 2.32 (s, 6H), 2.12 (s, 3H), 1.37 (d, J = 6.7 Hz, 3H). ^{13}C NMR (benzene-d_6): 138.86, 136.20, 135.95, 130.75, 130.68, 67.69, 67.56, 22.22, 22.17, 21.18, 21.13, 21.08, 21.00.

Hydrosilylation of 4-Methoxyacetophenone with 1.0 mol% 1: In a glove box, 4-methoxyacetophenone (75.7 mg, 0.504 mmol) and $PhSiH_3$ (62.1 μL, 0.504 mmol) were added sequentially to a 20 mL scintillation vial containing **1** (3.0 mg, 0.00504 mmol). The resulting red solution was dissolved in benzene-d_6 and transferred into a J. Young NMR tube and heated at 60 °C for 24 h. Greater than 99% conversion was observed *via* ^{1}H NMR spectroscopy. The solution was hydrolyzed with 1 mL of 10% $NaOH_{(aq)}$ and the organic product was extracted using Et_2O and dried over Na_2SO_4. The solvent was removed *in vacuo* and the product was identified as 1-(4-methoxyphenyl)ethanol (64.1 mg, 0.421 mmol, 83.6%). ^{1}H NMR (benzene-d_6): 7.19 (d, J = 8.3 Hz, 2H), 6.78 (d, J = 8.3 Hz, 2H), 4.65 (q, J = 6.1 Hz, 1H), 3.34 (s, 3H), 2.78 (s, 1H), 1.36 (d, J = 6.3 Hz, 3H). ^{13}C NMR (benzene-d_6): 159.66, 139.36, 127.36, 114.36, 70.17, 70.09, 55.21, 55.17, 26.02, 25.97.

Hydrosilylation of Dicyclohexyl Ketone with 1.0 mol% 1: In a glove box, dicyclohexylketone (125.8 μL, 0.638 mmol) and $PhSiH_3$ (78.7 μL, 0.638 mmol) were added sequentially to a 20 mL scintillation vial containing **1** (3.8 mg, 0.00638 mmol). The resulting red solution was dissolved in benzene-d_6 and transferred into a J. Young NMR tube and heated at 60 °C for 24 h. Greater than 99% conversion was observed *via* ^{1}H NMR spectroscopy. The solution was hydrolyzed with 1 mL of 10% $NaOH_{(aq)}$ and the organic product was extracted using Et_2O and dried over Na_2SO_4. The solvent was removed *in vacuo* and the product was identified as dicyclohexylmethanol (111.5 mg, 0.568 mmol, 89.0%). ^{1}H NMR (benzene-d_6): 2.91 (t, J = 5.5 Hz, 1H), 1.84 (d, J = 12.6 Hz, 2H), 1.74 (dd, J = 16.7, 7.1 Hz, 4H), 1.64 (dd, J = 6.8, 3.5 Hz, 2H), 1.49 (d, J = 12.5 Hz, 2H), 1.36 (m, 3H), 1.10 (m, 9H). ^{13}C NMR (benzene-d_6): 80.51, 40.67, 30.72, 28.11, 27.40, 27.31, 27.03.

Hydrosilylation of Cyclohexanone with 1.0 mol% 1: In a glove box, cyclohexanone (78.3 μL, 0.756 mmol) and $PhSiH_3$ (93.2 μL, 0.756 mmol) were added sequentially to a 20 mL scintillation vial containing **1** (4.5 mg, 0.00756 mmol). The resulting red solution was dissolved in benzene-d_6 and transferred into a J. Young NMR tube and heated at 60 °C for 24 h. Greater than 99% conversion was observed *via* ^{1}H NMR spectroscopy. The solution was hydrolyzed with 1 mL of 10% $NaOH_{(aq)}$ and the organic product was extracted using Et_2O and dried over Na_2SO_4. The solvent was removed *in vacuo* and the product was identified as cyclohexanol (42.6 mg, 0.425 mmol, 56.3%). ^{1}H NMR (benzene-d_6): 3.43 (m, 1H), 1.84 (bs, 1H), 1.75 (m, 2H), 1.59 (m, 2H), 1.35 (m, 1H), 1.21 (m, 2H), 1.09 (m, 3H). ^{13}C NMR (benzene-d_6): 30.37, 36.18, 26.33, 24.89.

Hydrosilylation of 2,4-dimethyl-3-pentanone with 1.0 mol% 1: In a glove box, 2,4-dimethyl-3-pentanone (85.6 μL, 0.605 mmol) and $PhSiH_3$ (74.5 μL, 0.605 mmol) were added sequentially to a 20 mL scintillation vial containing **1** (3.6 mg, 0.00605 mmol). The resulting red solution was dissolved in benzene-d_6 and transferred into a J. Young NMR tube and heated at 60 °C for 24 h. Greater than 99% conversion was observed *via* ^{1}H NMR spectroscopy. The solution was hydrolyzed with 1 mL of 10% $NaOH_{(aq)}$ and the organic product was extracted using Et_2O and dried over Na_2SO_4. The solvent was removed *in vacuo* and the product was identified as 2,4-dimethyl-3-pentanol (0.01458 mg, 0.125 mmol, 20.7%). ^{1}H NMR (benzene-d_6): δ 2.78 (t, J = 5.8 Hz, 1H), 1.60 (dh, J = 13.2, 6.7 Hz, 2H), 0.89 (d, J = 6.7 Hz, 6H), 0.81 (d, J = 6.8 Hz, 6H). ^{13}C NMR (benzene-d_6): δ 31.21, 20.37, 17.51.

Hydrosilylation of 2-Hexanone with 1.0 mol% 1: In a glove box, 2-hexanone (89.1 μL, 0.722 mmol) and $PhSiH_3$ (89.0 μL, 0.722 mmol) were added sequentially to a 20 mL

scintillation vial containing **1** (4.3 mg, 0.00722 mmol). The resulting red solution was dissolved in benzene-d_6 and transferred into a J. Young NMR tube and heated at 60 °C for 24 h. Greater than 99% conversion was observed *via* ^{1}H NMR spectroscopy. The solution was hydrolyzed with 1 mL of 10% $NaOH_{(aq)}$ and the organic product was extracted using Et_2O and dried over Na_2SO_4. The solvent was removed *in vacuo* and the product was identified as 2-hexanol (35.7 mg, 0.349 mmol, 63.1%). ^{1}H NMR (benzene-d_6): 3.54 (h, J = 5.7 Hz, 1H), 1.23 (m, 7H), 1.02 (d, J = 6.2 Hz, 3H), 0.87 (t, J = 7.0 Hz, 3H). ^{13}C NMR (benzene-d_6): 68.12, 68.03, 39.83, 28.75, 24.12, 24.07, 23.51, 14.70.

CHAPTER THREE

CATALYTIC C-O CLEAVAGE AS A ROUTE FOR PREPARATION OF SILYL ESTERS

3.1 Abstract

With the knowledge that **1** can mediate the reduction of ketones and aldehydes with $PhSiH_3$, expanding the scope of this chemistry led to the evaluation of ester hydrosilylation. Combining ethyl acetate and $PhSiH_3$ with 1.0 mol% **1** resulted in 80% conversion to $PhSi(OEt)H_2$ and $PhSi(OEt)_2H$ at 60 °C in 24 h. While this transformation did not occur with 6 other esters, when allyl acetate was utilized, a distinctly different reaction was observed. Upon addition of allyl acetate and $PhSiH_3$ to 1.0 mol% **1**, a colour change from red to yellow and gas evolution were immediately observed. Analysis via ^1H NMR spectroscopy revealed the complete conversion of allyl acetate to a single silaneyl triester and the generation of propylene within 30 min. This process was extended to 6 other allyl esters. Due to the highly sensitive nature of the silaneyl esters, they were isolated from the catalytic mixture by reacting **1** with 1 equivalent of I_2 to form an insoluble compound, that was removed via filtration. Silaneyl triesters were subsequently isolated in good yield. While substituted allylic type substrates did not result in ester C-O cleavage, allyl phenyl ether was partially converted to a similar product, although the alkene hydrosilylation product was also observed in significant quantity. Mechanistically, it is proposed that **1** undergoes rapid oxidative addition of the allylic ester C-O bond prior to σ-bond metathesis with $PhSiH_3$ to form propylene, followed by reductive elimination of the silyl ester. Addition of excess allyl acetate to **1** resulted in the formation of a yellow, paramagnetic

compound. However, attempts to characterize this material *via* single crystal X-ray diffraction were unsuccessful.

3.2 Ethyl Acetate Dihydrosilylation

Seeking to expand on the carbonyl hydrosilylation results outlined in Chapter 2, **1** was combined with ethyl acetate and $PhSiH_3$ in benzene-d_6, with the goal of catalyzing ester dihydrosilylation. At 1.0 mol% catalyst loading, after 24 h at 60 °C, 80% conversion was observed *via* ^{1}H NMR spectroscopy. A mixture of products was formed, with a 7:3 ratio of $Ph(OEt)_2SiH$ to $Ph(OEt)SiH_2$ noted.

Scheme 3.1 Ethyl acetate dihydrosilylation using 1.0 mol% **1** at 60 °C.

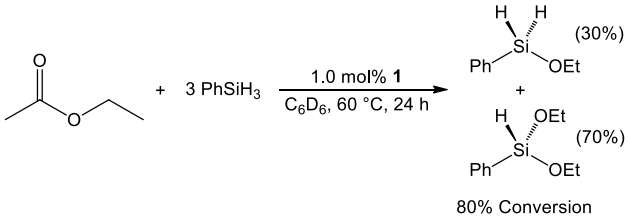

With this result in hand, a number of other esters and formates were screened to determine the scope of **1**-mediated dihydrosilylation. Unfortunately, methyl benzoate, ethyl benzoate, ethyl 4-fluorobenzoate, ethyl 4-methoxybenzoate, ethyl cinnamate, phenyl acetate, ethyl formate, and phenyl formate showed no conversion at 60 °C in 24. Increasing the temperature to 90 °C also had no effect. However, when allyl acetate and $PhSiH_3$ were combined with 1.0 mol% **1** in benzene-d_6, a colour change from red to yellow was immediately observed, followed by bubbling, indicating gas formation. Quickly transferring the solution to a J. Young style NMR tube and capping prevented all the evolved gas from escaping. After 30 min, analysis *via* ^{1}H NMR spectroscopy revealed that

there was >99% conversion of allyl acetate to propylene and a single silaneyl triester, phenylsilanetriyl triacetate.

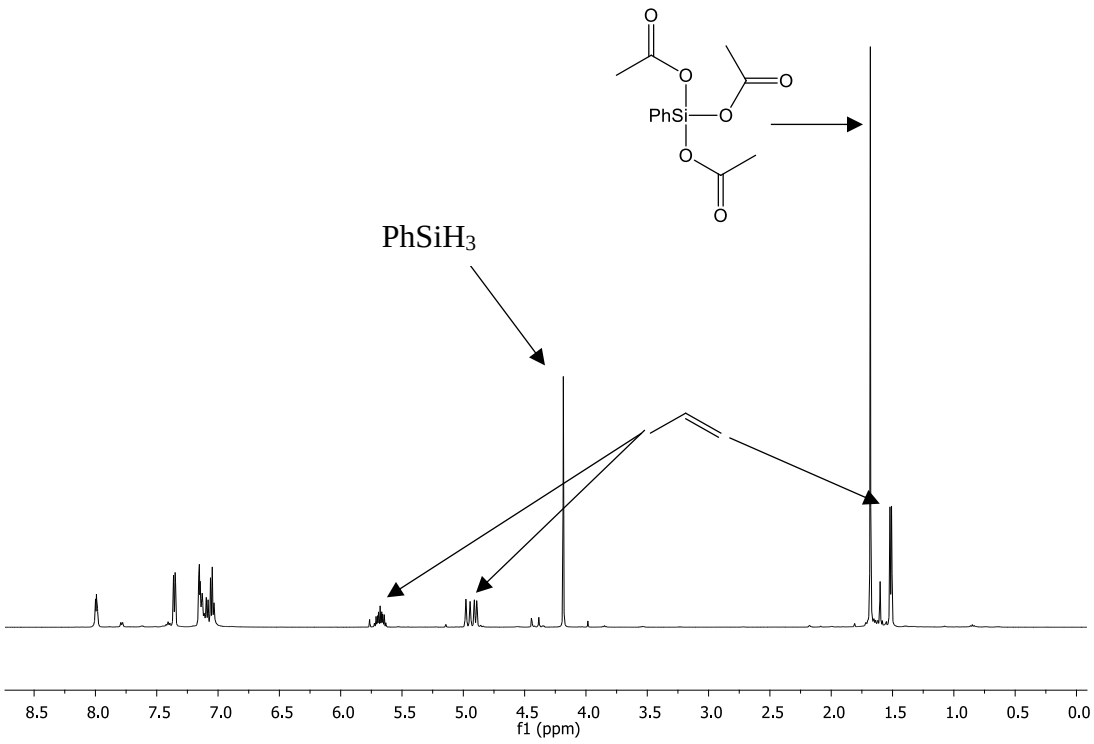

Fig. 3.1 ^{1}H NMR spectrum showing conversion of allyl acetate to propylene and phenylsilanetriyl triacetate in benzene-d_6.

3.3 Allyl Esters

With this alternate C-O ester cleavage pathway identified for allyl acetate, optimization of the reaction conditions was undertaken. First, an atom efficient experiment with a 3:1 ratio of allyl acetate to $PhSiH_3$ was performed. With 1.0 mol% **1** in benzene-d_6, >99% conversion was observed *via* ^{1}H NMR spectroscopy in 1 h. Second, the catalyst loading was lowered to 0.1 mol% to maximize the turnover frequency (TOF). In a neat solution of allyl acetate and $PhSiH_3$, 0.1 mol% **1** was able to efficiently generate phenylsilanetriyl triacetate in 1 h. With these optimized conditions, a scope of allyl esters was performed

(**Table 3.1**). A further 6 esters were converted to silaneyl triesters with TOFs of up to 990 h^{-1}, which is the highest reported for any catalyst for this transformation. The entries in **Table 3.1** are believed to be the first known examples of tricarboxysilane synthesis via ester C-O bond hydrosilylation.[27]

Table 3.1 Hydrosilylation of allyl esters using 1.0 mol% **1** and $PhSiH_3$ at 25 °C.[a,b]

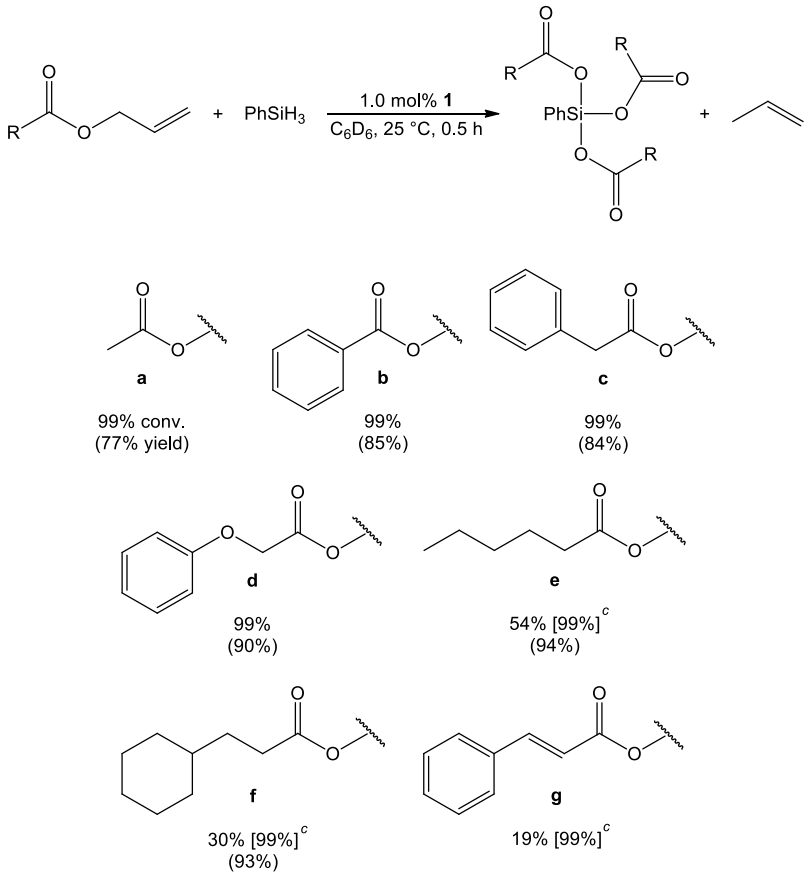

[a]Percent conversion determined by ^{1}H NMR spectroscopy. [b]Yield in parenthesis of isolated tricarboxyphenylsilane. [c]Determined after 3 h.

While generating the silaneyl ester products was straightforward, isolation of these materials proved more problematic, as they are extremely prone to hydrolysis, with the parent carboxylic acid forming in air within minutes. Even filtration through Celite under an inert atmosphere resulted in decomposition. To isolate **1** from the product in solution,

one equivalent of I_2 was added, which quickly oxidatively added to **1** to generate an insoluble iodide complex, **1-I₂**. **1-I₂** could then be removed via filtration and volatile compounds were removed *in vacuo* to yield the silaneyl trimester product. Only the cinnamyl ester was not isolated using this method, as the addition of I_2 causes substrate halogenation.

The observed selectivity and activity of **1**-mediated C-O bond hydrosilylation are noteworthy. While it is common for esters to undergo dihydrosilylation to yield a mixture of silyl ethers (**Scheme 3.1**),[67,69,75,96] it has been shown that ester reduction in the presence of silane can result in the formation of silyl acetals *via* carbonyl hydrosilylation[97] or ether formation following deoxygenation.[98] Selective ester C-O bond hydrosilylation to form carboxysilanes has been observed using $Co_2(CO)_8$ as a catalyst, although this transformation required 6 h at 200 °C to achieve completion (TOFs up to 4 h^{-1}).[99] Examples of catalytic allyl ester C-O bond hydrosilylation are very rare, though propylene formation was first noted by Speier in his initial publication,[25] and are limited to Pt-catalyzed allyl acetate hydrosilylation.[100] In each of these examples, a mixture of alkene hydrosilylation and C-O cleavage products was observed due to poor catalyst selectivity.[102]

3.4 Substituted Allylic Substrates

Seeking to bridge the primary findings of Chapters 2 and 3, and to investigate the utility of **1** as a potential biomass reduction catalyst, the hydrosilylation of the aldehyde and C-O bond hydrosilylation of 5-(acetoxymethyl)furfural was investigated, a suitable biomass analogue.[102] After mixing the substrate with 2 equivalents of $PhSiH_3$ and 1.0 mol% **1** in benzene-d_6 and allowing the reaction to sit for 3 h, the ^{1}H NMR spectrum was obtained. It revealed that there was complete reduction of the aldehyde to a mixture of silyl ethers but

no evidence for C-O cleavage to a silaneyl triester was observed. Heating this mixture to 90 °C for 24 h also resulted in no conversion.

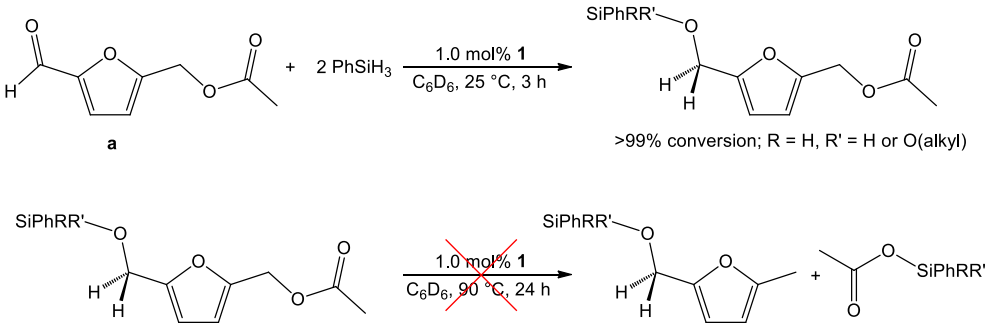

Scheme 3.2 Hydrosilylation of the carbonyl of 5-(acetoxymethyl)furfural but not the ester.

While this result was disappointing, it did not discount the possibility of cleaving other substituted allylic substrates. D-glucal triacetate, cinnamyl acetate, prenyl acetate, and *cis*-hex-2-enyl acetate were combined with $PhSiH_3$ and 1.0 mol% **1** in benzene-d_6 but no C-O cleavage hydrosilylation was observed after 24 h, either at ambient or 90 °C. This demonstrates the **1**-mediated C-O cleavage hydrosilylation is limited to α-allyl substrates.

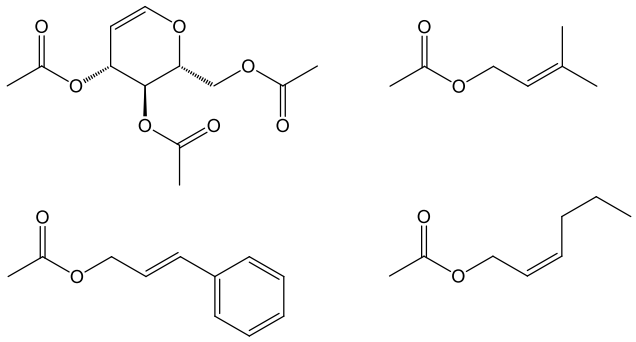

Fig. 3.2 Other allyl containing substrates that did not result in C-O cleavage hydrosilylation with 1.0 mol% **1** at 90 °C in 24 h.

3.5 Mechanism

Unlike the studies performed using ketones and aldehydes, there is a noticeable colour change during active allyl ester catalysis. Immediately upon addition of a mixture of ester and silane to **1**, there is a change from the characteristic red of **1** to pale yellow. This is proceeded by gas evolution indicating propylene formation. After catalysis is observed to be complete *via* ^{1}H NMR spectroscopy, the solution returns to red and the presence of **1** is confirmed *via* ^{31}P NMR spectroscopy.

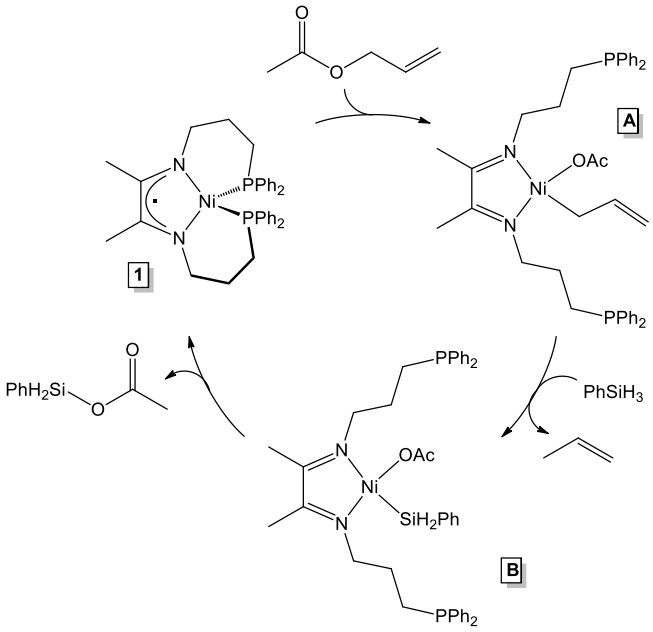

Fig. 3.3 Proposed catalytic cycle for C-O cleavage hydrosilylation of allyl esters.

To determine the identity of a catalytic intermediate, one equivalent of allyl acetate was added to **1** in toluene and let to sit for 24 h, after which time the solution had turned to pale yellow. This same result was also achieved within 1 h with the addition of 10 equivalents of allyl acetate. Characterization of this new product, proposed to be intermediate A in **Fig. 3.3**, proved challenging, as it displays no ^{1}H or ^{31}P NMR signals. Additionally, attempts to grow XRD quality crystals proved unsuccessful. This yellow compound was proven to be

a relevant intermediate, as addition of allyl acetate and $PhSiH_3$ to this compound resulted in the formation of phenylsilanetriyl triacetate, the evolution of propylene, and the reformation of **1** (as judged by ^{1}H and ^{31}P NMR spectroscopy).

3.6 Allyl Phenyl Ether

While working to expand the scope of substrates that undergo allyl C-O bond hydrosilylation, allyl phenyl ether and $PhSiH_3$ were combined with 1.0 mol% **1** in benzene-d_6 in a J. Young NMR tube. After 24 h at ambient temperature, it was determined using ^{1}H NMR spectroscopy that 39% of allyl phenyl ether was consumed, significantly slower than the observed rate for allyl esters. Interestingly, in addition to C-O cleavage products, the product of alkene hydrosilylation, $PhSiH_2((CH_2)_3OPh)$, was also observed.

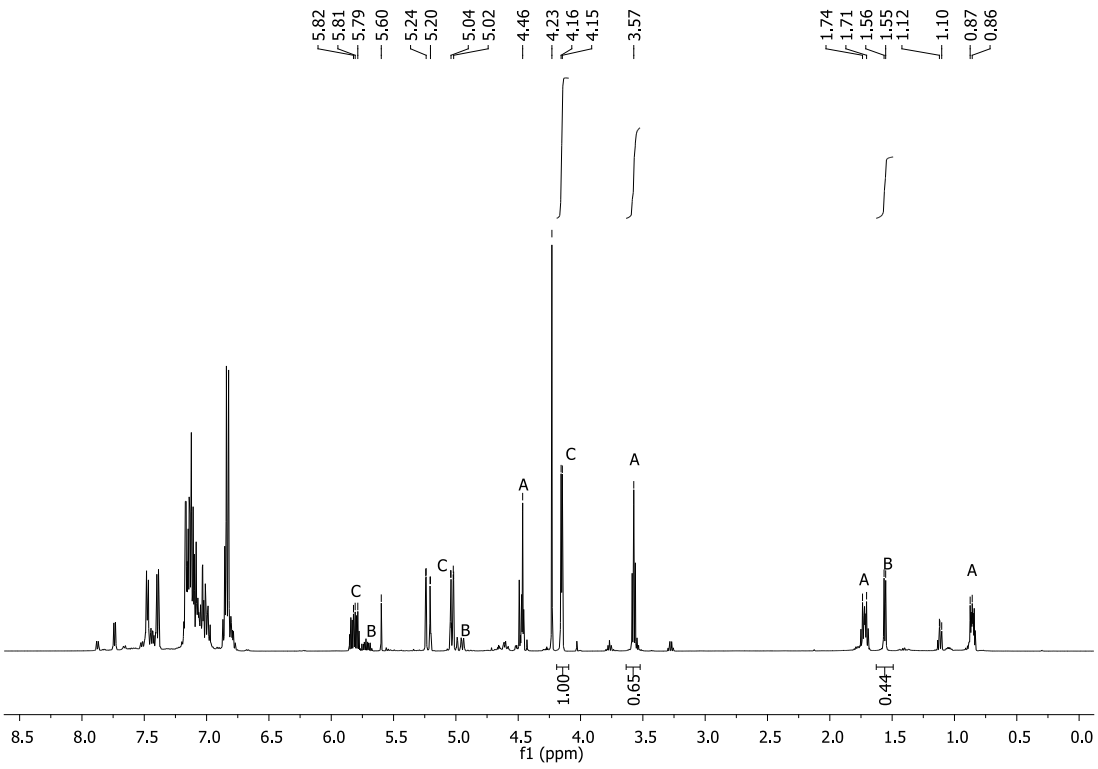

Fig. 3.4 ^{1}H NMR spectrum showing conversion of allyl phenyl ether (annotation C) with $PhSiH_3$ (s at 4.23 ppm) showing (3-phenoxypropyl)phenyl silane (A) and propylene (B).

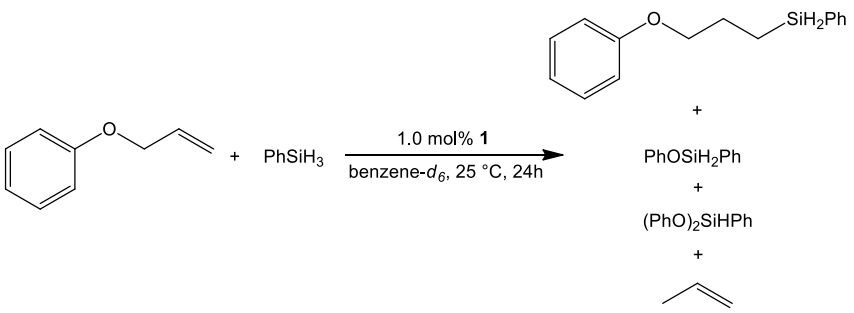

Scheme 3.3 Reaction of allyl phenyl ether with $PhSiH_3$ in the presence of **1**.

With the understanding that **1** is capable of catalyzing alkene hydrosilylation, a more in-depth investigation into this transformation was performed, as outlined in Chapter 4.

3.7 Conclusion

Evaluation of **1** as a catalyst for the dihydrosilylation of esters and formates led to the determination that while ethyl acetate could be 80% converted to a mixture of silyl ethers, most other esters and formates were unreactive. The exception is allyl esters, which underwent a different reaction pathway, with the ester C-O bond being cleaved to form a silyl ester and propylene. Combing allyl acetate and $PhSiH_3$ with 1.0 mol% **1** in benzene-d_6 resulted in the formation of a single silaneyl triester within 30 min. Isolation of these silyl esters proved challenging due to their sensitivity to hydrolysis. They were subsequently isolated from the catalyst by reacting **1** with an equivalent of I_2, producing an insoluble compound, **1-I$_2$**, that could be removed via filtration. The study of other allyl type substrates proved that **1**-mediated allyl C-O bond hydrosilylation is limited to primary

allyls. Moving to allyl ethers, the same C-O bond hydrosilylation was observed, although it was the minor product, observed along with the alkene hydrosilylation product.[93]

3.8 Experimental Details

Dihydrosilylation of Ethyl Acetate with 1.0 mol% 1: In a glove box, 90.7 µL of ethyl acetate (0.924 mmol) and 342.0 µL $PhSiH_3$ (2.77 mmol) were combined in a 20 mL scintillation vial and then added to a vial containing 5.5 mg **1** (0.00924 mmol) in 0.5 mL benzene-d_6. The red solution was then transferred into a J. Young NMR tube, sealed, and heated to 60 °C for 24 h. Analysis by ^{1}H NMR spectroscopy revealed 80% conversion of ethyl acetate to a mixture of silyl ethers.

Cleavage of Allyl Acetate Using 1.0 mol% 1: Under an inert atmosphere, allyl acetate (83.4 µL, 0.773 mmol) and $PhSiH_3$ (95.2 µL, 0.773 mmol) were combined in a 20 mL scintillation vial and then transferred to a vial containing **1** (4.6 mg, 0.00773 mmol) in 0.5 mL benzene-d_6. The red solution was transferred into a J. Young NMR tube and sealed. A color change to pale yellow was quickly observed. After 30 min, the solution returned to red and greater than 99% conversion was observed by ^{1}H NMR spectroscopy. The solution was diluted with benzene and a benzene solution containing 1 equivalent of I_2 (relative to Ni, 31.2 µL of a 0.248 M solution) was added. The mixture was allowed to sit for 1 h, after which it was filtered, and volatile compounds were removed under reduced pressure, yielding phenylsilanetriyl triacetate (55.9 mg, 0.198 mmol, 76.8%) as a dark yellow oil. ^{1}H NMR (benzene-d_6): δ 8.02 – 7.99 (m, J = 3.5 Hz, 2H), 7.19 – 7.08 (m, 3H), 1.67 (s, 9H). ^{13}C NMR (benzene-d_6): δ 169.11, 135.62, 132.70, 128.78, 127.19, 22.22.

Atom Efficient Cleavage of Allyl Acetate Using 1.0 mol% 1: Under an inert atmosphere, allyl acetate (90.6 µL, 0.840 mmol) and $PhSiH_3$ (34.5 µL, 0.280 mmol) were combined in

a 20 mL scintillation vial and then transferred to a vial containing **1** (5.0 mg, 0.00840 mmol) in 0.5 mL benzene-d_6. The red solution was transferred into a J. Young NMR tube and sealed. A color change to pale yellow was quickly observed. After 3 h, the solution returned to red and greater than 99% conversion was observed via ^{1}H NMR spectroscopy.

Cleavage of Allyl Acetate Using 0.1 mol% 1: Under an inert atmosphere, allyl acetate (0.94 mL, 8.73 mmol) and $PhSiH_3$ (1.08 mL, 8.73 mmol) were combined in a 20 mL scintillation vial and then transferred to a vial containing **1** (5.2 mg, 0.00521 mmol). A color change to pale yellow and vigorous bubbling was quickly observed. The vial was left loosely capped and after 1 h, the solution returned to red. Greater than 99% conversion was observed via ^{1}H NMR spectroscopy.

Cleavage of Allyl Benzoate Using 1.0 mol% 1: Under an inert atmosphere, allyl benzoate (93.1 µL, 0.605 mmol) and $PhSiH_3$ (75.6 µL, 0.605 mmol) were combined in a 20 mL scintillation vial and then transferred to a vial containing **1** (3.6 mg, 0.00605 mmol) in 0.5 mL benzene-d_6. The red solution was transferred into a J. Young NMR tube and sealed. A color change to pale yellow was quickly observed. After 30 min, the solution returned to red and greater than 99% conversion was observed via ^{1}H NMR spectroscopy. The solution was diluted with benzene and 1 equivalent of I_2 in benzene (relative to Ni, 24.4 µL of a 0.248 M solution) was added. The mixture was allowed to sit for 1 h, after which it was filtered, and volatile compounds were removed under reduced pressure, yielding phenylsilanetriyl tribenzoate (80.4 mg, 0.172 mmol, 85.1%) as a dark yellow oil. ^{1}H NMR (benzene-d_6): 8.27 (dd, J = 4.8, 2.3 Hz, 2H), 8.21 (d, J = 7.3 Hz, 6H), 7.14 (d, J = 6.6 Hz, 4H), 7.04 (t, J = 7.4 Hz, 3H), 6.93 (t, J = 7.7 Hz, 6H). ^{13}C NMR (benzene-d_6): δ 164.95, 135.89, 134.16, 132.83, 131.51, 131.42, 130.47, 129.06, 128.99.

Cleavage of Allyl Phenylacetate Using 1.0 mol% 1: Under an inert atmosphere, allyl phenylacetate (111.3 µL, 0.655 mmol) and $PhSiH_3$ (80.7 µL, 0.655 mmol) were combined in a 20 mL scintillation vial and then transferred to a vial containing **1** (3.9 mg, 0.00655 mmol) in 0.5 mL benzene-*d*$_6$. The red solution was transferred into a J. Young NMR tube and sealed. A color change to pale yellow was quickly observed. After 30 min, the solution returned to red and greater than 99% conversion was observed via ^{1}H NMR spectroscopy. The solution was diluted with benzene and 1 equivalent of I_2 in benzene (relative to Ni, 24.4 µL of a 0.248 M solution) was added. The mixture was allowed to sit for 1 h, after which it was filtered, and volatile compounds were removed under reduced pressure, yielding phenylsilanetriyl tris(2-phenylacetate) (94.1 mg, 0.184 mmol, 84.4%) as an off-white solid. ^{1}H NMR (benzene-*d*$_6$): δ 7.80 (d, *J* = 6.7 Hz, 2H), 7.16 – 6.99 (m, 18H), 3.41 (s, 6H). ^{13}C NMR (benzene-*d*$_6$): δ 169.66, 135.55, 134.06, 132.71, 130.18, 129.04, 128.72, 127.64, 126.58, 42.69.

Cleavage of Allyl Phenoxyacetate Using 1.0 mol% 1: Under an inert atmosphere, allyl phenoxyacetate (101.8 µL, 0.588 mmol) and $PhSiH_3$ (72.5 µL, 0.588 mmol) were combined in a 20 mL scintillation vial and then transferred to a vial containing **1** (3.5 mg, 0.00588 mmol) in 0.5 mL benzene-*d*$_6$. The red solution was transferred into a J. Young NMR tube and sealed. A color change to pale yellow was quickly observed. After 30 min, the solution returned to red and greater than 99% conversion was observed via ^{1}H NMR spectroscopy. The solution was diluted with benzene and 1 equivalent of I_2 in benzene (relative to Ni, 23.7 µL of a 0.248 M solution) was added. The mixture was allowed to sit for 1 h, after which it was filtered, and volatile compounds were removed under reduced pressure, yielding phenylsilanetriyl tris(2-phenoxyacetate) (98.1 mg, 0.176 mmol, 90%) as

an off-white solid. ^{1}H NMR (benzene-d_6): δ 7.81 (d, J = 6.8 Hz, 2H), 7.17 – 7.04 (m, 4H), 7.00 (t, J = 7.9 Hz, 6H), 6.75 (dd, J = 10.3, 4.5 Hz, 8H), 4.20 (s, 6H). ^{13}C NMR (benzene-d_6): δ 167.15, 158.38, 135.54, 133.35, 130.16, 129.01, 125.11, 122.27, 115.33, 65.59.

Cleavage of Allyl Hexanoate Using 1.0 mol% 1: Under an inert atmosphere, allyl hexanoate (118.0 µL, 0.672 mmol) and $PhSiH_3$ (83.0 µL, 0.672 mmol) were combined in a 20 mL scintillation vial and then transferred to a vial containing **1** (4.0 mg, 0.672 mmol) in 0.5 mL benzene-d_6. The red solution was transferred into a J. Young NMR tube and sealed. A color change to pale yellow was quickly observed. After 3 h, the solution returned to red and greater than 99% conversion was observed via ^{1}H NMR spectroscopy. The solution was diluted with benzene and 1 equivalent of I_2 in benzene (relative to Ni, 27.1 µL of a 0.248 M solution) was added. The mixture was allowed to sit for 1 h, after which it was filtered, and volatile compounds were removed under reduced pressure, yielding phenylsilanetriyl trihexanoate (94.8 mg, 0.210 mmol, 93.9%) as a dark yellow oil. ^{1}H NMR (benzene-d_6): δ 8.33 – 8.00 (m, 2H), 7.18 (m, 3H), 2.28 – 2.08 (m, 6H), 1.58 – 1.43 (m, 6H), 1.10 (m, 12H), 0.76 (m, 9H). ^{13}C NMR (benzene-d_6): δ 171.94, 135.68, 132.65, 128.80, 127.69, 35.98, 31.61, 24.95, 22.92, 14.37.

Cleavage of Allyl Cyclohexylpropanoate using 1.0 mol% 1: Under an inert atmosphere, allyl cyclohexylpropanoate (100.1 µL, 0.487 mmol) and $PhSiH_3$ (60.0 µL, 0.487 mmol) were combined in a 20 mL scintillation vial and then transferred to a vial containing **1** (2.9 mg, 0.00621 mmol) in 0.5 mL benzene-d_6. The red solution was transferred into a J. Young NMR tube and sealed. A color change to pale yellow was quickly observed. After 3 h, the solution returned to red and greater than 99% conversion was observed via ^{1}H NMR

spectroscopy. The solution was diluted with benzene and 1 equivalent of I_2 in benzene (relative to Ni, 19.6 µL of a 0.248 M solution) was added. The mixture was allowed to sit for 1 h, after which it was filtered, and volatile compounds were removed under reduced pressure, yielding phenylsilanetriyl tris(3-cyclohexylpropanoate) (86.3 mg, 0.151, 93.0%) as a dark yellow oil. ^{1}H NMR (benzene-d_6): δ 8.37 – 8.10 (m, 2H), 7.33 – 7.16 (m, 3H), 2.33 – 2.26 (m, 6H), 1.63 – 1.41 (m, 21H), 1.16 – 0.96 (m, 12H), 0.69 (m, 6H). ^{13}C NMR (benzene-d_6): δ 172.25, 135.71, 132.65, 128.80, 127.72, 37.50, 33.70, 33.43, 32.60, 27.17, 26.88.

Cleavage of Allyl Cinnamate Using 1.0 mol% 1: Under an inert atmosphere, allyl cinnamate (75.9 mg, 0.403 mmol) and $PhSiH_3$ (49.7 µL, 0.403 mmol) were combined in a 20 mL scintillation vial and then transferred to a vial containing **1** (2.4 mg, 0.00403 mmol) in 0.5 mL benzene-d_6. The red solution was transferred into a J. Young NMR tube and sealed. After 3 h, greater than 99% conversion was observed via ^{1}H NMR spectroscopy. Since I_2 addition was found to result in product alteration, this tricarboxyphenylsilane could not be isolated.

Hydrosilylation of 5-(acetoxymethyl)furfural with 1.0 mol% 1: Under inert atmosphere, 5-(acetoxymethyl)furfural (107.3 mg, 0.638 mmol) and $PhSiH_3$ (157.3 µL, 1.28 mmol) were added to a 20 mL scintillation vial containing **1** (3.8 mg, 0.00639 mmol) dissolved in benzene-d_6. After 3 h, greater than 99% conversion of the aldehyde to a mixture of silyl ethers was observed by ^{1}H NMR. Additional time and heating did not result in ester C-O bond hydrosilylation.

Hydrosilylation of allyl phenyl ether using 1.0 mol% 1. Under an inert atmosphere, allyl phenyl ether (85.3 µL, 0.621 mmol) and $PhSiH_3$ (76.5 µL, 0.621 mmol) were combined in

a 20 mL scintillation vial and added to a vial containing **1** (3.7 mg, 0.00621 mmol) dissolved in 0.6 mL of C_6D_6. The resulting red solution was then transferred into a J. Young NMR tube. Gas evolution was observed and after 24 h at ambient temperature, 39% conversion to (3-phenoxypropyl)phenyl silane, along with production of propylene, was observed.

CHAPTER FOUR

ANTI-MARKOVNIKOV TERMINAL AND *GEM*-OLEFIN HYDROSILYLATION

4.1 Abstract

Owing to the observation that **1** is active for alkene hydrosilylation with $PhSiH_3$ and allyl phenyl ether, optimal conditions for alkene hydrosilylation were sought. Using 1-hexene and 1.0 mol% **1**, a series of 8 silanes were screened over a period of 24 h at ambient temperature to determine the optimum reductant. It was found that only Ph_2SiH_2 results in >99% conversion to Ph_2(hexyl)SiH, with only the *anti*-Markovnikov product being observed and isolated. Additionally, adding 1-hexene and Ph_2SiH_2 to 1.0 mol% **1** at 60 °C resulted in >99% conversion within 1 h. Lowering the catalyst loading to 0.1 mol% resulted in complete conversion within 24 h at room temperature and 1 h at 60 °C under neat conditions, while a 0.01 mol% loading resulted in 89% conversion at ambient temperature within 72 h and 56% conversion within 6 h at 60 °C. Utilizing 1.0 mol% **1** and Ph_2SiH_2, 5 additional primary olefins were successfully hydrosilylated. When styrenes were investigated, there was no conversion at ambient temperature but >99% conversion was observed within 3 h at 60 °C. With a more complete understanding of the alkene hydrosilylation capabilities of **1**, allyl ether containing substrates were re-investigated. It was found that unlike allyl phenyl ether, allyl alkyl ethers did not undergo C-O cleavage, instead proceeding directly to the alkene hydrosilylation products under the same conditions as primary olefins. Additionally, vinyl phenyl ether and vinyl isobutyl ether did not undergo C-O cleavage, while the minor products when vinyl acetate was utilized were C-O cleavage products. Moving to more sterically demanding *gem*-olefins, 23% conversion of α-methylstyrene was observed with an equimolar amount of Ph_2SiH_2 and 1.0

mol% **1** after 24 h at 60 °C. Four additional days of heating resulted in only 60% conversion. A significant quantity of coupled silanes was also observed, which did not occur with primary olefins. Increasing the temperature to 90 °C resulted in 87% conversion within 24 h, although this number did not improve with additional time. The quantity of coupled silanes also increased, and the formation of the Markovnikov and quaternary silane products was observed. Subsequently, it was determined that 70 °C was the optimum temperature for catalysis, allowing for >99% conversion within 7 d. Seven additional *gem*-olefins were >99% converted under these conditions, with only the more sterically demanding 1,1-diphenyl ethene (38%) and 1,1-dicyclohexyl ethene (0%) remaining incomplete. Additionally, when 4-chloro-α-methylstyrene was combined with Ph_2SiH_2 and 1.0 mol% **1**, a significant amount of dehalogenation was observed, resulting in 69% olefin conversion with a product ratio of 3:2 of dehalogenated:halogenated hydrosilylated products. This dehalogenation was independently confirmed by combining chlorobenzene with Ph_2SiH_2 and 1.0 mol% **1**, which resulted in 67% conversion to benzene and Ph_2SiHCl after 7 d at 70 °C. It is proposed that **1** operates *via* a Chalk-Harrod alkene hydrosilylation mechanism, with alkene insertion into the Ni-H bond occurring after concurrent phosphine dissociation and silane oxidative addition. The more sterically demanding *gem*-olefins result in a slower insertion, allowing for competing silane coupling or dehalogenation pathways to occur.

4.2 1-Hexene

Given the complicated mixture of products generated in the **1** catalyzed hydrosilylation of allyl phenyl ether (**Scheme 3.3**), a simpler substrate was needed to determine the optimum conditions for **1** catalyzed alkene hydrosilylation. Combining 1-hexene and 1.0 mol% **1** in benzene-d_6, as well as either $PhSiH_3$, Ph_2SiH_2, or Ph_3SiH, allowed for preliminary determination of the optimal silane for this system. Interestingly, unlike the carbonyl reactions already optimized, $PhSiH_3$ proved to be a poor reductant for alkene hydrosilylation, with only 11% conversion to the alkene hydrosilylation product noted within 24 h at ambient temperature. Additionally, there was no observed conversion with Ph_3SiH; however, >99% conversion was observed *via* ^{1}H NMR spectroscopy when Ph_2SiH_2 was utilized (TOF = 4.1 h^{-1}). Heating this same series of reactions to 60 °C revealed a similar trend, with only Ph_2SiH_2 showing >99% conversion, this time in 1 h (TOF = 99 h^{-1}).

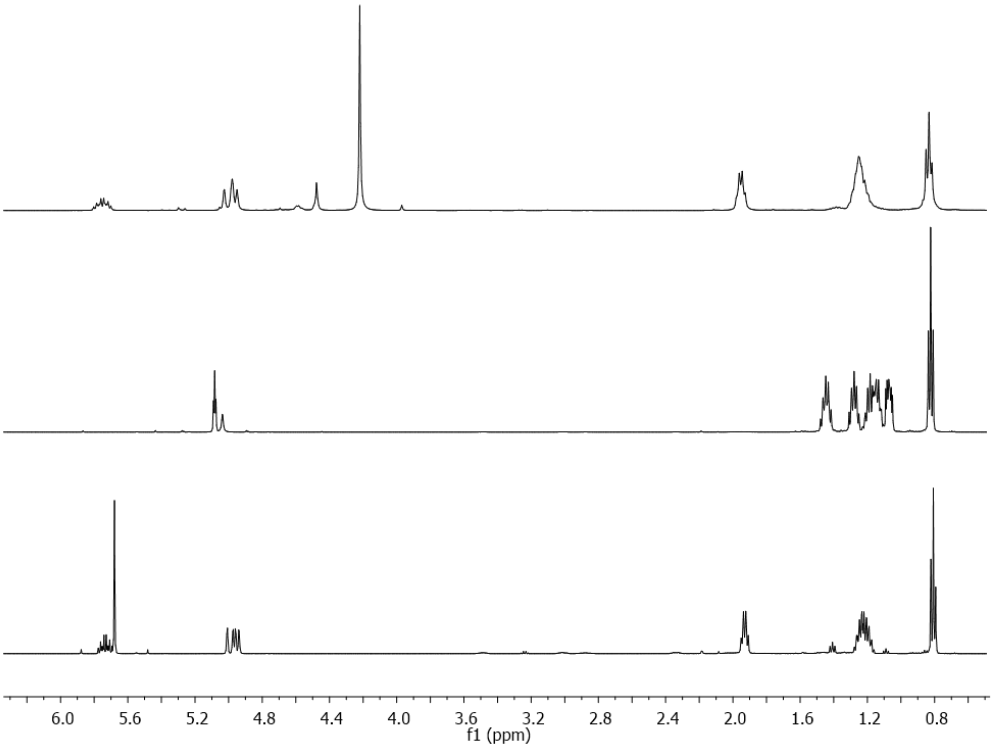

Fig. 4.1 ^{1}H NMR spectra showing **1** catalyzed 1-hexene hydrosilylation with $PhSiH_3$ (top, 11% conversion), Ph_2SiH_2 (middle, >99% conversion), and Ph_3SiH (bottom, 0% conversion).

In both the ambient temperature and heated reactions, only a single product is observed: the *anti*-Markovnikov alkene hydrosilylation product. There is no evidence for the formation of the Markovnikov or quaternary silane products. Screening additional secondary silanes (Et_2SiH_2, $^{i}Pr_2SiH_2$, $^{t}Bu_2SiH_2$, $(TMSO)_2SiH_2$, and $(Et_2N)_2SiH_2$) revealed that only Ph_2SiH_2 facilitated >99% conversion under these reaction conditions, with only Et_2SiH_2 (21%) and $(TMSO)_2SiH_2$ (56%) showing any conversion. To determine the limit of reactivity of **1**, the catalyst loading was first lowered to 0.1 mol%, with >99% conversion being observed in 24 h at ambient temperature (TOF 41 h^{-1}) or 1 h at 60 °C (TOF 990 h^{-1}) under neat conditions. Further lowering of the loading to 0.01 mol% **1** resulted in 89%

conversion in 72 h (TOF 124 h^{-1}) at ambient temperature and 58% conversion within 6 h at 60 °C (TOF 967 h^{-1}).

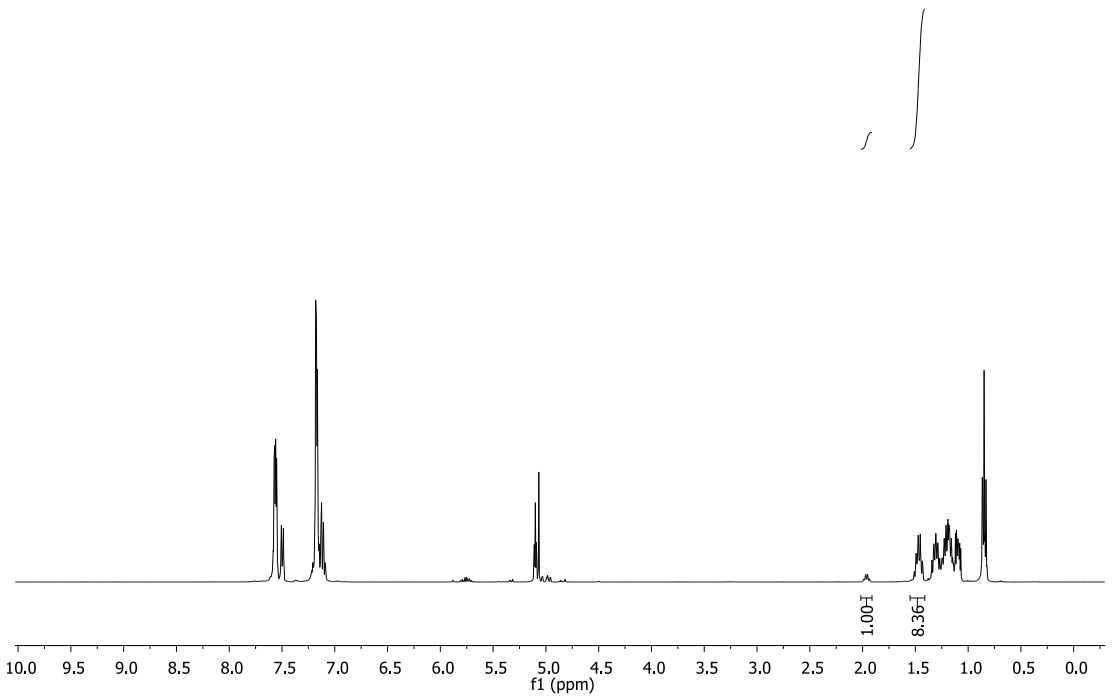

Fig. 4.2 ^{1}H NMR spectrum showing conversion of 1-hexene to Ph_2(hexyl)SiH with 0.01 mol% **1** at ambient temperature after 72 h.

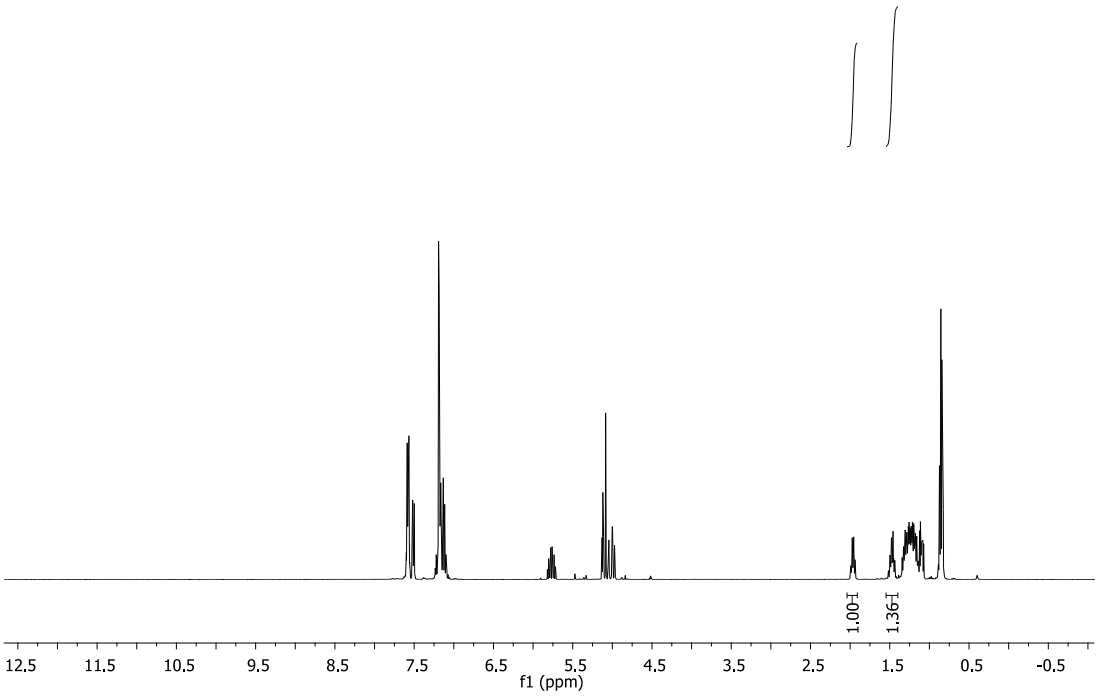

Fig. 4.3 ^{1}H NMR spectrum showing conversion of 1-hexene to Ph_2(hexyl)SiH with 0.01 mol% **1** at 60 °C after 6 h.

Owing to the long relaxation time inherent in ^{29}Si NMR, spectra for this nucleus were obtained using a DEPT135 experiment with a one bond coupling constant of 260 Hz, allowing for fast observation of Si-H resonances. Quaternary silanes were observed using the same experiment but with an 8 Hz one bond coupling constant. Standard ^{29}Si NMR were run with a relaxation delay of 30 seconds, which allowed for observation of multiple ^{29}Si environments. This experiment was only necessary for the hydrosilylated products of allyl trimethylsilane and allyl trimethylsilyl ether.

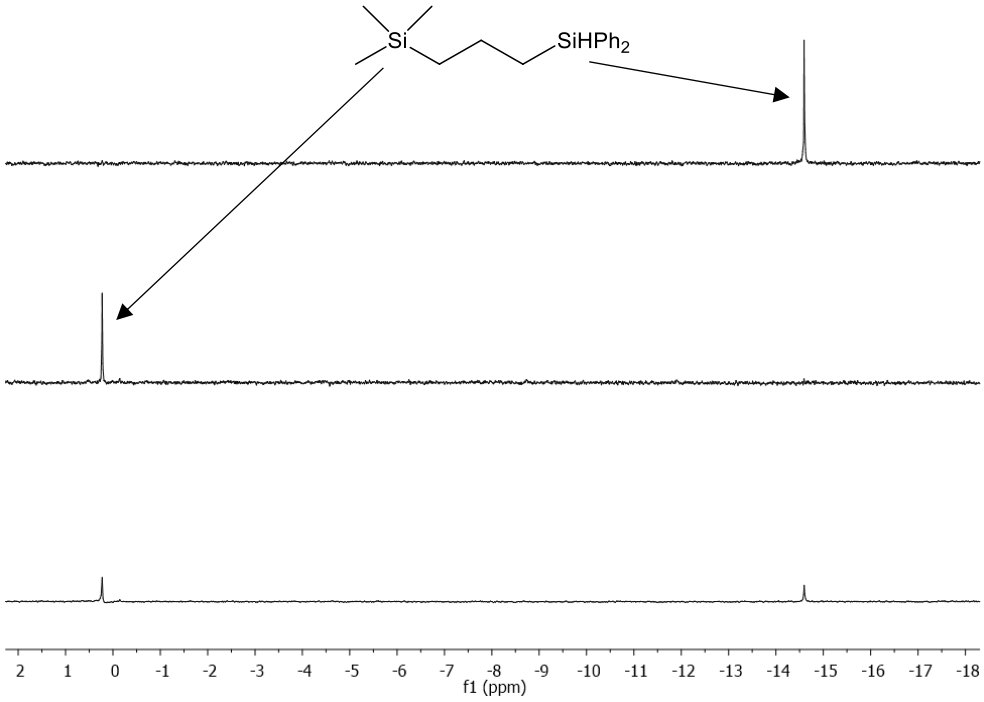

Fig. 4.4 ^{29}Si NMR spectra showing (3-(diphenylsilyl)propyl)trimethylsilane in benzene-d_6 as DEPT135 with a one bond coupling constant of 260 Hz (top), 8 Hz (middle), and a standard ^{29}Si with a 30 second relaxation delay.

4.3 Alkene Scope

With the optimized conditions for **1** catalyzed alkene hydrosilylation in hand, a scope of primary olefins was sought. Sterically un-encumbered alkenes 4-methyl-1-pentene, 1-tridecene, allyl trimethyl silane, and allyl benzene were all converted efficiently. The slightly bulkier vinyl cyclohexane was successfully hydrosilylated but the even bulkier vinyl trimethylsilane was not. Additionally, methyl acrylate, 6-chloro-1-hexene, 6-bromo-1-hexene, and 3,3,4,4,5,5,6,6,6-nonafluoro-1-hexene did not proceed to the alkene hydrosilylation products, with the halogenated substrates likely undergoing a dehalogenation deactivation reaction. Styrene proved unreactive at room temperature, while heating to 60 °C did result in conversion to the *anti*-Markovnikov product at a

slightly longer reaction time (3 h). Fluoro and chloro substituents on the aryl rings did not inhibit catalysis.

Table 4.1 Hydrosilylation of terminal alkenes with 1.0 mol% **1** and Ph_2SiH_2 at 25 °C.[a,b]

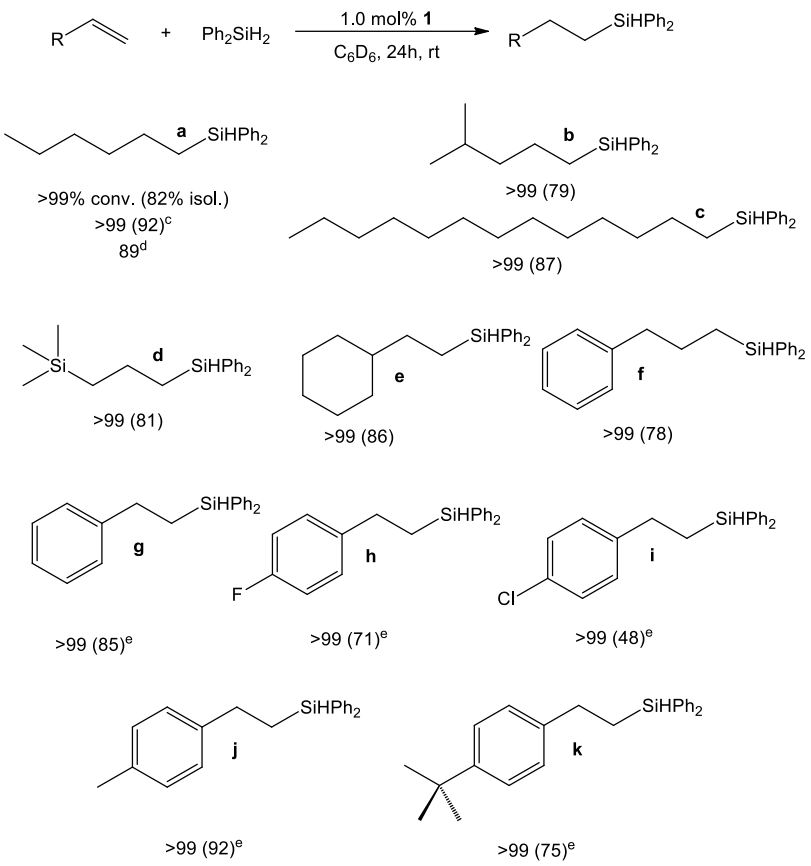

[a]Percent conversion as determined by ^{1}H NMR spectroscopy. [b]Isolated yields in parentheses. [c]Neat at 0.1 mol% **1**. [d]Neat at 0.01 mol% in 72 h. [e]3 h at 60 °C.

4.4 Allyl Ethers

With a better understanding of the alkene hydrosilylation capabilities of **1**, reinvestigation of allyl ethers was sought. While allyl phenyl ether continued to produce a mixture of products, even when Ph_2SiH_2 was utilized, allyl alkyl ethers did not undergo a similar C-O cleavage side reaction. Combining allyl alkyl ethers (**Table 4.1**, **l-q**) with Ph_2SiH_2 and 1.0 mol% **1** in benzene-d_6 resulted in >99% conversion to the *anti*-Markovnikov alkene hydrosilylation product within 24 h at ambient temperature or within 1 h at 60 °C.

Table 4.2 Hydrosilylation of allyl ethers and vinyl ether/ester with 1.0 mol% **1** and Ph_2SiH_2 at 25 °C.[a,b]

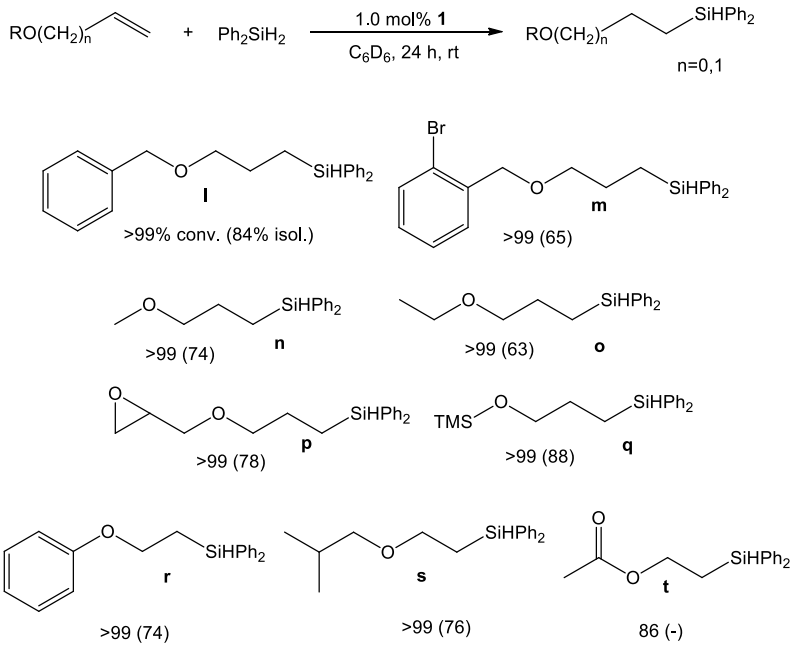

[a]Percent conversion as determined by ^{1}H NMR spectroscopy. [b]Isolated yields in parentheses.

Of note is the untouched epoxide group of allyl glycidyl ether (**p**); epoxides can be utilized for further functionalization, leading to cross-linked materials valuable for the silicone industry. Additionally, vinyl ethers **r** and **s** and vinyl acetate **t** were also investigated to determine their hydrosilylation pathway. It has previously been shown that Ni complexes capable of allyl ester cleavage are also capable of vinyl ester cleavage. However, **1**-mediated hydrosilylation of vinyl ethers proceeded to the *anti*-Markovnikov alkene hydrosilylation product only, while the *anti*-Markovnikov alkene hydrosilylation product was the primary product formed when vinyl acetate was utilized, with only a small percentage undergoing C-O cleavage hydrosilylation.

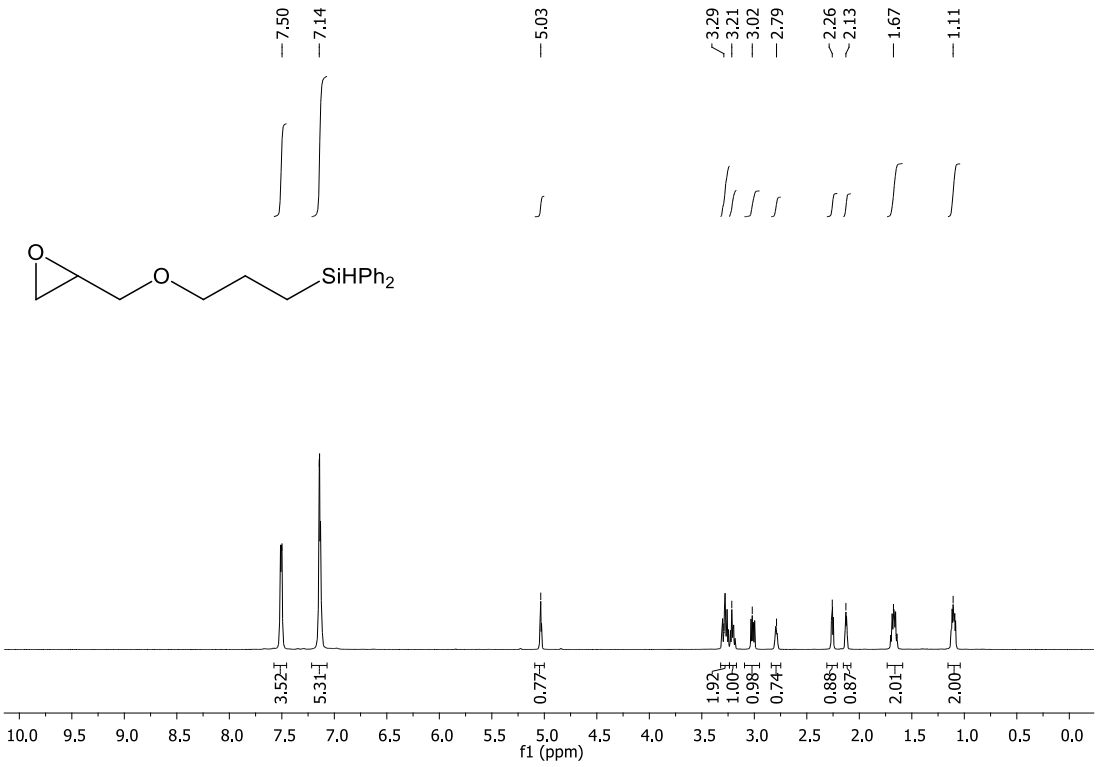

Fig. 4.5 Representative ^{1}H NMR spectrum of isolated (3-(oxiran-2-ylmethoxy)propyl) diphenyl silane in benzene-d_6.

4.5 *Gem*-Olefins

With a thorough understanding of the **1** catalyzed hydrosilylation of primary olefins, the conversion of more substituted olefins was sought. While **1** was unable to achieve the hydrosilylation of cyclohexene, it was found that there was 23% conversion of α-methylstyrene with Ph_2SiH_2 and 1.0 mol% **1** in benzene-d_6 at 60 °C in 24 h to the *anti*-Markovnikov product. Heating for an additional 4 d resulted in 60% conversion, as well as the observation of coupled silane products.[103] Repeating this trial at 90 °C resulted in 87% conversion within 24 h, although further heating did not result in increased conversion. Additionally, the elevated temperature increased the amount of coupled silanes and resulted in the formation of both the quaternary silane and Markovnikov addition products.

While there was no observation of coupled silanes in the terminal alkene hydrosilylation reactions, this result was anticipated as similar observations were noted in the ketone hydrosilylation experiments (**Fig. 2.11**). To overcome the issue of competing silane coupling, 1.25 equivalents of silane relative to substrate were utilized. To achieve >99% conversion, heating the reaction mixture to 70 °C for 7 d was required. This temperature limited the formation of coupled silanes and there was no observation of other products.

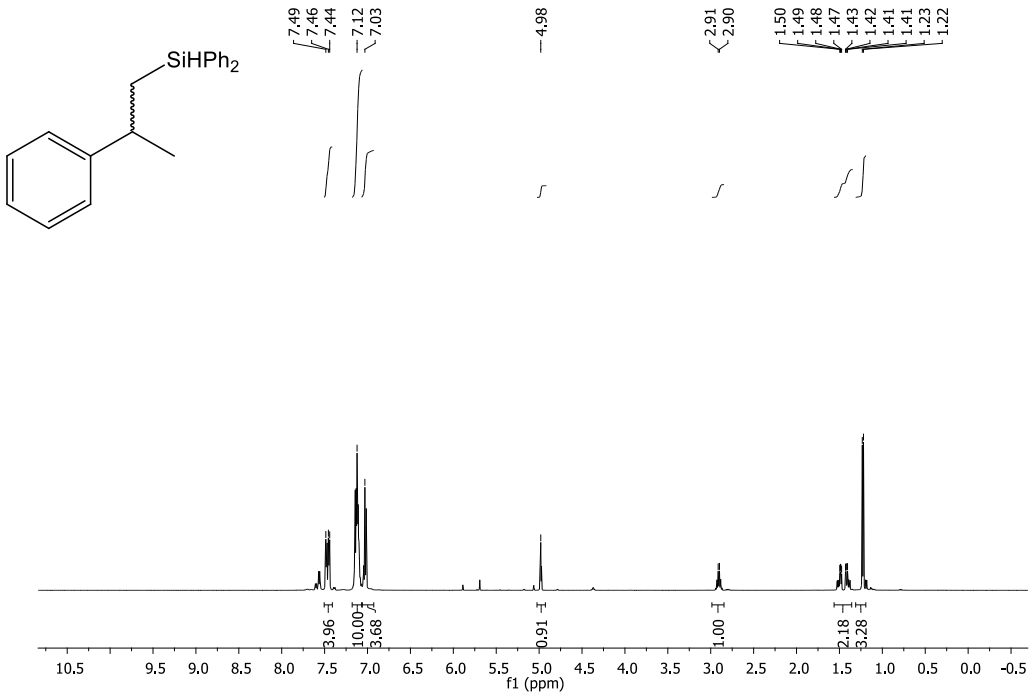

Fig. 4.6 Representative ^{1}H NMR spectrum of isolated (2-phenylpropyl) diphenyl silane in benzene-d_6.

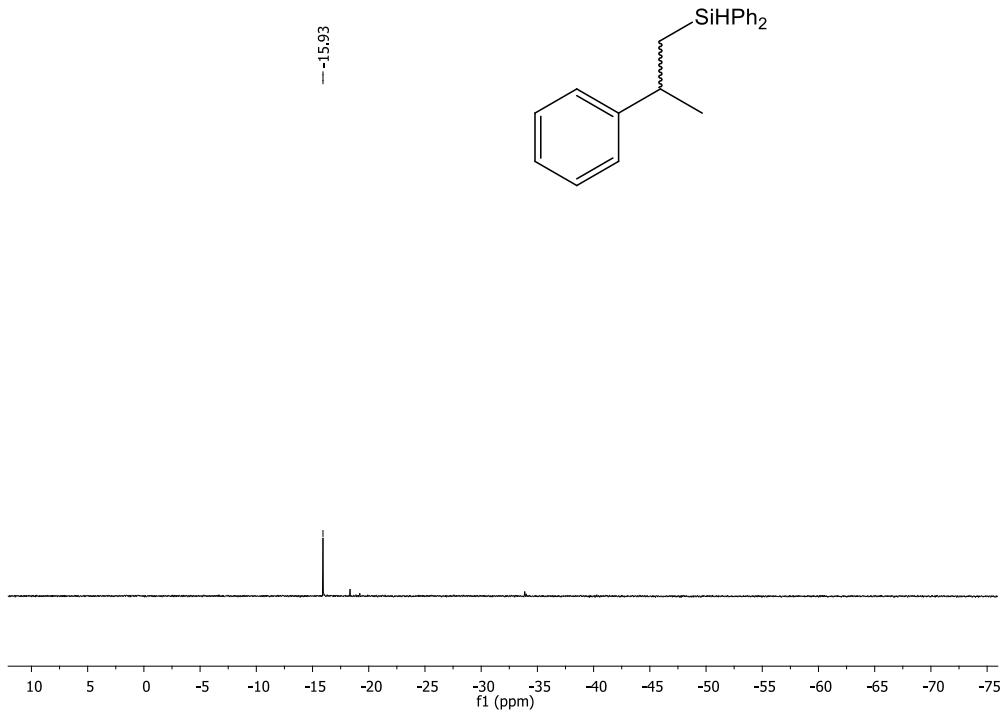

Fig. 4.7 Representative DEPT135 ^{29}Si NMR spectrum of isolated (2-phenylpropyl) diphenyl silane in benzene-d_6.

Completing a substrate scope of *gem*-olefins proved challenging, as only D-limonene and methyl methacrylate were commercially available. Fortunately, the remainder of the *gem*-olefins were readily synthesized from the parent ketone using a Wittig reaction, followed by isolation via flash column chromatography with hexanes.[104]

Scheme 4.1 Wittig synthesis of 4-fluoro-α-methylstyrene from 4-fluoroacetophenone.

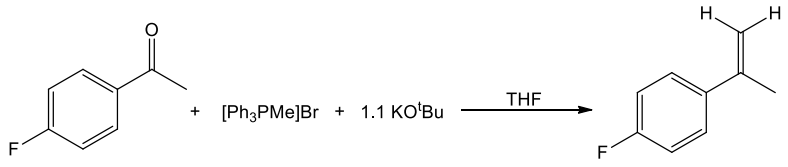

Using **1**, 4 additional α-methylstyrenes (**Table 4.3**, **v**, **x**-**z**) were successfully hydrosilylated and the racemic *anti*-Markovnikov products were isolated in good yield. An exception is

4-chloro-α-methylstyrene (**w**), which underwent partial dehalogenation prior to olefin hydrosilylation. At the end of 7 d, 69% of the olefin had been hydrosilylated, yielding a 3:2 ratio of (2-phenylpropyl) diphenyl silane to (2-(4-chlorophenyl)propyl) diphenyl silane. Primary silane products were also derived from D-limonene (**bb**), methyl methacrylate (**cc**), and 2-methyl-1-octene (**dd**). The more sterically demanding 1,1-diphenyl ethene (**aa**) and 1,1-dicyclohexyl ethene (**ee**) were significantly less reactive, with 1,1-diphenyl ethene reaching 38% conversion in 7 d at 70 °C, while 1,1-dicyclohexyl ethene did not convert at all.

Table 4.3 Hydrosilylation of *gem*-olefins with 1.0 mol% **1** and Ph_2SiH_2 at 70 °C.[a,b]

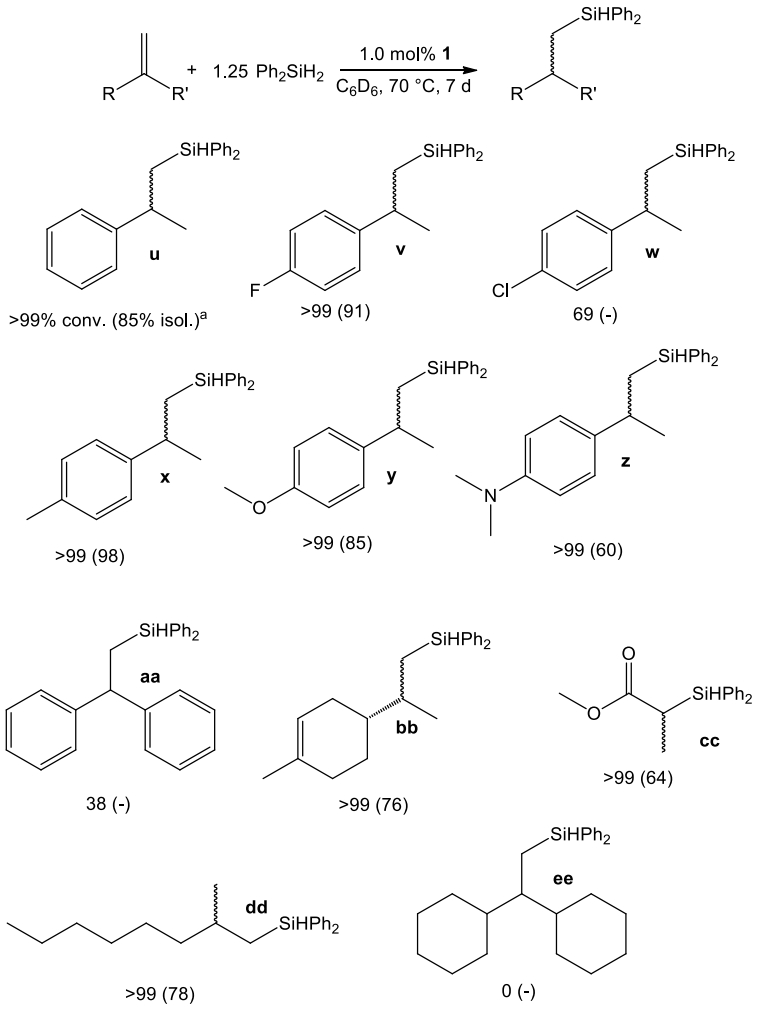

[a]Percent conversion as determined by ^{1}H NMR spectroscopy. [b]Isolated yields in parentheses.

Literature examples of nickel catalyzed *gem*-olefin hydrosilylation are rare. Kumada and coworkers reported low yields and optical purity for asymmetric α-methylstyrene, 2,3-dimethyl-1-butene, and 2-methyl-1-butene hydrosilylation using [(*R*)-$(PhCH_2)MePhP]_2NiCl_2$.[105] Hu and coworkers found that 1.0 mol% $(MeN_2N)Ni(OMe)$ (**Fig. 1.9**, **d**) mediates 2-methyl-1-heptene and α-methylstyrene hydrosilylation using Ph_2SiH_2 after 6 h at ambient temperature (TOF = 16.5 h^{-1}).[58] Two of Puerta and Valerga's (NHC)Ni(allyl) catalysts were found to mediate α-methylstyrene hydrosilylation at 60 °C,

although low yields were reported.[52] Although **1** exhibits lower alkene hydrosilylation TOFs than (MeN_2N)Ni(OMe), **Table 4.3** encompasses the first substantive scope for Ni-catalyzed *gem*-olefin hydrosilylation.

4.6 Mechanism

It is proposed that **1**-mediated alkene hydrosilylation follows a Chalk-Harrod mechanism (**Fig. 4.8**), where alkene insertion into the Ni-H follows Si-H oxidative addition. From the mechanistic insights gained in Chapter 2, it was ascertained that Si-H oxidative addition occurs concurrently with dissociation of one or both phosphine arms. This Ni(II) intermediate is not persistent and is not observed *via* ^{1}H or ^{31}P NMR spectroscopy. Alkene coordination to the metal centre and subsequent insertion into Ni-H then occurs. The new alkyl silane then rapidly reductively eliminates, at which point the phosphine arms can re-coordinate to generate the pre-catalyst.

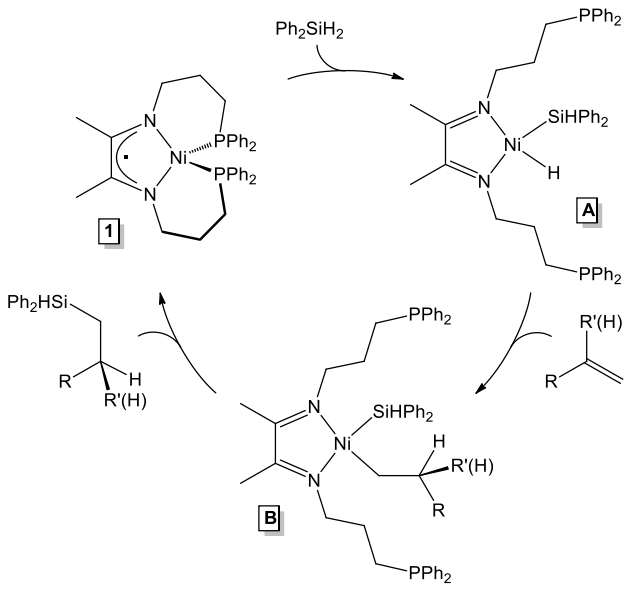

Fig. 4.8 Chalk-Harrod mechanism for **1**-mediated alkene hydrosilylation.

Several additional insights were gained through-out the alkene catalysis experiments that support the proposed mechanism. First, following the room temperature hydrosilylation of 1-hexene with Ph_2SiH_2 *via* ^{31}P NMR spectroscopy revealed only the presence of **1** during catalysis. However, upon completion of olefin hydrosilylation, a new singlet at 20.64 ppm appeared, though only in a very low percentage.

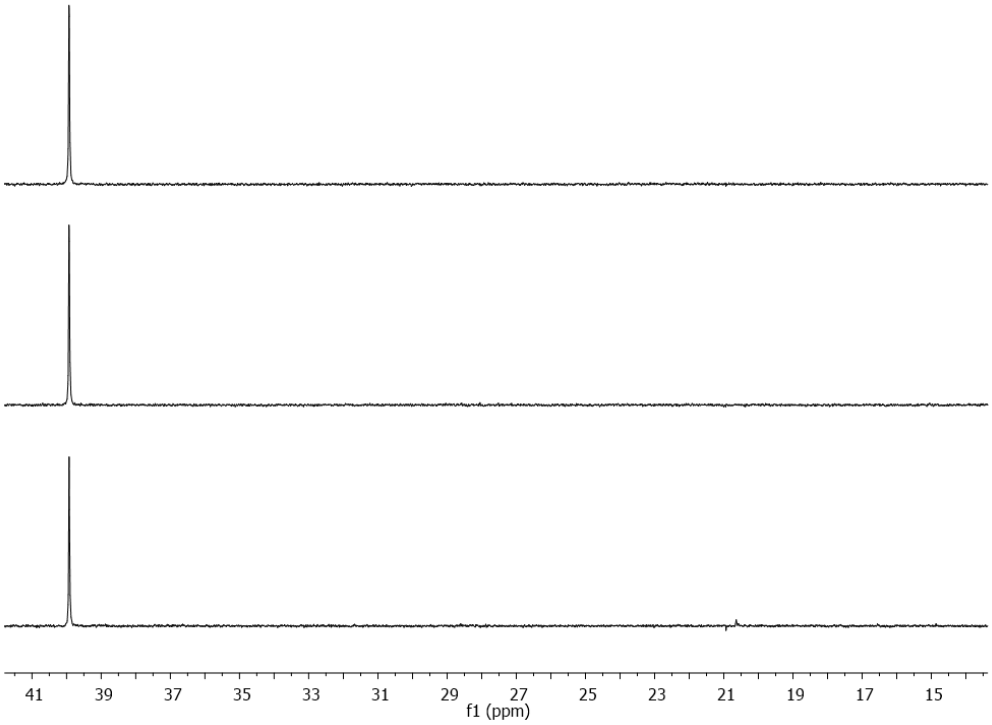

Fig. 4.9 ^{31}P NMR spectra during room temperature **1** catalyzed 1-hexene hydrosilylation with Ph_2SiH_2 after 1 h (top), 5 h (middle), and 24 h (bottom).

Second, is the observation of coupled silanes during catalytic trials featuring *gem*-olefins.[103] The more sterically demanding nature of these substrates inhibits their ability to coordinate to the metal centre, meaning that intermediate **A** more slowly reacts with alkenes than experiments featuring primary olefins. This allows for a second equivalent of silane to interact with the metal, likely involving a σ-bond metathesis step with Ni-H,

generating H_2 and a *bis*-silyl nickel species (**Fig. 4.10**, **C**). This new Ni(II) intermediate can rapidly reductively eliminate a coupled silane. Silane coupling is also observed in the absence of alkene. Addition of 1 equivalent of Ph_2SiH_2 to **1** and analysis *via* ^{31}P NMR spectroscopy resulted in observation of the same signal (20.64 ppm) as the post-alkene hydrosilylation experiments (**Fig. 4.9**), again in the same low percentage. Addition of further equivalents of silane did not result in further formation of this compound. It is proposed that this species is *trans*-(κ^4-*P*,*P*,*N*,*N*-^{Ph2PPr}DI)Ni($SiHPh_2$)$_2$ (**Fig. 4.10**, **D**), which cannot reductively eliminate a coupled silane but can lose the phosphine arms to reform intermediate **C**, which can reductively eliminate coupled silane. The *cis*-isomer of intermediate **D**, which is still capable of reductive elimination, is not observed, nor are the κ^4-versions of intermediate **A**.

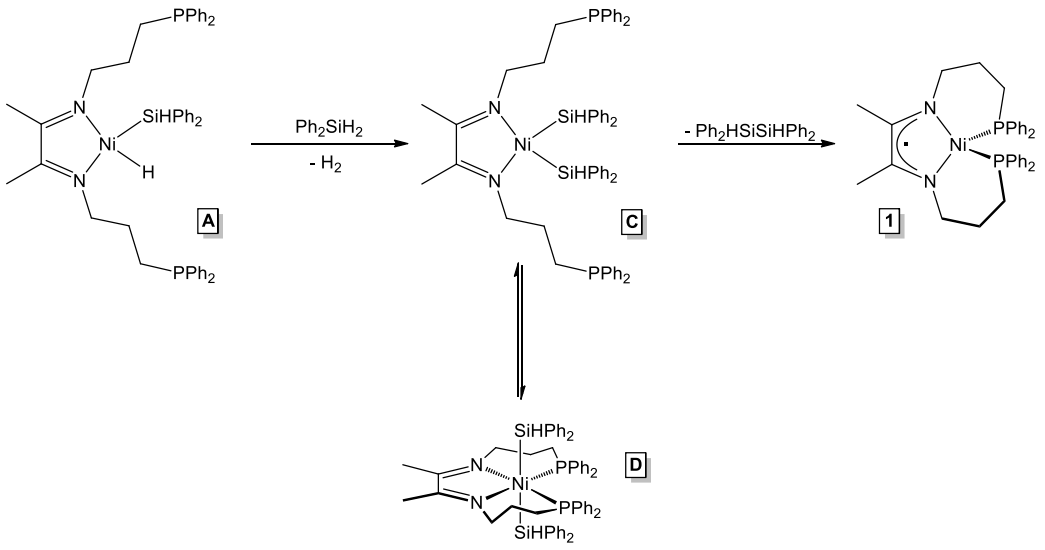

Fig. 4.10 Mechanism for generation of coupled silanes from Chalk-Harrod intermediate **A** with observable intermediate **D.**

The third important mechanistic note is the dechlorination observed with 4-chloro-α-methylstyrene, as presented in **4.7**.

4.7 Dechlorination

As noted in **4.5**, 4-chloro-α-methylstyrene produced two primary silyl products after 7 d at 70 °C; (2-phenylpropyl) diphenyl silane and (2-(4-chlorophenyl)propyl) diphenyl silane, in a ratio of 3:2. This result indicates that there is partial dechlorination of the aryl ring by **1**. To confirm that this is indeed the case, chlorobenzene and Ph_2SiH_2 were combined with 1.0 mol% **1** in toluene-d_8 and heated to 70 °C for 7 d. It was noted that 67% of the chlorobenzene was dechlorinated to benzene and a single silane product, Ph_2SiHCl (5.76 ppm in **Fig. 4.11**) was observed in the ^{1}H NMR spectrum.

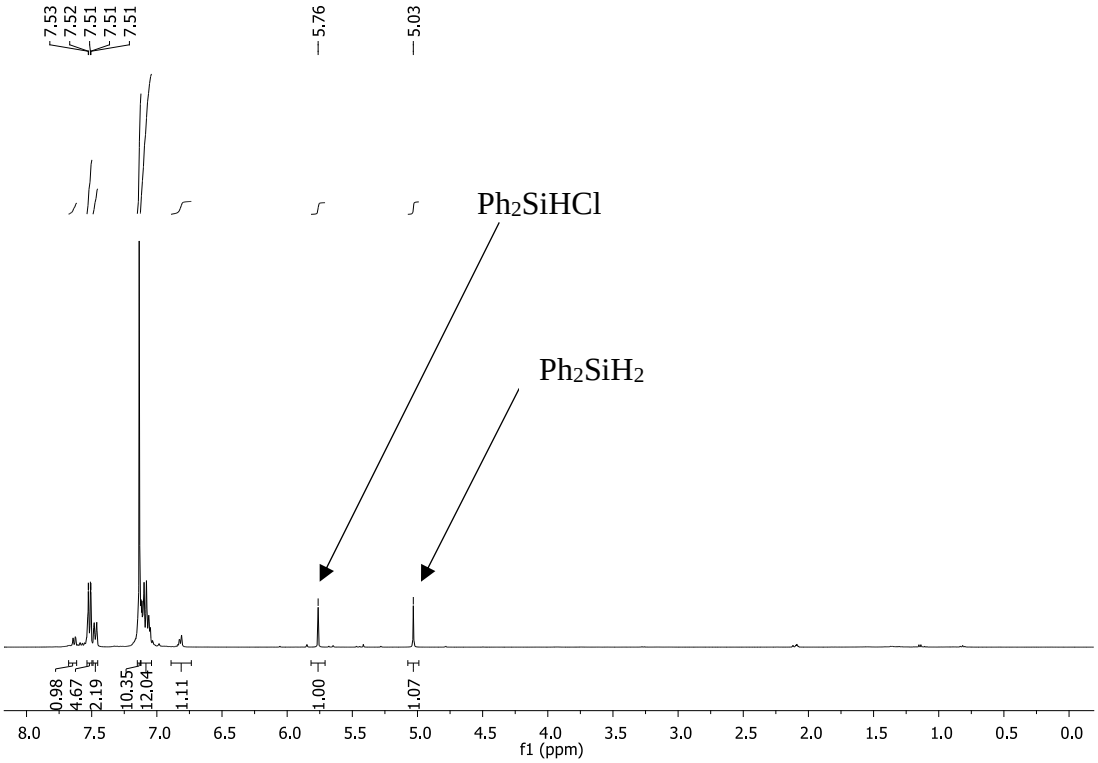

Fig. 4.11 ^{1}H NMR showing conversion of chlorobenzene to benzene and Ph_2SiHCl in toluene-d_8.

The absence of $Ph_2Si(CH_2CH(CH_3)Ph)Cl$ (and other chloroalkyl silanes) indicates that the dechlorination of 4-chloro-α-methylstyrene is occurring prior to alkene hydrosilylation. Notably, this phenomenon is not observed for other chlorinated substrates (4-chlorostyrene, 4-chlorobenzaldehyde, and 4-chloroacetophenone). This is likely due to the more sterically challenging coordination and insertion into the Ni-H bond (**Fig. 4.8**, intermediate **B**), which was noted as a side reaction leading to the formation of coupled silanes. Disfavoured insertion into the Ni-H bond allows for C-Cl oxidative addition to become competitive with Si-H oxidative addition that is the first step of the Chalk-Harrod alkene hydrosilylation mechanism. This competitive pathway results in much slower hydrosilylation of the alkene, as seen by the incomplete conversion of 4-chloro-α-methylstyrene to the mixed alkyl silane products.

4.8 Conclusion

In summary, **1** was shown to be active for the *anti*-Markovnikov hydrosilylation of primary olefins using Ph_2SiH_2, with >99% conversion being observed after 24 h at ambient temperature or after 1 h at 60 °C. Styrenes were unreactive at ambient temperature and required 3 h at 60 °C to reach >99% conversion. Previously, the hydrosilylation of allyl phenyl ether generated a mixture of products, including the alkene hydrosilylation and C-O cleavage products. However, allyl alkyl ether hydrosilylation only formed the alkene hydrosilylation product. Vinyl phenyl ether and vinyl isobutyl ether also selectively followed the alkene hydrosilylation pathway. Expanding the scope to more sterically demanding *gem*-olefins resulted in >99% conversion to the *anti*-Markovnikov hydrosilylation products after 7 d at 70 °C. Catalyst **1** also showed the ability to dehalogenate aryl halides under similar reaction conditions.[106]

4.9 Experimental Details

Hydrosilylation of 1-hexene using 1.0 mol% 1. Under an inert atmosphere, 1-hexene (105.0 µL, 0.840 mmol) and Ph_2SiH_2 (155.9 µL, 0.840 mmol) were combined in a 20 mL scintillation vial and added to a vial containing **1** (5.0 mg, 0.00840 mmol) dissolved in 0.6 mL of C_6D_6. The resulting red solution was then transferred into a J. Young NMR tube. After 24 h at ambient temperature, >99% conversion was observed *via* ^{1}H NMR spectroscopy. The reaction was then exposed to air to deactivate the catalyst, filtered through Celite, and volatile compounds were removed under reduced pressure to obtain diphenylhexyl silane in 82% yield (184.7 mg, 0.688 mmol). Diphenylhexyl silane was isolated in similar yield (84%) and quality when a mixture of 1-hexene (92.4 µL, 0.739 mmol), Ph_2SiH_2 (137.2 µL, 0.739 mmol), **1** (4.4 mg, 0.00739 mmol), and 0.6 mL C_6D_6 was heated to 60 °C for 1 h. ^{1}H NMR (benzene-d_6): 7.58 – 7.45 (m, 4H, *Ar*), 7.19 – 7.05 (m, 6H, *Ar*), 5.08 (t, *J* = 3.7 Hz, 1H, Si-*H*), 1.50 – 1.39 (m, 2H, -C*H*$_2$-), 1.33 – 1.25 (m, 2H, -C*H*$_2$-), 1.23 – 1.10 (m, 4H, -C*H*$_2$-), 1.09 – 1.04 (s, 2H, -C*H*$_2$-), 0.82 (t, *J* = 7.1 Hz, 3H, -C*H*$_3$). ^{13}C NMR (benzene-d_6): 135.89 (*Ar*), 135.35 (*Ar*), 130.15 (*Ar*), 128.69 (*Ar*), 33.60 (-*C*H$_2$-), 32.14 (-*C*H$_2$-), 25.16 (-*C*H$_2$-), 23.30 (-*C*H$_2$-), 14.67 (-*C*H$_2$-), 12.95 (-*C*H$_3$). DEPT135 ^{29}Si NMR (benzene-d_6): -13.71.

Hydrosilylation of 1-hexene using 0.1 mol% 1. Under an inert atmosphere, 1-hexene (6.3 mL, 5.04 mmol) and Ph_2SiH_2 (9.35 mL, 5.04 mmol) were combined in a 20 mL scintillation vial and added to a vial containing **1** (3.0 mg, 0.00504 mmol). The resulting red solution was then stirred for 24 h at ambient temperature, after which >99% conversion was observed *via* ^{1}H NMR spectroscopy. The reaction was then exposed to air to deactivate the

catalyst, filtered through Celite, and volatile compounds were removed under reduced pressure to obtain diphenylhexyl silane in 92% yield (1.245 g, 4.64 mmol). Diphenylhexyl silane was isolated in similar yield (90%) and quality when a mixture of 1-hexene (1.58 mL, 12.6 mmol), Ph_2SiH_2 (2.35 mL, 12.6 mmol), and **1** (7.5 mg, 0.0126 mmol) was heated to 60 °C for 1 h.

Hydrosilylation of 1-hexene using 0.01 mol% 1. Under an inert atmosphere, 1-hexene (7.17 mL, 57.1 mmol) and Ph_2SiH_2 (10.6 mL, 57.1 mmol) were added to a 100 mL round bottom flask containing **1** (3.4 mg, 0.00571 mmol). The resulting red solution was then stirred for 72 h at ambient temperature, after which 89% conversion was observed *via* ^{1}H NMR spectroscopy. Alternatively, 58% conversion was observed when a mixture of 1-hexene (1.58 mL, 12.6 mmol), Ph_2SiH_2 (2.35 mL, 12.6 mmol), and **1** (7.5 mg, 0.0126 mmol) was heated to 60 °C for 6 h.

Hydrosilylation of 4-methylpent-1-ene using 1.0 mol% 1. Under an inert atmosphere, 4-methylpent-1-ene (80.8 µL, 0.655 mmol) and Ph_2SiH_2 (121.6 µL, 0.655 mmol) were combined in a 20 mL scintillation vial and added to a vial containing **1** (3.9 mg, 0.00655 mmol) dissolved in 0.6 mL of C_6D_6. The resulting red solution was then transferred into a J. Young NMR tube. After 24 h at ambient temperature, >99% conversion was observed *via* ^{1}H NMR spectroscopy. The reaction was then exposed to air to deactivate the catalyst, filtered through Celite, and volatile compounds were removed under reduced pressure to obtain (4-methylpentyl)diphenyl silane in 79% yield (139.1 mg, 0.518 mmol). (4-Methylpentyl)diphenyl silane was isolated in similar yield (74%) and quality when a mixture of 4-methylpent-1-ene (64.3 µL, 0.521 mmol), Ph_2SiH_2 (96.7 µL, 0.521 mmol), **1** (3.1 mg, 0.00521 mmol), and 0.6 mL C_6D_6 was heated to 60 °C for 1 h. ^{1}H NMR (benzene-

d$_6$): 7.62 – 7.55 (m, 4H, *Ar*), 7.22 – 7.14 (m, 6H, *Ar*), 5.13 (t, *J* = 3.2 Hz, 1H, Si*H*), 1.56 – 1.37 (m, 3H, -C*H*$_2$-, -C*H*-), 1.23 (dd, *J* = 14.9, 7.2 Hz, 2H, -C*H*$_2$-), 1.13 – 1.05 (m, 2H, -C*H*$_2$-), 0.82 (d, *J* = 6.6 Hz, 6H, -C*H*$_3$). ^{13}C NMR (benzene-*d*$_6$): 135.88 (*Ar)*, 135.16 (*Ar)*, 130.17 (*Ar)*, 128.70 (*Ar)*, 43.20 (-*C*H$_2$-), 28.20 (-*C*H-), 23.09 (-*C*H$_3$), 22.96 (-*C*H$_2$-), 13.04 (-*C*H$_2$-). DEPT 135 ^{29}Si NMR (benzene-*d*$_6$): -13.74.

Hydrosilylation of 1-tridecene using 1.0 mol% 1. Under an inert atmosphere, 1-tridecene (104.0 µL, 0.437 mmol) and Ph_2SiH_2 (81.1 µL, 0.437 mmol) were combined in a 20 mL scintillation vial and added to a vial containing **1** (2.6 mg, 0.00437 mmol) dissolved in 0.6 mL of C_6D_6. The resulting red solution was then transferred into a J. Young NMR tube. After 24 h at ambient temperature, >99% conversion was observed *via* ^{1}H NMR spectroscopy. The reaction was then exposed to air to deactivate the catalyst, filtered through Celite, and volatile compounds were removed under reduced pressure to obtain diphenyltridecyl silane in 87% yield (123.6 mg, 0.337 mmol). Diphenyltridecyl silane was isolated in similar yield (90%) and quality when a mixture of 1-tridecene (91.9 µL, 0.386 mmol), Ph_2SiH_2 (71.7 µL, 0.386 mmol), **1** (2.3 mg, 0.00386 mmol), and 0.6 mL C_6D_6 was heated to 60 °C for 1 h. ^{1}H NMR (benzene-*d*$_6$): 7.61 – 7.53 (m, 4H, *Ar*), 7.21 – 7.14 (m, 6H, *Ar*), 5.10 (t, *J* = 3.7 Hz, 1H, Si*H*), 1.55 – 1.45 (m, 2H, -C*H*$_2$-), 1.41 – 1.19 (m, 20H, multiple -C*H*$_2$-), 1.15 – 1.08 (m, 2H, -C*H*$_2$-), 0.91 (t, *J* = 6.8 Hz, 3H, -C*H*$_3$). ^{13}C NMR (benzene-*d*$_6$): 135.90 (*Ar*), 135.35 (*Ar*), 130.15 (*Ar*), 128.69 (*Ar*), 34.00 (-*C*H$_2$-), 32.73 (-*C*H$_2$-), 30.55 (multiple -*C*H$_2$-), 30.52 (-*C*H$_2$-), 30.40 (-*C*H$_2$-), 30.21 (-*C*H$_2$-), 30.05 (-*C*H$_2$-), 25.26 (-*C*H$_2$-), 23.50 (-*C*H$_2$-), 14.76 (-*C*H$_2$-), 13.00 (-*C*H$_3$). DEPT135 ^{29}Si NMR (benzene-*d*$_6$): -13.72.

Hydrosilylation of allyl trimethylsilane using 1.0 mol% 1. Under an inert atmosphere, allyl trimethylsilane (109.0 µL, 0.689 mmol) and Ph_2SiH_2 (127.9 µL, 0.689 mmol) were combined in a 20 mL scintillation vial and added to a vial containing **1** (4.1 mg, 0.00689 mmol) dissolved in 0.3 mL of C_6D_6. The resulting red solution was then transferred into a J. Young NMR tube. After 24 h at ambient temperature, >99% conversion was observed *via* ^{1}H NMR spectroscopy. The reaction was then exposed to air to deactivate the catalyst, filtered through Celite, and volatile compounds were removed under reduced pressure to obtain (3-(diphenylsilyl)propyl)trimethyl silane in 81% yield (166.6 mg, 0.558 mmol). (3-(Diphenylsilyl)propyl)trimethyl silane was isolated in similar yield (78%) and quality when a mixture of allyl trimethylsilane (109.0 µL, 0.689 mmol), Ph_2SiH_2 (127.9 µL, 0.689 mmol), **1** (4.1 mg, 0.00689 mmol), and 0.6 mL C_6D_6 was heated to 60 °C for 1 h. ^{1}H NMR (benzene-d_6): 7.56 – 7.50 (m, 4H, *Ar*), 7.17 – 7.01 (m, 6H, *Ar*), 5.09 (t, J = 3.3 Hz, 1H, Si-*H*), 1.62 – 1.42 (m, 2H, -CH_2-), 1.16 (td, J = 7.9, 3.9 Hz, 2H, -CH_2-), 0.62 – 0.52 (m, 2H, -CH_2-), -0.12 (s, 9H, Si(CH_3)$_3$). ^{13}C NMR (benzene-d_6) 135.89 (*Ar*), 135.29 (*Ar*), 130.17 (*Ar*), 128.92 (*Ar*), 128.70 (*Ar*), 21.33 (-*C*H$_2$-), 19.88 (-*C*H$_2$-), 17.28 (-*C*H$_2$-), -1.15 (Si(*C*H$_3$)$_3$). ^{29}Si NMR (benzene-d_6): 0.23 (*Si*(CH$_3$)$_3$), -14.59 (*Si*-H).

Hydrosilylation of vinyl cyclohexane using 1.0 mol% 1. Under an inert atmosphere, vinyl cyclohexane (75.7 µL, 0.537 mmol) and Ph_2SiH_2 (99.7 µL, 0.537 mmol) were combined in a 20 mL scintillation vial and added to a vial containing **1** (3.2 mg, 0.00537 mmol) dissolved in 0.6 mL of C_6D_6. The resulting red solution was then transferred into a J. Young NMR tube. After 24 h at ambient temperature, >99% conversion was observed *via* ^{1}H NMR spectroscopy. The reaction was then exposed to air to deactivate the catalyst, filtered through Celite, and volatile compounds were removed under reduced pressure to

obtain diphenyl-(2-cyclohexyl)ethyl silane in 86% yield (136.2 mg, 0.462 mmol). Diphenyl-(2-cyclohexyl)ethyl silane was isolated in similar yield (85%) and quality when a mixture of vinyl cyclohexane (75.6 µL, 0.537 mmol), Ph_2SiH_2 (99.8 µL, 0.537 mmol), **1** (3.2 mg, 0.00537 mmol), and 0.6 mL C_6D_6 was heated to 60 °C for 1 h. ^{1}H NMR (benzene-d_6): 7.62 – 7.54 (m, 4H, *Ar*), 7.23 – 7.18 (m, 6H, *Ar*), 5.10 (t, *J* = 3.6 Hz, 1H, Si-*H*), 1.73 – 1.58 (m, 5H, -C*H*$_2$-, -C*H*-), 1.43 – 1.35 (m, 2H, -C*H*$_2$-), 1.24 – 1.04 (m, 6H, -C*H*$_2$-), 0.85 – 0.70 (m, 2H, -C*H*$_2$-). ^{13}C NMR (benzene-d_6): 135.89 (*Ar*), 135.36 (*Ar*), 130.16 (*Ar*), 128.69 (*Ar*), 41.11 (-*C*H$_2$-), 33.51 (-*C*H$_2$-), 32.63 (-*C*H-), 27.45 (-*C*H$_2$-), 27.14 (-*C*H$_2$-), 10.02 (-*C*H$_2$-). DEPT135 ^{29}Si NMR (benzene-d_6): -13.03.

Hydrosilylation of allyl benzene using 1.0 mol% 1. Under an inert atmosphere, allyl benzene (75.7 µL, 0.571 mmol) and Ph_2SiH_2 (106.0 µL, 0.571 mmol) were combined in a 20 mL scintillation vial and added to a vial containing **1** (3.4 mg, 0.00571 mmol) dissolved in 0.6 mL of C_6D_6. The resulting red solution was then transferred into a J. Young NMR tube. After 24 h at ambient temperature, >99% conversion was observed *via* ^{1}H NMR spectroscopy. The reaction was then exposed to air to deactivate the catalyst, filtered through Celite, and volatile compounds were removed under reduced pressure to obtain diphenyl(3-phenyl)propyl silane in 78% yield (135.2 mg, 0447 mmol). Diphenyl(3-phenyl)propyl silane was isolated in similar yield (80%) and quality when a mixture of allyl benzene (73.4 µL, 0.554 mmol), Ph_2SiH_2 (103.0 µL, 0.554 mmol), **1** (3.3 mg, 0.00554 mmol), and 0.6 mL C_6D_6 was heated to 60 °C for 1 h. ^{1}H NMR (benzene-d_6): 7.51 (d, *J* = 5.1 Hz, 4H, *Ar*), 7.21 – 7.09 (m, 8H, *Ar*), 7.08 – 6.96 (m, 3H, *Ar*), 5.08 (t, *J* = 3.3 Hz, 1H, Si-*H*), 2.52 (t, *J* = 7.5 Hz, 2H, -C*H*$_2$-), 1.76 (pseudo p, *J* = 7.8 Hz, 2H, -C*H*$_2$-), 1.13 – 1.04 (m, 2H, -C*H*$_2$-). ^{13}C NMR (benzene-d_6): 142.66 (*Ar*), 135.87 (*Ar*), 135.03 (*Ar*), 130.19 (*Ar*),

129.20 (*Ar*), 128.95 (*Ar*), 128.70 (*Ar*), 126.44 (*Ar*), 39.89 (-*C*H_2-), 27.06 (-*C*H_2-), 12.48 (-*C*H_2-). DEPT135 ^{29}Si NMR (benzene-d_6): -13.87.

Hydrosilylation of styrene using 1.0 mol% 1. Under an inert atmosphere, styrene (57.7 µL, 0.504 mmol) and Ph_2SiH_2 (93.5 µL, 0.504 mmol) were combined in a 20 mL scintillation vial and added to a vial containing **1** (3.0 mg, 0.00504 mmol) dissolved in 0.6 mL of C_6D_6. The resulting red solution was then transferred into a J. Young NMR tube. After 3 h at 60 °C, >99% conversion was observed *via* ^{1}H NMR spectroscopy. The reaction was then exposed to air to deactivate the catalyst, filtered through Celite, and volatile compounds were removed under reduced pressure to obtain diphenyl(2-phenyl)ethyl silane in 85% yield (125.9 mg, 0.430 mmol). ^{1}H NMR (benzene-d_6): 7.55 – 7.44 (m, 4H, *Ar*), 7.19 – 7.08 (m, 7H, *Ar*), 7.08 – 6.93 (m, 4H, *Ar*), 5.05 (t, *J* = 3.7 Hz, 1H, Si-*H*), 2.73 – 2.64 (m, 2H, -C*H*$_2$-), 1.42 – 1.33 (m, 2H, -C*H*$_2$-). ^{13}C NMR (benzene-d_6): 144.87 (*Ar*), 136.39 (*Ar*), 135.89 (*Ar*), 134.81 (*Ar*), 130.26 (*Ar*), 128.98 (*Ar*), 128.74 (*Ar*), 128.57 (*Ar*), 126.39 (*Ar*), 31.18 (-*C*H_2-), 15.04 (-*C*H_2-). DEPT135 ^{29}Si NMR (benzene-d_6): -14.48.

Hydrosilylation of 4-fluorostyrene using 1.0 mol% 1. Under an inert atmosphere, 4-fluorostyrene (64.0 µL, 0.537 mmol) and Ph_2SiH_2 (99.6 µL, 0.537 mmol) were combined in a 20 mL scintillation vial and added to a vial containing **1** (3.2 mg, 0.00537 mmol) dissolved in 0.6 mL of C_6D_6. The resulting red solution was then transferred into a J. Young NMR tube. After 3 h at 60 °C, >99% conversion was observed *via* ^{1}H NMR spectroscopy. The reaction was then exposed to air to deactivate the catalyst, filtered through Celite, and volatile compounds were removed under reduced pressure to obtain diphenyl-((4-fluoro)-phenyl)ethyl silane in 71% yield (116.3 mg, 0.380 mmol). ^{1}H NMR (benzene-d_6): 7.59 –

7.42 (m, 4H, *Ar*), 7.21 – 7.10 (m, 6H, *Ar*), 6.81 – 6.64 (m, 4H, *Ar*), 5.01 (t, *J* = 3.6 Hz, 1H, Si*H*), 2.61 – 2.45 (m, 2H, -C*H*$_2$-), 1.32 – 1.17 (m, 2H, -C*H*$_2$-). ^{13}C NMR (benzene-d_6): 162.06 (d, *J* = 243.0 Hz, *Ar*), 140.38 (d, *J* = 3.3 Hz, *Ar*), 135.85 (*Ar)*, 134.66 (*Ar)*, 130.33 (*Ar)*, 129.91 (d, *J* = 7.7 Hz, *Ar*), 128.76 (*Ar)*, 115.57 (d, *J* = 21.0 Hz, *Ar*), 30.28 (-*C*H$_2$-), 15.03 (-*C*H$_2$-). DEPT135 ^{29}Si NMR (benzene-d_6): -13.70.

Hydrosilylation of 4-chlorostyrene using 1.0 mol% 1. Under an inert atmosphere, 4-chlorostyrene (62.9 mg, 0.454 mmol) and Ph_2SiH_2 (84.2 µL, 0.454 mmol) were combined in a 20 mL scintillation vial, dissolved in 0.6 mL of C_6D_6 and added to a vial containing **1** (2.7 mg, 0.00454 mmol). The resulting red solution was then transferred into a J. Young NMR tube. After 3 h at 60 °C, >99% conversion was observed *via* ^{1}H NMR spectroscopy. The reaction was then exposed to air to deactivate the catalyst, filtered through Celite, and volatile compounds were removed under reduced pressure to obtain diphenyl-((4-chloro)-phenyl)ethyl silane in 48% yield (70.4 mg, 0.218 mmol). ^{1}H NMR (benzene-d_6): 7.52 – 7.42 (m, 4H, *Ar*), 7.20 – 7.10 (m, 6H, *Ar*), 7.05 (d, *J* = 8.3 Hz, 2H, *Ar*), 6.63 (d, *J* = 8.3 Hz, 2H, *Ar*), 4.99 (t, *J* = 3.6 Hz, 1H, Si*H*), 2.55 – 2.42 (m, 2H, -C*H*$_2$-), 1.26 – 1.17 (m, 2H, -C*H*$_2$-). ^{13}C NMR (benzene-d_6): 143.21 (*Ar*), 135.85 (*Ar*), 134.58 (*Ar*), 132.11 (*Ar*), 130.36 (*Ar*), 129.93 (*Ar*), 129.00 (*Ar*), 128.78 (*Ar*), 30.42 (-*C*H$_2$-), 14.80 (-*C*H$_2$-). DEPT135 ^{29}Si NMR (benzene-d_6): -14.21.

Hydrosilylation of 4-methylstyrene using 1.0 mol% 1. Under an inert atmosphere, 4-methylstyrene (73.0 µL, 0.554 mmol) and Ph_2SiH_2 (102.9 µL, 0.554 mmol) were combined in a 20 mL scintillation vial and added to a vial containing **1** (3.3 mg, 0.00554 mmol) dissolved in 0.6 mL of C_6D_6. The resulting red solution was then transferred into a J. Young NMR tube. After 24 h at ambient temperature, >99% conversion was observed

via ^{1}H NMR spectroscopy. The reaction was then exposed to air to deactivate the catalyst, filtered through Celite, and volatile compounds were removed under reduced pressure to obtain diphenyl-((4-methyl)-phenyl)ethyl silane in 92% yield (154.0 mg, 0.509 mmol). ^{1}H NMR (benzene-d_6): 7.58 – 7.47 (m, 4H, *Ar*), 7.23 – 7.12 (m, 6H, *Ar*), 7.00 – 6.95 (m, 4H, *Ar*), 5.08 (dd, *J* = 6.9, 3.3 Hz, 1H, Si-*H*), 2.79 – 2.66 (m, 2H, -C*H*$_2$-), 2.15 (s, 3H, -C*H*$_3$), 1.43 (ddd, *J* = 12.0, 5.2, 3.7 Hz, 2H, -C*H*$_2$-). ^{13}C NMR (benzene-d_6): 141.87 (*Ar*), 135.91 (*Ar*), 135.49 (*Ar*), 134.91 (*Ar*), 130.22 (*Ar*), 129.68 (*Ar*), 128.73 (*Ar*), 128.53 (*Ar*), 30.80, (-*C*H$_2$-), 21.42 (-*C*H$_3$), 15.17 (-*C*H$_2$-). DEPT135 ^{29}Si NMR (benzene-d_6): -14.11.

Hydrosilylation of 4-*tert*-butylstyrene using 1.0 mol% 1. Under an inert atmosphere, 4-*tert*-butylstyrene (113.8 µL, 0.621 mmol) and Ph_2SiH_2 (115.3 µL, 0.621 mmol) were combined in a 20 mL scintillation vial and added to a vial containing **1** (3.7 mg, 0.00621 mmol) dissolved in 0.6 mL of C_6D_6. The resulting red solution was then transferred into a J. Young NMR tube. After 3h at 60 °C, >99% conversion was observed *via* ^{1}H NMR spectroscopy. The reaction was then exposed to air to deactivate the catalyst, filtered through Celite, and volatile compounds were removed under reduced pressure to obtain diphenyl-((4-*t*-butyl)-phenyl)ethyl silane in 75% yield (160.5 mg, 0.466 mmol). ^{1}H NMR (benzene-d_6): 7.54 – 7.47 (m, 4H, *Ar*), 7.23 (d, *J* = 8.2 Hz, 2H, *Ar*), 7.19 – 7.12 (m, 6H, *Ar*), 7.03 (d, *J* = 8.2 Hz, 2H, *Ar*), 5.08 (t, *J* = 3.5 Hz, 1H, Si*H*), 2.77 – 2.70 (m, 2H, -C*H*$_2$-), 1.46 – 1.40 (m, 2H, -C*H*$_2$-), 1.23 (s, 9H, -C(C*H*$_3$)$_3$). ^{13}C NMR (benzene-d_6): 148.88 (*Ar*), 141.88 (*Ar*), 135.91 (*Ar*), 134.90 (*Ar*), 130.22 (*Ar*), 128.73 (*Ar*), 128.35 (*Ar*), 125.86 (*Ar*), 34.74 (-*C*(CH$_3$)$_3$), 31.98 (-C(*C*H$_3$)$_3$), 30.73 (-*C*H$_2$-), 15.20 (-*C*H$_2$-). DEPT135 ^{29}Si NMR (benzene-d_6): -14.07.

Hydrosilylation of allyl benzyl ether using 1.0 mol% 1. Under an inert atmosphere, allyl benzyl ether (86.0 µL, 0.554 mmol) and Ph_2SiH_2 (103.0 µL, 0.554 mmol) were combined in a 20 mL scintillation vial and added to a vial containing **1** (3.3 mg, 0.00554 mmol) dissolved in 0.6 mL of C_6D_6. The resulting red solution was then transferred into a J. Young NMR tube. After 24 h at ambient temperature, >99% conversion was observed *via* ^{1}H NMR spectroscopy. The reaction was then exposed to air to deactivate the catalyst, filtered through Celite, and volatile compounds were removed under reduced pressure to obtain (3-(benzyloxy)propyl)diphenylsilane in 84% yield (107.8 mg, 0.324 mmol). (3-(Benzyloxy)propyl)diphenylsilane was isolated in similar yield (81%) and quality when a mixture of allyl benzyl ether (101.6 µL, 0.655 mmol), Ph_2SiH_2 (121.6 µL, 0.655 mmol), **1** (3.9 mg, 0.00655 mmol), and 0.6 mL C_6D_6 was heated to 60 °C for 1 h. ^{1}H NMR (benzene-d_6): 7.51 (dt, *J* = 10.3, 4.8 Hz, 4H, *Ar*), 7.29 – 7.23 (m, 2H, *Ar*), 7.18 – 7.11 (m, 8H, *Ar*), 7.07 (t, *J* = 7.3 Hz, 1H, *Ar*), 5.07 (t, *J* = 3.6 Hz, 1H, Si-*H*), 4.27 (s, 2H, CH_2-), 3.26 (t, *J* = 6.4 Hz, 2H, CH_2-), 1.81 – 1.68 (m, 2H, CH_2-), 1.19 – 1.11 (m, 2H, -CH_2-). ^{13}C NMR (benzene-d_6): 139.80 (*Ar*), 135.88 (*Ar*), 135.03 (*Ar*), 130.19 (*Ar*), 128.87 (*Ar*), 128.70 (*Ar*), 128.08 (*Ar*), 127.90 (*Ar*), 73.22 (-CH_2-), 72.91 (-CH_2-), 25.53 (-CH_2-), 9.29 (-CH_2-). DEPT135 ^{29}Si NMR (benzene-d_6): -13.52.

Hydrosilylation of allyl (2-bromophenyl)methyl ether using 1.0 mol% 1. Under an inert atmosphere, allyl (2-bromophenyl)methyl ether (97.7 µL, 0.571 mmol) and Ph_2SiH_2 (106.0 µL, 0.571 mmol) were combined in a 20 mL scintillation vial and added to a vial containing **1** (3.4 mg, 0.00571 mmol) dissolved in 0.6 mL of C_6D_6. The resulting red solution was then transferred into a J. Young NMR tube. After 24 h at ambient temperature, >99% conversion was observed *via* ^{1}H NMR spectroscopy. The reaction was then exposed

to air to deactivate the catalyst, filtered through Celite, and volatile compounds were removed under reduced pressure to obtain (3-((2-bromobenzyl)oxy)propyl)diphenylsilane in 65% yield (151.9 mg, 0.369 mmol). (3-((2-Bromobenzyl)oxy)propyl)diphenylsilane was isolated in similar yield (76%) and quality when a mixture of allyl (2-bromophenyl)methyl ether (89.2 µL, 0.521 mmol), Ph_2SiH_2 (96.7 µL, 0.521 mmol), **1** (3.1 mg, 0.00521 mmol), and 0.6 mL C_6D_6 was heated to 60 °C for 1 h. ^{1}H NMR (benzene-d_6): 7.57 – 7.52 (m, 4H, *Ar*), 7.48 (d, *J* = 7.5 Hz, 1H, *Ar*), 7.34 (d, *J* = 7.9 Hz, 1H, *Ar*), 7.17 (s, 6H, *Ar*), 6.98 (t, *J* = 7.4 Hz, 1H, *Ar*), 6.72 (t, *J* = 7.3 Hz, 1H, *Ar*), 5.08 (t, *J* = 3.5 Hz, 1H, Si-*H*), 4.43 (s, 2H, -C*H*$_2$-), 3.28 (t, *J* = 6.4 Hz, 2H, -C*H*$_2$-), 1.75 (p, *J* = 6.4 Hz, 2H, -C*H*$_2$-), 1.22 – 1.11 (m, 2H, -C*H*$_2$-). ^{13}C NMR (benzene-d_6): 138.38 (*Ar*), 135.17 (*Ar*), 134.27 (*Ar*), 132.18 (*Ar*), 129.51 (*Ar*), 128.69 (*Ar*), 128.43 (*Ar*), 128.01 (*Ar*), 127.13 (*Ar*), 122.22 (*Ar*), 72.70 (-*C*H$_2$-), 71.80 (-*C*H$_2$-), 24.75 (-*C*H$_2$-), 8.54 (-*C*H$_2$-). DEPT135 ^{29}Si NMR (benzene-d_6): -13.51.

Hydrosilylation of allyl methyl ether using 1.0 mol% 1. Under an inert atmosphere, allyl methyl ether (39.4 µL, 0.420 mmol) and Ph_2SiH_2 (78.0 µL, 0.420 mmol) were combined in a 20 mL scintillation vial and added to a vial containing **1** (2.5 mg, 0.00420 mmol) dissolved in 0.6 mL of C_6D_6. The resulting red solution was then transferred into a J. Young NMR tube. After 24 h at ambient temperature, >99% conversion was observed *via* ^{1}H NMR spectroscopy. The reaction was then exposed to air to deactivate the catalyst, filtered through Celite, and volatile compounds were removed under reduced pressure to obtain (3-methoxypropyl)diphenylsilane in 74% yield (79.9 mg, 0.312 mmol). (3-Methoxypropyl)diphenylsilane was isolated in similar yield (77%) and quality when a mixture of allyl ethyl (39.4 µL, 0.420 mmol), Ph_2SiH_2 (78.0 µL , 0.420 mmol), **1** (2.5 mg, 0.00420 mmol), and 0.6 mL C_6D_6 was heated to 60 °C for 1 h. ^{1}H NMR (benzene-d_6): 7.57

– 7.51 (m, 4H, *Ar*), 7.16 (m, 6H, *Ar*), 5.08 (t, *J* = 3.6 Hz, 1H, Si-*H*), 3.15 (t, *J* = 6.3 Hz, 2H, -OC*H*$_2$-), 3.07 (s, 3H, -OC*H*$_3$), 1.76 – 1.66 (m, 2H, -C*H*$_2$-), 1.19 – 1.12 (m, 2H, -C*H*$_2$-). ^{13}C NMR (benzene-d_6): 135.87 (*Ar*), 135.13 (*Ar*), 130.16 (*Ar*), 128.68 (*Ar*), 75.15 (-O*C*H$_2$-), 58.51 (-O*C*H$_3$), 25.36 (-*C*H$_2$-), 9.28 (-*C*H$_2$-). DEPT135 ^{29}Si NMR (benzene-d_6): -13.51.

Hydrosilylation of allyl ethyl ether using 1.0 mol% 1. Under an inert atmosphere, allyl ethyl ether (62.8 µL, 0.554 mmol) and Ph_2SiH_2 (103.0 µL, 0.554 mmol) were combined in a 20 mL scintillation vial and added to a vial containing **1** (3.3 mg, 0.00554 mmol) dissolved in 0.6 mL of C_6D_6. The resulting red solution was then transferred into a J. Young NMR tube. After 24 h at ambient temperature, >99% conversion was observed *via* ^{1}H NMR spectroscopy. The reaction was then exposed to air to deactivate the catalyst, filtered through Celite, and volatile compounds were removed under reduced pressure to obtain (3-ethoxypropyl)diphenylsilane in 63% yield (93.6 mg, 0.346 mmol). (3-ethoxypropyl)diphenylsilane was isolated in similar yield (69%) and quality when a mixture of allyl ethyl (59.0 µL, 0.521 mmol), Ph_2SiH_2 (96.7 µL, 0.521 mmol), **1** (3.1 mg, 0.00521 mmol), and 0.6 mL C_6D_6 was heated to 60 °C for 1 h. ^{1}H NMR (benzene-d_6): 7.55 – 7.50 (m, 4H, *Ar*), 7.18 – 7.11 (m, 6H, *Ar*), 5.06 (t, *J* = 3.8 Hz, 1H, Si-*H*), 3.25 – 3.18 (m, 4H, -C*H*$_2$-), 1.75 – 1.67 (m, 2H, -C*H*$_2$-), 1.18 – 1.12 (m, 2H, -C*H*$_2$-), 1.07 (t, *J* = 7.0 Hz, 3H, -C*H*$_3$). ^{13}C NMR (benzene-d_6): 135.89 (*Ar*), 135.15 (*Ar*), 130.16 (*Ar*), 128.68 (*Ar*), 73.18 (-*C*H$_2$-), 66.46 (-*C*H$_2$-), 25.63 (-*C*H$_2$-), 15.91 (-*C*H$_2$-), 9.40 (-*C*H$_3$). DEPT135 ^{29}Si NMR (benzene-d_6): -13.49.

Hydrosilylation of allyl glycidyl ether using 1.0 mol% 1. Under an inert atmosphere, allyl glycidyl ether (71.7 µL, 0.605 mmol) and Ph_2SiH_2 (112.0 µL, 0.605 mmol) were combined in a 20 mL scintillation vial and added to a vial containing **1** (3.6 mg, 0.00605

mmol) dissolved in 0.6 mL of C_6D_6. The resulting red solution was then transferred into a J. Young NMR tube. After 24 h at ambient temperature, >99% conversion was observed *via* ^{1}H NMR spectroscopy. The reaction was then exposed to air to deactivate the catalyst, filtered through Celite, and volatile compounds were removed under reduced pressure to obtain (3-(oxiran-2-ylmethoxy)propyl)diphenyl silane in 78% yield (141.5 mg, 0.473 mmol). (3-(Oxiran-2-ylmethoxy)propyl)diphenyl silane was isolated in similar yield (77%) and quality when a mixture of allyl glycidyl ether (77.7 µL, 0.0.655 mmol), Ph_2SiH_2 (121.6 µL, 0.655 mmol), **1** (3.9 mg, 0.00655 mmol), and 0.6 mL C_6D_6 was heated to 60 °C for 1 h. ^{1}H NMR (benzene-d_6): 7.53 – 7.48 (m, 4H, *Ar*), 7.14 (m, 6H, *Ar*), 5.03 (t, *J* = 3.6 Hz, 1H, Si-*H*), 3.32 – 3.24 (m, 2H, -C*H*$_2$-), 3.21 (dt, *J* = 9.1, 6.4 Hz, 1H, -C*H*$_2$-), 3.01 (dd, *J* = 11.4, 5.9 Hz, 1H, -C*H*$_2$-), 2.79 (ddt, *J* = 5.9, 3.9, 2.9 Hz, 1H, -C*H*-), 2.26 (dd, *J* = 5.1, 4.3 Hz, 1H, -C*H*$_2$-), 2.13 (dd, *J* = 5.2, 2.5 Hz, 1H, -C*H*$_2$-), 1.67 (tt, *J* = 12.6, 6.4 Hz, 2H, -C*H*$_2$-), 1.17 – 1.06 (m, 2H, -C*H*$_2$-). ^{13}C NMR (benzene-d_6): 135.86 (*Ar*), 135.02 (*Ar*), 130.20 (*Ar*), 128.71 (*Ar*), 73.86 (-*C*H$_2$-), 72.21 (-*C*H$_2$-), 51.07 (-*C*H-), 43.96 (-*C*H$_2$-), 25.47 (-*C*H$_2$-), 9.18 (-*C*H$_2$-). DEPT135 ^{29}Si NMR (benzene-d_6): -13.50.

Hydrosilylation of allyl trimethylsilyl ether using 1.0 mol% 1. Under an inert atmosphere, allyl trimethylsilyl ether (96.6 µL, 0.588 mmol) and Ph_2SiH_2 (109.1 µL, 0.588 mmol) were combined in a 20 mL scintillation vial and added to a vial containing **1** (3.5 mg, 0.00588 mmol) dissolved in 0.6 mL of C_6D_6. The resulting red solution was then transferred into a J. Young NMR tube. After 24 h at ambient temperature, >99% conversion was observed *via* ^{1}H NMR spectroscopy. The reaction was then exposed to air to deactivate the catalyst, filtered through Celite, and volatile compounds were removed under reduced pressure to obtain (2-(diphenylsilyl)ethoxy)trimethyl silane in 88% yield (163.1 mg, 0.512

mmol). (2-(Diphenylsilyl)ethoxy)trimethyl silane was isolated in similar yield (84%) and quality when a mixture of allyl trimethylsilyl ether (121.7 µL, 0.722 mmol), Ph_2SiH_2 (134.0 µL, 0.722 mmol), **1** (4.3 mg, 0.00722 mmol), and 0.6 mL C_6D_6 was heated to 60 °C for 1 h. ^{1}H NMR (benzene-d_6): 7.61 – 7.42 (m, 4H, *Ar*), 7.20 – 7.05 (m, 6H, *Ar*), 5.06 (t, *J* = 3.6 Hz, 1H, Si-*H*), 3.45 (t, *J* = 6.4 Hz, 2H, -CH_2-), 1.69 (tt, *J* = 13.0, 6.5 Hz, 2H, -CH_2-), 1.15 – 1.09 (m, 2H, -CH_2-), 0.06 (s, 9H, -Si(CH_3)$_3$). ^{13}C NMR (benzene-d_6): 135.89 (*Ar*), 135.09 (*Ar*), 130.18 (*Ar*), 128.69 (*Ar*), 65.20 (-*C*H_2-), 28.41 (-*C*H_2-), 8.92 (-*C*H_2-), 0.07 (-Si(*C*H_3)$_3$). ^{29}Si NMR (benzene-d_6): 15.49 (*Si*(CH$_3$)$_3$), -13.48 (*Si*-H).

Hydrosilylation of vinyl phenyl ether using 1.0 mol% 1. Under an inert atmosphere, vinyl phenyl ether (81.0 µL, 0.454 mmol) and Ph_2SiH_2 (84.2 µL, 0.454 mmol) were combined in a 20 mL scintillation vial and added to a vial containing **1** (2.7 mg, 0.00454 mmol) dissolved in 0.6 mL of C_6D_6. The resulting red solution was then transferred into a J. Young NMR tube. After 24 h at ambient temperature, >99% conversion was observed *via* ^{1}H NMR spectroscopy. The reaction was then exposed to air to deactivate the catalyst, filtered through Celite, and volatile compounds were removed under reduced pressure to obtain (2-phenoxyethyl)diphenyl silane in 74% yield (102.4 mg, 0.336 mmol). (2-Phenoxyethyl)diphenyl silane was isolated in similar yield (71%) and quality when a mixture of vinyl phenyl ether (45.5 µL, 0.370 mmol), Ph_2SiH_2 (68.7 µL, 0.370 mmol), **1** (2.2 mg, 0.00370 mmol), and 0.6 mL C_6D_6 was heated to 60 °C for 1 h. ^{1}H NMR (benzene-d_6): 7.50 – 7.43 (m, 4H, *Ar*), 7.14 – 7.06 (m, 6H, *Ar*), 7.06 – 7.00 (m, 2H, *Ar*), 6.76 (dd, *J* = 10.6, 4.1 Hz, 1H, *Ar*), 6.71 (dt, *J* = 3.3, 1.8 Hz, 2H, *Ar*), 5.08 (t, *J* = 3.6 Hz, 1H, Si*H*), 3.88 (t, *J* = 7.8 Hz 2H, -CH_2-), 1.55 (td, *J* = 8.1, 3.6 Hz, 2H, -CH_2-). ^{13}C NMR (benzene-

d$_6$): 159.64 (*Ar*), 135.87 (*Ar*), 134.19 (*Ar*), 130.38 (*Ar*), 130.04 (*Ar*), 128.76 (*Ar*), 121.17 (*Ar*), 115.25 (*Ar*), 65.16 (-*C*H$_2$-), 14.41 (-*C*H$_2$-). DEPT135 ^{29}Si NMR (benzene-*d*$_6$): -17.09.

Hydrosilylation of vinyl isobutyl ether using 1.0 mol% 1. Under an inert atmosphere, vinyl isobutyl ether (59.1 µL, 0.454 mmol) and Ph_2SiH_2 (84.3 µL, 0.454 mmol) were combined in a 20 mL scintillation vial and added to a vial containing **1** (2.7 mg, 0.00621 mmol) dissolved in 0.6 mL of C_6D_6. The resulting red solution was then transferred into a J. Young NMR tube. After 24 h at ambient temperature, >99% conversion was observed *via* ^{1}H NMR spectroscopy. The reaction was then exposed to air to deactivate the catalyst, filtered through Celite, and volatile compounds were removed under reduced pressure to obtain (2-isobutoxyethyl)diphenyl silane in 76% yield (98.1 mg, 0.345 mmol). (2-Isobutoxyethyl)diphenyl silane was isolated in similar yield (73%) and quality when a mixture of isobutyl vinyl ether (59.1 µL, 0.454 mmol), Ph_2SiH_2 (84.3 µL, 0.454 mmol), **1** (2.7 mg, 0.00454 mmol), and 0.6 mL C_6D_6 was heated to 60 °C for 1 h. ^{1}H NMR (benzene-*d*$_6$): 7.60 – 7.55 (m, 4H, *Ar*), 7.20 – 7.16 (m, 6H, *Ar*), 5.15 (t, *J* = 3.6 Hz, 1H, Si-*H*), 3.52 (t, *J* = 7.6 Hz, 2H, -C*H*$_2$-), 2.97 (d, *J* = 6.5 Hz, 2H, -C*H*$_2$-), 1.79 (sep, *J* = 6.8 Hz, 1H, -C*H*-), 1.53 (td, *J* = 15.9, 8.0 Hz, 2H, -C*H*$_2$-), 0.88 (d, *J* = 6.8 Hz, 6H, -C*H*$_3$). ^{13}C NMR (benzene-*d*$_6$): 135.95 (*Ar*), 134.90 (*Ar*), 130.17 (*Ar*), 128.65 (*Ar*), 77.97 (-*C*H$_2$-), 68.13 (-*C*H$_2$-), 29.33 (-*C*H-), 20.04 (-*C*H$_3$), 15.00 (-*C*H$_2$-). DEPT135 ^{29}Si NMR (benzene-*d*$_6$): -16.34.

Hydrosilylation of vinyl acetate using 1.0 mol% 1. Under an inert atmosphere, vinyl acetate (48.2 µL, 0.521 mmol) and Ph_2SiH_2 (96.6 µL, 0.521 mmol) were combined in a 20 mL scintillation vial and added to a vial containing **1** (3.1 mg, 0.00521 mmol) dissolved in 0.6 mL of C_6D_6. After 24 h at ambient temperature, 86% conversion was observed via ^{1}H

NMR spectroscopy to a mixture of 2-(diphenylsilyl)ethyl acetate, diphenyl silyl diacetate, and diphenyl silyl acetate.

Hydrosilylation of α-methylstyrene using 1.0 mol% 1: Under an inert atmosphere, α-methylstyrene (74.3 µL, 0.571 mmol) and Ph_2SiH_2 (132.5 µL, 0.714 mmol) were combined in a 20 mL scintillation vial and then added to a vial containing **1** (3.4 mg, 0.00571 mmol) dissolved in 0.6 mL C_6D_6. The resulting red solution was transferred into a J. Young NMR tube and heated to 70 °C for 7 d, after which >99% conversion was observed *via* ^{1}H NMR spectroscopy. The reaction was then exposed to air to deactivate the catalyst, filtered through Celite, and volatile compounds were removed under reduced pressure to obtain diphenyl-(2-phenylpropyl) silane as a mixture of enantiomers in 85% yield (147.1 mg, 0.486 mmol). ^{1}H NMR (benzene-d_6): 7.50 – 7.43 (m, 4H, *Ar*), 7.17 – 7.09 (m, 7H, *Ar*), 7.06 – 7.00 (m, 4H, *Ar*), 4.98 (t, J = 4.0 Hz, 1H, Si*H*), 2.96 – 2.86 (m, 1H, -C*H*-), 1.54 – 1.36 (m, 2H, -CH_2-), 1.23 (d, J = 6.9 Hz, 3H, -CH_3). ^{13}C NMR (benzene-d_6): 149.53 (*Ar*), 136.57 (*Ar*), 135.87 (*Ar*), 135.80 (*Ar*), 130.43 (*Ar*), 130.15 (*Ar*), 130.11 (*Ar*), 129.03 (*Ar*), 128.77 (*Ar*), 128.67 (*Ar*), 128.66 (*Ar*), 127.30 (*Ar*), 126.63 (*Ar*), 36.99 (-*C*H-), 25.87 (-*C*H_3), 23.27 (-*C*H_2). DEPT135 ^{29}Si NMR (benzene-d_6): -15.93.

Hydrosilylation of α-methylstyrene using 0.1 mol% 1: Under an inert atmosphere, α-methylstyrene (0.7 mL, 5.37 mmol) and Ph_2SiH_2 (1.25 mL, 6.71 mmol) were combined in a 20 mL scintillation vial and then added to a vial containing **1** (3.2 mg, 0.00537 mmol). The resulting red solution was transferred into a 100 mL thick walled glass bomb and heated to 70 °C for 7 d, after which 74% conversion was observed *via* ^{1}H NMR spectroscopy.

Hydrosilylation of 4-fluoro-α-methylstyrene using 1.0 mol% 1: Under an inert atmosphere, 4-fluoro-α-methylstyrene (84.4 µL, 0.605 mmol) and Ph_2SiH_2 (140.3 µL, 0.765 mmol) were combined in a 20 mL scintillation vial and then added to a vial containing **1** (3.6 mg, 0.00605 mmol) dissolved in 0.6 mL of C_6D_6. The resulting red solution was transferred into a J. Young NMR tube and heated to 70 °C for 7 d, after which >99% conversion was observed via ^{1}H NMR spectroscopy. The reaction was then exposed to air to deactivate the catalyst, filtered through Celite, and volatile compounds were removed under reduced pressure to obtain (2-(4-fluorophenylpropyl) diphenyl silane as a mixture of enantiomers in 91% yield (177.0 mg, 0.552 mmol). ^{1}H NMR (benzene-d_6): 7.50 – 7.41 (m, 4H, *Ar*), 7.22 – 7.08 (m, 6H, *Ar*), 6.80 – 6.75 (m, 4H, *Ar*), 4.93 (t, *J* = 4.0 Hz, 1H, Si*H*), 2.89 – 2.74 (m, 1H, -C*H*-), 1.45 – 1.28 (m, 2H, -CH_2-), 1.16 (d, *J* = 6.9 Hz, 3H, -CH_3). ^{13}C NMR (benzene-d_6): 162.06 (d, *J* = 243.2 Hz), 145.01 (d, *J* = 3.1 Hz), 136.56 (*Ar*), 135.82 (*Ar*), 135.75 (*Ar*), 130.22 (*Ar*), 130.17 (*Ar*), 128.72 (*Ar*), 128.72 (*Ar*), 128.67 (*Ar*), 128.64 (*Ar*), 115.63 (d, *J* = 20.9, *Ar*), 36.26 (-*C*H-), 25.99 (-*C*H_3), 23.31 (-*C*H_2-). DEPT135 ^{29}Si NMR(benzene-d_6): -15.73.

Hydrosilylation of 4-chloro-α-methylstyrene using 1.0 mol% 1: Under an inert atmosphere, 4-chloro-α-methylstyrene (76.3 µL, 0.537 mmol) and Ph_2SiH_2 (124.6 µL, 0.671 mmol) were combined in a 20 mL scintillation vial and then added to a vial containing **1** (3.2 mg, 0.00537 mmol) dissolved in 0.6 mL of C_6D_6. The resulting green solution was transferred into a J. Young NMR tube and heated to 70 °C for 7 d, after which 69% olefin hydrosilylation was observed *via* ^{1}H NMR spectroscopy. Additionally, de-chlorination of the aromatic ring and consumption of Ph_2SiH_2 to form Ph_2HSiCl was

observed. The ratio of hydrosilylated products is 3:2 (2-phenylpropyl) diphenyl silane:(2-(4-chlorophenyl)propyl) diphenyl silane.

Hydrosilylation of 4,α-dimethylstyrene using 1.0 mol% 1: Under an inert atmosphere, 4,α-dimethylstyrene (63.7 µL, 0.437 mmol) and Ph_2SiH_2 (101.4 µL, 0.546 mmol) were combined in a 20 mL scintillation vial and then added to a vial containing **1** (2.6 mg, 0.00437 mmol) dissolved in 0.6 mL of C_6D_6. The resulting red solution was transferred into a J. Young NMR tube and heated to 70 °C for 7 d, after which >99% conversion was observed *via* ^{1}H NMR spectroscopy. The reaction was then exposed to air to deactivate the catalyst, filtered through Celite, and volatile compounds were removed under reduced pressure to obtain (2-(4-methylphenyl)propyl) diphenyl silane as a mixture of enantiomers in 98% yield (125.4 mg, 0.396 mmol). ^{1}H NMR (benzene-d_6): 7.63 – 7.53 (m, 1H, *Ar*), 7.51 – 7.43 (m, 3H, *Ar*), 7.18 – 7.02 (m, 7H, *Ar*), 6.99 – 6.93 (m, 3H, *Ar*), 4.98 (t, *J* = 3.9 Hz, 1H, -Si*H*), 2.92 (h, *J* = 7.0 Hz, 1H, -C*H*-), 2.12 (s, 3H, -CH_3), 1.56 – 1.38 (m, 2H, -CH_2-), 1.25 (d, *J* = 6.9 Hz, 3H, -CH_3). ^{13}C NMR (benzene-d_6): δ 146.54 (*Ar*), 136.58 (*Ar*), 135.90 (*Ar*), 135.82 (*Ar*), 135.72 (*Ar*), 135.43 (*Ar*), 135.26 (*Ar*), 135.09 (*Ar*), 130.89 (*Ar*), 130.42 (*Ar*), 130.11 (*Ar*), 130.04 (*Ar*), 129.69 (*Ar*), 128.77 (*Ar*), 128.65 (*Ar*), 128.62 (*Ar*), 127.25 (*Ar*), 36.64 (-*C*CH_3), 26.09 (-*C*H-), 23.39 (-*C*H_3), 21.42 (-*C*H_2-). DEPT135 ^{29}Si NMR (benzene-d_6): -15.63.

Hydrosilylation of 4-methoxy-α-methylstyrene using 1.0 mol% 1: Under an inert atmosphere, 4-methoxy-α-methylstyrene (67.2 mg, 0.454 mmol) and Ph_2SiH_2 (105.3 µL, 0.568 mmol) were combined in a 20 mL scintillation vial and then added to a vial containing **1** (2.7 mg, 0.00454 mmol) dissolved in 0.6 mL of C_6D_6. The resulting red solution was transferred into a J. Young NMR tube and heated to 70 °C for 7 d, after which

>99% conversion was observed *via* ^{1}H NMR spectroscopy. The reaction was then exposed to air to deactivate the catalyst, filtered through Celite, and volatile compounds were removed under reduced pressure to obtain diphenyl-(2-(4-methoxyphenyl)propyl) silane as a mixture of enantiomers in 85% yield (127.7 mg, 0.384 mmol). ^{1}H NMR (benzene-d_6): 7.51 – 7.45 (m, 4H, *Ar*), 7.18 – 7.07 (m, 6H, *Ar*), 6.97 – 6.92 (m, 2H, *Ar*), 6.76 – 6.72 (m, 2H, *Ar*), 4.98 (t, *J* = 3.9 Hz, 1H, Si*H*), 3.32 (s, 3H, -OC*H*$_3$), 2.91 (h, *J* = 7.1 Hz, 1H, -C*H*-), 1.54 – 1.38 (m, 2H, -C*H*$_2$-), 1.25 (d, *J* = 6.9 Hz, 3H, -C*H*$_3$). ^{13}C NMR (benzene-d_6): 158.89 (*Ar*), 141.45 (*Ar*), 136.57 (*Ar*), 135.90 (*Ar*), 135.81 (*Ar*), 130.12 (*Ar*), 130.06 (*Ar*), 128.67 (*Ar*), 128.63 (*Ar*), 128.19 (*Ar*), 114.50 (*Ar*), 55.16 (-O*C*H$_3$), 36.25 (-*C*H-), 26.33 (-*C*H$_3$), 23.54 (-*C*H$_2$-). DEPT135 ^{29}Si NMR (benzene-d_6): -15.91.

Hydrosilylation of 4-(*N*,*N*-dimethylamino)-α-methylstyrene using 1.0 mol% 1: Under an inert atmosphere, 4-(*N*,*N*-dimethylamino)-α-methylstyrene (78.5 mg, 0.487 mmol) and Ph_2SiH_2 (113.0 µL, 0.609 mmol) were combined in a 20 mL scintillation vial and then added to a vial containing **1** (2.9 mg, 0.00487 mmol) dissolved in 0.6 mL of C_6D_6. The resulting red solution was transferred into a J. Young NMR tube and heated to 70 °C for 7 d, after which >99% conversion was observed *via* ^{1}H NMR spectroscopy. The reaction was then exposed to air to deactivate the catalyst, filtered through Celite, and volatile compounds were removed under reduced pressure to obtain diphenyl-(2-(4-(*N*,*N*-dimethylamino)phenyl)propyl) silane as a mixture of enantiomers in 60% yield (100.5 mg, 0.290 mmol). ^{1}H NMR (benzene-d_6): 7.60 – 7.48 (m, 4H, *Ar*), 7.20 – 7.12 (m, 6H, *Ar*), 7.09 – 7.04 (m, 2H, *Ar*), 6.65 – 6.58 (m, 2H, *Ar*), 5.05 (t, *J* = 4.0 Hz, 1H, Si*H*), 3.07 – 2.93 (m, 1H, -C*H*-), 2.55 (s, 6H, -N(C*H*$_3$)$_3$), 1.66 – 1.46 (m, 2H, -C*H*$_2$-), 1.34 (d, *J* = 6.9 Hz, 3H, -C*H*$_3$). ^{13}C NMR (benzene-d_6): 149.99 (*Ar*), 137.72 (*Ar*), 136.57 (*Ar*), 135.95 (*Ar*), 135.86

(*Ar*), 130.04 (*Ar*), 129.97 (*Ar*), 128.64 (*Ar*), 127.87 (*Ar*), 113.79 (*Ar*), 41.03 (N(*C*H_3)$_3$), 36.16 (-*C*H-), 26.49 (-*C*H_3), 23.68 (-*C*H_2-). DEPT 135 ^{29}Si NMR (benzene-d_6): -15.87.

Hydrosilylation of 1,1-diphenylethene using 1.0 mol% 1: Under an inert atmosphere, 1,1-diphenylethene (73.9 µL, 0.420 mmol) and Ph_2SiH_2 (97.4 µL, 0.525 mmol) were combined in a 20 mL scintillation vial and then added to a vial containing **1** (2.5 mg, 0.00420 mmol) dissolved in 0.6 mL of C_6D_6. The resulting red solution was transferred into a J. Young NMR tube and heated to 70 °C for 7 d, after which 38% conversion was observed *via* ^{1}H NMR spectroscopy.

Hydrosilylation of D-limonene using 1.0 mol% 1: Under an inert atmosphere, D-limonene (76.1 µL, 0.470 mmol) and Ph_2SiH_2 (109.0 µL, 0.588 mmol) were combined in a 20 mL scintillation vial and then added to a vial containing **1** (2.8 mg, 0.00470 mmol) dissolved in 0.6 mL of C_6D_6. The resulting red solution was transferred into a J. Young NMR tube and heated to 70 °C for 7 d, after which >99% conversion was observed *via* ^{1}H NMR spectroscopy. The reaction was then exposed to air to deactivate the catalyst, filtered through Celite, and volatile compounds were removed under reduced pressure to obtain ((*rac*)-2-((R)-4-methylcyclohex-3-en-1-yl)propyl)diphenylsilane as a mixture of diastereomers in 76% yield (114.9 mg, 0.358 mmol). ^{1}H NMR (benzene-d_6): 7.58 – 7.51 (m, 4H, *Ar*), 7.18 – 7.09 (m, 6H, A*r*), 5.38 (s, 1H, =C*H*), 5.15 (m, 1H, Si*H*), 1.93 – 1.79 (m, 3H, -C*H*-, -C*H*$_2$-), 1.79 – 1.62 (m, 3H, -C*H*-, -C*H*$_2$-), 1.61 (s, 3H), 1.59 – 1.50 (m, 1H, -C*H*-), 1.43 – 1.33 (m, 1H, -C*H*-), 1.32 – 1.24 (m, 1H, -C*H*-), 1.22 – 1.10 (m, 1H, -C*H*-), 0.98 – 0.93 (m, 1H, -C*H*-), 0.91 (d, *J* = 2.5 Hz, 3H, -C*H*$_3$), 0.90 (d, *J* = 2.5 Hz, 3H, -C*H*$_3$). ^{13}C NMR (benzene-d_6): 136.58 (*Ar*), 135.91 (*Ar*), 135.90 (*Ar*), 135.82 (*Ar*), 135.80 (*Ar*), 135.48 (*Ar*), 133.96 (*Ar*), 133.95 (*Ar*), 130.42 (*Ar*), 130.15 (*Ar*), 130.10 (*Ar*), 130.09 (*Ar*),

128.71 (*Ar*), 128.67 (*Ar*), 128.67 (*Ar*), 121.86 (=*C*H), 121.82 (=*C*H), 41.62 (-*C*H-), 41.56 (-*C*H-), 34.69 (-*C*H_2-), 34.53 (-*C*H_2-), 31.58 (-*C*H_2-), 31.50 (-*C*H_2-), 29.44 (-*C*H_2-), 28.63 (-*C*H_2-), 27.38 (-*C*H_2-), 26.21 (-*C*H_2-), 24.10 (-*C*H_3), 24.09 (-*C*H_3), 19.76 (=C*C*H_3), 19.36 (=C*C*H_3), 18.33 (-*C*H_2Si-), 17.83 (-*C*H_2Si-). DEPT135 ^{29}Si NMR (benzene-*d*$_6$): -14.64, -14.93.

Hydrosilylation of 2-methyloctene using 1.0 mol% 1: Under an inert atmosphere, 2-methyloctene (61.5 µL, 0.386 mmol) and Ph_2SiH_2 (89.6 µL, 0.483 mmol) were combined in a 20 mL scintillation vial and then added to a vial containing **1** (2.3 mg, 0.00386 mmol) dissolved in 0.6 mL of C_6D_6. The resulting red solution was transferred into a J. Young NMR tube and heated to 70 °C for 7 d, after which >99% conversion was observed *via* ^{1}H NMR spectroscopy. The reaction was then exposed to air to deactivate the catalyst, filtered through Celite, and volatile compounds were removed under reduced pressure to obtain (2-methyloctyl)diphenyl silane as a mixture of enantiomers in 78% yield (93.1 mg, 0.300 mmol). ^{1}H NMR (benzene-*d*$_6$): 7.72 – 7.40 (m, 4H, *Ar*), 7.27 – 6.99 (m, 6H, *Ar*), 5.19 (t, *J* = 4.2 Hz, 1H, Si-*H*), 1.74 (ddd, *J* = 12.0, 8.1, 6.5 Hz, 1H, -C*H*-), 1.49 – 1.12 (m, 10H, -C*H*$_2$-), 0.99 (d, *J* = 6.6 Hz, 3H, -C*H*$_3$), 0.89 (t, *J* = 7.0 Hz, 3H, -C*H*$_3$). ^{13}C NMR (benzene-*d*$_6$): 136.80 (*Ar*), 135.88 (*Ar*), 135.85 (*Ar*), 130.11 (*Ar*), 130.09 (*Ar*), 128.69 (*Ar*), 128.67 (*Ar*), 40.83 (-*C*H_2-), 32.63 (-*C*H_2-), 30.44 (-*C*H_2-), 30.25 (-*C*H_2-), 27.72 (-*C*H_2-), 23.45 (-*C*H_3), 23.28 (-*C*H_2-), 21.47 (-*C*H_2-), 14.74 (-*C*H_3). DEPT135 ^{29}Si NMR (benzene-*d*$_6$): -15.56.

Hydrosilylation of 1,1-dicyclohexylethene using 1.0 mol% 1: Under an inert atmosphere, 1,1-dicyclohexylethene (86.5 µL, 0.403 mmol) and Ph_2SiH_2 (93.5 µL, 0.504 mmol) were combined in a 20 mL scintillation vial and then added to a vial containing **1**

(2.4 mg, 0.00403 mmol) dissolved in 0.6 mL of C_6D_6. The resulting red solution was transferred into a J. Young NMR tube and heated to 70 °C for 7 d, after which no conversion was observed *via* ^{1}H NMR spectroscopy.

Hydrosilylation of methyl methacrylate using 1.0 mol% 1: Under an inert atmosphere, methyl methacrylate (66.2 µL, 0.621 mmol) and Ph_2SiH_2 (144.0 µL, 0.776 mmol) were combined in a 20 mL scintillation vial and then added to a vial containing **1** (3.7 mg, 0.00621 mmol) dissolved in 0.6 mL of C_6D_6. The resulting red solution was transferred into a J. Young NMR tube and heated to 70 °C for 7 d, after which >99% conversion was observed *via* ^{1}H NMR spectroscopy. The reaction was then exposed to air to deactivate the catalyst, filtered through Celite, and volatile compounds were removed under reduced pressure to obtain methyl 3-(diphenylsilyl)-2-methylpropanoate in 64% yield (113.2 mg, 0.378 mmol). ^{1}H NMR (benzene-d_6): 7.51 – 7.46 (m, 4H, *Ar*), 7.16 – 7.05 (m, 6H *Ar*), 5.05 (t, *J* = 3.9 Hz, 1H, Si*H*), 3.21 (s, 3H, -OCH_3), 2.59 (h, *J* = 7.1 Hz, 1H, -C*H*-), 1.65 – 1.57 (m, 1H, -C*H*-), 1.23 – 1.18 (m, 1H, -C*H*-), 1.11 (d, *J* = 7.0 Hz, 3H, -CH_3). ^{13}C NMR (benzene-d_6): 176.92 (*C*=O), 135.90 (*Ar*), 135.83 (*Ar*), 130.29 (*Ar*), 130.26 (*Ar*), 128.72 (*Ar*), 128.70 (*Ar*), 51.39 (-O*C*H$_3$), 36.33 (-*C*H-), 20.49 (-*C*H$_2$-), 18.13 (-*C*H$_3$). DEPT135 ^{29}Si NMR (benzene-d_6): -15.85.

De-chlorination of chlorobenzene with 1.0 mol% 1. Under an inert atmosphere, chlorobenzene (49.4 µL, 0.487 mmol) and Ph_2SiH_2 (113.0 µL, 0.609 mmol) were combined in a 20 mL scintillation vial and then added to a vial containing **1** (2.9 mg, 0.00487 mmol) dissolved in 0.6 mL toluene-d_8. The resulting red solution was transferred into a J. Young NMR tube and heated to 70 °C for 7 d, after which time 67% conversion

was observed *via* ^{1}H NMR spectroscopy. Products were identified as benzene and Ph_2SiHCl.

CHAPTER FIVE

COBALT CATALYZED NITRILE DIHYDROBORATION

5.1 Abstract

Addition of ^{Ph2PPr}DI to $CoCl_2$ in acetonitrile allowed for the isolation of (^{Ph2PPr}DI)$CoCl_2$ (**4**). Crystals of **4** grown from an acetonitrile solution were diffracted using single crystal X-ray diffraction. The structure revealed a κ^4-^{Ph2PPr}DI chelate and *cis*-chloride ligands. Since DI ligands are known for their redox non-innocence, the bond distances were analyzed; however, they did not reveal any ligand reduction, meaning **4** exists as a Co(II), 19 e^- compound. This was confirmed using electron paramagnetic resonance spectroscopy, which which revealed a broad and nearly isotropic signal extending over 90 mT, consistent with a low-spin ^{59}Co(II) (d^7, S_{Co}= 1/2, I_{Co}= 7/2) electronic struture. Treatment of **4** with excess $NaEt_3BH$ yielded the diamagnetic hydride complex (^{Ph2PPr}DI)CoH (**5**). Crystals suitable for single crystal XRD were grown from diethyl ether and analysis revealed a square pyramidal structure with an apical and an equatorial phosphine. Analysis of the chelate bond lengths revealed elongated C-N and contracted C-C bonds, consistent with a singly reduced chelate, where the ligand radical is antiferromagnetically coupled to a Co based electron. This determination was confirmed using density functional theory calculations. Compound **5** was found to be active for alkyne hydroboration, yielding alkenyl borate esters. Furthermore, **5** was also found to reduce nitriles to diboryl amines with turnover frequencies of up to 4.1 h^{-1} at 60 °C. Diboryl amine products were isolated in good yield after recrystallization using pentane.

5.2 Introduction

Beginning in 1979, alkenyl boronate esters were shown to be precursors for palladium catalyzed cross-coupling reactions, now know as Suzuki coupling reactions. Utilizing a Pd(0) source and an aryl halide, new carbon-carbon bonds were formed.[107]

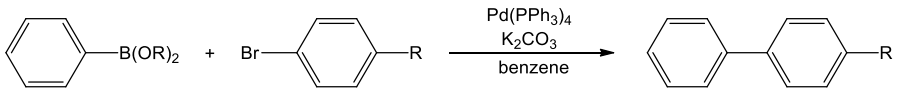

Fig. 5.1 General format for Suzuki coupling.

These reagents are typically prepared through the addition of Grignard or organolithium reagents to trialkyl borates.[108] However, more efficient direct addition[109] or catalyzed methods[110] are needed and sought after. One such reaction that has been evaluated is transition metal catalyzed alkyne hydroboration. Several notable catalysts of this transformation include a (PNP)$RuH_2(H_2)$ complex developed by Leitner,[111] which resulted in *Z*-alkenyl boronate esters with TOFs up to 41.6 h^{-1} (**Scheme 5.1**), and a $[(PC^{BIm}P)Rh(ACN)]PF_6$ complex developed by Rieger,[112] which resulted in *E*-alkenyl boronate esters with TOFs up to 2.0 h^{-1} (**Scheme 5.2**).

Scheme 5.1 Ruthenium catalyzed formation of *cis*-alkenyl borolanes

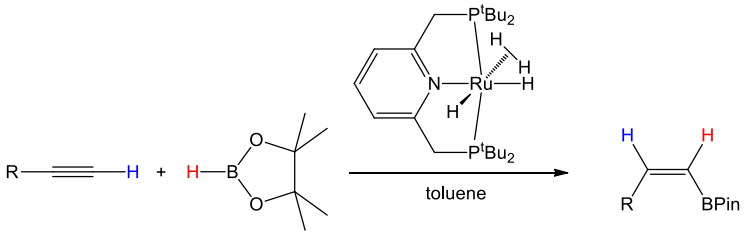

Scheme 5.2 Rhodium catalyzed formation of *trans*-alkenyl borolanes.

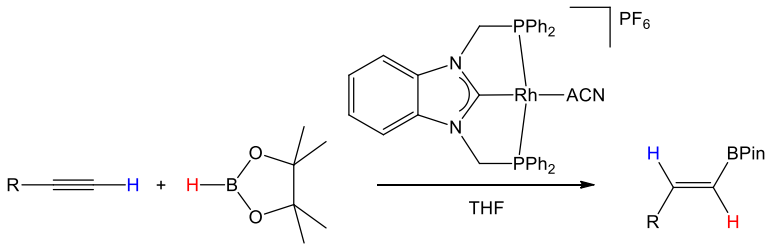

Few examples of cobalt-mediated alkyne hydroboration have been reported. In 2015, it was determined by Chirik that the bis(imino)pyridine cobalt alkyl complex, ($^{2,6\text{-iPr2Ph}}$PDI)$CoCH_3$, affords *E*-alkenyl boronate esters, while cyclohexyl-substituted (^{Cy}PDI)$CoCH_3$ yields *Z*-alkenyl boronate esters with TOFs of up to 6 h^{-1} at ambient temperature.[113] Zuo and Huang subsequently reported that *in situ* activation of (IPO)$CoCl_2$ with 2 equiv. of $NaEt_3BH$ allows for alkyne dihydroboration TOFs of up to 3 h^{-1} (6 h^{-1} based on pinacol borane, HBPin).[114]

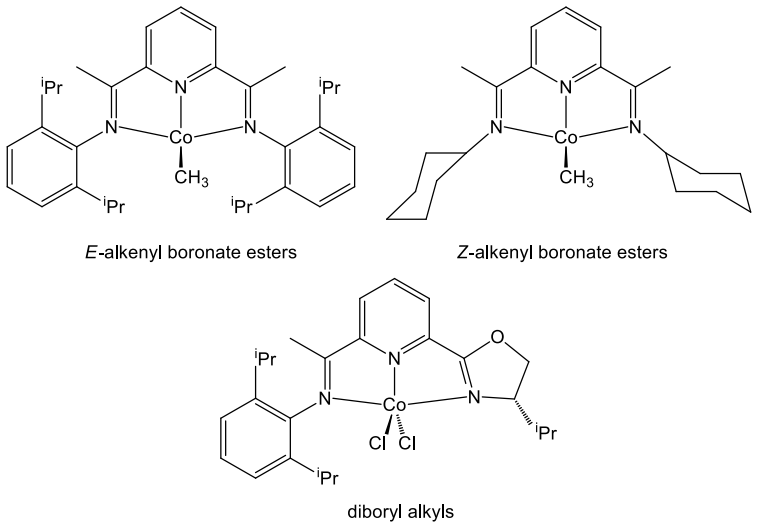

Fig. 5.2 Cobalt catalysts active for alkyne hydroboration.

Moreover, few catalysts for nitrile dihydroboration have been described in the literature. In 2012, Nikonov and coworkers reported that (2,6-$^{i}Pr_2C_6H_3N$)$MoH(Cl)(PMe_3)_3$ (**Fig. 5.3**,

a) catalyzes the dihydroboration of acetonitrile and benzonitrile in the presence of catechol borane (HBCat) at 5.0 mol% loading after 12 h at 22 °C.[115] Subsequently, this catalyst and related compounds, (2,6-$^{i}Pr_2C_6H_3N$)$MoH_2(PMe_3)_3$ and (η^3-2,6-$^{i}Pr_2C_6H_3NHBCat$)$MoH_2(PMe_3)_3$ were found to reduce an expanded nitrile scope with HBCat.[116] Fu proposed a mechanism involving the formation of a boryl-imine intermediate in their studies with (XantPhos)Rh(B((OCH$_2$)$_2$C(CH$_3$)$_2$)) (**Fig. 5.3**, **b**).[117] In 2016, Hill and co-workers achieved nitrile dihydroboration using HBPin and a butylmagnesium *β*-diiminate catalyst (**Fig. 5.3**, **c**) at 60 °C with 10 mol% catalyst loading, converting propionitrile to the *N*,*N*-diborylpropylamine within 30 min.[118] A loading of 5.0 mol% was used by Szymczak when investigating the substrate scope and functional group tolerance of [(BH$_0$PI)Ru(PPh$_3$)$_2$][K(18-crown-6)] (**Fig. 5.3**, **d**) catalyzed nitrile dihydroboration at 45 °C using HBPin.[119] [(*p*-Cymene)RuCl$_2$]$_2$ (**Fig. 5.3**, **e**) was found to mediate the slow dihydroboration of benzylnitrile at ambient temperature, with complete turnover after 24 h at 60 °C.[120] A broad substrate scope was effectively reduced with HBPin over 15-36 h. In 2017, Fout reported a (^{DIPP}CCC)Co(N$_2$) (**Fig. 5.3**, **f**) complex that catalyzed nitrile dihydroboration with HBPin at 70 °C with TOFs up to 2.5 h^{-1} which, along with the study presented herein, are the first reported examples of cobalt catalyzed nitrile dihydroboration.[121] These new diborylamines represent a new class of substrates that may be utilized for cross coupling reactions or as precursors for the synthesis of amines.

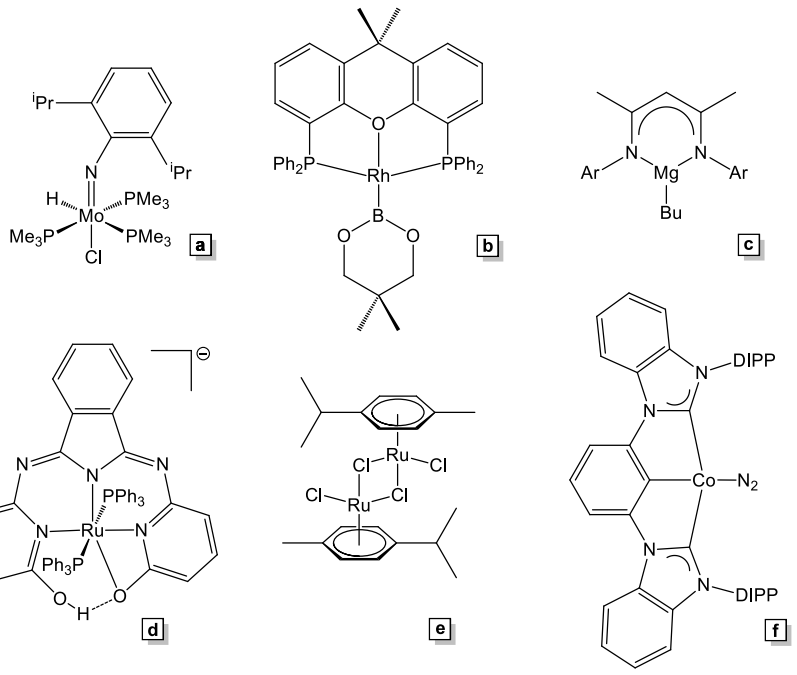

Fig. 5.3 Catalysts active for nitrile hydroboration

5.3 (^{Ph2PPr}DI)$CoCl_2$

An equimolar amount of ^{Ph2PPr}DI was added to a suspension of $CoCl_2$ in acetonitrile and stirred for 24 h, yielding a dark red compound identified as (^{Ph2PPr}DI)$CoCl_2$ (**4**). ^{1}H NMR spectroscopy revealed that **4** is a paramagnetic compound, exhibiting resonances from -14 to 23 ppm. Additionally, it was determined that **4** has two different binding modes at ambient temperature, with one predominating at -20 °C.

Scheme 5.3 Synthesis of **4**.

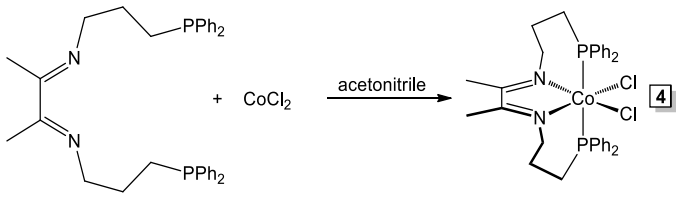

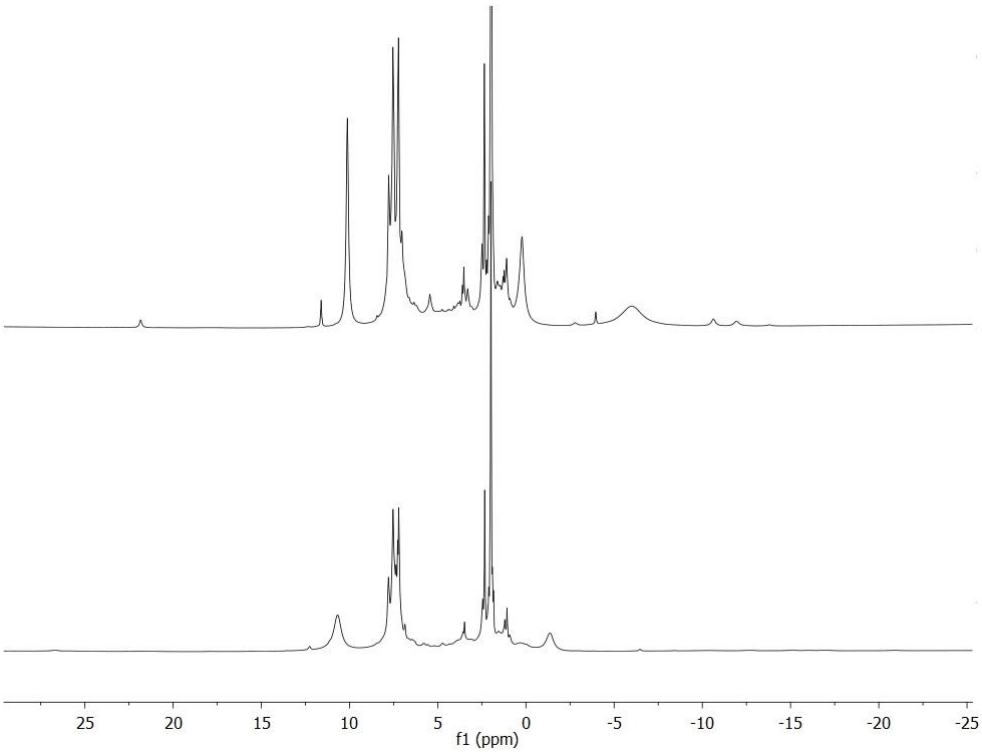

Fig. 5.4 ^{1}H NMR spectrum of **4** in acetonitrile-d_3 at 23 °C (top) and -20 °C (bottom).

Compound **4** was determined to have a magnetic moment of 2.8 μ_B at 25 °C as determined by both Evans method[122] and with a magnetic susceptibility balance. Crystals suitable for single crystal XRD were grown from a saturated solution in acetonitrile at -35 °C.

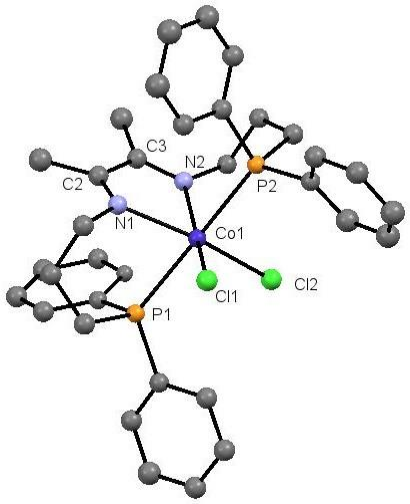

Fig. 5.5 Solid state structure of **4**, drawn with 30% probability ellipsoids. Hydrogen atoms omitted for clarity.

Analysis of the bond lengths reveals C=N distances of 1.273(10) and 1.303(10) Å and a C-C distance of 1.492(10) Å indicating a neutral DI (no ligand reduction) and a Co(II) centre. To confirm this assignment, an electron paramagnetic resonance (EPR) spectrum was collected at 9.4 GHz and 113 K, which revealed a broad and nearly isotropic signal extending over 90 mT, consistent with a low-spin ^{59}Co(II) (d^7, S_{Co}= 1/2, I_{Co}= 7/2) electronic structure.

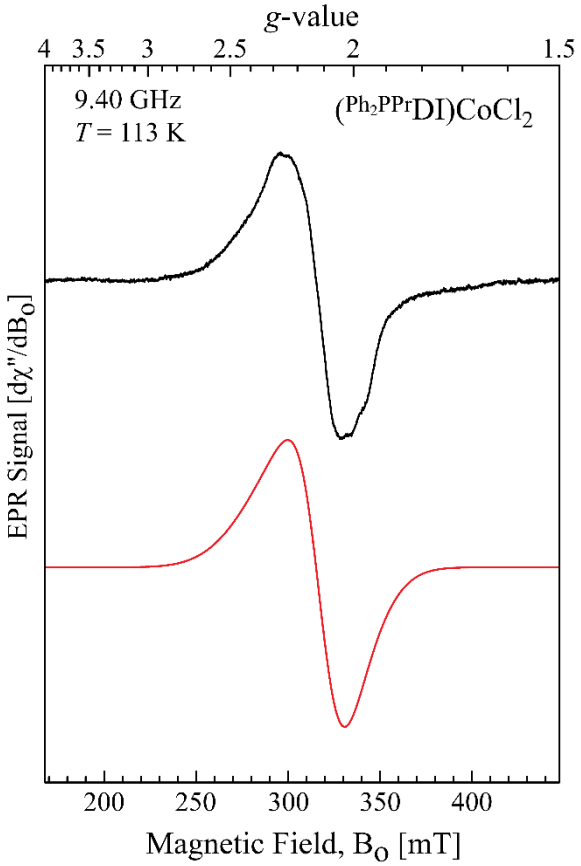

Fig. 5.6 EPR spectrum of **4** in acetonitrile at 113 K.

5.4 ^{Ph2PPr}DICoH

Suspension of **4** in diethyl ether and the addition of 2.1 equivalents of $NaEt_3BH$ allowed for the isolation of (^{Ph2PPr}DI)CoH (**5**), first characterized by Hagit Levin. Crystals of **5** suitable for XRD were grown from diethyl ether and analysis revealed C=N distances of 1.347(2) and 1.357(2) Å and a C-C distance of 1.401(3) Å, indicating that **5** likely possesses a singly reduced DI chelate and a Co(II) centre.

Scheme 5.4 Synthesis of **5**.

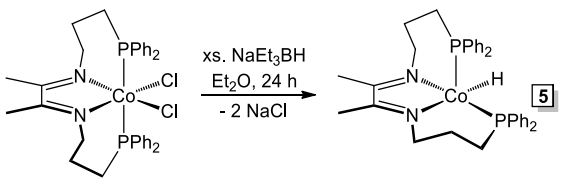

To confirm the electronic structure proposed from the observed bond lengths, density functional theory (DFT) calculations were performed (by Amanda C. Bowman at Colorado College). An unrestricted Kohn-Sham (UKS) calculation converged to the restricted Kohn-Sham (RKS) solution, which features highly mixed molecular orbitals (e.g., the HOMO possesses only 28% Co character, **Fig. 5.7**).

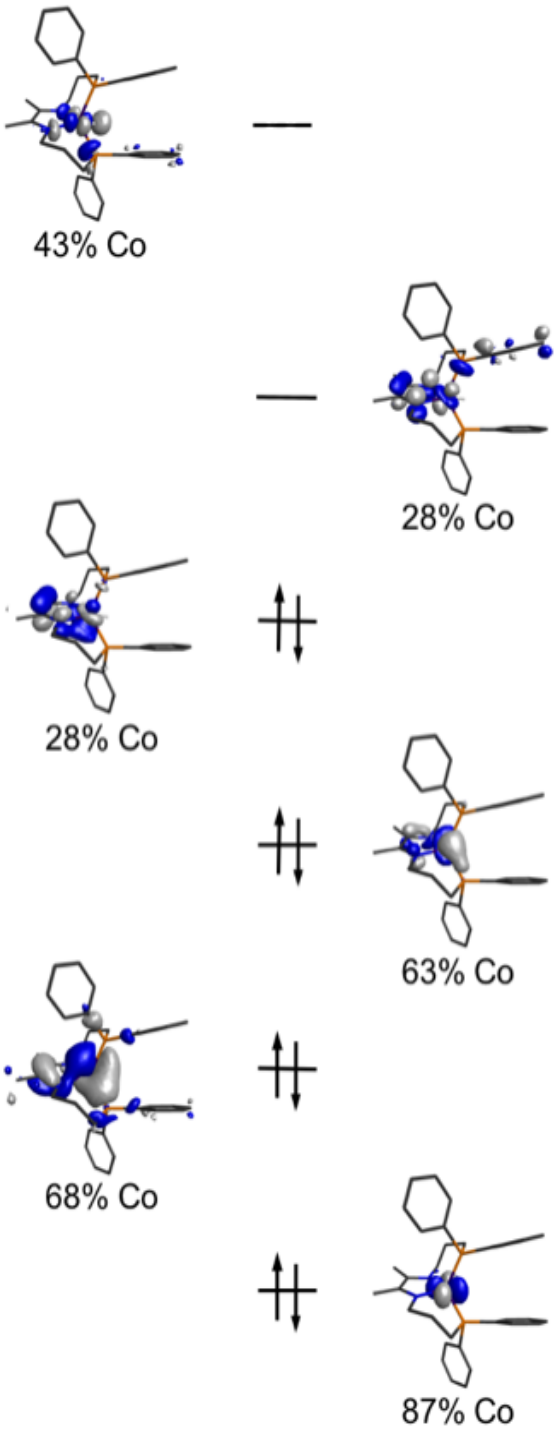

Fig. 5.7 Qualitative molecular orbital diagram and representations for the **5** rks (S = 0) solution.

A broken symmetry calculation [BS(1,1)] was then performed, revealing a low-spin Co(II) metal centre that is antiferromagnetically coupled to a DI based electron (S = 0.66).

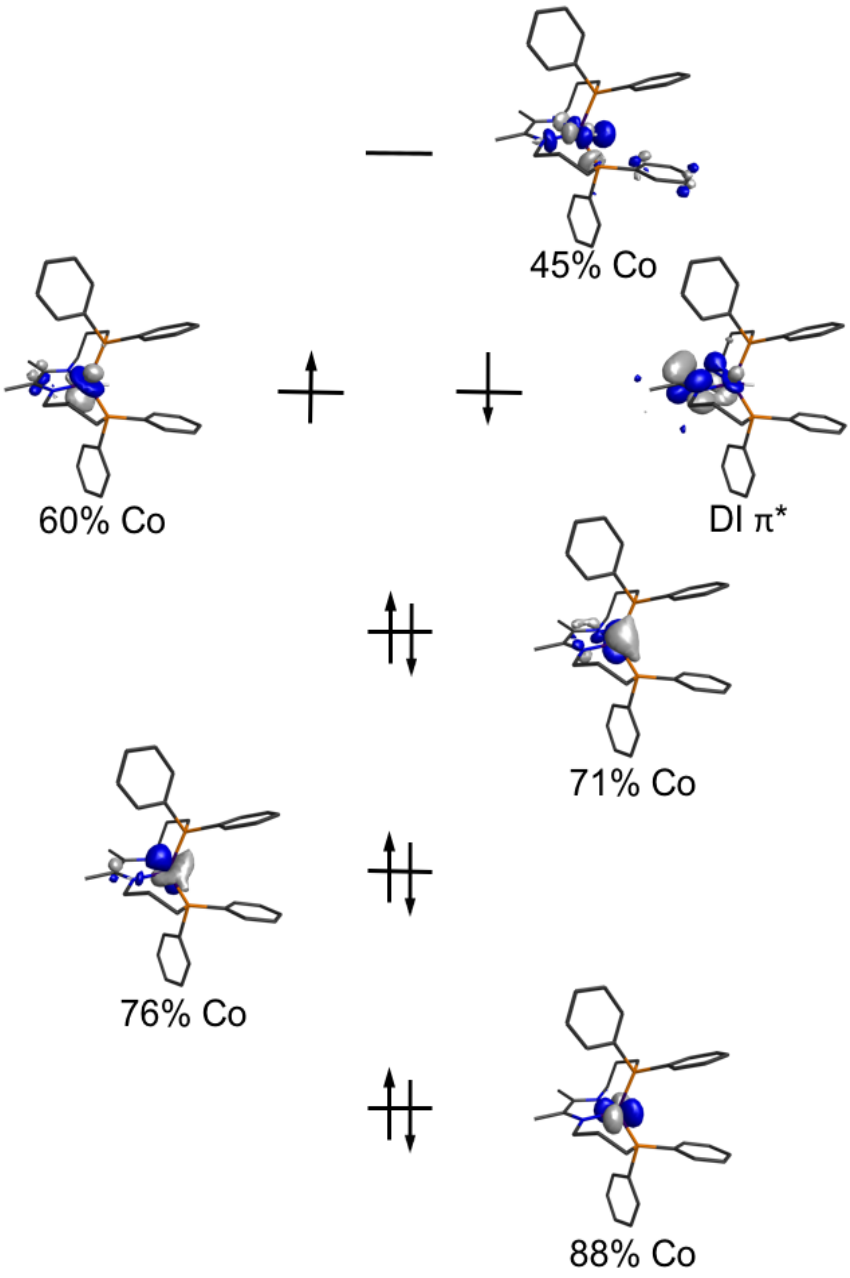

Fig. 5.8 Qualitative molecular orbital diagram and representations for the **5** BS(1,1) solution.

The spin density plot for this solution features a charge of +0.74 on the metal and an overall charge of -0.72 on the DI backbone (**Fig. 5.9**). The RKS and BS(1,1) solutions reasonably match the experimental metrical parameters determined for **5** (**Table 5.5**), and the BS(1,1) solution was found to be 1.2 kcal/mol lower in energy. Performing single point UKS and BS(1,1) calculations using the solid-state structure coordinates revealed a smaller preference for BS(1,1) of 0.6 kcal/mol. Given this slight preference, the electronic structure of **5** is consistent with a low-spin Co(II) centre that is antiferromagnetically coupled to a DI radical anion (**Fig. 5.10**).

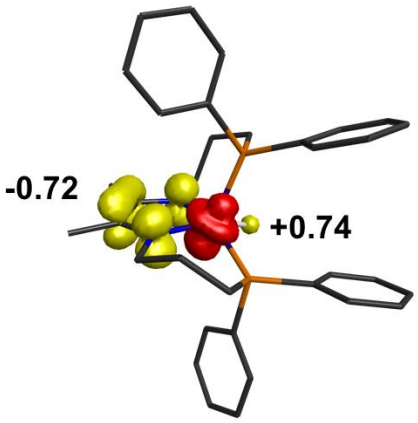

Fig. 5.9 Mulliken Spin density plot of BS(1,1) solution of **5**.

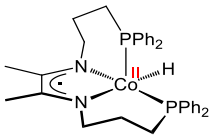

Fig. 5.10 Updated electronic structure of **5**.

Addition of pinacol borane (HBPin) to 1-hexyne with 1.0 mol% **5** in benzene-d_6 resulted in >99% conversion to the *E*-alkenyl boronate ester. Adding excess HBPin did not result in dihydroboration. Lowering the catalyst loading to 0.1 mol% under neat conditions resulted in 90% alkyne hydroboration within 1 h, with >99% conversion observed via ^{1}H

NMR within 2 h (maximum TOF of 900 h^{-1}). This work was done cooperatively by Levin and the author.

Table 5.1 Hydroboration of alkynes with 1.0 mol% **5** and HBPin.

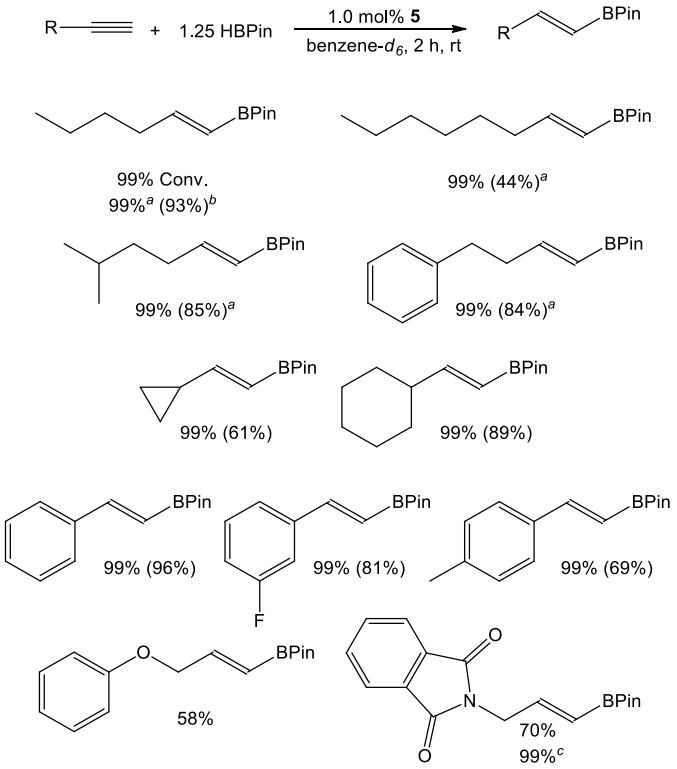

[a]Trial performed at 0.1 mol% **5** under neat conditions. [b]Isolated yields shown in parenthesis. [c]Conversion after 6 h.

5.5 Nitrile Dihydroboration

With the understanding that **5** is an effective alkyne hydroboration catalyst, expansion of this work to other multiple bond systems was explored. While the conversion of alkenes to alkyl boranes was unsuccessful, the conversion of nitriles to diboryl amines was observed. Adding an equimolar amount of HBPin and benzonitrile to 1.0 mol% **5** resulted in partial conversion of benzonitrile to the *N*,*N*-diborylated product after 6 h at ambient temperature. After a further 18 h, ^{1}H NMR spectroscopy revealed further, but incomplete, conversion.

It was quickly determined that HBPin was the limiting reagent, and the reaction was promptly repeated with 2.2 equivalents. Complete conversion to the diboryl amine was observed after 24 h at 60 °C, with a solid product being isolated after removal of solvent and recrystallization from pentane.

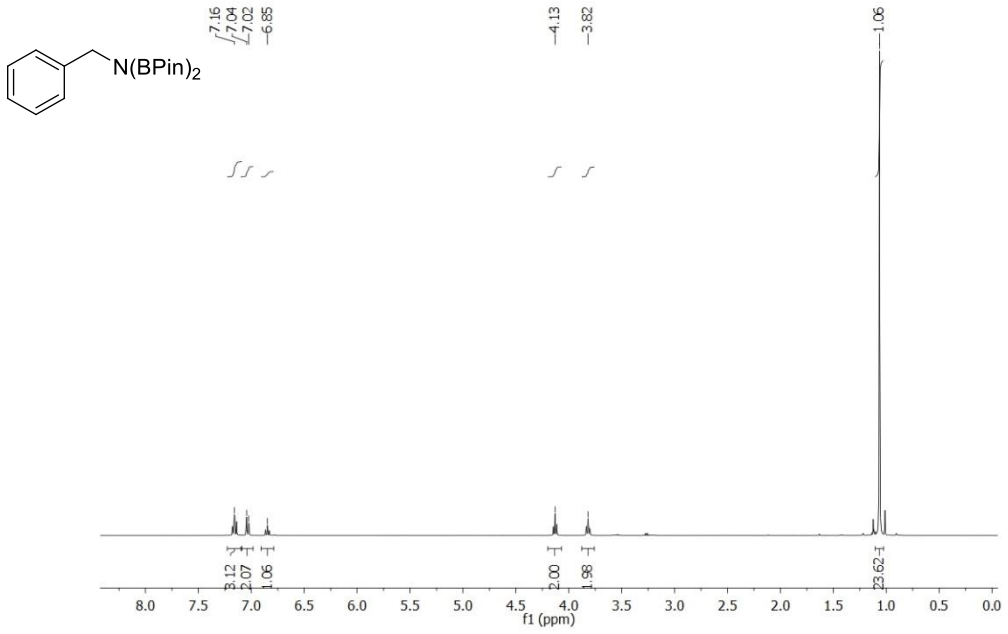

Fig. 5.11 ^{1}H NMR spectrum of isolated *N*-benzyl-4,4,5,5-tetramethyl-*N*-(4,4,5,5-tetramethyl-1,3,2-dioxaborolan-2-yl)-1,3,2-dioxaborolan-2-amine in benzene-d_6.

Attempts to lower the catalyst loading to 0.1 mol% and run the reactions under neat conditions proved unsuccessful, as the solid product inhibits complete conversion. A further 6 nitriles were successfully dihydroborated and isolated (**Table 5.2**). At 60 °C **5**-mediated nitrile dihydroboration was found to operate at TOFs of up to 4.1 h^{-1}.

Table 5.2 Dihydroboration of nitriles using 1.0 mol% **5** at 60 °C.

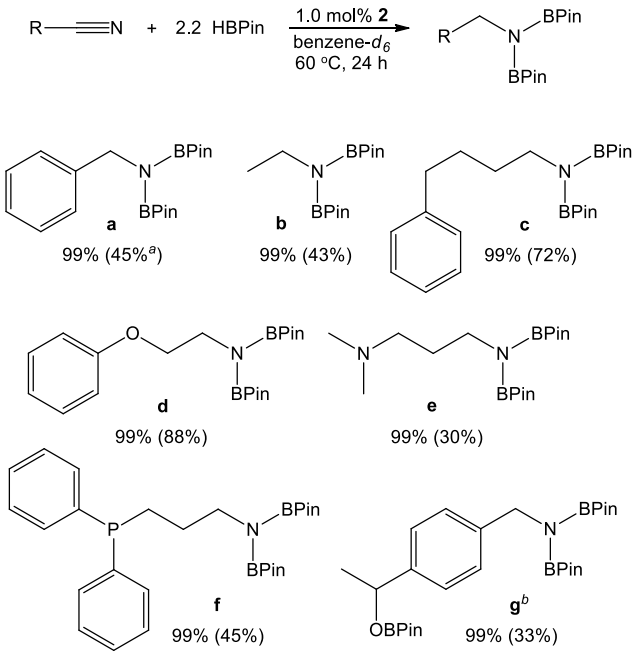

[a]Isolated yields in parenthesis. [b]Trial conducted with 3.3 equiv. HBPin.

Of note are the donating groups present in 3-(diphenylphosphino)propanenitrile and 3-(*N*,*N*-dimethylamino)propanenitrile; these coordinating groups could inhibit catalysis by binding to the metal centre in place of substrate. However, it does not appear as though this is the case, as there is no reduction in the rate of catalysis for these substrates when compared to their donor-free counterparts. Also of note is the use of 3.3 equivalents of HBPin for the reduction of 4-cyano-acetophenone. The use of 2.2 equivalents of HBPin resulted in complete carbonyl hydroboration, with partial nitrile dihydroboration, within 30 minutes. The use of 3.3 equivalents allowed for >99% conversion to the trihydroborated product, indicating that **5** is a highly active carbonyl hydroboration catalyst, although this transformation was not further explored during this project. Furthermore, it can be noted that **5** is the first example of cobalt catalyzed nitrile dihydroboration reported in the

literature, along with a CCC-pincer Co(N_2) complex reported by Fout, as both studies were published concurrently.[114]

5.6 Lewis Acid Catalysis

To ensure that the dihydroboration of nitriles is indeed catalyzed through a **5** mediated pathway that utilizes traditional transition metal pathways and not through an ion catalyzed reaction, several control experiments were performed. First, benzonitrile was combined with 2.2 equivalents of HBPin in the absence of any catalyst. No reaction was observed at either ambient temperature or 60 °C, either under neat conditions or dissolved in benzene-d_6. A series of Lewis Acids were then screened to check for their efficacy for this transformation. Adding 10 mol% BH_3·THF to a neat mixture of benzonitrile and 2.2 equivalents of HBPin resulted in 24% conversion within 5 h at ambient temperature, while 51% conversion was observed at 60 °C in the same time. BH_3·THF proved to be the most efficient of the screened catalysts, although it did not approach the established efficiency of **5**. It should be noted that HBPin is typically prepared from pinacol and BH_3, so impure materials may lead to "self-catalyzed" reactions.[123]

Table 5.3 Benzonitrile dihydroboration percent conversions by Lewis Acid catalysts.

Catalyst	10 mol% RT 5 h	10 mol% 60 °C 5 h
none	0	0
BH_3·THF	24%	51%
BF_3·Et_2O	10%	16%
$FeCl_2$	0%	0%
$FeBr_3$	0%	0%
$Fe(OTf)_2$	0%	0%
$La(OTF)_3$	0%	0%
$AlCl_3$	0%	0%
$Al(^iBu)_3$	0%	0%

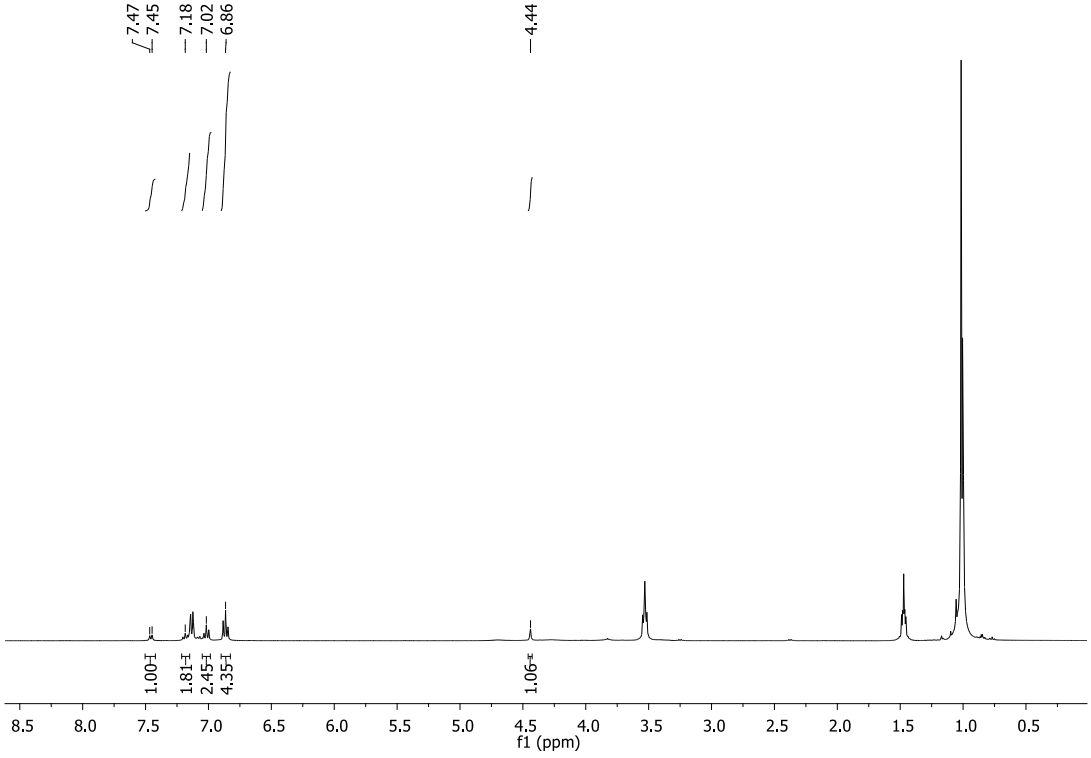

Fig. 5.12 Representative ^{1}H NMR spectrum of benzonitrile with 2.2 equivalents of HBPin catalyzed by 10% BH_3·THF at ambient temperature.

5.7 Conclusion

In summary, ^{Ph2PPr}DI was added to $CoCl_2$ to form (^{Ph2PPr}DI)$CoCl_2$ (**4**), which had two binding modes based on variable temperature paramagnetic ^{1}H NMR spectroscopy but yielded an octahedral complex when crystals suitable for XRD were grown. Adding an excess of $NaEt_3BH$ resulted in the formation of (^{Ph2PPr}DI)CoH (**5**), which was found to be an active catalyst for the hydroboration of alkynes. Compound **5** was subsequently found to be active for nitrile dihydroboration, with >99% conversion being observed after 24 h at 60 °C. Diboryl amines were isolated in good yield after recrystallization from pentane. **5** is one of the first reported examples of a cobalt based nitrile dihydroboration catalyst. Control reactions performed during the course of this study determined that this transformation can be catalyzed by Lewis Acids, with 10 mol% BH_3·THF being the most efficient of these, resulting in 51% conversion after 5 h at 60 °C.[124]

5.8 Experimental Details

General Considerations: All reactions were performed inside an MBraun glovebox under an atmosphere of purified nitrogen. Toluene, tetrahydrofuran, diethyl ether, and pentane were purchased from Sigma-Aldrich, purified using a Pure Process Technology solvent system, and stored in the glovebox over activated 4Å molecular sieves and sodium before use. Benzene-d_6 was purchased from Cambridge Isotope Laboratories or Oakwood Chemicals and dried over 4Å molecular sieves and potassium. Acetonitrile-d_3 was obtained from Oakwood Chemicals and dried over 3Å molecular sieves prior to use. Chloroform-*d* was purchased from Cambridge Isotope Laboratories and dried over 4Å molecular sieves. Celite was purchased from Acros Organics. Cobalt dichloride was purchased from Strem.

1-Octyne and phenyl propargyl ether were purchased from Fisher Scientific. 4-Ethynyltoluene was purchased from Santa Cruz Biotechnology. 5-Methyl-1-hexyne and cyclohexylacetylene were purchased from Alfa Aesar. 2-Phenoxyacetonitrile, 3-fluorophenylacetylene, and 4-phenyl-1-butyne were obtained from Oakwood Chemicals. Cyclopropylacetylene, *N*-propargyl phthalimide, and 4-ethynylanisole were purchased from Combi-Blocks. Benzonitrile was purchased from TCI. 1-Hexyne, phenylacetylene, anisole, 1,4-dioxane, pinacolborane, catecholborane, 4-phenylbutyronitrile, 4-acetylbenzonitrile, and sodium triethyl borohydride were purchased from Sigma Aldrich. Acetonitrile was purchased from Sigma Aldrich and dried over 3Å molecular sieves prior to use. All substrates were dried over 4Å molecular sieves prior to catalyst screening. 3-(diphenylphosphino)propanenitrile[95] and ^{Ph2PPr}DI[23] were synthesized according to literature procedures.

Solution nuclear magnetic resonance (NMR) spectra were recorded at room temperature on a Varian 400 MHz, a Bruker 400 MHz, or a Varian 500 MHz NMR spectrometer. All ^{1}H NMR and ^{13}C NMR chemical shifts (ppm) are reported relative to $Si(Me)_4$ using ^{1}H (residual) and ^{13}C chemical shifts of the solvent as secondary standards. ^{31}P NMR chemical shifts (ppm) are reported relative to phosphoric acid. Elemental analyses were performed at the Goldwater Environmental Laboratory at Arizona State University and Robertson Microlit Laboratories Inc. (Ledgewood, NJ). Solution phase magnetic susceptibility was determined using Evans method. Solid state magnetic susceptibility was determined at 25 °C using a Johnson Matthey magnetic susceptibility balance calibrated with $HgCo(SCN)_4$.

X-ray Crystallography: Single crystals suitable for X-ray diffraction were coated with polyisobutylene oil in the glovebox and transferred to a glass fiber with Apiezon N grease, which was then mounted on the goniometer head of a Bruker APEX Diffractometer equipped with Mo Kα radiation (Arizona State University). A hemisphere routine was used for data collection and determination of the lattice constants. The space group was identified and the data was processed using the Bruker SAINT+ program and corrected for absorption using SADABS. The structures were solved using direct method (SHELXS) completed by subsequent Fourier synthesis and refined by full-matrix, least square procedures on [F^2] (SHELXL). The solid-state structure of **(^{Ph2PPr}DI)CoCl$_2$** was found to feature two molecules in the asymmetric unit with two co-crystallized acetonitrile molecules; however, the data is not of sufficient quality to report in CIF format (R = 0.0984).

DFT Calculations: All DFT calculations were carried out using the ORCA program,[125] and all compounds were optimized with the B3LYP functional.[126] Empirical van der Waals corrections were included in the geometry optimization of all molecules.[127] The self-consistent field (SCF) calculations were tightly converged (1×10^{-8} E_h in energy, 1×10^{-7} E_h in density charge). Ahlrichs triple-ξ valence basis sets with one set of first polarization functions (def2-TZVP) were used for the cobalt, phosphorus, and nitrogen atoms.[128] Ahlrichs split valence basis sets with one set of first polarization functions (def2-SVP) were used for the carbon and hydrogen atoms.[128] Auxiliary basis sets were chosen to match the orbital basis sets used. Molecular orbitals were visualized using the Molekel program.[129]

Table 5.4 Relative energies calculated for **5**.

	Energy (Hartree)	ΔE (kJ/mol)	ΔE (kcal/mol)
rks	-3492.163067931415	4.915345	1.174783
uks (*S* = 0)	-3492.163068074221	4.914970	1.174694
BS(1,1)	-3492.164940087330	0.000000	0.000000
uks (*S* = 0) xtal (no opt)	-3491.617720739870	2.648872	0.633089
BS(1,1) xtal (no opt)	-3491.618729641740	0.000000	0.000000

Table 5.5 A comparison of metrical parameters calculated for **5**.

	Expt.	rks	uks (S = 0) xtal (no opt)	uks (S = 0)	BS(1,1)	BS(1,1) xtal (no opt)
C-N	1.347 1.357	1.349 1.355	1.347 1.357	1.349 1.355	1.347 1.352	1.347 1.357
C-C	1.401	1.414	1.401	1.414	1.420	1.401
Co-N_{DI}	1.887 1.916	1.894 1.922	1.887 1.916	1.894 1.922	1.924 1.961	1.887 1.916
Co-H	1.439	1.498	1.439	1.498	1.502	1.439
Co-P	2.146 2.137	2.173 2.165	2.146 2.137	2.173 2.165	2.238 2.183	2.146 2.137
P-Co-P	114.4	115.6	114.4	115.6	111.7	114.4
N-Co-N	81.9	82.1	81.9	82.1	81.7	81.9
$N_{DI,1}$-Co-H	95.0	91.6	95.0	91.6	91.4	95.0
$N_{DI,2}$-Co-H	165.0	159.8	165.0	159.8	159.7	165.0
$N_{DI,1}$-Co-P_1	93.8	94.6	93.8	94.6	94.2	93.8
$N_{DI,1}$-Co-P_2	148.5	146.7	148.5	146.7	153.0	148.5
$N_{DI,2}$-Co-P_1	115.9	117.0	115.9	117.0	115.3	115.9
$N_{DI,2}$-Co-P_2	96.9	95.0	96.9	95.0	93.5	96.9

Electron Paramagnetic Resonance Spectroscopy:

Instrumentation. Studies were performed at the EPR Facility of Arizona State University. Continuous wave (CW) EPR spectra were recorded at 113 K using a Bruker ELEXSYS E580 CW X-band spectrometer (Bruker, Rheinstetten, Germany) equipped with a liquid nitrogen temperature control system (ER 4131VT). The magnetic field modulation frequency was 100 kHz with a field modulation of 1 mT peak-to-peak. The microwave power was 4 mW, the microwave frequency was 9.40 GHz and the sweep time was 168 seconds.

Spin Hamiltonian. The EPR spectrum of **(^{Ph2PPr}DI)CoCl$_2$** was interpreted using a spin Hamiltonian, $\mathcal{H}$, containing the electron Zeeman interaction with the applied magnetic field B_o and the hyperfine coupling (hfc) term:[130]

$$\mathcal{H} = \beta_e \, S.\boldsymbol{g}.\mathbf{Bo} + h \, \mathbf{S}.\boldsymbol{A}.\mathbf{I} \qquad (1)$$

where **S** is the electron spin operator, **I** is the nuclear spin operator of ^{59}Co, $\boldsymbol{A}$ is the hfc tensor in frequency units, $\boldsymbol{g}$ is the electronic *g*-tensor, β_e is the electron magneton, and *h* is Planck's constant. The best fit of the spectrum was obtained considering a single Co(0) ion (S = ½, I = 7/2).

Fitting of EPR spectra. To quantitatively compare experimental and simulated spectra, we divided the spectra into N intervals, i.e. we treated the spectrum as an N-dimensional vector **R**. Each component R_j has the amplitude of the EPR signal at a magnetic field B_j, with j varying from 1 to N. The amplitudes of the experimental and simulated spectra were normalized so that the span between the maximum and minimum values of R_j is 1. We compared the calculated amplitudes R_j^{calc} of the signal with the observed values R_j defining a root-mean-square deviation σ by:

$$\sigma(p_1, p_2, \ldots, p_n) = [\sum_j (R_j^{calc}(p_1, p_2, \ldots, p_n) - R_j^{exp})^2/N]^{½} \qquad (2)$$

where the sums are over the N values of j, and p's are the fitting parameters that produced the calculated spectrum. For our simulations, N was set equal to 2048. The EPR spectra were simulated using EasySpin (v 5.0.20), a computational package developed by Stoll and Schweiger[131] and based on Matlab (The MathWorks, Natick, MA, USA). EasySpin calculates EPR resonance fields using the energies of the states of the spin system obtained by direct diagonalization of the spin Hamiltonian (see Eq. 1). The EPR fitting procedure

used a Monte Carlo type iteration to minimize the root-mean-square deviation, σ (see Eq. 2) between measured and simulated spectra. We searched for the optimum values of the following parameters: the principal components of $\boldsymbol{g}$ (i.e. g_x, g_y, g_z), the principal components of the hfc tensor $\boldsymbol{A}$ (i.e. A_x, A_y, A_z) and the peak-to-peak line-widths (ΔB_x, ΔB_y, and ΔB_z).

Preparation of (^{Ph2PPr}DI)$CoCl_2$ (4): Under inert atmosphere, acetonitrile solutions (approx. 8 mL) of $CoCl_2$ (0.060 g, 0.458 mmol) and ^{Ph2PPr}DI (0.247 g, 0.461 mmol) were prepared in 20 mL scintillation vials and stirred for 15 min. The ligand solution was then pipetted into the $CoCl_2$ solution and the reaction was stirred for 24 h. The solution was filtered through Celite, the solvent was removed under reduced pressure, and the product was washed with pentane (10 mL). A dark red microcrystalline solid was isolated, yielding 0.213 g (0.151 mmol, 80%) of **4**. Magnetic Susceptibility (Evans method and magnetic susceptibility balance, 25 °C): $\mu_{eff} = 2.8\ \mu_B$. Analysis for $C_{34}H_{38}N_2P_2CoCl_2$ (666.44): Calcd. C, 61.27%; H, 5.75%; N, 4.20%. Found: C, 61.48%; H, 5.82%; N, 4.01%. ^{1}H NMR (acetonitrile-d_3, 25 °C, 500 MHz, peak width at half height in parenthesis): δ 21.84 (69.24), 11.60 (30.70), 10.12 (73.97), 0.22 (163.75), -2.80 (193.01), -3.96 (39.01), -6.00 (705.03), -10.63 (134.17), -11.93 (160.24), -13.81 (144.94). ^{1}H NMR (acetonitrile-d_3, -20 °C): δ 10.67 (244.02), -1.36 (265.41).

Preparation of (^{Ph2PPr}DI)CoH (5): Under inert atmosphere, a scintillation vial was charged with diethyl ether (12 mL) and **4** (0.138 g, 0.207 mmol). A 1.0 M solution of $NaEt_3BH$ in toluene (0.45 mL, 0.45 mmol) was then added and the reaction rapidly turned dark green as a soluble product formed. The solution was stirred for 24 h, filtered through Celite, and dried under reduced pressure. A dark green microcrystalline solid was isolated,

yielding 0.082 g (0.137 mmol, 66%) of **5**. Analysis for $C_{34}H_{39}N_2P_2Co$ (596.57): Calcd. C, 68.45%; H, 6.59%; N, 4.70%. Found: C, 68.86%; H, 7.51%; N, 4.86%. ^{1}H NMR (benzene-d_6, 400 MHz, 25 °C): δ 7.63 (t, 8.4 Hz, 2H, *phenyl*), 7.12 (t, 8.4 Hz, 2H, *phenyl*), 7.00 (m, 5H, *phenyl*), 6.88 (m, 6H, *phenyl*), 6.72 (t, 7.4 Hz, 3H, *phenyl*), 6.65 (t, 7.4 Hz, 2H, *phenyl*), 4.81 (t, 12.1 Hz, 1H, CH_2), 4.51 (m, 1H, CH_2), 3.26 (m, 1H, CH_2), 3.09 (m, 1H, CH_2), 2.52 (m, 2H, CH_2), 2.11 (m, 4H, CH_2), 2.00 (pseudo q, 2H, CH_2), 1.51 (dd, 22.3 Hz, 7.8 Hz, 6H, CH_3), -19.80 (dd, 90.2 Hz, 39.3 Hz, 1H, Co*H*). ^{13}C{^{1}H} NMR (benzene-d_6, 125 MHz, 25 °C): δ 142.66 (*phenyl*), 140.09 (*phenyl*), 139.72 (*phenyl*), 139.52 (*phenyl*), 135.72 (d, J_{CP} = 13.0 Hz, *phenyl*), 133.42 (d, J_{CP} = 11.4 Hz, phenyl), 131.05 (dd, J_{CP} = 10.3, 3.2 Hz, *phenyl*), 128.83 (*phenyl*), 128.74 (*phenyl*), 128.65 (*phenyl*), 128.46 (*phenyl*), 128.27 (*phenyl*), 128.09 (*phenyl*), 128.05 (*phenyl*), 128.02 (*phenyl*), 127.99 (*phenyl*), 127.94 (*phenyl*), 127.87 (*phenyl*), 127.64 (*C*CH$_3$), 127.43 (*C*CH$_3$), 61.79 (*C*H$_2$), 55.19 (*C*H$_2$), 31.12 (d, J_{CP} = 25.2 Hz, *C*H$_2$), 30.54 (*C*H$_2$), 28.95 (d, J_{CP} = 15.7 Hz, *C*H$_2$), 26.86 (d, J_{CP} = 12.6 Hz, *C*H$_2$), 17.25 (d, J_{CP} = 4.0 Hz, *C*H$_3$), 15.19 (d, J_{CP} = 4.0 Hz, *C*H$_3$). ^{31}P{^{1}H} NMR (benzene-d_6, 162 MHz, 25 °C): δ 75.33 (br), 50.59 (br).

Dihydroboration of benzonitrile using 1.0 mol% 5: Under an inert atmosphere, benzonitrile (97 µL, 0.939 mmol) and pinacolborane (300 µL, 2.07 mmol) were combined in a 20 mL scintillation vial with 0.5 mL benzene-d_6. This solution was transferred to a vial containing 0.0056 g of **5** (0.00939 mmol). The vial was sealed and stirred at 60 °C for 24 h. The solution was then exposed to air to deactivate the catalyst. Greater than 99% conversion was observed by ^{1}H NMR spectroscopy. Solvent and remaining borane were removed under reduced pressure, resulting in a white solid. Recrystallization from pentane at -35 °C yielded 0.153 g (45 %) of *N*-benzyl-4,4,5,5-tetramethyl-*N*-(4,4,5,5-tetramethyl-

1,3,2-dioxaborolan-2-yl)-1,3,2-dioxaborolan-2-amine. ^{1}H NMR (benzene-d_6): 7.58 (d, J = 7.6 Hz, 2H, *Ar*), 7.27-7.22 (m, 2H, *Ar*), 7.14-7.08 (m, 1H, *Ar*), 4.60 (s, 2H, CH_2), 1.03 (s, 24H, CH_3). ^{13}C NMR (benzene-d_6): 144.11 (*Ar*), 128.68 (*Ar*), 126.98 (*Ar*), 82.91 (*C*CH_3), 48.25 (*C*H_3), 25.06 (*C*H_3), one phenyl resonance not located.

Dihydroboration of acetonitrile using 1.0 mol% 5: Under an inert atmosphere, acetonitrile (55 µL, 1.06 mmol) and pinacolborane (338 µL, 2.33 mmol) were combined in a 20 mL scintillation vial with 0.5 mL benzene-d_6. This solution was transferred to a vial containing 0.0063 g of **5** (0.0106 mmol). The vial was sealed and stirred at 60 °C for 24 h. The solution was then exposed to air to deactivate the catalyst. Greater than 99% conversion was observed using ^{1}H NMR spectroscopy. Solvent and residual borane were removed under reduced pressure, resulting in a white solid. Recrystallization from pentane at -35 °C yielded 0.134 g (43%) of *N*-ethyl-4,4,5,5-tetramethyl-*N*-(4,4,5,5-tetramethyl-1,3,2-dioxaborolan-2-yl)-1,3,2-dioxaborolan-2-amine. ^{1}H NMR (benzene-d_6, 400 MHz): 3.49 (q, J = 7.0 Hz, 2H, CH_2), 1.34 (t, J = 7.0 Hz, 3H, CH_3), 1.07 (s, 24H, CH_3). ^{13}C NMR (benzene-d_6): 82.58 (*C*CH_3), 39.51 (*C*H_2), 25.11 (*C*H_3), 19.58 (*C*H_3).

Dihydroboration of 4-phenylbutyronitrile using 1.0 mol% 5: Under an inert atmosphere, 4-phenylbutyronitrile (130 µL, 0.872 mmol) and pinacolborane (278 µL, 1.91 mmol) were combined in a 20 mL scintillation vial with 0.5 mL benzene-d_6. This solution was transferred to a vial containing 0.0052 g of **5** (0.00872 mmol). The vial was sealed and stirred at 60 °C for 24 h. The solution was then exposed to air to deactivate the catalyst. By ^{1}H NMR spectroscopy, it was determined that 85% conversion was reached. Solvent and remaining borane were removed under reduced pressure, resulting in a white solid. Recrystallization from pentane at -35 °C yielded 0.250 g (72%) of 4,4,5,5-tetramethyl-*N*-

(4-phenylbutyl)-*N*-(4,4,5,5-tetramethyl-1,3,2-dioxaborolan-2-yl)-1,3,2-dioxaborolan-2-amine. ^{1}H NMR (benzene-d_6): 7.22 – 7.14 (m, 2H, *Ar*), 7.11 – 7.05 (m, 3H, *Ar*), 3.45 (t, *J* = 6.9 Hz, 2H, CH_2), 2.58 (t, *J* = 7.3 Hz, 2H, CH_2), 1.81 – 1.61 (m, 4H, CH_2), 1.08 (s, 24H, CH_3). ^{13}C NMR (benzene-d_6): 143.32 (*Ar*), 129.15 (*Ar*), 128.78 (*Ar*), 126.16 (*Ar*), 82.57 (*C*CH_3), 44.45 (*C*H_2), 36.37 (*C*H_2), 33.56 (*C*H_2), 29.24 (*C*H_2), 25.09 (*C*H_3).

Dihydroboration of 2-phenoxyacetonitrile using 1.0 mol% 5: Under an inert atmosphere, 2-phenoxyacetonitrile (117.0 µL, 0.955 mmol) and pinacolborane (305 µL, 2.10 mmol) were combined in a 20 mL scintillation vial with 0.5 mL benzene-d_6. This solution was transferred to a vial containing 0.0057 g of **5** (0.00955 mmol). The vial was sealed and stirred at 60 °C for 24 h. The solution was then exposed to air to deactivate the catalyst. Greater than 99% conversion was observed by ^{1}H NMR spectroscopy. Solvent and remaining borane were removed under reduced pressure, resulting in a white solid. Recrystallization from diethyl ether/pentane at -35 °C yielded 0.325 g (88%) of 4,4,5,5-tetramethyl-*N*-(2-phenoxyethyl)-*N*-(4,4,5,5-tetramethyl-1,3,2-dioxaborolan-2-yl)-1,3,2-dioxaborolan-2-amine. ^{1}H NMR (chloroform-*d*): 7.16 (m, 2H, *Ar*), 7.03 (m, 2H, *Ar*), 6.85 (m, 1H, *Ar*), 4.13 (t, *J* = 6.5 Hz, 2H, CH_2), 3.82 (t, *J* = 6.5 Hz, 2H, CH_2), 1.06 (s, 24H, CH_3). ^{13}C NMR (chloroform-*d*): 160.27 (*Ar*), 130.03 (*Ar*), 121.00 (*Ar*), 115.33 (*Ar*), 82.93 (*C*CH_3), 69.59 (*C*H_2), 43.71 (*C*H_2), 25.07 (*C*H_3).

Dihydroboration of 3-(dimethylamino)propanenitrile using 1.0 mol% 5: Under an inert atmosphere, 3-(dimethylamino)propanenitrile (106.0 µL, 0.939 mmol) and pinacolborane (300 µL, 2.07 mmol) were combined in a 20 mL scintillation vial with 0.5 mL benzene-d_6. This solution was transferred to a vial containing 0.0056 g of **5** (0.00939 mmol). The vial was sealed and stirred at 60 °C for 24 h. The solution was then exposed to

air to deactivate the catalyst. Greater than 99% conversion was observed by ^{1}H NMR spectroscopy. Solvent and remaining borane were removed under reduced pressure, resulting in a white solid. Recrystallization from pentane at -35 °C yielded 0.0996 g (30%) of N^1,N^1-dimethyl-N^3,N^3-*bis*-(4,4,5,5-tetramethyl-1,3,2-dioxaborolan-2-yl)propane-1,3-diamine. ^{1}H NMR (chloroform-*d*): 3.56 (t, *J* = 7.5 Hz, 2H, C*H*$_2$), 2.35 (t, *J* = 7.0 Hz, 2H, C*H*$_2$), 2.17 (s, 6H, NC*H*$_3$), 1.98 (t, *J* = 7.3 Hz, 2H, C*H*$_2$), 1.08 (s, 24H, C*H*$_3$). ^{13}C NMR (chloroform-*d*): 82.63 (*C*CH$_3$), 58.21 (-*C*H$_2$-), 45.97 (N*C*H$_3$), 43.16 (-*C*H$_2$-), 32.65 (-*C*H$_2$-), 25.12 (-*C*H$_3$).

Dihydroboration of 3-(diphenylphosphino)propanenitrile using 1.0 mol% 5: Under an inert atmosphere, 3-(diphenylphosphino)propanenitrile (225.7 mg, 0.955 mmol) and pinacolborane (305 µL, 2.10 mmol) were combined in a 20 mL scintillation vial with 0.5 mL benzene-d_6. This solution was transferred to a vial containing 0.0057 g of **5** (0.00955 mmol). The vial was sealed and stirred at 60 °C for 24 h. The solution was then exposed to air to deactivate the catalyst. Greater than 99% conversion was observed by ^{1}H NMR spectroscopy. Solvent and remaining borane were removed under reduced pressure, resulting in a white solid. Recrystallization from diethyl ether at -35 °C yielded 0.211 g (45%) of *N*-(3-(diphenylphosphino)propyl)-4,4,5,5-tetramethyl-*N*-(4,4,5,5-tetramethyl-1,3,2-dioxaborolan-2-yl)-1,3,2-dioxaborolan-2-amine. ^{1}H NMR (benzene-d_6): 7.45 (t, *J* = 6.7 Hz, 4H, *Ar*), 7.12 – 7.02 (m, 6H, *Ar*), 3.48 (t, *J* = 6.9 Hz, 2H, -C*H*$_2$-), 2.12 – 2.03 (m, 2H, -C*H*$_2$-), 1.96 – 1.80 (m, 2H, -C*H*$_2$-), 1.03 (s, 24H, -C*H*$_3$). ^{13}C NMR (benzene-d_6): 139.76 (d, *J* = 15.1 Hz, *Ar*), 132.81 (d, *J* = 18.5 Hz, *Ar*), 130.79 (d, *J* = 9.0 Hz, *Ar*), 128.21 (d, *J* = 6.2 Hz, *Ar*), 81.95 (*C*CH$_3$), 45.15 (d, *J* = 14.8 Hz, -*C*H$_2$-), 29.70 (d, *J* = 15.7 Hz, -*C*H$_2$-), 25.52 (d, *J* = 12.3 Hz, -*C*H$_2$-), 24.38 (-*C*H$_3$). ^{31}P NMR (benzene-d_6): -16.20.

Trihydroboration of 4-acetylbenzonitrile using 1.0 mol% 5: Under an inert atmosphere, 4-acetylbenzonitrile (124.0 mg, 0.855 mmol) and pinacolborane (409 µL, 2.82 mmol) were combined in a 20 mL scintillation vial with 0.5 mL benzene-d_6. This solution was transferred to a vial containing 0.0051 g of **5** (0.00855 mmol). Bubbling and heat generation was observed. The solution was stirred at 25 °C for 30 min, after which >99% carbonyl reduction was observed by ^{1}H NMR spectroscopy. The vial was sealed and stirred at 60 °C for 24 h. The solution was then exposed to air to deactivate the catalyst. Greater than 99% conversion was observed by ^{1}H NMR spectroscopy. Solvent and remaining borane were removed under reduced pressure, resulting in a white solid. Recrystallization from diethyl ether/pentane at -35 °C yielded 0.150 g (33%) of 4,4,5,5-tetramethyl-*N*-(4,4,5,5-tetramethyl-1,3,2-dioxaborolan-2-yl)-*N*-(4-(1-(4,4,5,5-tetramethyl-1,3,2-dioxaborolan-2-yloxy)ethyl)benzyl)-1,3,2-dioxaborolan-2-amine. ^{1}H NMR (benzene-d_6): 7.54 (d, *J* = 8.1 Hz, 2H, *Ar*), 7.42 (d, *J* = 8.2, 2H, *Ar*), 5.44 (q, *J* = 6.2, 1H, -C*H*-), 4.58 (s, 2H, -CH_2-), 1.48 (d, *J* = 6.4 Hz, 3H, -CH_3), 1.03 (s, 24H, -CH_3), 1.01 (s, 12H, -CH_3). ^{13}C NMR (benzene-d_6): 143.72 (*Ar*), 142.96 (*Ar*), 125.86 (*Ar*), 82.90 (*C*CH_3), 82.78 (*C*CH_3), 73.28 (*C*H), 47.98 (-*C*H_2-), 26.02 (-*C*H_3), 25.07 (-*C*H_3), 24.93 (-*C*H_3).

BIBLIOGRAPHY

1. a) Hoff, R.; Mathers, R. T. *Handbook of Transition Metal Polymerization Catalysts (Online ed.).* John Wiley & Sons, 2010. b) Natta, G.; Danusso, F. *Stereoregular Polymers and Stereospecific Polymerizations*, Pergamon Press, 1967.

2. a) Vineyard, B.D.; Knowles, W.S.; Sabacky, M. J.; Bachman, G. L.; Weinkauff, D. J. *J. Am. Chem. Soc.*, **1977**, *99* (18), 5946-5952. b) Noyori, R.; Ohkuma, T.; Kitamura, M.; Takaya, H.; Sayo, N.; Kumobayashi, H.; Akutagawa, S. *J. Am. Chem. Soc.*, **1987**, 109, 5856. c) Kolb, H. C.; Van Nieuwenhze, M. S.; Sharpless, B.K. *Chem. Rev.* **1994**, *94* (8), 2483-2547.

3. a) Bazan, G.C.; Oskam, J. H.; Cho, H. N.; Park, L. Y.; Schrock, R. R. *J. Am. Chem. Soc.* **1991**, *109* (18), 6899-6907. b) Schwab, P.; Grubbs, R. H.; Ziller, Joseph W. *J. Am. Chem. Soc.*, **1996**, *118*, 100-110. c) Scholl, M.; Trnka, T. M.; Morgan, J. P.; Grubbs, R. H. *Tetrahedron Lett.* **1999**, *40* (12), 2247-2250.

4. a) Heck, R. F.; Nolley, J. P. *J. Org. Chem.* **1972**, *37* (14), 2320-2322. b) King A. O.; Okukado, N.; Negishi, E. *J. Chem. Soc., Chem. Commun*. **1977**, *19*, 683. c) Miyaura, N.; Yamada, K.; Suzuki, A. *Tetrahedron Lett*. **1979**, *20* (36), 3437-3440.

5. Hartwig, J. F. *Organotransition Metal Chemistry - From Bonding to Catalysis*, University Science Books, 2010.

6. Osborn, J. A.; Jardine, F. H.; Young, J. F.; Wilkinson, G. *J. Chem. Soc.* **1966**, *12*, 1711-1732.

7. Fröhlich, P.; Lorenz, T.; Martin, G.; Brett, B.; Bertau, M. *Angew. Chem., Int. Ed*., **2017**, *56*, 2544.

8. (a) Madias, N. E.; Harrington, J. T. *Am. J. Med*., **1978**, *65*, 307; (b) Schmid, M.; Zimmermann, S.; Krug, H.F.; Sures, B. *Environ. Int*., **2007**, *33*, 385.

9. Barbalance, K. Periodic Table of Elements, https://environmentalchemistry.com/yogi/periodic (accessed: October 8th, 2018).

10. Yu, R. P.; Darmon, J. M.; Hoyt, J. M.; Margulieux, G. R.; Turner, Z.; Chirik, P. J. *ACS Catal.* **2012**, *2*, 1760-1764.

11. Hostier, T.; Neouchy, Z.; Ferey, V.; Gomez Pardo, D.; Cossy, J. *Org. Lett*. **2018**, *20*, 1815-1818.

12. Smieja, J. M.; Sampson, M. D.; Grice, K. A.; Benson, E. E.; Froehlich, J. D.; Kubiak, C. P. *Inorg. Chem*. **2013**, *52*, 2484-2491.

13. a) Lyaskovskyy, V.; de Bruin, B. *ACS Catal*. **2012**, *2*, 270-279. b) Chirik, P. J.; Wieghardt, K. *Science* **2010**, 327, 794-795.

14. a) Jørgensen, C. K. *Coord. Chem. Rev.*, **1966**, *1*, 164. b) Baker-Hawkes, M. J.; Billig, E.; Gray, H. B. *J. Am. Chem. Soc*., **1966**, *88*, 4870-4875.

15. Stubbert, B. D.; Peters, J. C.; Gray, H. B. *J. Am. Chem. Soc*., **2011**, *133*, 18070.

16. Luca, O. R.; Konezny, S. J.; Blakemore, J. D.; Saha, S.; Colosi, D. M.; Brudvig, G. W.; Batista, V. S.; Crabtree, R. H. *New J. Chem*., **2012**, *36*, 1149.

17. Chaudhuri, P.; Hess, M.; Müller, J.; Hildenbrand, K.; Bill, E.; Weyhermüller, T.; Wieghardt, K. *J. Am. Chem. Soc*. **1999**, *121*, 9599.

18. a) Gibson, V. C.; Redshaw, C.; Solan, G. A. *Chem. Rev.* **2007**, *107*, 1745-1776. b) Small, B. L.; Brookhart, M.; Bennett, A. M. A. *J. Am. Chem. Soc.* **1998**, *120*, 4049-4050. c) Britovsek, G. J. P.; Gibson, V. C.; Kimberley, B. S.; Maddox, P. J.; McTavish, S. J.; Solan, G. A.; White, A. J. P.; Williams, D.J. *Chem. Commun.* **1998**, 849-850.

19. a) Bart, S. C.; Lobkovsky, E.; Bill, E.; Chirik, P. J. *J. Am. Chem. Soc*. **2004**, *126*, 13794-13807. b) Trovitch, R. J.; Lobkovsky, E.; Bill, E.; Chirik, P. J. *Organometallics* **2008**, *27*, 1470. c) Sylvester, K. T.; Chirik, P. J. *J. Am. Chem. Soc.* **2009**, *131*, 8772-8774. d) Hoyt, J. M.; Schmidt, V. A.; Tondreau, A. M.; Chirik, P. J. *Science*, **2015**, *349*, 960-963.

20. a) Johnson, L. K.; Killian, C. M.; Brookhart, M. *J. Am. Chem. Soc*., **1995**, *117*, 6414. b) Killian, C. M.; Tempel, D. J.; Johnson, L. K.; Brookhart, M. *J. Am. Chem. Soc*., **1996**, *118*, 11664.

21. For PDI: a) de Bruin, B.; Bill, E.; Bothe, E.; Weyhermüller, T.; Wieghardt, K. *Inorg. Chem*. **2000**, *39*, 2936-2947. b) Knijnenburg, Q.; Gambarotta, S.; Budzelaar, P. H. M. *Dalton Trans.* **2006**, 5442-5448. For DI: c) Khusniyarov, M. M.; Harms, K.; Burghaus, O.; Sundermeyer, J. *Eur. J. Inorg. Chem*., **2006**, 2985; d) Muresan, N.; Chlopek, K.; Weyhermüller, T.; Nesse, F.; Wieghardt, K. *Inorg. Chem*., **2007**, *46*, 5327. e) Khusniyarov, M. M.; Weyhermüller, T.; Eckhard, B.; Wieghardt, K. *J. Am. Chem. Soc.*, **2009**, 131, 1208-1221.

22. Ben-Daat, H.; Hall, G. B.; Groy, T. L.; Trovitch, R. J. *Eur. J. Inorg. Chem.* **2013**, 4430-4442.

23. Porter, T. M.; Hall, G. B.; Groy, T. L.; Trovitch, R. J. *Dalton Trans.*, **2013**, 42, 14689-14692.

24. Karstedt, B. D. General Electric Company. U.S. Patent US3775452A **1973**.

25. Speier, J. L.; Webster, J. A.; Barnes, G. H. *J. Am. Chem. Soc*. **1957**,*79*, 974-979.

26. For a review of precious metal catalyzed olefin hydrosilylation see: Troegel, D.; Stohrer, J. *Coord. Chem. Rev.*, **2011**, *255*, 1440-1459.

27. For a comprehensive review of base metal olefin hydrosilylation see: Du, X.; Huang, Z. *ACS Catal*. **2017**, *7*, 1227-1243.

28. Carney, J. R.; Dillon, B. R.; Campbell, L.; Thomas, S. P. *Angew. Chem. Int. Ed.* **2018**, **57**, 10620-10624.

29. Mukhopadhyay, T. K.; Flores, M.; Groy, T. L.; Trovitch, R. J. *Chem. Sci.* **2018**, *9*, 7673-7680.

30. a) Freidlina, R. K.; Chukovskaya, E. T.; Tsao, I.; Nesmeyanov, A. N. *Dokl. Akad. Nauk SSSR* **1960**, *132*, 374-377. b) Nesmeyanov, A. N.; Freidlina, R. K.; Chukovskaya, E. C.; Petrova, R. G.; Belyavsky, A. B. *Tetrahedron* **1962**, *17*, 61-68.

31. a) Graham, W. A. G.; Jetz, W. *Inorg. Chem*. **1971**, *10*, 4-9. b) Schroeder, M. A.; Wrighton, M. S. *J. Organomet. Chem*. **1977**, *128*, 345-358.

32. Sunada, Y.; Tsutsumi, H.; Shigeta, K.; Yoshida, R.; Hashimoto, T.; Nagashima, H. *Dalton Trans*. **2013**, *42*, 16687-16692.

33. Bart, S. C.; Lobkovsky, E.; Chirik, P. J. *J. Am. Chem. Soc*. **2004**, *126*, 13794-13807.

34. Tondreau, A. M.; Atienza, C. C. H.; Weller, K. J.; Nye, S. A.; Lewis, K. M.; Delis, J. G. P.; Chirik, P. J. *Science*, **2012**, *335*, 567-570.

35. Greenhalgh, M. D.; Frank, D. J.; Thomas, S. P. *Adv. Synth. Catal*., **2014**, *356*, 584-590.

36. Challinor, A. J.; Calin, M.; Nichol, G. S.; Carter, N. B.; Thomas, S. P. *Adv. Synth. Catal*. **2016**, *358*, 2404-2409.

37. a) Kamata, K.; Suzuki, A.; Nakai, Y.; Nakazawa, H. *Organometallics* **2012**, *31*, 3825-3828. b) Tondreau, A. M.; Atienza, C. C. H.; Darmon, J. M.; Milsmann, C.; Hoyt, H. M.; Weller, K. J.; Nye, S. A.; Lewis, K. M.; Boyer, J.; Delis, J. G. P.; Lobkovsky, E.; Chirik, P. J. *Organometallics* **2012**, *31*, 4886-4893.

38. Hayasaka, K.; Kamata, K.; Nakazawa, H. *Bull. Chem. Soc. Jpn*. **2016**, *89*, 394-404.

39. Peng, D.; Zhang, Y.; Du, X.; Zhang, L.; Leng, X.; Walter, M. D.; Huang, Z. *J. Am. Chem. Soc*. **2013**, *135*, 19154-19166.

40. Du, X.; Zhang, Y.; Peng, D.; Huang, Z. *Angew. Chem., Int. Ed*. **2016**, *55*, 6671-6675.

41. For other Fe examples see: a) Bellachioma, G.; Cardaci, G.; Colomer, E.; Corriu, R. J. P; Vioux, A. *Inorg. Chem*., **1989**, 28, 519-525. b) Marciniec, B.; Majchrzak, M. *Inorg. Chem. Commun*., **2000**, *3*, 371-375. c) Bart, S. C.; Lobkovsky, E.; Chirik, P. J. *J. Am. Chem. Soc*., **2004**, *126*, 13794-13807. d) Archer, A. M.; Bouwkamp, M. W.; Cortez, M.-P.; Lobkovsky, E.; Chirik, P. J. *Organometallics*, **2006**, *25*, 4269-4278. e) Peng, D.; Zhang, Y.; Du, X.; Zhang, L.; Leng, X.; Walter, M. D.; Huang, Z. *J. Am. Chem. Soc*., **2013**, *135*, 19154-19166. f) Chen, J.; Cheng, B.; Cao, M.; Lu, Z. *Angew. Chem., Int. Ed*., **2015**, *54*, 4661-4664. g) Gilbert-Wilson, H.; Chu, W.-Y.; Rauchfuss, T. B. *Inorg. Chem*., **2015**, *54*, 5596-5603. h) Marciniec, B.; Kownacka, A.; Kownacki, I.; Hoffmann, M.; Taylor, R. *J. Organomet. Chem*., **2015**, *791*, 58-65. i) Sunada, Y.; Noda, D.; Soejima, H.; Tsutsumi, H.; Nagashima,

H. *Organometallics*, **2015**, *34*, 2896-2906. j) Nikonov, G.I. *ChemCatChem*, **2015**, *7*, 1918-1919. k) Jia, X.; Huang, Z. *Nat. Chem*., **2016**, *8*, 157-161. l) Noda, D.; Tahara, A.; Sunada, Y.; Nagashima, H. *J. Am. Chem. Soc*., **2016**, *138*, 2480-2483. m) Du, X.; Zhang, Y.; Peng, D.; Huang, Z. *Angew. Chem., Int. Ed*., **2016**, *55*, 6671-6675. n) Hayasaka, K.; Kamata, K.; Nakazawa, H. *Nat. Chem*., **2016**, *89*, 394-404. o) Toya, Y.; Hayasaka, K.; Nakazawa, H. *Organometallics*, **2017**, *36*, 1727-1735. p) Hu, M.-Y.; He, Q.; Fan, S.-J.; Wang, Z.-C.; Liu, L.-Y.; Mu, Y.-J.; Peng, Q.; Zhu, S.-F. *Nat. Commun*., **2018**, *9*, 221. q) Cheng, B.; Liu, W.; Lu, Z. *J. Am. Chem. Soc*., **2018**, *140*, 5014-5017.

42. Chalk, A. J.; Harrod, J. F.; *J. Am. Chem. Soc*., **1965**, *21*, 1133-1135.

43. Brookhart M.; Grant, B. E. *J. Am. Chem. Soc*., **1993**, *115*, 2151-2156.

44. Mo, Z.; Liu, Y.; Deng, L. *Angew. Chem., Int. Ed.* **2013**, *52*, 10845-10849.

45. Chen, C.; Hecht, M. B.; Kavara, A.; Brennessel, W. W.; Mercado, B. Q.; Weix, D. J.; Holland, P. L. *J. Am. Chem. Soc*., **2015**, *137*, 13244-13247.

46. Chen, C.; Dugan, T. R.; Brennessel, W. W.; Weix, D. J.; Holland, P. L. *J. Am. Chem. Soc*. **2014**, *136*, 945-955.

47. Schuster, C. H.; Diao, T.; Pappas, I.; Chirik, P. J. *ACS Catal*. **2016**, *6*, 2632-2636.

48. Ibrahim, A. D.; Entsminger, S. W.: Zhu, L.; Fout, A. R. *ACS Catal*., **2016**, *6*, 3589-3593.

49. For other Co examples see: a) Magomedov, G. K. I.; Andrianov, K. A.; Shkolnik, O. V.; Izmailov, B. A.; Kalinin, V. N. *J. Organomet. Chem*., **1978**, *149*, 29-36. b) Seki, Y.; Kawamoto, K.; Chatani, N.; Hidaka, A.; Sonoda, N.; Ohe, K.; Kawasaki, Y.; Murai, S. *J. Organomet. Chem*., **1991**, *403*, 73-84. c) Chatani, N.; Kodama, T.; Kajikawa, Y.; Murakami, H.; Kakiuchi, F.; Ikeda, S.-I.; Murai, S. *Chem. Lett*., **2000**, *29*, 14-15. d) Atienza, C. C. H.; Diao, T.; Weller, K. J.; Nye, S. A.; Lewis, K. M.; Delis, J. G. P.; Boyer, J. L.; Roy, A. K.; Chirik, P. J. *J. Am. Chem. Soc*., **2014**, *136*, 12108-12118. e) Sun, J.; Deng, L. *ACS Catal*., **2016**, *6*, 290-300. f) Gorczynski, A.; Zaranek, M.; Witomska, S.; Bocian, A.; Stefankiewicz, A. R.; Kubicki, M.; Patroniak, V.; Pawlu´c, P. *Catal. Commun*., **2016**, *78*, 71-74. g) Raya, M.; Biswas, S.; RajanBabu, T. V. *ACS Catal*., **2016**, *6*, 6318-6323. h) Chu, W.-Y.; GilbertWilson, R.; Rauchfuss, T. B.; *Organometallics*, **2016**, *35*, 2900-2914. i) Wang, C.; Teo, W. J.; Ge, S. *ACS Catal*., **2017**, *7*, 855-863. j) Raya, B.; Jing, S.; Balasanthiran, V.; RajanBabu, T.V. *ACS Catal*., **2017**, *7*, 2275-2283. k) Liu, Y.; Deng, L. *J. Am. Chem. Soc.*, **2017**, *139*, 1798-1801. l) Wang, C.; Teo, W.J.; Ge, S. *Nat. Commun*., **2017**, *8*, 2258. m) Cheng, B.; Lu, P.; Zhang, H.; Cheng, X.; Lu, Z. *J. Am. Chem. Soc*., **2017**, *139*, 9439-9442.

50. For early examples see: (a) Petrov, A. D.; Mironov, V. F.; Vdovin, V. M.; Sakykh-Zade, S. I. *Russ. Chem. Bull.* **1956**, *5*, 247-248. (b) Nozakura, S.; Konotsune, S. *Bull. Chem. Soc. Jpn.* **1956**, *29*, 326-331. (c) Chukovskaya, E. T.; Freidlina, R. K. *Russ. Chem. Bull.* **1963**, *12*, 685-686. (d) Kumada, M.; Kiso, Y.; Umeno, M. *J. Chem. Soc. D, Chem. Commun.* **1970**, 611. (e) Kiso, Y.; Kumada, M.; Tamao, K.; Umeno, M. *J. Organomet. Chem.* **1973**,

50, 297-310. (f) Kiso, Y.; Kumada, M.; Maeda, K.; Sumitani, K.; Tamao, K. *J. Organomet. Chem.* **1973**, *50*, 311-318.

51. a) Fontaine, R.-G.; Nguyen, R.-V.; Zargarian, D. *Can. J. Chem.* **2003**, *81*, 1299-1306. b) Fontaine, R.-G.; Zargarian, D. *J. Am. Chem. Soc.* **2004**, *126*, 8786-8794. c) Chen, Y.; Sui-Seng, C.; Boucher, S.; Zargarian, D. *Organometallics* **2005**, *24*, 149-155. d) Chen, Y.; Zargarian, D. *Can. J. Chem.* **2009**, *87*, 280-287.

52. Benítez Junquera, L.; Puerta, M. C.; Valerga, P. *Organometallics* **2012**, *31*, 2175-2183.

53. Kuznetsov, A.; Gevorgyan, V. *Org. Lett.* **2012**, *14*, 914-917.

54. Lipschutz, M. I.; Tilly, D. T. *Chem. Commun.* **2012**, *48*, 7146-7148.

55. Srinivas, V.; Nakajima, Y.; Ando, W.; Sato, K.; Shimada, S. *Catal. Sci. Technol.* **2015**, *5*, 2081-2084.

56. Srinivas, V.; Nakajima, Y.; Ando, W.; Sato, K.; Shimada, S. *J. Organomet. Chem.* **2016**, *809*, 57-62.

57. a) Mathew, J.; Nakajima, Y.; Choe, Y.-K.; Urabe, Y.; Ando, W.; Sato, K.; Shimada, S. *Chem. Commun.* **2016**, *52*, 6723-6726. b) Nakajima, Y.; Sato, K.; Shimada, S. *Chem. Rec.* **2016**, *16*, 2379-2387.

58. Buslov, I.; Becouse, J.; Mazza, S.; Montandon-Clerc, M.; Hu, X. *Angew. Chem. Int. Ed.* **2015**, *54*, 14523-14526.

59. Pappas, I.; Treacy, S.; Chirik, P. J. *ACS Catal*. **2016**, *6*, 4105-4109.

60. a) Ojima, I.; Nihonyanagi, M.; Nagai, Y. *J. Chem. Soc., Chem. Commun.*, **1972**, 938. b) Ojima, I.; Kogure, T.; Nihonyanagi, M.; Nagai, Y. *Bull. Chem. Soc. Japan*, **1972**, *45*, 3506.

61. For early examples see: a) Ojima, I.; Kogure, T.; Nagai, Y. *Chem. Lett.*, **1973**, *541*. b) Dumont, W.; Poulin, J.-C.; Dang, T.-P.; Kagan, H. B. *J. Am. Chem. Soc.*, **1973**, *95*, 8295. c) Yamamoto, K.; Hayashi, T.; Kumada, M. *J. Organomet. Chem.*, **1973**, *54*, C45.

62. a) Vijjamarri, S.; Chidara, V. K.; Du, G. *ACS Omega*, **2017**, *2*, 582. b) Vijjamarri, S.; Streed, S.; Serum, E. M.; Sibi, M. P.; Du, G. *ACS Sustainable Chem. Eng.*, **2018**, *6*, 2491.

63. Cavanaugh, M. D.; Gregg, B. T.; Cutler, A.R. *Organometallics* **1996**, *15*, 2764-2769.

64. Son, S.U.; Paik, S.-J.; Lee, I.S.; Lee, Y.-A.; Chung, Y.K.; Seok, W. K.; Lee, H. N. *Organometallics*, **1999**, *18*, 4114-4118.

65. Son, S. U.; Paik, S.-J.; Chung, Y. K. *J. Mol. Catal. A: Chem.*, **2000**, *151*, 87-90.

66. Mukhopadhyay, T. K.; Rock, C. L.; Hong, M.; Ashley, D. C.; Groy, T. L.; Baik, M.-H.; Trovitch, R. J. *J. Am. Chem. Soc.*, **2017**, *139*, 4901-4915.

67. Mukhopadhyay, T. K.; Flores, M.; Groy, T. L.; Trovitch, R. J. *J. Am. Chem. Soc.*, **2014**, *136*, 882-885.

68. a) Ghosh, C.; Mukhopadhyay, T. K.; Flores, M.; Groy, T. L.; Trovitch, R. J. *Inorg. Chem.*, **2015**, *54*, 10398. b) Mukhopadhyay, T. K.; Ghosh, C.; Flores, M.; Groy, T. L.; Trovitch, R. J. *Organometallics*, **2017**, *36*, 3477.

69. Kelley, C. M.; McDonald, R.; Sydora, R. O.; Stradiotto, M.; Turculet, L. *Angew. Chem. Int. Ed.*, **2017**, *56*, 15901-15904.

70. Tondreau, M.; Lobkovsky, E.; Chirik, P. J. *Org. Lett.*, **2008**, *10*, 2789-2792.

71. Tondreau, M.; Darmon, J. M.; Wile, B. M.; Floyd, S. K.; Lobkovsky, E.; Chirik, P. J. *Organometallics*, **2009**, *28*, 3928-3940.

72. Kandepi, V. V. K. M.; Cardoso, J. M. S.; Peris, E.; Royo, B. *Organometallics*, **2010**, *29*, 2777-2782.

73. Yang, J.; Tilley, D. T. *Angew. Chem. Int. Ed.*, **2010**, *49*, 10186-10188.

74. Bhattacharya, P.; Krause, J. A.; Guan, H. *Organometallics*, **2011**, *30*, 4720-4729.

75. Ruddy, J.; Kelly, C. M.; Crawford, S. M.; Wheaton, C. A.; Sydora, O. L.; Small, B. L.; Stradiotto, M.; Turculet, L. *Organometallics*, **2013**, *32*, 5581-5588.

76. Brunner, H.; Amberger, K. *J. Organomet. Chem.*, **1991**, *417*, C63.

77. Yu, F.; Zhang, X.-C.; Wu, F.-F.; Zhou, J.-N.; Fang, W.; Wu, J.; Chan, A.S.C. *Org. Biomol. Chem.*, **2011**, *9*, 5652.

78. Sauer, D. C.; Wadepohl, H.; Gade, L. H. *Inorg. Chem.*, **2012**, *51*, 12948.

79. Niu, Q.; Sun, H.; Li, X.; Klein, H.-F.; Flörke, U. *Organometallics*, **2013**, *32*, 5235.

80. Zhou, H.; Sun, H.; Zhang, S.; Li, X. *Organometallics*, **2015**, *34*, 1479.

81. Nesbit, M. A.; Suess, D. L. M.; Peters, J. C. *Organometallics*, **2015**, *34*, 4741.

82. Chakraborty, S.; Krause, J. A.; Guan, H. *Organometallics*, **2009**, *28*, 582.

83. Tran, B. L.; Pink, M.; Mindiola, D. J. *Organometallics*, **2009**, *28*, 2234.

84. Postigo, L.; Royo, B. *Adv. Synth. Catal.*, **2012**, *354*, 2613.

85. Wei, Y.; Liu, S.-X.; Mueller-Bunz, H.; Albrecht, M. *ACS Catal.*, **2016**, *6*, 8192.

86. Bheeter, L. P.; Henrion, M.; Brelot, L.; Darcel, C,; Chetcuti, M. J.; Sortais, J.-B.; Ritleng, V. *Adv. Synth. Catal.*, **2012**, *354*, 2619.

87. MacMillan, S. N.; Harman, W. H.; Peters, J. C. *Chem. Sci.*, **2014**, *5*, 590.

88. Tafazolian, H.; Yoxtheimer, R.; Thakuri, R. S.; Schmidt, J. A. R.; *Dalton Trans.*, **2017**, *46*, 5431.

89. a) Ojima, I.; Nihonyanagi, M.; Kogure, T.; Kumagai, M.; Horiuchi, S.; Nakatsugawa, K.; Nagai, Y. *J. Organomet. Chem.* **1975**, *94*, 449-461. b) Reyes, C.; Prock, A.; Giering, W. P. *Organometallics* **2002**, *21*, 546-554.

90. Söllradl, H.; Hengge, E. *J. Organomet. Chem.*, **1983**, *243*, 257.

91. Pinkas, J.; Císařová, I.; Karban, J.; Schraml, J.; Sýkora, J. *J. Organomet. Chem.*, **2012**, *710*, 20.

92. Tolman, C. A. *Chem. Rev.* **1977**, *77* (3), 313-348.

93. This chapter was published in: Rock, C. L.; Groy, T. L.; Trovitch, R. J. *Dalton Trans.* **2018**, *47*, 8807-8816.

94. Jia, W.; Chen, X.; Guo, R.; Sui-Seng, C.; Amoroso, D.; Lough, A. J.; Abdur-Rashid, K. *Dalton Trans.*, **2009**, 8301.

95. Li, Y.; Li, Z.; Li, F.; Wang, Q.; Tao, F. *Tetrahedron Lett.*, **2005**, *46*, 6159.

96. a) Mimoun, H. *J. Org. Chem.*, **1999**, *64*, 2582. b) Boyer, J.; Corriu, R. J. P; Perz, R.; Poirier, M.; Reye, C. *Synthesis*, **1981**, 558. c) Berk, S. C.; Kreutzer, K. A.; Buchwald, S. L. *J. Am. Chem. Soc.*, **1991**, *113*, 5093. d) Berk, S. C.; Buchwald, S. L. *J. Org. Chem.*, **1992**, *57*, 3751. e) Barr, K. J.; Berk, S. C.; Buchwald, S. L. *J. Org. Chem.*, **1994**, *59*, 4323. f) Ohta, T.; Kamiya, M.; Kusui, K.; Michibata, T.; Nobutomo, M.; Furukawa, I. *Tetrahedron Lett.*, **1999**, *40*, 6963. g) Matsubara, K.; Iura, T.; Maki, T.; Nagashima, H. *J. Org. Chem.*, **2002**, *67*, 4985. h) Fernandes, A. C.; Romão, C. C. *J. Mol. Catal. A: Chem.*, **2006**, *253*, 96. i) Nakanishi, J.; Tatamidani, H.; Fukumoto, Y.; Chatani, N. *Synlett*, **2006**, 869. j) Pehlivan, L.; Métay, E.; Laval, S.; Dayoub, W.; Delbrayelle, D.; Mignani, G.; Lemaire, M. *Eur. J. Org. Chem.*, **2011**, 7400. k) Bézier, D.; Venkanne, G.T.; Castro, L.C.M.; Zheng, J.; Roisnel, T.; Sortais, J.-B.; Darcel, C. *Adv. Synth. Catal.*, **2012**, *354*, 1879. l) Junge, K.; Wendt, B.; Zhou, S.; Beller, M. *Eur. J. Inorg. Chem.*, **2013**, 2061. m) Fernández-Salas, J.; Manzini, S.; Nolan, S. P. *Chem. Commun.*, **2013**, *49*, 9758. n) Revunova, K.; Nikonov, G. I. *Chem. Eur. J.*, **2014**, *20*, 839. o) Kovalenko, O. O.; Adolfsson, H. *Chem. Eur. J.*, **2015**, *21*, 2785. p) Corre, Y.; Rysak, V.; Trivelli, X.; Agbossou-Niedercorn, F.; Michon, C. *Eur. J. Org. Chem.*, **2017**, 4820.

97. a) Parks, D. J.; Piers, W. E. *J. Am. Chem. Soc.*, **1996**, *118*, 9440. b) Igarashi, M.; Mizuno, R.; Fuchikami, T. *Tetrahedron Lett.*, **2001**, *42*, 2149. c) Cheng, C.; Brookhart, M. *Angew. Chem. Int. Ed.*, **2012**, *51*, 9422. d) Li, H.; Castro, L. C. M.; Zheng, J.; Roisnel, T.; Dorcet, V.; Sortais, J.-B.; Darcel, C. *Angew. Chem. Int. Ed.*, **2013**, 8045. e) Matsumoto, K.; Sanja, K. V.; Satoh, Y.; Sato, K.; Shimada, S. *Angew. Chem. Int. Ed.*, **2017**, *56*, 3168. f) Li; J. P.; Cassagnau, P.; Da Cruz-Boisson, F.; Mélis, F.; Alcouffe, P.; Lucas, C.; Bounor-Legaré, V. *J. Polym. Sci. A: Polym. Chem.*, **2017**, *55*, 1855.

98. a) Mao, Z.; Gregg, B. T.; Cutler, A.R. *J. Am. Chem. Soc.*, **1995**, *117*, 10139. b) Park, S.; Brookhart, M. *Organometallics*, **2010**, *29*, 6507. c) Das, S.; Li, Y.; Junge, K.; Beller, M. *Chem. Commun.*, **2012**, *48*, 10742. d) Xu, S.; Boschen, J. S.; Biswas, A.; Kobayashi, T.; Pruski, M.; Windus, T. L.; Sadow, A. D. *Dalton Trans.*, **2015**, *44*, 15897.

100. a) Chatani, N.; Murai, S.; Sonoda, N. *J. Am. Chem. Soc.*, **1983**, *105*, 1370. b) Chatani, N.; Fujii, S.; Wamasaki, Y.; Murai, S.; Sonoda, N. *J. Am. Chem. Soc.*, **1986**, *108*, 7361.

101. a) Belyakova, Z. V.; Pomerantseva, M. G.; Efimova, L. A.; Chernyshev, E. A.; Storozhenko, P.A. *Russ. J. Gen. Chem.*, **2010**, *80*, 728. b) Igarashi, M.; Kobayashi, T.; Sato, K.; Ando, W.; Matsumoto, T.; Shimada, S.; Hara, M.; Uchida, H. *J. Organomet. Chem.*, **2013**, *725*, 54. c) Igarashi, M.; Matsumoto, T.; Kobayashi, T.; Sato, K.; Ando, W.; Shimada, S.; Hara, M.; Uchida, H. *J. Organomet. Chem.*, **2014**, *749*, 421.

102. Bozell, J. J.; Petersen, G. R. *Green Chem.* **2010**, *12*, 539.

103. Schmidt, D.; Zell, T.; Schaub, T.; Radius, U. *Dalton Trans.* **2014**, *43*, 10816-10827.

104. a) Wittig, G.; Schöllkopf, U. *Chemische Berichte.* **1954**, *87* (9), 1318. b) Young, P.C.; Hadfield, M.S.; Arrowsmith, L.; Macleod, K.M.; Mudd, R.J.; Jordan-Hore, J.A.; Lee, A.-L. *Org. Lett.* **2012**, *14*, 3, 898-901.

105. Yamamoto, K.; Hayashi, T.; Uramoto, Y.; Ito, R.; Kumada, M. *J. Organomet. Chem.* **1976**, *118*, 331-348.

106. This chapter was published in: Rock, C. L.; Trovitch, R. J. *Dalton Trans*. **2018**, *manuscript submitted.*

107. a) Miyaura, N.; Yamada, K.; Suzuki, A. *Tetrahedron Lett.*, **1979**, *36*, 3437. b) Miyaura, N.; Suzuki, A. *J. Chem. Soc., Chem. Commun.*, **1979**, 866. c) Suzuki, A. *J. Organomet. Chem.* **1999**, *576*, 147. d) Martin, R.; Buchwald, S. L. *Acc. Chem. Res.*, **2008**, *41*, 1461.

108. a) Gerrard, W., in *The Organic Chemistry of Boron*, Academic Press, New York, NY, 1961. b) Matteson, D. S., in *The Chemistry of the Metal-Carbon Bond*, Patai, S. Hartley, F. R. Eds.; John Wiley & Sons, New York, NY, 1987, Vol. 4, Ch. 3. c) Miyaura, N.; Suzuki, A. *Chem. Rev.* **1995**, *95*, 2457. d) Hall, D. G., in *Boronic Acids*, John Wiley & Sons, Weinheim, Germany, 2012.

109. a) Brown, H. C.; Gupta, S. K. *J. Am. Chem. Soc.*, **1972**, *94*, 4370. b) Brown, H. C.; Gupta, S. K. *J. Am. Chem. Soc.*, **1975**, *97*, 5249. c) Tucker, E.; Davidson, J.; Knochel, P. *J. Org. Chem.*, **1992**, *57*, 3482.

110. a) Pereira, S.; Srebnik, M. *Organometallics*, **1995**, *14*, 3127. b) He, X.; Hartwig, J. F. *J. Am. Chem. Soc.*, **1996**, *118*, 1696. c) Pereira, S.; Srebnik, M. *Tetrahedron Lett.*, **1996**, *37*, 3283. d) Lee, T.; Baik, C.; Jung, I.; Song, K.-H.; Kim, S.; Kim, D.; Kang, S.-O.; Ko, J. *Organometallics*, **2004**, *23*, 4569. e) Semba, K.; Fujihara, T.; Terao, J.; Tsuji, Y. *Chem. Eur. J.*, **2012**, *18*, 4179. f) Nielson, B. M.; Bielawski, C. W. *Organometallics*, **2013**, *32*, 3121.

111. Gunanathan, C. Hölcher, M., Pan, F., Leitner, W., *J. Am. Chem. Soc.* **2012**, *134*, 14349-14352.

112. Plikhta, A., Pöthig, A., Herdtweck, E., Rieger, B., *Inorg. Chem.* **2015**, *54*, 9517-9528.

113. Obligacion, J. V.; Neely, J. M.; Yazdani, A. N.; Pappas, I.; Chirik, P. J. *J. Am. Chem. Soc.*, **2015**, *137*, 5855.

114. Zuo, Z.; Huang, Z. *Org. Chem. Front.*, **2016**, *3*, 434.

115. Khalimon, A. Y.; Farha, P. M.; Kuzmina, L. G.; Nikonov, G. I. *Chem. Commun.*, **2012**, *48*, 455.

116. Khalimon, A. Y.; Farha P. M.; Nikonov, G. I. *Dalton Trans.*, **2015**, *44*, 18945.

117. Jiang, Y.; Yu, H.; Fu, Y. *Organometallics*, **2013**, 32, 926-936.

118. Weetman, C.; Anker, M. D.; Arrowsmith, M.; Hill, M. S.; Kociok-Köhn, G.; Liptrot, D. J.; Mahon, M. F. *Chem. Sci.*, **2016**, *7*, 628.

119. Geri, J. B.; Szymczak, N. K. *J. Am. Chem. Soc.*, **2015**, *137*, 12808.

120. Kaithal, A.; Chatterjee, B.; Gunanathan, C. *J. Org. Chem.* **2016**, *81*, 11153.

121. Ibrahim, A.D.; Entsminger, S.W.; Fout, A.R. *ACS Catal*., **2017**, *7*, 3730-3734.

122.a) Evans, D. F. *J. Chem. Soc.*, **1959**, 2003. b) Schubert, E. M. *J. Chem. Educ.*, **1992**, *69*, 62.

123. Tucker, C. E.; Davidson, J.; Knochel, P. *J. Org. Chem*. **1992**, *57*, 3482.

124. This chapter was published in: Ben-Daat, H.; Rock, C. L.; Flores, M.; Groy, T. L.; Bowman, A. C.; Trovitch, R. J. *Chem. Commun.* **2017**, *53*, 7333-7336.

125. Neese, F. *Orca, an Ab Initio, Density Functional and Semiempirical Electronic Structure Program Package*, version 2.9.1; Max Planck Institute for Bioinorganic Chemistry: Mülheim an der Ruhr, Germany, 2012.

126. a) Becke, A. D. *J. Chem. Phys*., **1993**, *98*, 5648. b) Lee, C. T.; Yang, W. T.; Parr, R. G. *Phys. Rev.*, **1988**, *37*, 785.

127. Grimme, S. *J. Comput. Chem.*, **2006**, *27*, 1787.

128. Pantazis, D. A.; Chen, X. Y.; Landis, C. R.; Neese, F. *J. Chem. Theory Comput*., **2008**, *4*, 908.

129. Molekel, Advanced Interactive 3D-Graphics for Molecular Sciences; Swiss National Supercomputing Center; http:// www.cscs.ch/molekel.

130. Weil, J. A.; Bolton, J. R. *Electron paramagnetic resonance: Elementary theory and practical applications.* Wiley, Hoboken, NJ, 2007.

131. Stoll, S.; Schweiger, A. *J. Magn. Reson.*, **2006**, *178*, 42.

APPENDIX A

UNPUBLISHED BIS(IMINO)PYRIDINE MANGANESE CHEMISTRY

A1. Synthesis of ^{HOPr}PDI

Under an inert atmosphere, 3-aminopropanol (1.50 g, 20 mmol) and diacetylpyridine (1.61 g, 10 mmol) were combined in 10 mL of toluene in a thick walled glass bomb. 5 mg of *p*-TSA and 4 Å molecular sieves were added. The reaction was heated to 80 °C for 3 days, after which the reaction was filtered, and solvents removed. The crude residue was washed with pentane and then recrystallized from diethyl ether at -35 °C and **^{HOPr}PDI** was isolated as an off-white solid. Analysis for $C_{15}H_{23}N_3O_2$: Calc. C, 64.96% H, 8.36%, N, 15.15% Found C, 65.16% H, 8.27% N, 15.05%. ^{1}H NMR (benzene-d_6): 8.04 (d, J = 7.8 Hz, 2H, *Ar*), 7.08 (t, J = 7.8 Hz, 1H, *Ar*), 3.87 (bs, 4H, -CH_2-), 3.50 (bs, 2H, -O*H*), 3.34 (t, J = 6.1 Hz, 4H, -CH_2-), 2.14 (s, 6H, -CH_3), 1.91 – 1.79 (m, 4H, -CH_2-). ^{13}C NMR (benzene-d_6): 167.35 (*Ar*), 156.23 (*Ar*), 137.25 (*Ar*), 121.63 (*Ar*), 63.32 (*C*=N), 51.87 (-*C*H$_2$-), 33.58 (-*C*H$_2$-), 13.81 (-*C*H$_2$-).

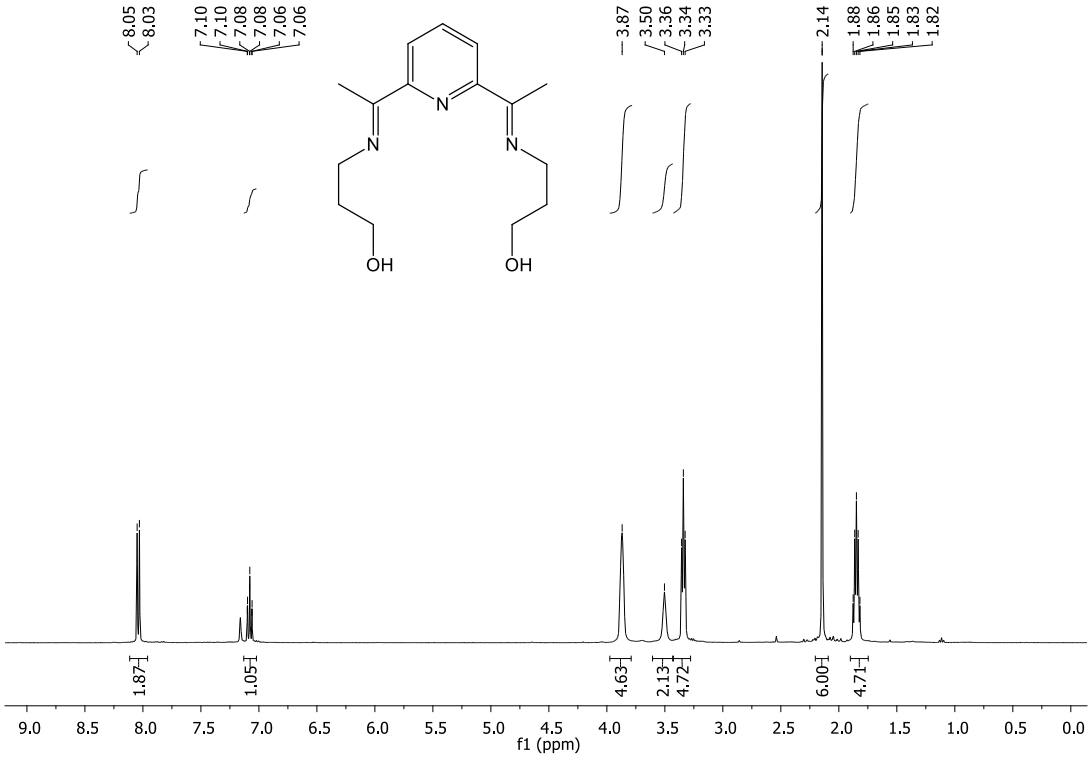

Fig. A.1 ^{1}H NMR spectrum of ^{HOPr}PDI in benzene-d_6.

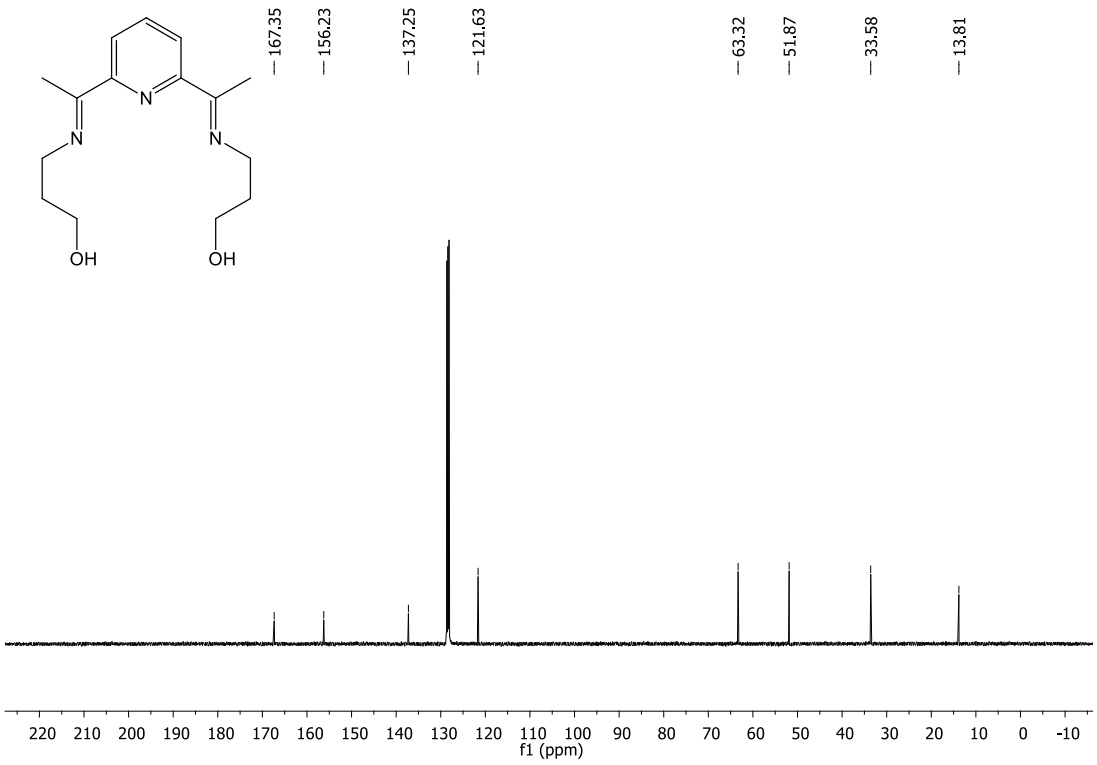

Fig. A.2 ^{13}C NMR spectrum of ^{HOPr}PDI in benzene-d_6.

A2. Synthesis of (^{HOPr}PDI)$MnCl_2$

Under an inert atmosphere, **^{HOPr}PDI** (84.7 mg, 0.305 mmol) and $MnCl_2 \cdot THF_2$ (82.4 mg, 0.305 mg) were combined in a thick walled glass bomb with 10 mL of toluene. The reaction was stirred at 85 °C overnight, after which **(^{HOPr}PDI)$MnCl_2$** was collected on a frit as an orange solid. Crystals suitable for single crystal XRD were grown from a saturated solution of THF at -35 °C after an attempt at reduction.

Reduction of **(^{HOPr}PDI)$MnCl_2$** proved unsuccessful with Na/Hg, K/Hg, and Na/Hg with COT, even though colour changes from orange to blue to red were observed over a period of 48 h. Crystals of **(^{HOPr}PDI)$MnCl_2$** were isolated from the reduction and diffracted.

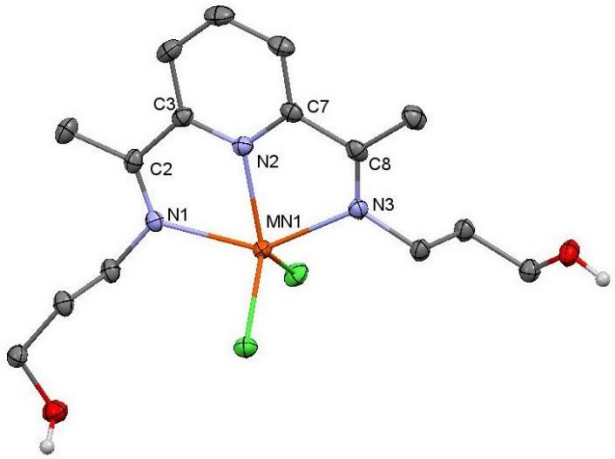

Fig. A.3 Solid state structure of (^{HOPr}**PDI)MnCl$_2$**, drawn with 30% probability ellipsoids. Hydrogen atoms are removed for clarity.

Table A.1 Select bond distances and angles for (^{HOPr}**PDI)MnCl$_2$**.

	Distance (Å)
C7-C8	1.501
C2-C3	1.501
C8-N3	1.279
C2-N1	1.278
N1-Mn	2.261
N2-Mn	2.194
N3-Mn	2.263
	Angle (°)
N1-Mn-N2	71.5
N3-Mn-N2	71.5
Cl1-Mn-Cl2	113.0

APPENDIX B

UNPUBLISHED BIS(IMINO)PYRIDINE TITANIUM CHEMISTRY

B1. Synthesis of **[(κ^3-*N*,*N*,*N*-^{Ph2PPr}PDI)TiCl$_3$]Cl**

Under an inert atmosphere, 0.49 mL of a 1.0 M solution of $TiCl_4$ in toluene (0.49 mmol) was diluted with 5 mL of toluene in a 20 mL scintillation vial. ^{Ph2PPr}DI (301.0 mg, 0.49 mmol) was dissolved in 5 mL of toluene and added to the $TiCl_4$ solution, which was stirred for 24 h, after which time a brick red solid was collected on a frit and washed with pentane. The isolated material is proposed to be **[(κ^3-*N*,*N*,*N*-^{Ph2PPr}PDI)TiCl$_3$]Cl** based on solubility and ^{31}P NMR spectroscopy.

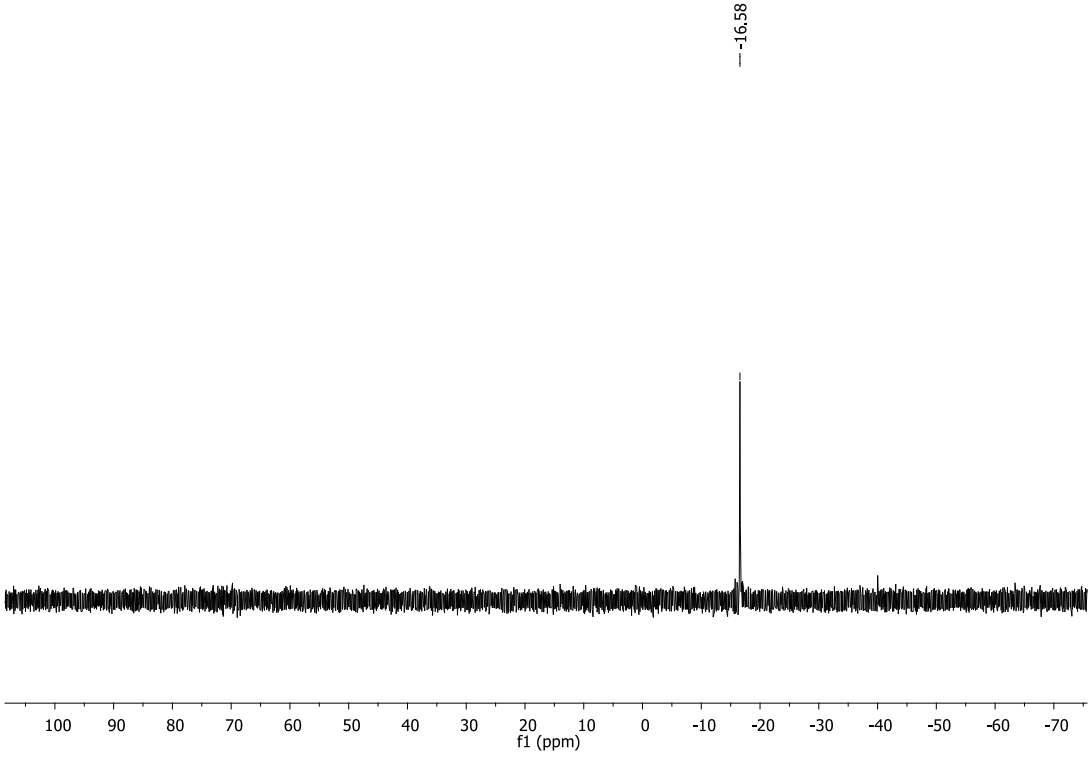

Fig. B.1 ^{31}P NMR spectrum of **[(κ^3-*N*,*N*,*N*-^{Ph2PPr}PDI)TiCl$_3$]Cl** in benzene-d_6.

Scheme B.1 Proposed synthesis of **[(κ^3-*N*,*N*,*N*-^{Ph2PPr}PDI)TiCl$_3$]Cl**.

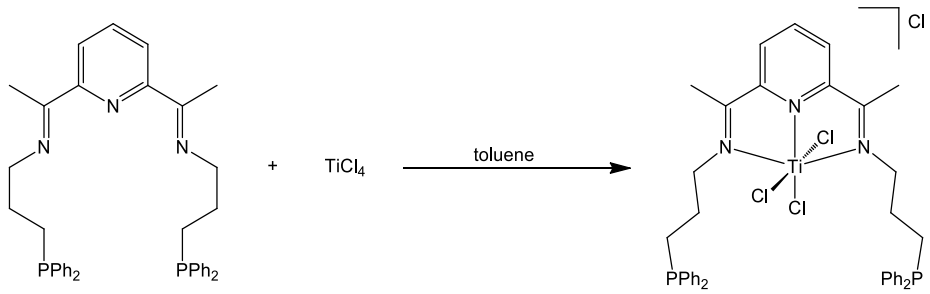

B2. Synthesis of (^{Ph2PPr}PDI)TiCl

Under an inert atmosphere, a 20 mL scintillation vial was charged with 9.3 g of mercury (46.3 mmol) and 5 mL toluene. Potassium (36.0 mg, 0.93 mmol) was added and the cloudy grey mixture was stirred for 30 min until it became clear. Solid **[(κ^3-*N*,*N*,*N*-^{Ph2PPr}PDI)TiCl$_3$]Cl** was added and the mixture diluted with 10 mL toluene. After 4 d, the mixture was filtered through Celite and volatile compounds from the resulting blue solution were removed *in vacuo*. Crystals suitable for XRD were grown from toluene layered with pentane at -35 °C.

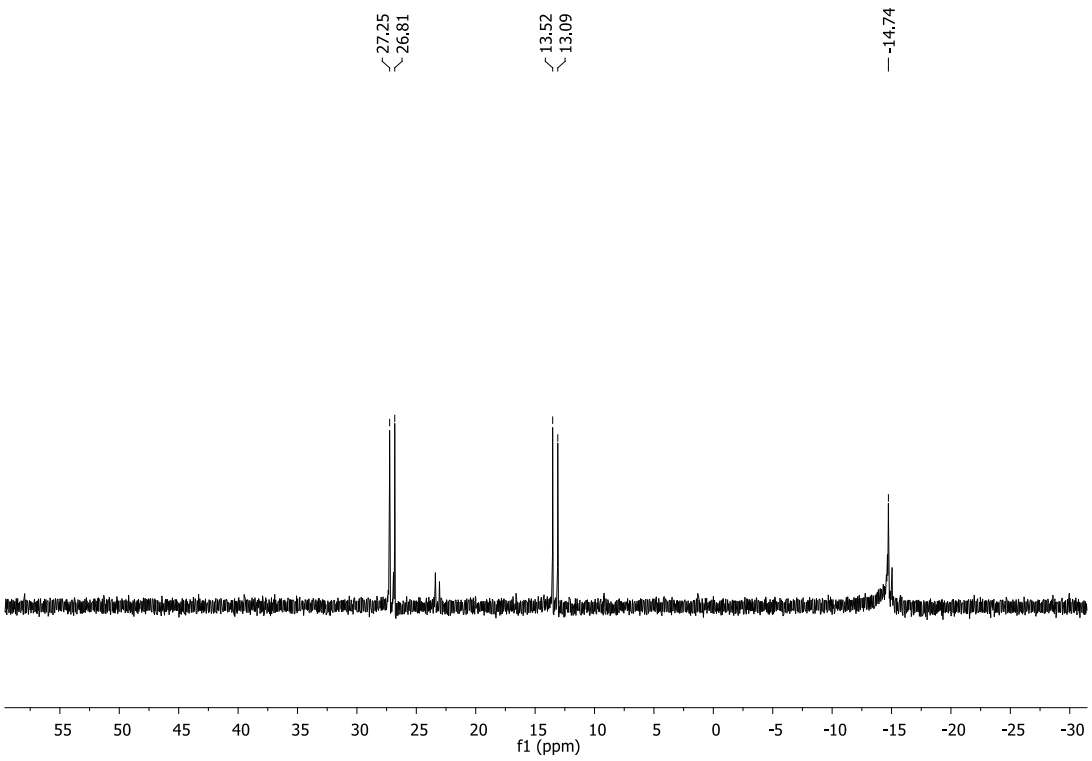

Fig. B.2 ^{31}P NMR spectrum of (**^{Ph2PPr}PDI)TiCl** in benzene-d_6.

Scheme B.2 Synthesis of (**^{Ph2PPr}PDI)TiCl**.

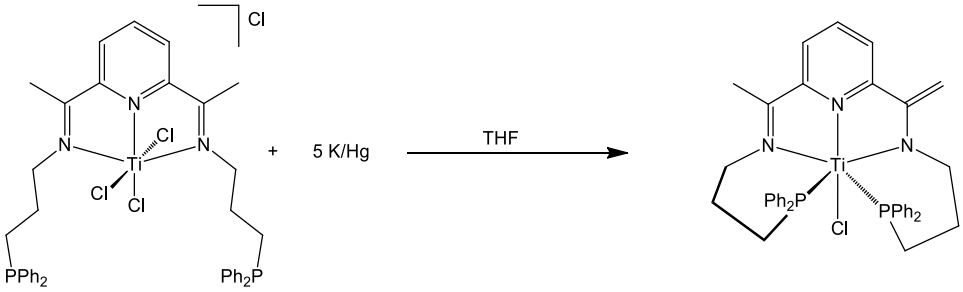

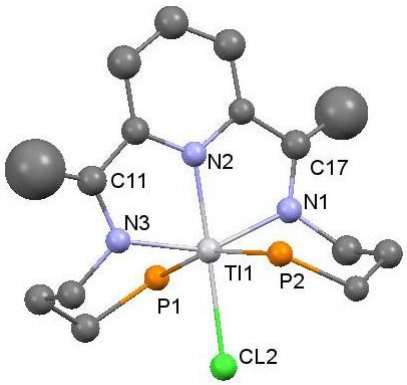

Fig. B.3 Solid state structure of (**^{Ph2PPr}PDI)TiCl**, drawn with 30% probability ellipsoids. Hydrogen atoms are removed for clarity.

Additional reactions performed include adding 2 or 4 equivalents of either PhLi or $NaEt_3BH$ to **(κ^3-*N,N,N*-Ph2PPrPDI)TiCl$_3$]Cl**. These experiments resulted in complicated mixtures of diamagnetic materials, the separations of which were unsuccessful. Sample ^{31}P NMR spectra are shown below.

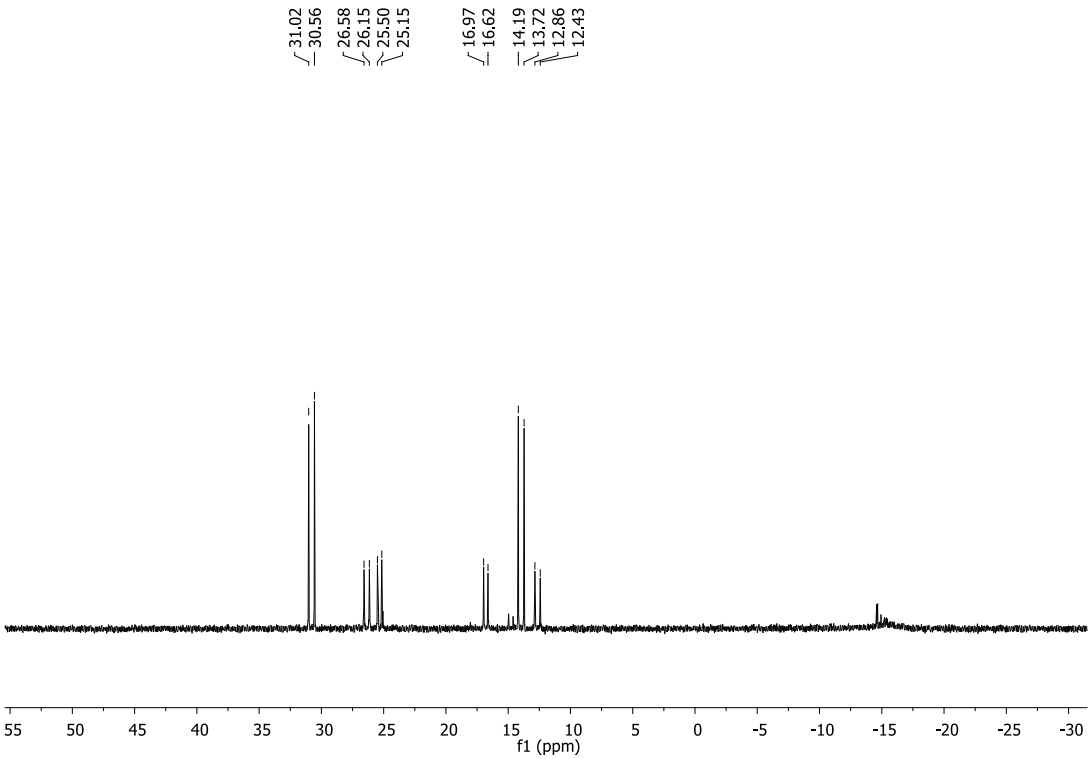

Fig. B.4 ^{31}P NMR spectrum of **(κ^3-*N*,*N*,*N*-Ph2PPrPDI)TiCl$_3$]Cl** after the addition of 2 equivalents of PhLi in toluene. Spectra in benzene-d_6.

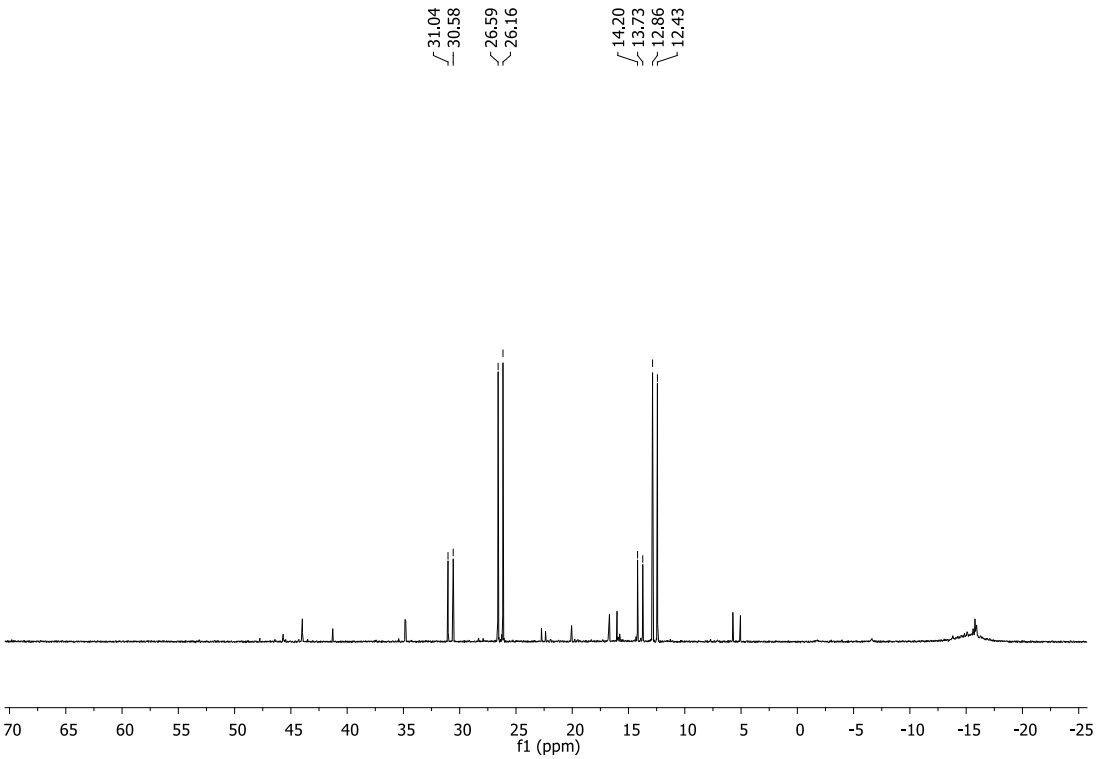

Fig. B.5 ^{31}P NMR spectrum of **(κ^3-*N*,*N*,*N*-Ph2PPrPDI)TiCl$_3$]Cl** after the addition of 4 equivalents of $NaEt_3BH$ in toluene. Spectra in benzene-d_6.

APPENDIX C

UNPUBLISHED DIIMINE MANGANESE CARBONYL CHEMISTRY

C1. Synthesis of [(^{Ph2PPr}DI)Mn(CO)$_2$]Br

Under an inert atmosphere, a thick walled glass bomb was charged with ^{Ph2PPr}DI (83.5 mg, 0.154 mmol) and $Mn(CO)_5Br$ (42.3 mg, 0.154 mmol) in 10 mL of toluene. The headspace was removed under vacuum and the reaction heated to 125 °C for 2 d. The reaction turned red within minutes of heating. The headspace was removed again and the reaction was heated to 125 °C for an additional 24 h. A red precipitate formed during this time, which was collected on a frit and washed with pentane. IR spectroscopy revealed C=O stretches at 1931 and 1859 cm^{-1} and ^{31}P NMR spectroscopy revealed a single resonance at 77.89 ppm. Based on this, the compound is identified as **[(^{Ph2PPr}DI)Mn(CO)$_2$]Br**. Needle like crystals were grown from acetone but did not diffract.

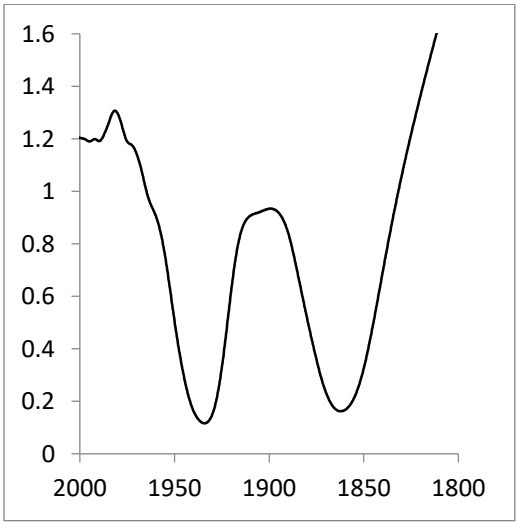

Fig. C.1 IR spectrum of **[(^{Ph2PPr}DI)Mn(CO)$_2$]Br** showing carbonyl stretching region.

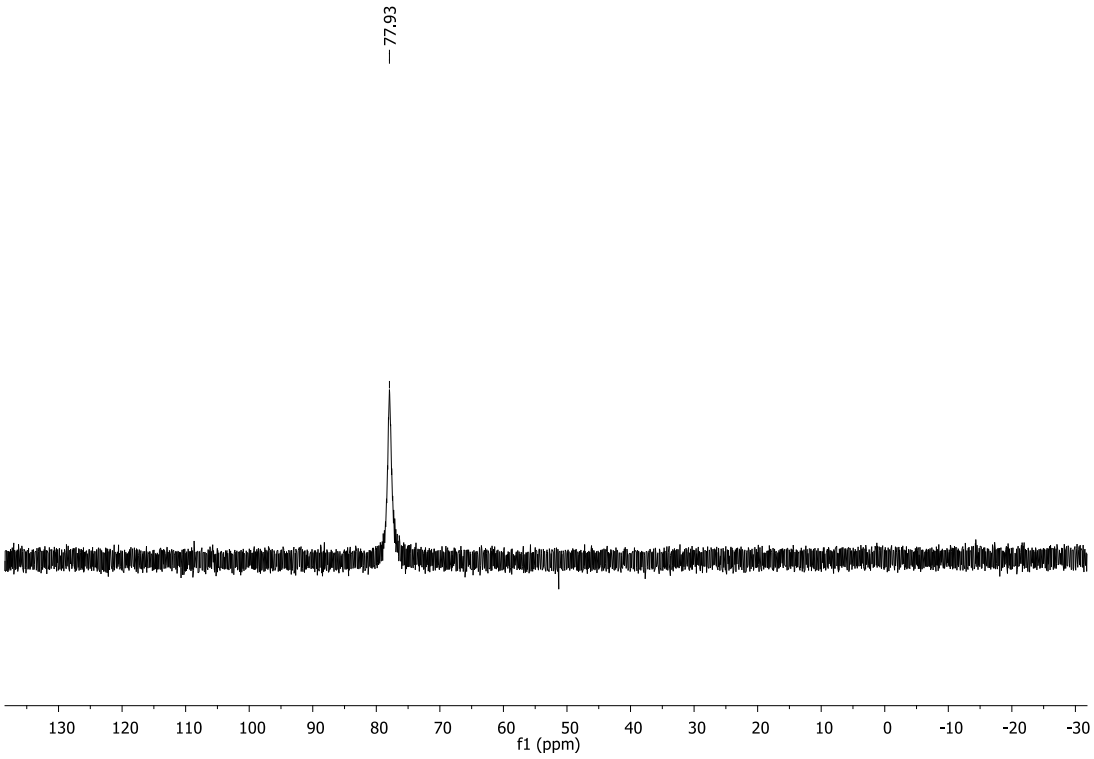

Fig. C.2 ^{31}P NMR spectrum of **[(^{Ph2PPr}DI)Mn(CO)$_2$]Br** in chloroform-*d*.

Scheme C.1 Proposed synthesis of **[(^{Ph2PPr}DI)Mn(CO)$_2$]Br**.

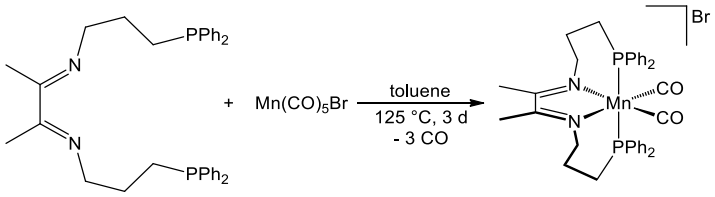

C2. Cyclic voltammetry of [(^{Ph2PPr}DI)Mn(CO)$_2$]Br

To screen for the electrocatalytic capabilities of **[(^{Ph2PPr}DI)Mn(CO)$_2$]Br**, the cyclic voltammograms of **[(^{Ph2PPr}DI)Mn(CO)$_2$]Br** alone and with 3.0 M H_2O under a saturated CO_2 atmosphere were obtained. Cyclic voltammetry run in 0.1 M [^{n}Bu$_4$N][PF_6] in CH_3CN with a glassy carbon electrode, platinum counter electrode, and a Ag/AgCl reference. Scan rate = 0.1 V/s.

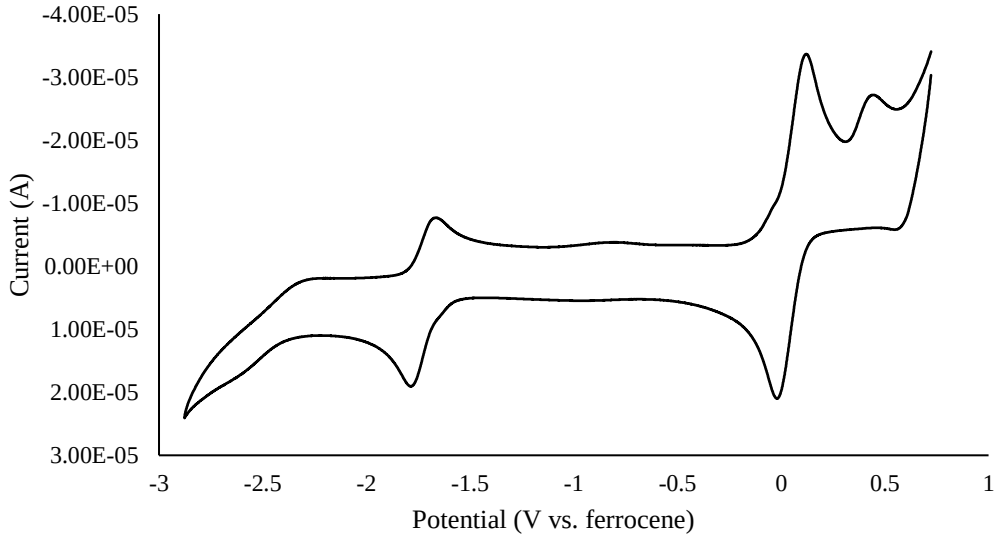

Fig. C.3 Cyclic voltammogram of **[(^{Ph2PPr}DI)Mn(CO)$_2$]Br** in acetonitrile vs ferrocene.

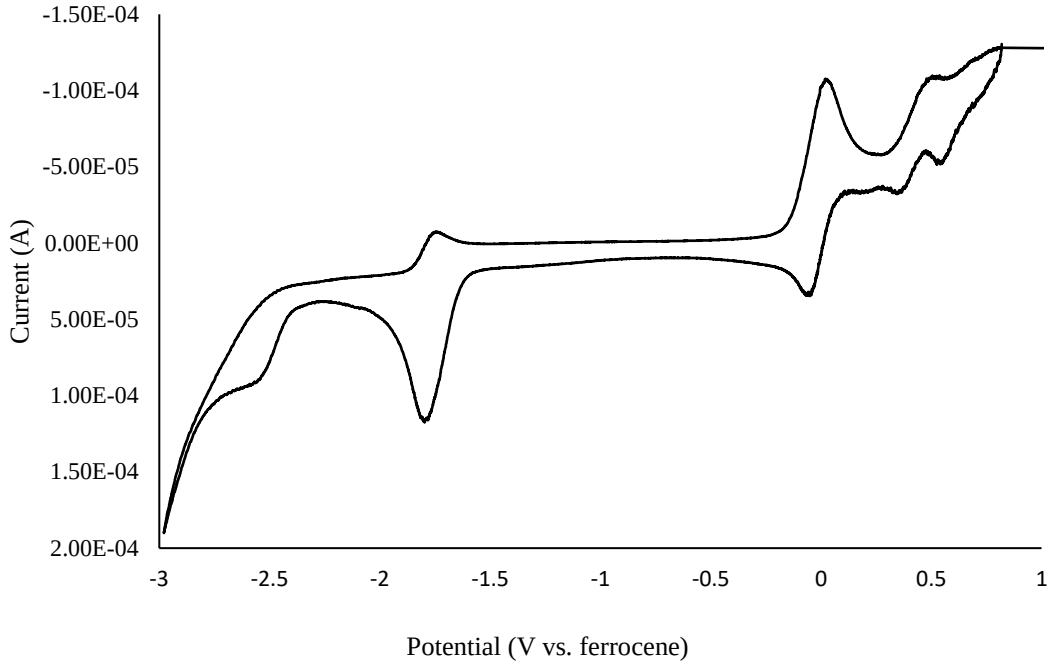

Fig. C.4 Cyclic voltammogram of **[(^{Ph2PPr}DI)Mn(CO)$_2$]Br** in acetonitrile with 3.0 M H_2O and a saturated CO_2 atmosphere vs ferrocene.

APPENDIX D

PHOSPHINO β-DIKETIMINATE LIGAND

D1. Synthesis of $(Ph_2P(CH_2)_3)NH(CH_3)CH(CO)CH_3$

Under an inert atmosphere, 2,4-pentanedione (191.4 mg, 1.19 mmol) and $Ph_2P(CH_2)_3NH_2$ (304.1 mg, 1.25 mmol) were combined with 10 mL toluene in a thick-walled glass bomb. 5 mg *p*-TSA and 4 Å molecular sieves were added. The reaction was heated to 80 °C for 2 days, after which it was filtered through Celite and solvents removed. The residue was washed with pentane and recrystallized to yield **$(Ph_2P(CH_2)_3)NH(CH_3)CH(CO)CH_3$** as an off white solid. Analysis for $C_{20}H_{24}NOP$: Calc. C, 73.81% H, 7.23%, N, 4.53% Found C, 73.83% H, 7.44% N, 4.31%.^{1}H NMR (benzene-d_6): 11.26 (s, 1H, N*H*), 7.44 – 7.37 (m, 4H, *Ar*), 7.13 – 7.01 (m, 6H, *Ar*), 4.88 (s, 1H, =C*H*), 2.64 (q, *J* = 6.6 Hz, 2H, -CH_2-), 2.06 (s, 3H, -CH_3), 1.85 (dd, *J* = 9.1, 6.6 Hz, 2H, -CH_2-), 1.40 (dt, *J* = 15.9, 8.0 Hz, 2H, -CH_2-), 1.34 (s, 3H, -CH_3). ^{13}C NMR (benzene-d_6): 194.79 (*C*=O), 162.17 (*C*-N), 139.54 (d, *J* = 14.2 Hz, *Ar*), 133.45 (d, *J* = 18.8 Hz, *Ar*), 129.16 (d, *J* = 3.0 Hz, *Ar*), 129.11 (*Ar*), 95.89 (=*C*H), 43.73 (d, *J* = 13.8 Hz, -*C*H_2-), 29.35 ((C=O)*C*H_3), 27.35 (d, *J* = 16.8 Hz, -*C*H_2-), 25.64 (d, *J* = 13.1 Hz, -*C*H_2-), 18.65 (H_3*C*-C-N). ^{31}P NMR (benzene-d_6): -16.67.

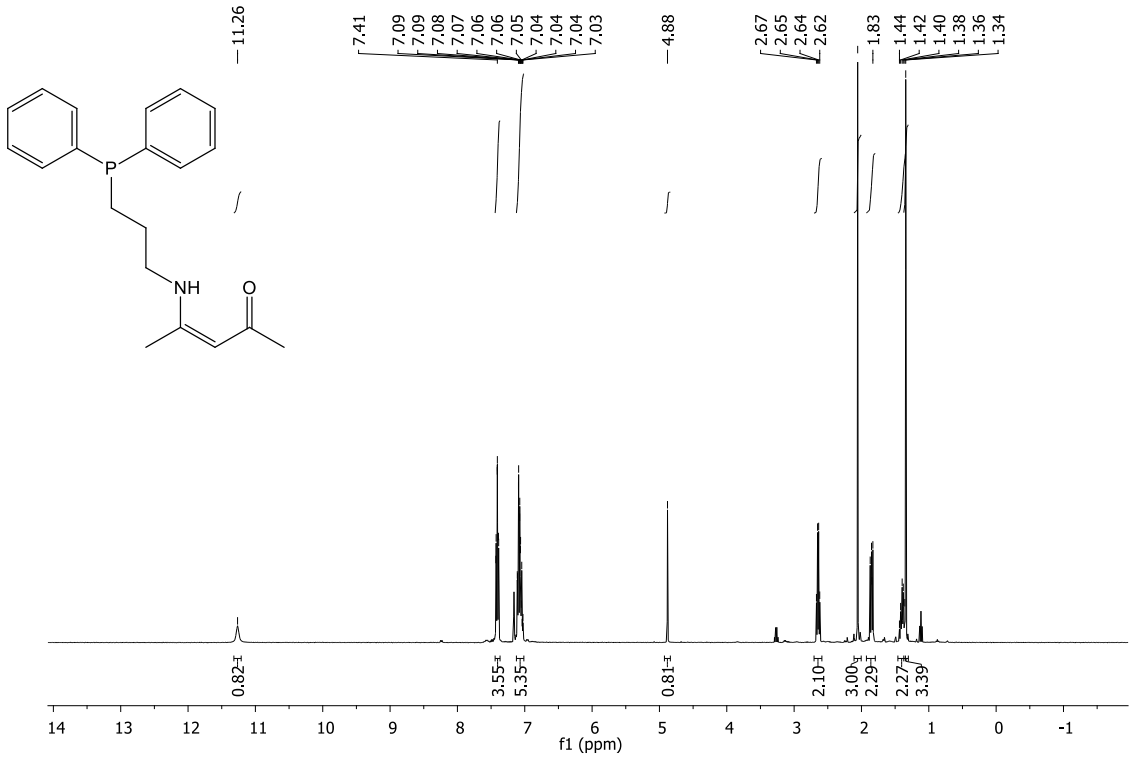

Fig. D.1 ^{1}H NMR spectrum of **$(Ph_2P(CH_2)_3)NH(CH_3)CH(CO)CH_3$** in benzene-$d_6$.

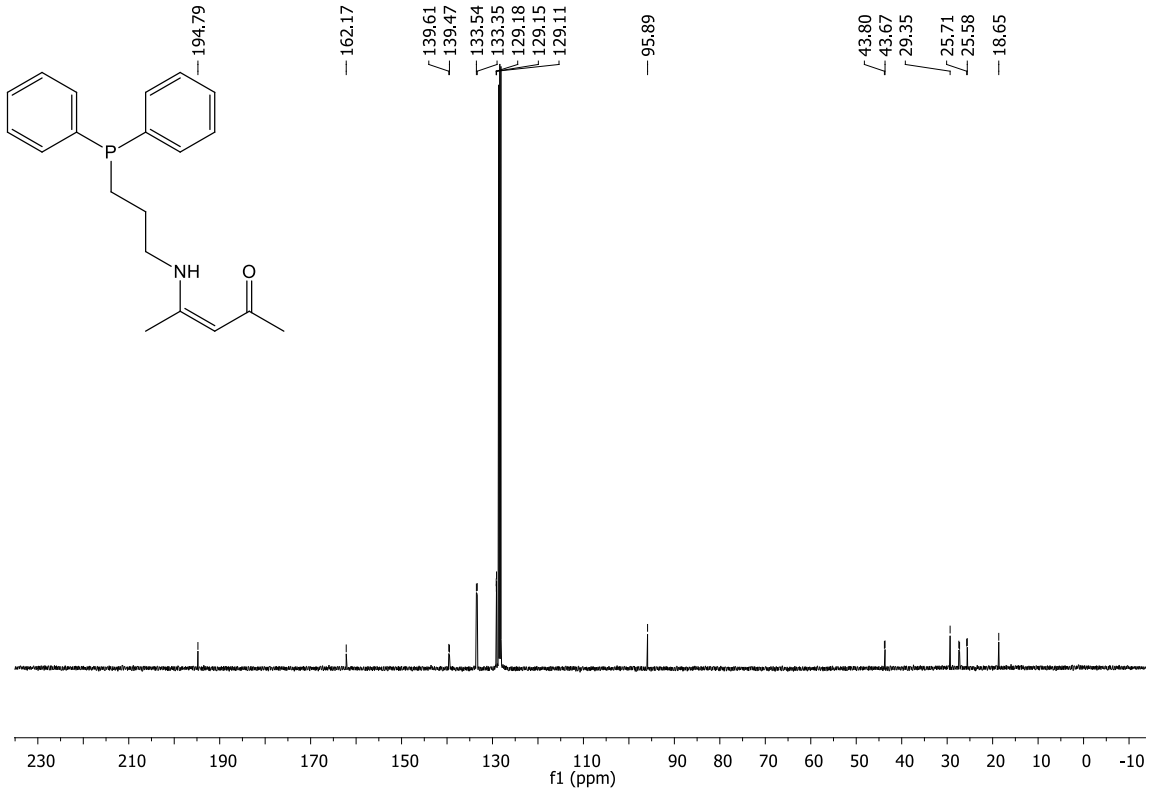

Fig. D.2 ^{13}C NMR spectrum of **$(Ph_2P(CH_2)_3)NH(CH_3)CH(CO)CH_3$** in benzene-$d_6$.

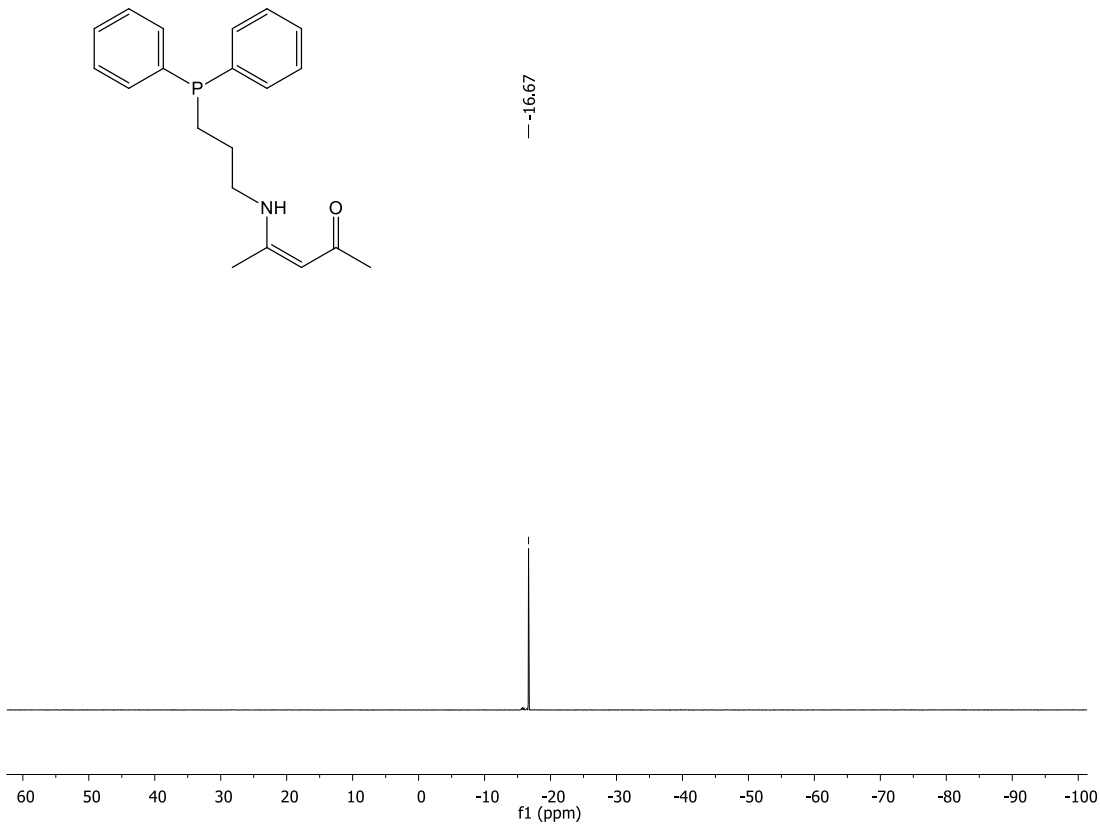

Fig. D.3 ^{31}P NMR spectrum of **$(Ph_2P(CH_2)_3)NH(CH_3)CH(CO)CH_3$** in benzene-$d_6$.

D2. Meerwein's Salt

While aryl amines will readily form the doubly condensed product with stoichiometric acid, this does not extend to alkyl amines, which will only form a singly condensed product. Reports by Wolczanski[1] and Glover[2] utilized cationic alkyl sources to active the remaining ketone, allowing for the formation of ^{pyCH2}BDI and ^{allyl}BDI. This same method does not extend to **$(Ph_2P(CH_2)_3)NH(CH_3)CH(CO)CH_3$**, which results on addition to the phosphine. Protection of the phosphorus with BH_3·THF did not prevent alkyl addition, as alkyl phosphines are typically deprotected with excess amine.

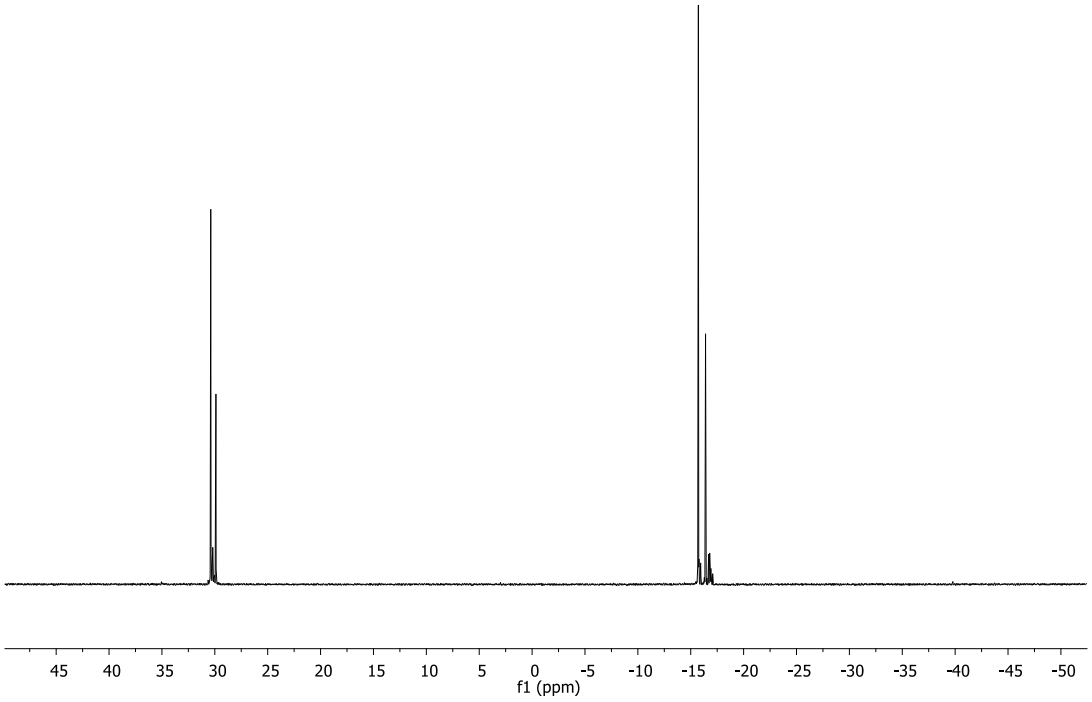

Fig. D.4 ^{31}P NMR spectrum of **$(Ph_2P(CH_2)_3)NH(CH_3)CH(CO)CH_3$** after the addition of Meerwein's salt.

D3. Other Methods

Other methods attempted include addition of 2 equivalents of vinyl diphenylphosphine to ^{allyl}BDI, along with Grubb's Catalyst (metathesis coupling), addition of 2 equivalents of Ph_2PH to ^{allyl}BDI under basic or radical conditions (similar to the addition of Ph_2PH to acrylonitrile), complexing ^{allyl}BDI to either Rh or Co, then adding 2 equivalents of Ph_2PH (metal catalyzed hydrophosphination), and the formation of ^{HOEt}BDI from ethanolamine and 2,4-pentanedione (could then be added to Ph_2PCl to make a phosphite ligand). None of these attempts were successful.

D4. References

1. Williams, V. A.; Wolczanski, P. T.; Sutter, J.; Meyer, K.; Lobkovsky, E. M; Cundari, T. R. *Inorg. Chem.* **2014**, *53*, 4459−4474.

2. Bradley, A. Z.; Thorn, D. L.; Glover, G. V. *J. Org. Chem.*, **2008**, *73* (21),8673–8674.

BIOGRAPHICAL SKETCH

Christopher Lewis Rock was born March 7th, 1988 in Calgary, AB, Canada to David and Lee Rock. He is the older brother to Lauren. He attended high school in Cochrane, AB, before moving to Kelowna, BC to pursue a Bachelor of Science degree from the University of British Columbia – Okanagan. In the summer of 2009, he received an Irving K. Barber Undergraduate Research Award and began working on synthesizing new metal containing polymethacrylates in the lab of Dr. Alaa Abd-El-Aziz. Christopher continued his work as an honours project and graduated with an Honours B.Sc. in 2010. He decided to continue his work with Dr. Abd-El-Aziz and pursued a Master of Science. In 2012, Dr. Abd-El-Aziz took a position at the University of Prince Edward Island and moved his research group there. Christopher completed his work on metal containing polynorbornenes and graduated in 2013 before moving to Arizona to pursue a Ph.D at Arizona State University under Dr. Ryan Trovitch. After some slow progress, Christopher settled in to study the reactivity of nickel and cobalt catalysts, publishing 3 papers on this work. He is the husband to Amanda and together they enjoy football, exercise, and taking care of their zoo. At present, Christopher is working as a Post-Doctoral researcher, synthesizing new chelated gadolinium complexes for contrast MRI.